

वास्तविक समय कैमरा आधारित खरपतवारनाशी छिड़काव यंत्र का विकास

**DEVELOPMENT OF A CAMERA BASED REAL TIME
WEEDICIDE APPLICATOR**

KONGA UPENDAR



ICAR-INDIAN AGRICULTURAL RESEARCH INSTITUTE

NEW DELHI - 110012

2022

**DEVELOPMENT OF A CAMERA BASED REAL TIME
WEEDICIDE APPLICATOR**

A thesis

By

KONGA UPENDAR

Submitted to the Faculty of Post Graduate School
ICAR-Indian Agricultural Research Institute, New Delhi
in partial fulfilment of the requirements
for the award of degree of

DOCTOR OF PHILOSOPHY

IN

AGRICULTURAL ENGINEERING

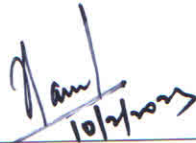
(Farm Power and Equipment)

(ICAR- IARI PG Outreach Programme at ICAR-CIAE, Bhopal)

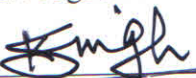
2022

Approved by:

Chairperson :

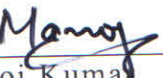

K. N. Agrawal

Co-Chairman :


Karan Singh

Members :


N.S. Chandel


Manoj Kumar



ICAR-Central Institute of Agricultural Engineering,
Nabi Bagh, Berasia Road, Bhopal-462038



K. N. Agrawal
Principal Scientist

CERTIFICATE

This is to certify that the thesis entitled "**Development of a Camera Based Real Time Weedicide Applicator**" submitted to the Faculty of Post Graduate School, Indian Agricultural Research Institute, New Delhi, in partial fulfilment of the requirements for the degree of **Doctor of Philosophy in Agricultural Engineering**, by **Mr. Konga Upendar**, Roll No. 10956 embodies the results of a *bona fide* research work carried out by him under my guidance and supervision. No part of the thesis has been submitted for any other degree or diploma.

It is further certified that any help or source of information, as has been availed for this work, has been duly acknowledged by him.

Date: 10/2/2023

Place: ICAR-CIAE, Bhopal

(Kamal Nayan Agrawal)

Chairperson, Advisory Committee

ACKNOWLEDGEMENT

Every single thing that is done for a good cause will end up well, without god almighty nothing would have been possible. I humbly place before the throne of the Almighty, my most sincere gratitude. His grace and tender mercy have renewed me every day, all the way on the journey through my life. This adage realizes me of the fact that I could make it to the thesis submission, which at one point of time was an impossible task for me. The task of acknowledging the help that was offered to me throughout this study by my teachers and friends is bigger than the study itself. Under this decorum I would like to recall all of them with utmost gratitude.

*At first, I would like to express my wholehearted gratitude and sincere thanks my Chairperson of advisory committee to **Dr. K. N. Agrawal**, Project Coordinator, ICAR-CIAE, Bhopal for providing me an opportunity to work under his excellent guidance, wholehearted support throughout the research, keen interest, constructive criticism, and the encouragement given to me will always remain in my heart with great respect.*

*I express my deep sense of reverence to Former Co-Chairperson, **Dr.P.S. Tewari**, Co-Chairperson, **Dr. Karan Singh**, Advisory Committee, **Dr. N.S Chandel** and **Dr. Manoj Kumar**, members for their valuable suggestions, creative comments in conducting research and the encouragement given to me for my career advancement will always remain in my heart with great respect and for their moral support and cooperation extended to me during the course of investigation. I would like to thank **Dr. C.R Mehta.**, Professor and Director, ICAR- CIAE, Bhopal for extending the research support.*

I am profoundly grateful to the all scientific and research staff of ICAR-CIAE, Bhopal, and also I am overwhelmed to express my gratitude Technical staff Subhasis, Bharathi, Ranjit, Suren Jhat and Kum Kum Dubey.

No words can express my gratitude to my dear friends Jithender, Shushant, Prabhakar sukla, Premveer, Anupam, Anjali, Pagare, Pramod, Manisha, Sanket and Mausami for their unending love, moral support, and assistance. I am also thankful to Ph.D. seniors, juniors and colleagues.

*On a Personal note I record my respectful gratitude to my beloved parents and siblings **Srinivas, Swarajyam, Shankar and Nirosha**, whose prayers were my strength to go*

ahead, whose love and affection have no equivalent and always aroused my spirits to do more, to achieve higher.

Finally, I acknowledge the financial assistance received from IARI, New Delhi and UGC National Fellowship (Govt. of India) during the tenure of research work.

Above all, I thank them for the blessings showered on me in my life. Any omission in this brief acknowledgement does not mean lack of gratitude.



Date: 28-12-2022

Place: ICAR-CIAE, Bhopal

(Konga Upendar)

CONTENTS

CHAPTER	TITLE	PAGE NO.
I	INTRODUCTION	1-7
II	REVIEW OF LITERATURE	8-37
III	MATERIALS AND METHODS	38-85
IV	RESULTS	86-134
V	DISCUSSION	135-146
VI	SUMMARY AND CONCLUSIONS	147-154
	BIBLIOGRAPHY	155-166
	ABSTRACT	I-III
	सारांश	IV-VI
	APPENDICES	VII-XVIII

LIST OF TABLES

Table No.	Title	Page No.
2.1	Critical period of weed control	9
2.2	List of weedicides and susceptible crops	10
2.3	List of visible spectral colour indices and formulas	17
2.4	List of visible spectral colour indices with their advantages and disadvantage	18
2.5	Types of features	20
2.6	Advantages and disadvantages of texture, shape and colour based weed detection	21
2.7	List colour models	24
2.8	Weeding robots developed in recent years	34
3.1	Logitech C525 webcam specification	41
3.2	Plan of experiment to test colour difference (ΔE_{ab}) of weed detection sensor	42
3.3	Technical details of lux meter	43
3.4	Supported image resolution (pixels) of Logitech (C525) webcam	45
3.5	Dimensions of test chart and megapixels suitability	46
3.6	Selection of illumination intensity and image resolution based on desirability value	47
3.7	Plan of experiment to test sensitivity of R, G, B, ExG and ExGR values of green and soil pixels	48
3.8	ExG and ExGR intensity values from RGB channels intensity values of green and soil colour patches	51
3.9	Experimental plan to measure the effect of image resolution, working distance and plant segmentation methods on response variables	57
3.10	Experimental plan to test effect of soil type on response variables	67
3.11	Plan of experiment to test effect of operating pressure and solenoid valve opening time on discharge rate	77
3.12	Hardware components used for site specific weedicide applicator	78

Table No.	Title	Page No.
4.1	Analysis of variance (ANOVA) of colour difference (ΔE_{ab})	88
4.2	Desirability values of 16 combinations of categorical factor levels	88
4.3	Analysis of variance (ANOVA) of red, green and blue channel intensity	91
4.4	Analysis of variance of ExG and ExGR channel intensity	94
4.5	Threshold values of ExG, ExGR, HSV and CIELAB models	103
4.6	Performance metrics of plant segmentation methods at different working height and image resolution	106-107
4.7	Analysis of variance (ANOVA) of precision, recall and false positive rate of ExG method	108
4.8	Analysis of variance (ANOVA) of precision, recall and false positive rate of ExGR method	108
4.9	Analysis of variance (ANOVA) of precision, recall and false positive rate of HSV method	109
4.10	Analysis of variance (ANOVA) of precision, recall and false positive rate of CIELAB method	109
4.11	Dynamic threshold values of plant segmentation methods at four working heights and image resolutions	116
4.12	Performance metrics of CIELAB method with pre-defined threshold value	117
4.13	Analysis of variance of precision and recall of CIELAB with pre-defined threshold value	118
4.14	Distance between weed detection sensor and spraying nozzle at different forward speed	121
4.15	Frame grabbing interval of weed detection sensor at different forward speed	123
4.16	Calculation of reduction in weedicide use by site specific weedicide application	131
4.17	Weeding efficiency of two spraying methods	132

LIST OF PLATES

Plate No.	Title	Page No.
3.1	Development of light source testing platform	40
3.2	Webcam (Logitech C525)	41
3.3	LED bulbs	43
3.4	Lux meter	43
3.5	ISO12233 edge spatial frequency response (eSFR) test chart	46
3.6	X-Rite colour chart checker	49
3.7	Microcontroller (Raspberry Pi)	54
3.8	Test images	59
3.9	Preparation of ground truth image	63
3.10	Plastic green patch	73
3.11	Compact setup for mounting microcontroller, LCD screen, motor driver and	80
3.12	Prototype and components of single row site specific camera based weedicide applicator	81
3.13	Field set up of tractor mounted site specific weedicide applicator	82
3.14	Field evaluation of developed system (Cotton field)	84
4.1	Measurement of spray foot print at different duration of solenoid valve opening	126
4.2	Effect of solenoid valve opening time spray coverage	127
4.3	Weeding efficiency	133
4.4	Water sensitive paper	133
4.5	Water sensitive paper attached to cotton plants	134

LIST OF FIGURES

Figure No.	Title	Page No.
1.1	Yield loss due to several factors	2
1.2	Weedicide spraying methods	4
1.3	Effect of optimization of operational parameters	6
2.1	Agrochemical spraying methods	12
3.1	Standard RGB values of green and soil colour patches	50
3.2	Excess green index (ExG) values of selected leaf	52
3.3	Excess red index (ExR) values of selected leaf	52
3.4	Excess green minus red index (ExGR) values of selected leaf	53
3.5	GPIO pin layout and colour coding of each pin of Raspberry Pi	55
3.6	Operating system installation procedure	56
3.7	Working height	58
3.8	Field of view of camera	58
3.9	Track bars window	60
3.10	Feature extraction using filters, model development and prediction	64
3.11	Weed and soil pixels classification and performance metrics computation	65
3.12	Solenoid valve	69
3.13	L298N motor driver module	69
3.14	Circuit diagram of Raspberry Pi 4B and L298N motor driver interface	70
3.15	Flowchart of site specific weedicide applicator	72
3.16	Green patch area and field of view of weed detection sensor	73
3.17	Center to center distance between weed detection sensor and spraying nozzle	75
3.18	Optimization of frame grab interval of weed detection sensor	75-76
3.19	Functional block diagram of the site specific weedicide application system	79
3.20	Set up for fixing webcam, light, solenoid valve, batteries and microcontroller	80

Figure No.	Title	Page No.
3.21	Schematic diagram of a single row site specific camera based weedicide applicator	81
3.22	Illustration of intersection over union (IoU) metric	83
4.1	Effect of illumination intensity and image resolution on colour difference (ΔE_{ab})	87
4.2	Red, green and blue channel intensity values of green patches	90
4.3	Red, green and blue channel intensity values of soil patches	90
4.4	Red, green and blue channel intensity values of green leaves	92
4.5	Red, green and blue channel intensity values of soil sample	92
4.6	Effect of illumination intensity and image resolution on ExG intensity values	93
4.7	Effect of illumination intensity and image resolution on ExGR intensity	94
4.8	ExG and ExGR intensity values of green leaves and soil sample	95
4.9	Test images and corresponding ground truth images	96
4.10	Output of developed software to compute performance metrics	96-97
4.11	Performance metrics of excess green index (ExG) method at different threshold values	98
4.12	Performance metrics of excess green minus red index (ExGR) method at different threshold values	99
4.13	Performance metrics of HSV method at different threshold values	100
4.14	Performance metrics of CIELAB method at different threshold values	100
4.15	GUI of excess green index	101
4.16	GUI of excess green minus red index (ExGR)	102
4.17	GUI of HSV method	102
4.18	GUI of CIELAB method	103
4.19	Effect of plant segmentation methods with pre-defined threshold value and working height on weed and soil pixels classification accuracy	110
4.20	Effect of plant segmentation methods with dynamic threshold value and working height on weed and soil pixels classification accuracy	111

Figure No.	Title	Page No.
4.21	Effect of plant segmentation methods with pre-defined threshold value and image resolution on weed and soil pixels classification accuracy	112
4.22	Effect of plant segmentation methods with dynamic threshold value and image resolution on weed and soil pixels classification accuracy	113
4.23	Effect of plant segmentation methods with pre-defined threshold value and test images on weed and soil pixels classification accuracy	114
4.24	Effect of plant segmentation methods with dynamic threshold value and test images on weed and soil pixels classification accuracy	115
4.25	Dynamic threshold values of plant segmentation methods	116
4.26	CIELAB method performance at three soil type	119
4.27	Effect of optimization of operational parameters on detection and spraying	120
4.28	Overlap among successive frames of weed detection sensor	123
4.29	Measurement of nozzle discharge and spray distribution pattern	124
4.30	Input image and segmented image	128
4.31	Real time site specific weedicide application	129
4.32	Variation of weed coverage percentage at different location of cotton field	130

LIST OF ABBREVIATIONS

AC	Alternate Current
ACC	Artificial Cloud Chamber
ANN	Artificial Neural Network
ANOVA	Analysis of Variance
Anon	Anonymous
B	Blue
CAGR	Compound Annual Growth Rate
CCD	Charge-Coupled Device
CCM	Colour Co-Occurrence Matrix
CIAE	Central Institute of Agricultural Engineering
CIELAB	International Commission on Illumination's LAB Colour Space
CIVE	Colour Index of Vegetation Extraction
CMOS	Complementary Metal-Oxide-Semiconductor
CNN	Convolutional Neural Network
CO. LTD	Limited Company
COM	Combined Exg, Exgr, CIVE and VEG Indexes
CPWC	Critical Period of Weed Control
CRD	Completely Randomized Design
DC	Direct Current
DM-HSI _{SD}	STEPDISC Data Model For Hue, Saturation, Intensity
DSLR	Digital Single-Lens Reflex
DF	Degree of Freedom
e.g.	For Example
eSFR	Edge Spatial Frequency Response
ExG	Excess Green
ExGR	Excess Green Minus Excess Red
ExR	Excess Red
FD	Fourier Descriptors
FN	False Negative
FOV	Field Of View
FP	False Positive
FPR	False Positive Rate
FY	Financial Year
G	Green
GGCM	Gray-Level Gradient Co-Occurrence Matrix
GIS	Geographic Information System
GLCM	Gray-Level Co-occurrence Matrix
GPIO	General Purpose Input and Output
GPS	Global Positioning System
GUI	Graphical User Interface
GVA	Gross Value Added
H	Hue
HDMI	High Definition Multimedia Interface
HID	High Intensity Discharge

HSD	Honestly Significant Difference
HTP	Horizontal Triplex Piston Pump
I	Intensity
i.e.	That Is
IC	Integrated Circuit
ICAR	Indian Council of Agricultural Research
IDE	Integrated Development Environment
IDS	International Design Services
IFRAO	International Federation of Rock Art Organizations
INC.	Incorporated
IR	Infra-Red
ISO	International Organization For Standardization
KNN	K-Nearest Neighbors
L	Luminance
LBP	Local Binary Pattern
LCD	Liquid Crystal Display
LED	Light Emitting Diode
LIDAR	Light Detection And Ranging
MA	Massachusetts
MExG	Modified Excess Green
MI	Michigan
MS	Microsoft
MSP	Mixed Signal Processing
MVRG	Modified Variable Rate Granular
NC	Normally Closed
NDI	Normalized Difference Index
NDVI	Normalized Difference Vegetation Index
NGRDI	Normalized Green-Red Difference Index
Nil	Nothing at All
NIR	Near Infra-Red
NO	Normally Open
NOOBS	New Out of Box Software
NTSC	National Television Standards Committee
OS	Operating System
PAC	Percentage Area Coverage
PC	Personal Computer
PTO	Power Take off Shaft
PWM	Pulse Width Modulation
R	Red
RAM	Random Access Memory
RGB	Red Green Blue
S	Saturation
SD	Standard Deviation
SSWM	Site Specific Weed Management
SVM	Support Vector Machine
TN	True Negative

TP	True Positive
UA	Uniform Application
US	United States
USA	United States of America
USB	Universal Serial Bus
V	Value
VF	Variable Frequency
VR	Variable Rate
VRA	Variable Rate Application
VRT	Variable Rate Technology
WCP	Weed Coverage Percentage
Wi-Fi	Wireless Fidelity
YOLO	You Only Look Once
YUV	Luma/Brightness, Blue Projection, Red Projection

LIST OF SYMBOLS

ΔE_{ab}	Colour difference
T	Temperature
ns	Non-significant
Σ	Sigma
σ	Standard deviation
μ	Mean
\$	USD
₹	Indian Rupees
%	Percentage

LIST OF UNITS

°C	Degree celsius
µm	Micrometer
A	Ampere
cm	Centimeter
cm ³	Cubic centimeter
g	Gram
h	Hour
hp	Horse power
Hz	Hertz
J	Joule
K	Kelvin
kg	Kilogram
km	Kilometer
kPa	Kilo Pascal
kV	Kilovolt
kW	Kilowatt
l	Litre
m	Meter
m ²	Square meter
m ³	Cubic meter
mg	Milligram
min	Minute
ml	Millilitre
mm	Millimeter
N	Newton
Pa	Pascal
rpm	Revolutions per minute
Rs.	Rupees
s	Second
V	Volt
W	Watt

Chapter 1

Introduction

Chapter-1

Introduction

India is the second most populous country in the world after China. It homes over 17 % of total world population with 2.4 % of land area. With a burgeoning population, it has always been a challenge to meet both the food and nutritional security. India is a global agricultural powerhouse among the major producers and exporters of many agricultural commodities. Agriculture is the primary source of livelihood for about 58 % of India's population. The share of agriculture and allied sectors in India's gross value added (GVA) at current prices stood at 17.8 % in FY 2020-21. The total agricultural and allied products exports stood at US\$ 41.25 billion in FY 2020-21. The Economic Survey of India 2020-21 report stated that in FY 2020-21, the total food grain production in the country was recorded at 296.65 million tonnes-up by 11.44 million tonnes compared with 285.21 million tonnes in FY 2018-2019. In FY 2020-21, production was recorded at 303.34 million tonnes against a target of 301 million tonnes (Economic survey, 2021-2022).

Agriculture is an important sector of the Indian economy and employs over 50 % of the domestic workforce and contributes to around 17 % to gross domestic product and about 11 % to country exports. In order to ensure self-sufficiency in food grain production in the backdrop of increasing population, state agencies have assumed a greater role as facilitators of technology adoption (Anonymous, 2022). Indian agriculture especially practiced on small farms was seen as being traditional and low productive activity. The productivity of farms depends mainly on the judicious use of available natural resources, farm inputs and available farm power. Moreover, under the situation of labour scarcity and high cost of labour due to urbanization and modernization, timely field operations have become a problem. Therefore, farm mechanization has immense scope in improving the agricultural productivity by reducing the labour requirement and the drudgery involved.

All the chemicals used to enhance crop yields, like pesticides and fertilizers, are known as agrochemicals. There are also insecticides, herbicides and fungicides in this group. Indian pesticide consumption is set to reach 69,450 metric ton by 2026 from 64,120 metric ton in 2021, growing 1.3 % year on year CAGR (India Agrochemical Industry Outlook, 2022-2026). Year on year, the Indian market has increased by 1.8 % since 1995. The United States, Brazil, and

Argentina were ranked second, third and fourth in this ranking, respectively. Witnessing the rising demand for food and constant population growth, agrochemicals today are the most practical method for improving crop yield and meeting the increasing demand of food worldwide. They are widely used in fields to protect crops and maximize output.

In today's input-intensive agricultural system, minimizing economic losses in agricultural production caused by biotic and abiotic factors is crucial. Among the major biotic constraints, weeds are considered harmful to agricultural production. They indirectly affect crop production because they compete with main crops for resources, provide shelter for crop pests and reduce crop yield and quality. Weeding is one of the most difficult and time consuming operations and accounts for the major share of the cost of agricultural production. During early establishment, the weeds make 20-30 % of their growth while the crop makes 2-3 % of its growth. Often several weeding operations are necessary to maintain weed free situation during the critical period of crop weed competition, which is approximately upto 25-40 days after sowing. It was estimated that reduction in yield due to weeds alone is 20-30 % depending on the crops, weed infestation intensity and location, which might increase up to 50 % if adequate crop management practices were not observed (Basavaraj et al., 2016). Fig 1.1 presents the yield loss due to different agents such as weed, insects, disease and other causes. The maximum yield loss of 37 % was observed due to weed infestation followed by insects and diseases (Kumawat et al., 2019).

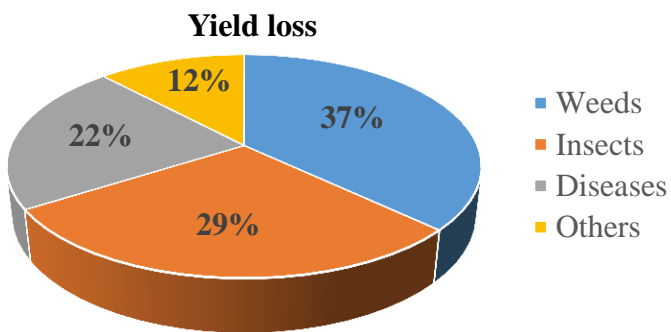


Fig. 1.1: Yield loss due to several factors

Various weed control methods are manual, mechanical, chemical and biological. Manual weeding has been done by hand or hand tools like hoes and khurpi in the bending posture which involves a lot of drudgery. Manual weeding can give a clean weeding, but it was a very slow

process (Biswas, 1990). Manually operated, animal operated, power operated and tractors mounted sprayers have been used for chemical spraying of weedicides. Weeds should be destroyed at an early stage to reduce yield loss. Weeds were present non-uniformly in a field, tilling the entire field with mechanical weeders results in more energy consumption. At present, research has been more inclined towards conservation tillage instead of conventional tillage. Conservation tillage focuses on minimal soil disturbance, moisture conservation and reducing unnecessary soil compaction due to the repeated movement of farm vehicles. A mechanical method of weed management needs more energy in terms of labour and power requirements than a chemical method of weed management. However, based on availability, both methods have been commonly used for inter-row weed management.

There was strong evidence that weeds were spread randomly and non-uniform in agriculture field (Agrawal et al., 2012; Steward & Tian, 1999). But, in case of chemical weeding weedicides were applied to whole field. Similarly, in case of mechanical weeding the entire field was tilled. It leads to wastage of chemicals and wastage of energy. Hence, the site specific weed management method is need of an hour. Precision agriculture tools can make it possible to assess and manage variability to improve production and productivity of farming practices (Gebhardt & Kühbauch, 2007). Precision agriculture (Molin et al., 2002) uses several technologies, such as sensors, information systems, improved machinery and informed management, to maximize production while considering the variability and uncertainty of agricultural systems. These modern agriculture practices were both in spatial and temporal domain based on the idea that a production area was not homogeneous; it varies greatly both in spatial and temporal domain, thus, using agricultural inputs and management techniques uniform for areas with different characteristics was not appropriate (Gianessi & Reigner, 2007). The development and convergence of numerous technologies, such as microcomputers, control automation, remote sensing, mobile computing, advanced information processing and telecommunications, have largely benefited precision agriculture. These technologies made it possible to analyze spatial and temporal variability by collecting data, managing information, applying inputs at different rates and then evaluating the results in terms of their economic and environmental effects (Triantafyllou et al., 2019).

Site-specific weedicide application technology eliminates the blanket application (Fig 1.2a) of weedicides by spraying only on weed-infested areas (Fig 1.2b); a potential weedicide

saving amount was reported as 30-75 % (Hamuda et al., 2016). Weed sensing and precision spraying control systems are components of site-specific weed management (SSWM). For site-specific weed management, an automated detection system was crucial for weed identification. Several non-contact sensing devices have been developed to detect weeds.

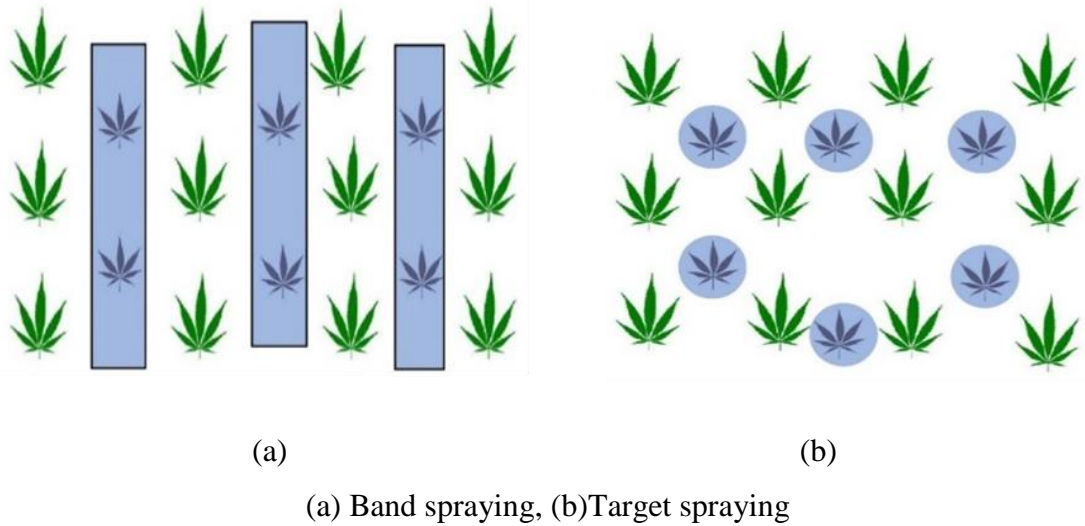


Fig 1.2: Weedicide spraying methods

Detect-Spray, Green-Seeker, Weed-IT and Weed-Seeker sensors have been developed and deployed for patch spraying to detect and extract herbaceous plants. All these sensors work in reflection mode (Schmittmann & Schulze, 2017). In order to determine the green colour, the measuring spot area should be $20 \times 10^2 \text{ mm}^2$. Another sensor, ‘AmaSpot,’ was a sensor and nozzle unit reported by (Schmittmann & Schulze, 2017). A recommended scanned area of the ‘AmaSpot’ sensor was $300 \times 300 \text{ mm}^2$, out of which 3 % of the area must be the green surface for successful green plant recognition. According to reports, a $500 \times 500 \text{ mm}^2$ scanning area must be included in a total scanning area of $70 \times 10^2 \text{ mm}^2$. It was reported that to use opto-electric sensors, either the weeds needed to be well developed or there needed to be a lot of weed coverage, making it easier to identify plants and apply weedicide. Distance measurement sensors (laser and ultrasonic) have been engaged in plant/weed identification (Farooque et al., 2013; Swain et al., 2009; Zaman et al., 2011). Due to the measurement speed, the small size of weeds at the early stage, the dynamic oscillation of the carrier vehicle and the sensitivity to small changes in distance, this method was ineffective for weed detection at an early stage. The disadvantage of this technology was that target weeds need to be taller to be sensed using ultrasonic sensors. Real-time ground measurements using machine vision (imaging sensor) for site-specific weed

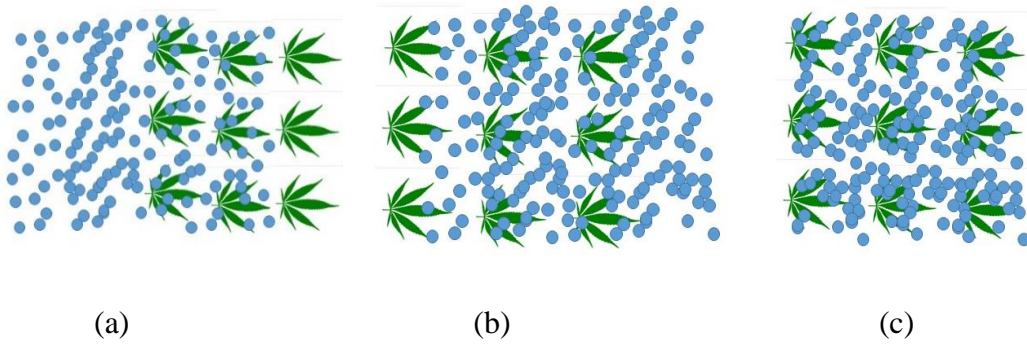
management were thought to overcome these limitations of opto-electric and ultrasonic sensors (Zaman et al., 2011).

Image processing techniques have been commonly employed for fast and accurate weed detection in a non-destructive way in crop fields (Sujaritha et al., 2017). Colour, shape and texture features have been employed for weed detections. In the case of colour-based site-specific weed management, all the plant material found between the crop rows was considered a weed (Agrawal et al., 2012; Chandel et al., 2018; Tangwongkit et al., 2008). Many researchers have employed the colour feature in plant segmentation to separate crops/weeds from the soil (Hamuda et al., 2016; Kirk et al., 2009; Meyer & Neto, 2008).

Colour-based weed and soil pixel classification is severely affected by outdoor light especially sun light and clouds. The illumination intensity varies throughout the day and this factor profoundly affects colour and texture based weed identification process (Mahmud et al., 2020). The image quality of digital colour camera is greatly affected by external illumination since the camera works on reflected light. Under field condition there were several factors affecting the performance of imaging sensors. They were variable illumination (Chandel et al., 2018), camera parameters (Mahmud et al., 2019), image acquisition speed (Esau et al., 2017) and image inappropriate feature selection (Chang et al., 2012; Rehman et al., 2018). Digital colour cameras store colour information in the RGB (red, green and blue) colour format. Instead of directly using the RGB intensity values of digital colour cameras, visible spectral colour indices and colour models have been engaged in weed and soil pixels classification. Visible spectral colour indices and colour models are formed by combining the RGB values through simple arithmetic operations to produce relative colour indices which are less sensitive to illumination or other factors affecting the RGB gray levels (El-Faki et al., 2000; Meyer & Neto, 2008). Accurate weed and soil pixels classification depends on threshold values of visible spectral colour indices and colour models. Under varying lighting conditions, this pre-defined threshold value shows under segmentation or over segmentation. To overcome problem of outside light effect on weed detection sensor performance several studies suggested use of artificial light source and protective cloth (Kazmi et al., 2015; Mahmud et al., 2019; Sujaritha et al., 2017; Tangwongkit et al., 2006; Tewari et al., 2014).

Other factors limiting development and deployment of site specific weedicide applicator include slow processing time and large memory requirement of application software. An image

processing software task is to extract salient features from digital colour images. High computing power and image processing software are needed for colour feature extraction, colour transformation and performing real-time site-specific weedicide applications. There is a need of a microcontroller to perform the operations mentioned earlier. Moreover, the power requirement of hardware components is also a significant factor because, during field operations, either power has to be taken from the prime mover or additional batteries are to be used. Hence, low power consumption, compact and robust hardware components are necessary for field applications.



(a) Spraying starts before reaching the detection area, (b) Spraying starts after crossing the detection area, (c) Spraying exactly on detection area

Fig 1.3: Effect of optimization of operational parameters

The optimization of operational parameters (distance between the sensing unit and spraying nozzle, frame grab interval of the weed detection sensor, and quantity of weedicide application) is of utmost importance because the chemical to be sprayed is in the weed-detection zone (the field of view of the camera); otherwise, the purpose of site-specific weedicide application has no meaning. The distance between the webcam and the nozzle depends on the time a microprocessor takes to execute the developed algorithm and the forward speed of the prime mover. Three conditions can be observed while optimizing the operational parameters. The situation in Fig. 1.3 (a) happens when the distance between the webcam and the nozzle is closer and the solenoid valve responds quickly. The Fig 1.3 (b) condition occurs when the distance between the webcam and nozzle is wider and the response time of the solenoid valve is too slow. Fig 1.3 (c) depicts precise spraying on weed patches detected by the webcam. Hence, there is a need to optimize the operational parameters of a site-specific weedicide applicator.

Weedicide is an essential input utilized by farmers to control weeds in the crops; most of the weedicide is applied as preventive measure. The recommendations of the weedicide

application were mostly done on whole area basis while occurrence of the weeds in the field was in random or non-uniform. Application of weedicide on site-specific manner leads to saving of the costly chemical apart from achieving desired goal of weed control. Map based system has its limitation due to limitation of remote sensing images taken. With advent of opto-electronic system, a number of attempts have been made in different parts of the world to develop real time weedicide application system. Moreover, considering the size of land holding in India, it is more realistic to have on the go system which is considered to be more accurate and reliable. In the current research, a real-time site specific weedicide applicator was developed. The proposed application was a vision-based approach using a web camera for image acquisition attached to a vehicle moving at constant speed. Fast colour-based weed and soil pixels classification algorithm was developed to meet the requirement of real-time weed detection. This study focused on detecting weeds in between crop rows for real-time application, hence, all vegetation in between rows was considered as weeds.

The objectives of research work are:

1. To optimize the factors affecting weed detection in a camera based image acquisition system
2. To develop a algorithm and real time validation of image acquisition and spraying system
3. To develop a camera based real time weedicide applicator

Chapter 2

Review of Literature

Chapter-2

Review of Literature

This chapter deals with the comprehensive review of the literature related to weeds and its control methods, importance of site specific weed management, advancement in weed detection technology, factors affecting colour based weed-soil classification, importance of plant segmentation and performance evaluation of site specific weedicide applicator. This chapter has been presented under the following main headings:

- 2.1 Weed and its control methods
- 2.2 Variable rate technology (VRT) in agriculture applications
- 2.3 Sensor for weed detection
- 2.4 Factors affecting computer vision based weed and soil pixels classification
- 2.5 Plant segmentation in agriculture
- 2.6 Automatic and robotic weeding methods
- 2.7 Performance evaluation of site specific weedicide applicator
- 2.8 Review summary

2.1 Weed and its control methods

A plant other than the main crop or a plant in the wrong place is considered a weed. Immediate action to remove weeds once they emerge is an essential task of weed management because weeds compete with the main crop for water, sunlight and nutrients. Otherwise, substantial yield loss may be encountered. The yield loss due to weeds alone was reported at 37 % (Kumawat et al., 2019). Weeds were classified as annual, biennial or perennial (Radosevich et al., 1997). Annual weeds can produce seeds quickly and in large quantities over a one-year life span. Biennial weeds grow their roots and leaves in the first year. After entering dormancy in the colder winter months, they produce flowers/seeds during the second summer. Perennials are typically the hardest to eradicate because they grow yearly (Mulligan & Findlay, 1970). Zimdahl, (2018) defined the critical period of weed control (CPWC) as "a period between that period after seeding or emergence when weed competition does not contribute in reducing crop yield and the time after which weed competition will no longer reduce crop yield." A more quantitative

definition is the number of weeks after crop emergence during which a crop must be weed free to prevent yield loss greater than 5 % (Hamuda et al., 2016; Knezevic et al., 1994). According to studies, crops should remain weed-free during the CPWC to prevent yield loss (Karkanis et al., 2012). The critical period of weed control for different crops is provided in Table 2.1. The weeding operating must be performed in critical period of weed growth, otherwise weeds negatively affects crop growth and yield. Weed control was as old as farming itself. However, progress in mechanized weed control did not start until the early 1800s, when Jethro Tull invented a seed planter for row crops. This intervention allowed for the killing of weeds between the rows by cultivating the soil.

Table 2.1: Critical period of weed control (Kumawat et al., 2019)

Crops	Critical period (days after sowing)	
	From	To
Rice (Transplanted)	15	45
Upland Rice	15	45
Wheat	30	45
Maize	15	45
Sorghum	15	45
Finger Millet	25	45
Soybean	15	45
Blackgram	30	60
Cotton	15	120
Sugarcane	30	50
Groundnut	30	45
Sunflower	30	60
Castor	30	45

Various common weed control methods are manual, mechanical, chemical and biological. Manual weeding has been done by hand or hand tools like hoes and khurpi in the bending posture which involves a lot of drudgery. Manual weeding can give a clean weeding, but it was a very slow process (Biswas, 1990). Mechanical and chemical weeding methods have been more commonly used than other weeding methods for weeding of large agriculture fields. Mechanical and chemical methods have been employed for inter-row and intra-weed management. Manually operated, animal operated, power operated and tractors mounted mechanical weeders and sprayers have been available for effective weed control. In the case of chemical weeding, weedicides were applied directly to weed plants using sprayers.

Mechanical weeders till the soil that is present between crop rows. Even though tillage is an effective way to get rid of annual weeds, it can leave the soil vulnerable to wind erosion when it is dry and water erosion when it is extremely wet (DiTomaso, 1997). Weedicides are typically regarded as the most cost-effective and efficient approach to manage weed in agricultural and non-crop situations. Improper weedicide use can result in several possible issues, including spray drift, water contamination, toxicity to humans or animals, developing weedicide resistance in weeds and a decline in plant diversity (DiTomaso, 1997).

Table 2.2: List of weedicides and susceptible crops (Kumawat et al., 2019)

Weedicides	Susceptible crops
Barban	Oat, rye
Chlorbromuron	Sugarbeet, cole crops, cucurbits, tomato, okra, rice
Chloroxuron	Sugarbeet, cole crops
2, 4 – D (amine)	Dicot plants
2, 4 – DEP (falone)	Cotton, Tobacco, tomato, onion, grapes
Dicamba	Soybean, beans, small-seeded legumes, ornamentals, vegetables
Dinoseb	Cruciferous crops
Flumeturon	Sugarbeet, cole crops, cucurbits, brinjal
Fluorodifen	Sugarbeet, cucurbits, tomato, alfalfa
Metribuzin	Sugarbeet, cole crops, cruciferous crops, onion, pea, sunflower, sweet-potato, cotton and tobacco
Neptalam	Sugar beet, tomato, spinach
Picloram	Broadleaved plants except cruciferous crops
Propazine	Sugarbeet, vegetables
Simazine	Sugarbeet, vegetables, tobacco

Pesticides offer a variety of advantages over other control methods (Edwards-Jones, 2008). It includes ease of use, rapid weed control, consistency of control and significantly higher yields. Weedicides are now the most commonly used since weeds were the major yield limiting factor in many crops (Gianessi & Reigner, 2007). Weedicides damage plants by interfering with the normal function of one or more of their vital processes, including photosynthesis, amino acid, protein synthesis, lipid synthesis, respiration, cell division and maintenance of membrane integrity (Gianessi & Reigner, 2007). Synthetic pesticides were among the most widely used chemicals in the world (Yao et al., 2008). Contact weedicides kill the parts of the weed that directly interact with the weedicide. Systemic weedicides kill by getting absorbed into the target weed's root system, usually with the water or nutrients used by that particular weed. The timing of weedicide application was broken into two categories, i.e. pre-emergence and post-emergence.

Pre-emergence weedicide was applied before the germination of the target weeds. Post-emergence weedicides were effective against weeds that have already grown. The list of weedicides and susceptible crops are given in Table 2.2. These weedicides have been using to control weeds growth.

2.2 Variable rate technology (VRT) in agriculture applications

The benefits of VRT can be seen in areas with high variability in weed growth and soil fertility, where variable rate input application was required throughout a field. VRT can control inputs applied to crops. The technology results in reducing the cost of production and minimizes the risk of environmental pollution due to over application of inputs in the crops (Earl et al., 1996). The variable rate technology plays an important role in the application of inputs such as seed, pesticide, fertilizer and other input at appropriate level in the management zone. In the field of VRT, there is enough scope to focus on development of site specific weedicide applicator.

Variable rate application technologies are being commonly used in areas such as site specific weed management application and variable rate granular or liquid fertilizer application. The non-uniform distribution of weeds and the potential for weedicide savings are driving the development of site-specific weedicide applicator. Site-specific weed management (SSWM) is a part of precision agriculture where equipment or machinery is embedded with technologies so that weeds present in an agriculture field can be detected and controlled successfully. Precision agriculture offers the promise of increasing productivity, decreasing production cost with optimum use of resources and minimizing the environmental impact (National Research Council, 1997). This technology mainly benefits from the emergence and convergence of several technologies, including the Global Positioning System (GPS), and incorporating the computer software interface component of database, mapping and interpretation with Geographic Information System (GIS) (Schmoldt, 2001).

2.2.1 Site specific weed management approaches

It is general perception that the weed distribution was uniform in agriculture field. Moreover, the weedicide recommendation was on hectare basis. Weedicides were applied uniformly to the entire field irrespective of weed presence. There was strong evidence that weeds were spread randomly in agriculture field at an early stage (Agrawal et al., 2012; Steward &

Tian, 1999), but weedicide recommendations were based on hectares. The entire field was tilled in the case of the mechanical method of weeding or weedicides were applied uniformly to the entire field in the case of the chemical method of weeding. Since, over application can lead to environmental damages. This increases farmer's production cost and prone to groundwater contamination. To overcome the problem of excess weedicide application, either the weedicide recommendation needs to be improved to precisely reflect individual field characteristics or farmers have to be informed about the authenticity of the agronomic advice and the consequences of applying excess weedicides.

Three different types of agrochemical spraying methods are used as shown in Fig 2.1. Broadcast, band and targeted spraying were the three main methods used in agriculture (Hong et al., 2012). Broadcast has been most commonly used spray application method that covers the entire field with a blanket agrochemical application. Band spraying has been used for row crops where only selected strips in the field were sprayed. Targeted spraying has been the hardest way to apply agrochemicals because it needs sensors to determine where the chemicals need to be applied. Target spraying can lower the amount of agrochemical spray by 60-70 %, allowing for a substantial cost reduction to farmers (Hong et al., 2012). Target spraying can also minimize environmental risk to ensure a sustainable agriculture sector.

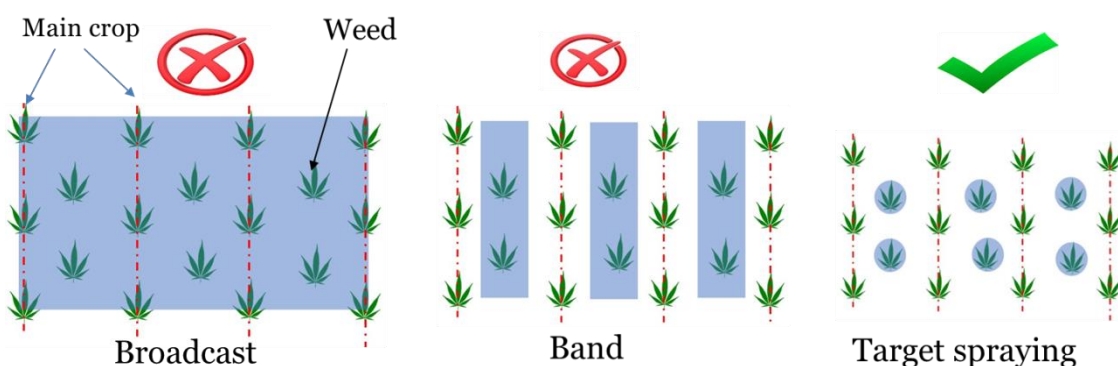


Fig 2.1: Agrochemical spraying methods

The map-based approach and the sensor-based approach have been using for weed recognition. Satellite and aerial-based sensing have been commonly used for large-scale field monitoring in applications such as variable rate weedicide spraying (Lan et al., 2009). These platforms have a lower spatial resolution and the working time was affected by the weather

condition (Moran et al., 1997). A spot specific prototype sprayer was developed (Michaud et al., 2006). It applies chemicals based on prescription maps. The prescription maps of the wild blueberry fields were developed using aerial spectral scans. The system was prone to positional error caused by the global positioning system (GPS) and obtaining up-to-date aerial photography was expensive, the quality was quite variable and data processing for weed detection was also intensive and difficult. Satellite based remote sensing was, in general, limited as a tool for real-time and in-field weed monitoring because of its insufficient spatial resolution. Moreover, this technique was not likely to be adopted extensively due to its high cost.

Sensor-based approach allows less dependency on positioning devices, an advantage over map based approach with higher position accuracy and real time application (Zhang et al., 2003). Sensing and low-altitude aerial-based sensing can acquire higher spatial resolution plant imagery enabling accurate detection of crop rows and plant localization for applications such as real-time, weed control (Hassanein et al., 2019; Li & Tang, 2018). Ground vehicle-based methods, however, must meet requirements such as having clearance over the crop, matching the crop row spacing and being able to traverse the field under a range of soil conditions (Hague et al., 2000).

Data collection of weed presence and processing in sensor-based VRA are to be made fractions of seconds before weedicide application, avoiding the need to generate a previous map of the area. Sensor-based systems have the ability to vary application rate without any mapping or prior data collection. Sensors measure in real time the desired properties while they are in motion. The measurements made by the system are processed immediately and sent to the controller who will perform the application at a varied rate. Thus, it is an easier-to-use system, consumes less time and has greater accuracy when compared to the map-based method. Its current limitation is related to the state of the development of sensors and algorithms with sufficient accuracy to collect and process more detailed information of plants and soil.

2.3 Sensors for weed detection

Several non-contact and nondestructive ground based sensing techniques have been available for weed detection. Opto-electronic sensors like Detect-Spray, Green-Seeker, Weed-IT and Weed-Seeker sensors have been developed and engaged for patch spraying for inter row to detect and extract herbaceous plants (Schmittmann & Schulze, 2017). All these sensors work in reflection mode. The detection principle of all sensors listed above was that green plants absorb

red light in the range of 630 to 660 nm. Moreover, green plants were more reflective in the NIR range of 750 to 1200 nm. All sensors listed earlier consist of two monochromatic diodes that were used for the R and IR range. A ratio of the R channel and IR channel was used to implement a plant identification decision criterion. In order to determine the green colour, the measuring spot area should be 20×10^2 mm². Another sensor, ‘AmaSpot,’ was a sensor nozzle unit reported by (Schmittmann & Schulze, 2017). A recommended scanned area of the ‘AmaSpot’ sensor was 300×300 mm², out of which 3 % area must be the green surface for successful green plants recognition. It was reported that 500×500 mm² scanning area needs to be a weed in a total scanning area of 70×10^2 mm². From above case studies it was observed that in order to use opto-electric sensors, either weed has to be well developed or a high degree of coverage by weeds supports successful plant recognition and weedicide application.

Distance measurement sensors (laser and ultrasonic sensors) have been engaged in plant/weed identification. Due to the measurement speed, the small size of weeds at the early stage, dynamic oscillation of the carrier vehicle and the sensitivity to small changes in distance, this method was ineffective for weed detection at an early stage. Swain et al., (2009) developed and tested an ultrasonic system for weeds (taller than plants) and bare spots (completely bare of vegetation) detection and mapping within wild blueberry fields. However, the variations in wild blueberry plant height from 100 mm to 400 mm (Farooque et al., 2013) and plant density from 870 to 1230 stems m² (Eaton, 1989) limit the use of ultrasonic sensors to detect short weeds and bare spots in wild blueberry fields. Zaman et al., (2011) developed a prototype sprayer that operated in real-time for tall weed detection. The disadvantage with using this technology was that target weeds were not tall enough to sense using ultrasonic sensors. Real-time ground measurements using machine vision for site-specific management were thought to overcome these limitations of ultrasonic sensors. Agrawal et al., (2012) developed a laser sensor based weedicide applicator. Findings of the study were laser sensor helps in reducing the time lag from detection to application of the spray. The drawbacks of system were the aperture area covered on the ground by laser beam was very small and the missing percentage varied between 5 to 26 %. It was reported that due to small aperture area covered by ultrasonic and LIDAR sensor, limited their application in weed detection (Llorens et al., 2011).

With the rapid growth in high resolution vision systems, image processing techniques and embedded computing devices (Agrawal et al., 2012; Hamuda et al., 2016), the imaging sensors playing vital role in precision agriculture. The advantage of imaging sensors especially RGB colour cameras over remaining sensor is available at low cost. Moreover, there is wide availability of image processing libraries for processing RGB images. With advancement of conventional neural networks the more emphasis has been given RGB image based weed or disease detection and classification. Imaging sensor was employed for weed detection (Chandel et al., 2018; B. Tangwongkit et al., 2008; Tewari et al., 2014). The performance of imaging sensor was affected by several factors. The output of a digital colour camera depends on the light source (Adelkhani et al., 2012), variable illumination (Chandler, 2003; El-Faki et al., 2000; Mahmud et al., 2020; Steward & Tian, 1999; Tian & Slaughter, 1998) and type of camera (El-Faki et al., 2000). Details of each factor are discussed in the following section.

2.4 Factors affecting computer vision based weed and soil pixels classification

Accurate classification of weed and soil pixels is required for precise chemical application and with good performance at this stage; the volume of weedicides that are applied to the fields can be minimized. Colour, shape and texture features have been most commonly employed for pixel level weed and soil pixels classification. The advantage and disadvantage of these three features employing for weed and soil pixels classification was listed in following section. This section also contains plant segmentation methods used for pixel level weed and soil classification. The role of dynamic threshold methods in weed and soil pixel classification was elaborated. The effect of illumination intensity and camera parameters on weed and soil pixels classification was mentioned. The strategies employed to overcome the problem of field level deployment of imaging sensors were reported. Factors affecting computer vision based weed and soil pixel classification are discussed in following sub headings.

2.4.1 Effect of feature selection

Traditional image processing based computer vision consider several features for weed detection. Colour, shape, texture and spectral features of soil background and weed are essential for computer vision based weed and soil pixel classification.

2.4.1.1 Colour feature

Colour is defined as the visible electromagnetic spectrum reflected by an object and perceivable by a sensor within its detection range, being one of the most important attributes of objects' appearance. Although the spectrum is continuous with no clear boundaries between one colour and the next ones, colour ranges have been established as an approximation for coordinate definition (Bruno & Svoronos, 2005).

Colour feature has been most commonly used for weed pixels segmentation from soil background. The accuracy of colour based classification mainly depends on colour difference and plant being studied. The colour feature was robust to scale position and size (Wu et al., 2021). The colour feature was not enough to classify the main crop from weeds or different types of weeds because main crop and weeds in almost all cases were green. Colour was most commonly used feature by various researchers (Agrawal et al., 2012; Chandel et al., 2018; Tangwongkit et al., 2008; Tewari et al., 2014) for weed and soil pixels classification and development of inter-row site specific weedicide applicator. Green ratio was used for separating green vegetation from complex soil background (Mahmud et al., 2020).

Visible spectral colour indices have been developed based on RGB colour information for weed and soil pixels classification. The list of colour indices engaged for weed and soil pixels classification is reported in following section.

2.4.1.1.1 Visible spectral colour indices

The digital colour camera stores colour information in RGB colour space. In case of traditional image processing most of the cases the image background has been segmented by converting RGB image to grayscale image. This technique is possible only when the grayscale values of background and foreground elements are different. For example, if colour image contains black and white pixels and converting colour image into grayscale image the white pixels intensity values approximately more than 200 and black pixels intensity values approximately less than 100. In this situation by placing threshold values as 125 one can convert grayscale image into binary image. In case of weeds and soil pixels classification the above technique is not possible. It was reported that directly converting RGB pixels values into grayscale scale do not yield a good segmentation because plant and soil background contain

similar grayscale values. Hence, visible spectral colour indices derived from RGB image have been employed for weed and soil pixels classification (Tian & Slaughter, 1998).

A widely used colour index (Neto, 2004; Vidović et al., 2016), has been called excess green (ExG) (Woebbecke et al., 1995). It uses the red, green and blue normalized chromatic coordinates to calculate the index value pixel by pixel. This results in a grayscale image that was suitable to separate between weeds and soil background by choosing a meaningful threshold (hand-crafted fixed threshold). There is a need of suitable threshold value of colour indices to distinguish between weed and soil pixels. Other threshold based colour indices work the same way except for the different calculation formula (Table 2.3). A review on visible spectral colour indices and their advantages and disadvantages are given in Table 2.4.

Table 2.3: List of visible spectral colour indices and formulas

Colour index	Formula
Excess Green (Woebbecke et al., 1995)	$ExG = 2 \times G - R - B$
Excess Red (G. Meyer et al., 1999)	$ExR = 1.4 \times R - G$
Colour Index of Vegetation Extraction (CIVE) (Kataoka et al., 2003)	$CIVE = 0.441 \times R - 0.811 \times G + 0.385 \times B + 18.787$
Excess Green minus Excess Red (ExGR) (Meyer & Neto, 2008)	$ExGR = ExG - ExR$
Normalized Green-Red Difference Index (NGRDI) (Hunt et al., 2005)	$NGRDI = \frac{(G - R)}{G + R}$
Modified Excess Green (MExG) (Burgos-Artizzu et al., 2011)	$MExG = 1.262 \times g - 0.884 \times r - 0.311 \times b$

Excess green index provides a near-binary intensity image, hence it was commonly employed for weed and soil pixels classification by several studies (Guijarro et al., 2011; Meyer & Neto, 2008; Woebbecke et al., 1995; Yang et al., 2015). Then, with the help of a suitable threshold value, each set of images were segmented into foreground and background pixels. Colour indices have been recommended and extensively used for vegetation identification as they can work under different crop residue conditions and were less sensitive to lighting variations (Campbell & Wynne, 2011). Excessive redness from several sources may be overcast and hamper digital image quality, making it more difficult to identify green plants with simple colour indices (Meyer et al., 1999). Image redness may be related to illumination and it may also

be associated with redness from the soil and residue. The excess red index was introduced to overcome excess red components in a digital colour image. Excess red index ($\text{ExR} = 1.4 \times R - G$) was proposed (Meyer et al., 1999) but has not been examined well in later studies.

Table 2.4: List of visible spectral colour indices with their advantages and disadvantage

Plant segmentation method	Description
Excess Green Index (ExG) (Woebbecke et al., 1995)	It was widely employed and simple to calculate. The sensitivity of this method to background and lighting issues was low. In a natural environment, it exhibited strong adaptability. It performs poorly when the light was too bright or too dim.
Excess Red Index (ExR) (Meyer et al., 1999)	Computing it was simple. It still extracts green pixels despite relying only on the red component. Both high and low light conditions degrade its performance. Compared to ExG, it was less precise.
Excess Green minus Excess Red Index (ExGR) (Neto, 2004)	It showed a high degree of environmental adaptability. This method was capable of extracting green by using ExG and removing background noise by using ExR. It performs poorly when the light was high or low. It segments the pixel of shadow as a plant pixel (over-segmentation).
Normalized Difference Index(NDI) (Woebbecke et al., 1995)	This method can be calculated easily. Other than extreme values, it can withstand lighting in some circumstances. Low or high light levels have a negative impact on its performance. False positives and false negatives were frequently misclassified.
Colour Index of Vegetation Extraction (CIVE) (Kataoka et al., 2003)	The running time for this method was low. It demonstrated good adaptability in an outdoor setting. When the light was weak or strong, it performs poorly. This method was not very adaptable to plant shadows.
Combined ExG, ExGR, CIVE, and VEG indexes (COM) (Montalvo et al., 2013)	It has demonstrated good adaptability in outdoor settings. This method requires a lot of computation. Both high and low light conditions degrade its performance. This method was also sensitive to plant shadows. It considers plant shadows as plant pixels (over segmentation).

Performance of several vegetation indices, i.e. excess green index (ExG), excess red index (ExR), excess green minus red index (ExGR) on green vegetation segmentation accuracy was studied (Hamuda et al., 2016). Normalized difference vegetation index (NDI) for greenness identification was used (Perez et al., 2000). It uses green and red channels only for image

segmentation. Normalized difference vegetation index, modified hue and ExG indices were used and tested their accuracy in plant matter identification under soil backgrounds (Mao et al., 2003). It was reported that excess green index (ExG) was shown superior performance in plant matter classification to the other methods tested. A crucial step in colour index-based vegetation segmentation was to select an optimum threshold value to divide image into white and black pixel image (Binary image). A study was conducted to detect powdery mildew disease using imaging sensor (Mahmud et al., 2020). In this study the first stage was background removal and then extracts texture features from segmented image. The soil background was removed from an input image by using green ratio. The threshold value 86 was used for green ratio. If pixel green ratio greater than 86, then that pixel was considered as green otherwise soil background. Only one threshold value (86) was used in this study. The performance of three colour indices on vegetation segmentation under three soil background and single plants i.e. soybean, sunflower, red root pigweed and velvetleaf was studied (Meyer & Neto, 2008). The three colour indices were excess green index (ExG), excess green minus excess red (ExG-ExR) and normalized difference index (NDI).

2.4.1.2 Shape feature

Shape feature has been most commonly used for weeds or crops detection or crop species detection. A list of shape features is provided in Table 2.5. Shape features have been employed successfully for plant species recognition tasks (Deng, 2009). Colour and shape analysis was proposed for weed detection in cereal fields (Perez et al., 2000). The green and red channels of colour images were used to build the image index (normalized difference index, NDI) to discriminate between vegetation and background. The shape feature was considered to distinguish between crops and weeds. The performance of the weed detection algorithms was assessed by comparing the results from visual surveying. The results showed that the correlation improved from 75 to 85 % when shape analysis was used.

2.4.1.3 Texture feature

Plant leaves are typically flat, with varying vein textures and leaf surface roughness. In texture-based weed or plant disease detection, the most commonly used techniques for feature extraction are given in Table 2.5. Texture information obtained from the main crop, weeds or disease plants plays a significant role in classification tasks (Dryden et al., 2003).

Table 2.5: Types of features

Category	Technique
Colour feature (Meng et al., 2015)	
Colour models	Red (R), Green (G), Blue (B) Hue (H), Saturation (S), Value (V) Luminance, Chrominance, Chroma (YUV)
Shape features (Wu et al., 2021)	
Shape parameters	Perimeter, compactness, area, diameter, minor axis length, rectangularity, major axis length, circularity, eccentricity, convexity and solidity
Region based descriptors	Two dimensional fourier descriptors (FD) and Hu moment invariants
Contour based descriptors	Spatial position descriptor, one dimensional FD, curvature scale descriptors
Texture features (Wu et al., 2021)	
Statistical method	Gray level co-occurrence matrix (GLCM): 10 statistics, Gray level gradient co-occurrence matrix (GGCM): 15 statistics
Structural method	Local binary pattern (LBP)
Model based method	Fractal dimension
Transform based method	Gabor based

Colour and texture features were used for weeds identification (Gebhardt & Kühbauch, 2007). The weed identification percentage was about 90 %. However, the problem was texture calculation algorithm involves complex calculations. Due to this complex calculation, the weed detection algorithm consumes much time and this method has the poor real-time capability. Grey level co-occurrence matrix (GLCM) was employed to extract features (Chang et al., 2012) and used to identify wild blueberry plants, bare spots and weeds. Forty-four textural features were extracted from hue, saturation, intensity, and NTSC luminance (L) channel. Choosing one algorithm over another depended on whether processing speed or accuracy was more important for the end-user application. The features extraction procedure suggested that the hue and saturation (HS) features influenced accuracy more than other colour space features. Grey level colour co-occurrence matrix (GLCM) was used for texture feature extraction from goldenrod within wild blueberry fields (Rehman et al., 2018). Goldenrod was a creeping herbaceous perennial weed present in 90 % of wild blueberry fields surveyed in Nova Scotia. He reported the overall accuracy (> 90 %) in both training and test set of goldenrod detection in wild blueberry fields using hue and saturation features.

Table 2.6: Advantages and disadvantages of texture, shape and colour based weed detection (Wu et al., 2021)

Features	Advantages	Disadvantages
Texture	Texture feature has high accuracy, strong adaptability, and robustness	Texture feature extraction using grey-level co-occurrence matrix (GLCM) takes a long time and requires high computational power. It may not meet the real-time processing requirements.
Shape	Independent of geometric translation, scaling, or rotation; robust to noise	Shapes are deformed by disease, insect eating, and man-made or mechanical damage and incomplete under overlap and occlusion
Colour	Insensitive to the adjustment of proportion, size, and position	Colour feature perform good results while segmenting background from main crop and weed. But colour feature not helps in segmentation main crop from weed. Because crops and weeds have similar colour and plant seasonality will change colour.

Grey level colour co-occurrence matrix-based (GLCM) texture analysis was used for strawberry powdery mildew disease detection under natural lighting conditions and artificial cloud lighting conditions (Mahmud et al., 2019). The colour image was converted into HSI (Hue, Saturation and Intensity) image and then ten features were extracted from the HSI colour channel. The extracted features were Contrast, Homogeneity, Entropy, Dissimilarity, Angular 2nd Moment, Inverse Difference Moment, Average, Sum of Squares, Product Moment and Correlation. The offset and orientation angles were 1 and 0°, respectively. Colour co-occurrence matrix-based texture analysis was used for feature extraction from strawberry powdery mildew disease images (Mahmud et al., 2020). Also used artificial neural network (ANN) technique to process images and classify them as disease and non-disease images. It was reported that a slight deviation in the developed image segmentation algorithm was observed. That may be due to high wind speeds (>8 km/h), leaf overlapping, leaf angle and the presence of spider mite disease

during field testing. The advantages and disadvantages of colour, shape and texture features are given in Table 2.6.

2.4.1.4 Spectral feature

Along with colour, shape and texture features, spectral feature also play a significant role in plants or weed classification problems. When spectral reflectance of weed class was significantly different from main crop spectral feature the same can be employed for distinguishing weeds and main crop (Jinglei et al., 2017). Compared to shape and texture features, the spectral feature was robust to partial occlusion of leaves (Tian & Slaughter, 1998).

2.4.2 Effect of light

The colour in a digital image depends on a number of factors: spectral characteristics of the illumination source, spectral reflectance of the objects, position of the illumination source, and the relative position of the camera with respect to the objects (Matas et al., 1995). Visible spectral colour indices require pre-defined threshold value for foreground and background pixels classification. Adverse light condition affects the imaging sensor performance. Consequently, the pre-defined threshold value leads to under segmentation or over segmentation. To overcome the problem associated with pre-defined threshold value, dynamic threshold value technique was introduced. Moreover, several colour models have been employed instead of visible spectral colour indices to cope up with variable illumination. Moreover, artificial light source and light blocking screen have been employed to cope up with variable illumination.

2.4.2.1 Dynamic threshold techniques

Otsu method was one of the most commonly used image segmentation methods for separating the objects from background (Yang et al., 2015). It travels from the lowest gray level of an image to the highest to find the optimal threshold. Each time it uses the current gray level as the threshold and partition the whole image into two groups and then calculates the between group variance. When the travel ends, the right gray level which makes the maximal between-group variance was the optimal threshold. After the segmentation, the white pixels represented the green plants.

The threshold value to excess green index (ExG) and normalized difference index (NDI) was set by Otsu method, whereas, the threshold value of excess green minus excess red (ExG-ExR) was fixed as zero. The visible spectral colour indices (ExG, ExR, NDVI) proved their

ability to segment plants and they do not present high sensitivity to soil types or weather condition. Global thresholding method called Otsu and adaptive threshold algorithm were employed (Milioto et al., 2018).

The automatic Otsu thresholding method was applied for binarizing ExG and the normalized difference index (NDI) (Meyer & Neto, 2008). Instead of automatic thresholding such as Otsu, the statistical mean value of the transformed image obtained with the vegetation indices was used for image thresholding (Guizarro et al., 2011). They justify its choice because Otsu's method gives a threshold value higher than the mean and produces over-segmentation.

2.4.2.2 Colour transformation

The RGB colour sensor output has been transferred to HSV, LAB and YCrCb colour spaces to cope with problem of variable light condition at field level. The performance HSV colour model was tested on images captured under different environmental conditions (Yang et al., 2015). The image dataset consists of maize seedlings, dark green leaf, tender green leaf, red soil, yellow soil, black soil, corn straw and wheat straw. The performance of HSV colour model was compared with the visible spectral colour indices such as the excess green index, the excess green minus excess red index, the vegetative index, the colour index of vegetation extraction and the combined index. It was found that hue values of green maize leaves ranged from 50 to 150. The hue value of corn straw was far greater than the 150. The hue values of plastic film, yellow soil, red soil, black soil and straw ash were found below 50. Therefore, it was easy to separate maize seedlings from different colour soil and residue background. HSV colour model worked better than visible spectral colour indices under different soil background and crop residues.

Generally, the colour spaces applied in product classification are the standard RGB (sRGB; red, green, blue) and L*a*b* (CIELAB). The standard RGB image can be obtained using computer vision systems. Outputs signals are generated by the camera sensors (e.g. CCD or CMOS), but the rendering was device-dependent, since the range of colours varies according to the display device specifications (Cubero et al., 2011; Mendoza et al., 2006; Menesatti et al., 2012). In order to overcome this problem, sRGB values are often transformed to other colour spaces such L*a*b*. Moreover, even the result of such transformation was device-dependent (Ford & Roberts, 1998).

Table 2.7: List colour models (Mahmud et al., 2019; Yang et al., 2015)

Green ratio	$\frac{(G \times 255)}{R + G + B}$
Luminance (L_m)	$0.1140 \times B + 0.5870 \times G + 0.2989 \times R$
Θ_h	$\cos^{-1} \left\{ \frac{\frac{1}{2}[(R - G) + (R - B)]}{[(R - G)^2 + (R - G)(G - B)]^{(1/2)}} \right\}$
H	$\begin{cases} \frac{\Theta_h}{360} \times 255 & \text{if } B \leq G \\ \frac{360 - \Theta_h}{360} \times 255 & \text{if } B > G \end{cases}$
S	$255 \times \left\{ 1 - \frac{3}{(R+G+B)} (\min(R, \min(G, B))) \right\}$
I	$\frac{R + G + B}{3}$

A modified excess green index (G-R>T & G-B>T) was used locating crop rows (Nan et al., 2015). Moreover, Otsu dynamic threshold technique was employed to cope with variation in outside illumination intensity. Outdoor images require a camera with a wide dynamic range due to the potential for brightness variations (Nayar & Mitsunaga, 2000). Illumination invariant image transformation was used instead of excess green index (ExG) for weed and soil pixels classification (Suh et al., 2014). The illumination-invariant transformation value was found to be above 0.42 for green pixels, while soil pixels found to be below 0.40.

A machine vision system was presented based on the hypothesis that nonconventional elements including shadow, pixel saturation, noise, light variations and important camera characteristics should not affect segmentation (Hernández et al., 2016). Thus, their proposed system could choose a colour space based on field lighting. There were eight colour models used in this study. They were RGB, HSL, YCbCr, YUV, L*a*b*, L*u*v*, TSL and XYZ.

2.4.2.3 Artificial light and light blocking screen

Different illumination factors should be deeply considered prior to any colorimetric measurement, when not properly evaluated it could yield important biases (Stevens et al., 2007). A possible way to reduce or avoid illumination biases is then represented by taking pictures

under standardized light conditions. To reduce effects of natural light source over acquired images, the system often equipped with some assistant devices for acquiring field images. A plastic inspection area was used to acquire field images (Tangwongkit et al., 2006; Zhang et al., 2003). Variable illumination issue was resolved by employing artificial lighting at night (Font et al., 2015).

A digital colour camera for thistle detection in a sugar beet field under shade and outdoor field conditions was employed (Kazmi et al., 2015). To restrict the intensity of sunlight entering the camera's field of view, an adjustable wooden shade was installed and this condition was considered as shade condition. Under the shade, the illumination intensity varied from 8 to 10 klx, whereas, under direct sunlight, the illumination intensity was 105 klx. The results showed that the illumination (sun light) was important factor affecting the classification efficiency of the proposed vegetation segmentation algorithms. It was also reported that best results were obtained for images of young sugar beet under a shade.

An attempt was made by developing artificial cloud lighting condition for improving the machine vision based disease detection accuracy (Mahmud et al., 2019). Testing platform was covered by black cloth and LED light source was provided. The illumination intensity inside testing platform was measured by lux meter (LX101BS, V&A Instrument CO., LTD., Shanghai, China). The illumination inside artificial cloud lighting conditions (ACC) chamber ranged between 800 and 900 lx during experiments. At artificial cloud lighting conditions (ACC), the performance measures, i.e., recall, precision and F-measures were 95.26 %, 95.45 % and 95.37 %. Compared to ACC, the detection percentage of strawberry powdery mildew disease detection was decreased under natural lighting conditions. The performance measures, i.e., recall, precision and F-measures, were reported as 81.54 %, 72 % and 75.95 % at natural lighting condition.

The mango fruit images were taken from a controlled image system composed of a digital camera and the lighting system. The distance between mango and camera was fixed at 200 mm. Four lamps with two fluorescent tubes each were used to give brightness to the image. The angle between the axis of the lens and the sources of illumination was approximately 45 degree. Polarising filters were placed in front of the lamps and camera lenses in order to reduce the impact of reflections (Limsripraphan et al., 2019). A portable image acquisition system was

developed for field level powdery mildew disease evaluation (Gong et al., 2022). The portable phenotype platform consists of a dark box and its dimensions were 250 mm × 490 mm × 320 mm. It consists of a tablet PC, a top diffuser, a top LED strip and a bottom diffuser. In addition, the top outer side of the dark box has a handle to make it easy for researchers to carry.

Different light source options are readily available in the market. A LED-powered illumination system specifically for use with machine vision systems that require consistent light colour and intensity (Dowling et al., 2003). An efficient LED illumination system with reflectors for area-based scanning equipment such as video cameras was developed (Hecht, 2005). It was observed that typical incandescent or HID light sources were not ideal because they were inefficient and consume more energy and generate large amounts of heat as compared to LED illumination systems.

2.4.2.4 Calibration of acquired image and minimization of variation in image acquisition

Accurate characterization (profiling) of a capture system is essential to have the system accurately reproduce the colours in a scene. ISO 17321 describe two methods to achieve this calibration. One based on standard reflective targets (chart-based method) and the other on making accurate measurements of the cameras responsivity functions and the spectral power distribution of the deployed illuminant. The more prominent of the two was the chart-based method for the reason that it involves a simple capture of an inexpensive, standard colour pattern (e.g. Macbeth/X-Rite colour checker).

Colorimetric calibration of three cameras was performed with help of an X-Rite colour checker chart (X-Rite) and custom colour patches (Varghese et al., 2014). The standard RGB values of colour patches information was measured using spectrometer to provide ground truth data. Colour error or colour difference was used to report error in colorimetric calibration.

Different types of colour charts were used for colour calibration *i.e.*, from colour checker 7-patches to 140-patches by different researchers. However, the results suggest that use of colour checker with 24-patches was sufficient to resume the entire colour space, while 7-patches were insufficient and 140-patches oversamples, without giving a decisive efficiency increase. Moreover, the error (Δ RGB) resulted significantly greater when the distance of a colour from the closer reference ones was greater. This result suggests the use of new colour checkers with 24-30 patches better distributed in the colour space. A possible way to reduce or avoid illumination biases was then represented by taking pictures under standardized light conditions. Nevertheless,

this was a difficult condition to satisfy, not only in the field but even in the laboratory (Menesatti et al., 2012).

Colour calibration require standard colour chart and needs dedicated software. Most of available calibration software read RAW image format. But, several low cost webcam do not provide RAW image format. Hence, it is difficult to calibrate camera that do not provide RAW image files. Red, green and blue standard primary colour plates were used instead of actual leaf, stem and soil samples for threshold values calibration of visible spectral colour indices and to study the effects of illumination on colour indices (El-Faki et al., 2000). Similar attempt made by Suh et al., (2014) that instead of camera calibration, threshold values of illumination invariant image transformation function and excess green index methods with help of standard colour chart were calibrated. The weed and soil pixels classification accuracy of illumination invariant image transformation was compared with excess green index method (ExG) under natural illumination condition (Suh et al., 2014). Instead of actual plant and soil images, the X-Rite colour chart checker (Grand Rapids, MI, USA) images were captured with a colour camera resolution of 1280×720 pixels on different days under different outdoor illumination conditions. Among 24 colour patches of X-Rite colour chart checker, Foliage, Yellow Green and Green colour patches were considered as plant pixels, and Dark Skin, Moderate Red and Magenta were considered as soil pixels. The six colour patches information was analyzed with illumination-invariant transformation and excess green index (ExG). The experimental results demonstrated that illumination-invariant transformation has shown robust plant segmentation performance under outdoor natural illumination conditions as compared with ExG method.

2.4.3 Effect of camera parameters

The effect of camera type and working height on weed detection accuracy in wild berry fields was studied by (Hennessy et al., 2022). YOLOv3-Tiny deep learning model was used to identify weeds, sheep sorrel and hair fescue. Three cameras Canon T6 DSLR camera (5184×3456 pixels), Logitech c920 webcam (1920×1080 pixels) and LG G6 smartphone (4160×3120 pixels) were used. The three working distances were 570, 980 and 1290 mm, respectively. As a performance metrics precision, recall and F1-score were used to compare significance of each combination of camera type and working height on target detection. The highest F1-score observed to detect at least one hair fescue tuft by LG G6 and Canon T6 was 0.97 at working height of 980 mm. The F1-score observed as 0.94 and 0.93 to detect at least one

sheep sorrel at working height of 570 mm by LG G6 and Canon T6 DSLR camera. Sheep sorrel was undetectable in images from the Logitech c920 webcam. It was reported that the detection accuracy was affected by not only camera type and working height, but also size of training set.

Two digital colour cameras were employed for vegetation segmentation using visible spectral colour indices (Meyer & Neto, 2008). First camera was DC120 (Kodak Digital Science Rochester, NY). The DC120 digital colour camera of image resolution 1280×960 pixels was mounted at a height of 1000 mm. The spatial resolution of camera with ground was 0.5 mm/pixel. The second camera was Olympus E-10 (Olympus Imaging America Inc.). The resolution of digital colour camera was 2240×1680 pixels. The spatial resolution of camera with ground was 0.25 mm/pixel. Sony digital colour camera was employed to acquire maize seedling images under field conditions (Yang et al., 2015). The acquired digital images were stored in 24 bit. The resolution of digital colour camera was 800×600 pixels.

Two digital colour cameras (IDS Imaging Development System INC., Woburn, MA, USA) were used to acquire two crop rows images (Mahmud et al., 2019). The image resolution maintained during image acquisition was 640×256 pixels. The acquired digital images were stored in 24 bit format. The wide angle field of view of lens with 3.5 mm focal length was set up to a fixed aperture (f/4.0) and infinity focus. Effect of different camera heights on powdery mildew disease detection was studied by Mahmud et al., (2019). The working depths chosen for the study were 100, 200, 300 and 400 mm. Camera mount holder was used for varying the camera height. The results reported that disease detection accuracy of digital colour camera was decreased with increasing of working depth. The accuracy, precision and F-measure found highest at 300 mm camera height. The detection accuracy was found lowest with increasing working depth greater than 300 mm. It was also reported that working depths 100 and 200 mm reported less detection accuracy when compared with the 300 mm working depth. This study reported that the image quality significantly affected by working depth.

A dataset containing six food crops and eight weed species was used by Sudars et al., (2020). Three RGB digital colour cameras were employed for capturing crops and weeds images at the different growth stages. The image resolutions used for capturing food crops and weed species images were 640×360, 720×1280, 480×384, 640×480, 1000×750 pixels. The effect spatial resolution on main crop and weed detection was studied (Mathanker et al., 2007). The

field of view of camera was $1600 \times 1200 \text{ mm}^2$. Three features colour, texture and shape were used for classifying vegetation into main crop (wheat) and weeds. After 21 days of wheat seeding, the field images contain wheat, weed (broad leaf weed) and soil background were captured using digital colour camera at three image resolutions (128×128 , 64×128 and 64×64 pixels). When shape considered for image segmentation the classification accuracy was reported as 73 % at image resolution of 128×128 pixels but the classification accuracy decreased drastically by decreasing the image resolution from 128×128 to 64×64 pixels. When texture and green colour features considered for object detection, the classification accuracy was reported as 86.7 % at image resolution of 128×128 pixels. Even at image resolution of 64×64 pixels the classification accuracy was reported as 80 %. The performance accuracy was not affected by the image resolution when texture and green colour features were considered.

2.4.4 Effect of image acquisition speed

Effect of image acquisition speed on detection accuracy was studied (Mahmud et al., 2019). Five forward speeds selected for the study were 1.0, 1.5, 2.0, 2.5 and 3.0 km/h. The performance metrics recall, precision and F-measures found highest at forward speed with 1.0 km/h. There was a slight deviation in the performance measures were observed between 1.0 and 1.5 km/h. The images were blurred by increasing forward speed of system more than 1.5 km/h. The frame rate of chosen digital colour camera was 25.8 fps. This study recommended that image acquisition speed 1.5 km/h was suggested for powdery mildew disease detection in strawberry field. It was recommended that the system speed can be increased by increasing frame rate (>25.8 fps).

Performance of the MVRG fertilizer spreader was evaluated under two different lighting conditions and three ground speeds (Chattha et al., 2015). The ground speeds of 1.6 and 3.2 km/h were found to be suitable for real-time detection and fertilizer application under sunny and cloudy conditions. Poor performance of the MVRG fertilizer spreader was observed at a ground speed of 4.8 km/h under both lighting conditions. The combination of higher ground speed (4.8 km/h) and undulating topography of the wild blueberry field induced movement in the front camera boom, which might have resulted in the detection failure of bare spots by the GLCM algorithm due to blurred images. The MVRG fertilizer spreader was successfully operated for spot application at a ground speed of 3.2 km/h for actual fertilization in wild blueberry fields.

2.4.5 Preparation of ground truth image

The performance metrics have been used for quantifying image segmentation techniques performance. Before going to the computation of true positive (TP), true negative (TN), false negative (FN) and false positive (FP) metrics, the actual pixels labels of image are to be identified. It means in a given image what are pixels belongs to green class and soil background class. If the actual pixels labels in the input image are known, then one can compare it with the output image that is segmented by the image segmentation techniques.

Reference image dataset was generated manually using Adobe Photoshop 5.0 LE for each reference image (Meyer & Neto, 2008). It was reported that manual painting become more difficult with too many broadleaf images/weeds and complex soil background. Under such conditions the reference image was cropped into small rectangles using MATLAB *imcrop* function and then ground truth images were created. It was reported that creating ground truth image for segmentation accuracy classification more tedious operation but it was necessary to measure and indicate the accuracy of vegetative indices. In addition, based on the empirical knowledge related to powdery mildew, the powdery mildew spot areas in each image were manually marked: the powdery mildew areas were marked as white and the non-powdery mildew areas were marked as black (Gong et al., 2022). Different size of images and working depth were used to see effect of image resolution on classification accuracy. Ground truth image creation was very difficult for image size of 32×32 pixels (Rehman et al., 2018). Different working depths were used to see effect of working depth on classification accuracy (Mahmud et al., 2019).

It was observed section 2.4 that several ground based sensing techniques were available for weed detection. It can be pointed out that the aforementioned optoelectronic sensors were well evaluated in former times, but they were not able to detect small plants in early leaf stages (smaller than 3% of the measuring spot). Due to limitation of opto-electric sensors and ultrasonic sensors in weed detection, RGB colour camera was employed for weed detection over other methods. The advantage of imaging cameras especially RGB colour camera over remaining sensor was available at low cost. Moreover, there has been wide availability of imaging processing libraries for processing RGB images. With advancement of convolutional neural networks the more emphasis has been given to RGB image based weed or disease detection and classification. Colour, shape and texture features have been commonly employed for weed

identification. The shape feature may be useful in enhancing the performance and promoting robustness against the field-deployable system's environmental factors. However, the challenges of occlusion still exist. Another drawback of the shape-based weed identification approach was the overlapping of leaves. Texture-based and leaf area estimation methods involve complex mathematics and they require high computation time. The shape feature detection algorithm requires an occlusion algorithm and it was computationally intensive. In case of site specific weedicide application for inter row crops, everything that present between crops rows were considered as weed. Colour feature has been most commonly used for plant segmentation (weed/crop). Nevertheless, colour feature was not scale invariant and not sensitive like shape and texture features.

It was observed of literature that the visible spectral colour indices and colour models have been employed plant segmentation. These indices shows good segmentation results under controlled condition but fails under open field condition (Hamuda et al., 2016). A threshold value of visible spectral colour indices has to be defined for weed segmentation (Hassanein et al., 2019; Meyer & Neto, 2008; Yang et al., 2015). Due to variation in illumination intensity at field level a fixed threshold value of visible spectral colour indices yields over segmentation or under segmentation problem (Hamuda et al., 2016). In order to develop successful machine vision based weed detection and weedicide application system, a research on optimization of field factors and camera parameters was highly essential for accurate image segmentation. To cope with variable illumination dynamic thresholding techniques were employed for weed and soil pixels classification. It was also suggested to use artificial light source and light blocking screen to cope with outside variable illumination. It was observed from previous studies that manually selecting each pixel and labelling them as green or soil pixel was tedious and time consuming operation. Moreover, manually painting each pixel was prone to error.

2.5 Plant segmentation in agriculture

The computer vision based monitoring was non-destructive and continuous. Many precision agriculture applications need reliable computer vision outputs to keep their promise of efficient use of agrochemicals. Plant segmentation was a computer vision task, which aims to discriminate between soil and plants/weeds in colour images and was often used to identify plant canopies in field crops. In contrast, plant classification aims to distinguish between crops and

weeds to perform precise weed control. Plant segmentation refers to separate the pixels in the input image either it belongs to vegetation (weed) or soil background. In the first stage a plant region of interest was identified with colour feature, in second stage advanced image processing operations such as texture, shape and convolutional neural networks may be applied for identification of weed species or plant disease for strategic weed and pest control. An autonomous robot was developed to classify input image pixels into crop, weed and soil pixels (Haug & Ostermann, 2015). The plant segmentation algorithm consists of three stages. In the first stage plant segmentation was performed using deep learning convolutional neural networks. To improve plant segmentation results as input to network along with RGB image, a set of visible spectral colour indices like excess green index (ExG), excess red index (ExR), colour index of vegetation and extraction (CIVE) and normalized difference index (NDI). In the second stage number of blobs (plant pixels) was extracted. In the third stage the extracted blobs were passed through CNN to classify plant and weed pixels (Haug & Ostermann, 2015).

Plant segmentation applied in several applications such as plant growing phase determination (Kataoka et al., 2003; Yang et al., 2015), guide the robot for weed killing (Yang et al., 2015), even estimate the nutrition deficiency of crops (Montalvo et al., 2013) and estimation of leaf area of segmented image (Kirk et al., 2009; Meyer & Neto, 2008; Rasmussen et al., 2007). More recent applications use deep learning methods, where plant segmentation can be used to increase the dataset size or to highlight regions of interest (Kamilaris & Prenafeta-Boldú, 2018). The result of plant segmentation can be used for subsequent analysis of the plant properties (Meyer et al., 2004; Neto, 2004; Wang et al., 2019), such as camera-based crop row detection or plant classification for weed detection. Crop row detection was used for precise usage of a variable rate spot spraying system (Ji & Qi, 2011), for machine guidance by vision control (Vidović et al., 2016) and for navigation of field robots (Winterhalter et al., 2018). With help of digital colour camera and image processing the rice crop growth stage estimation and nutrient status of nitrogen were performed (Lee & Lee, 2013). No matter what we want to do by analyzing the crop images, the key job was to identify the plants, i.e. the green objects in the captured images.

2.6 Automatic and robotic weeding methods

Researchers have made several attempts to develop automatic and robotics site-specific weedicide applicators. A small tractor-mounted sprayer with a track width of 1100 mm was used to apply weedicide between sugarcane crop rows (Tangwongkit et al., 2006). It was reported that the developed weedicide applicator reduced the application rate by 20.6 % by applying 146 l/ha of weedicide with an average application rate of 2.08 l/min. At the same time, the uniform application method required a weedicide amount of 709 l/ha with an average application rate of 2.62 l/min. It was also reported that the operating speed of the variable rate application system was lower than the constant application system. However, the variable rate application system cuts down on the use of weedicide and saves the environment from the damage that comes from using too many chemicals. A contact-type microcontroller-based manually operated three-row weedicide applicator for inter-row was developed (Tewari et al., 2014). The colour based traditional image processing approach was followed for weed identification. In real-time image processing, the system automatically calculates the amount of weedicide to be applied to the weeds. The experimental results revealed that the application efficiency of the weedicide applicator was 90% and the reduction in weedicide amount was about 40 %. It was also reported that the contact roller-type weedicide applicator eliminated both weedicide drift and over application.

Opto-electronic sensors like Detect-Spray, Green-Seeker, Weed-IT and Weed-Seeker sensors have been developed and used for inter-row patch spraying to detect and extract herbaceous plants (Schmittmann & Schulze, 2017). A two-row tractor-operated laser sensor based weedicide applicator was developed (Agrawal et al., 2012). It was operated at different operating speeds between 1.28–3.3 km/h.

The performance of a robotic weed control system in outdoor and indoor conditions was compared for tomato cotyledons (Lee et al., 1999). The system could only properly spray 47.6 % of weeds with 24.2 % over-sprayed tomato plants in a real-time commercial application. Using a Raspberry Pi microcontroller, cameras, tiny light sources, and powered motors, a weed-detection robotic prototype was developed (Sujaritha et al., 2017). Using rotation and scale invariant texture features and a fuzzy real-time classifier, the prototype of the weed-detection robot successfully distinguished sugarcane crops from nine different weed species (92.9 %). A self-driving robot platform was developed (Utstumo et al., 2018). The proposed robot was

created to make drop on demand weedicide applications. Weed detection was accomplished through the use of computer vision and deep learning. Individual weedicide droplets were applied to each weed in the row without damaging the crop. The robot effectively controlled all weeds in the carrot field test while using ten times less weedicide.

A PMW drive motor was used to control the spray rate by changing the duty cycle of the motor based on the greenness ratio (Tangwongkit et al., 2008). The developed software using the Borland C++ builder program acquires the field images using a webcam and processes and activates the nozzle if the greenness level exceeds the threshold value. A direct injection system was developed to control the amount of pesticide applied (Smith & Thomson, 2003). Pulse width modulation technology was used in variable-rate field sprayers and proved to be an effective weed control spraying method. The closing and opening of valves were controlled by the electromechanical system that receives the instruction from the microcontroller (Ishak et al., 2011). The nozzle was closed when the percentage of weeds detected was less than 2 %. It was half open at 3 to 50 % and fully open at more than 51 %. It was reported that the use of PWM give the better result for monitoring the opening of the nozzles. The PWM nozzle was very precise and very expensive for the farmers or for agricultural operations. Normally open solenoid valve was employed for delivering weedicide amount at weed infested locations (Agrawal et al., 2012). To avoid spraying of weedicide on useful plants guards were provided on either side of the nozzle.

Table 2.8: Weeding robots developed in recent years (Zhang et al., 2022)

Crop	Country	Sensor	Method	Year
Sugar beet	Germany	RGB, NIR camera, and ultrasonic sensor	Mechanical	2015
Bean, cotton, rapeseeds	Switzerland	RGB camera	Chemical	2020
Lettuce, cauliflower and broccoli	Australia	Hyper spectral and thermal camera	Chemical	2015
Thistle, feather top Rhodes grass and wild oats	Australia	RGB camera	Mechanical	2015
Maize, soybean	America	RGB camera	-----Nil---	2018
Paddy field	Japan	---Nil---	Mechanical	2018
Paddy field	Japan	---Nil---	Mechanical	2018

A real-time weed-detection system was developed for wheat fields (Wang et al., 2007). The machine consisted of a weed sensor, Ag GPS, radar sensor, PWM, microcontroller and electrically controlled nozzles. A precision weedicide applicator was developed (Muangkasem et al., 2010). The operation of the motor was controlled by a microcontroller based on pulse width modulation signals generated by MSP 430.

Most of robots mentioned earlier are at developing stage. Research is under progress to deploy them at field level. Developing autonomous robots require time and efforts. In terms of cost also is high. Robotics platform need accurate guidance system. However, conventional neural network based deep learning based models employed for crop detection and row identification, they need high configured hardware and computationally intensive. Moreover field undulations and variable nature of environmental parameters are limiting factors for their deployment at field level.

2.7 Performance evaluation of site specific weedicide applicator

The simplest way of site-specific weedicide application was turning-off the sprayer wherever no weed were detected. The performance evaluation of weedicide applicator was reported in terms of field capacity, field efficiency, weeding efficiency, plant damage and chemical saving.

The application flow rate accuracy of developed system was about 91.7 % (Tangwongkit et al., 2006). The distance between webcam and spraying nozzle was 770 mm at forward speed of 2.7 km/h. One second programming delay was provided for nozzle activation. By shifting towards variable rate weedicide application the weedicide saving amount was reported as 20.6 %. It was reported that this weedicide reduction could be stochastic and depending upon the amount of weed density in the field, further tests would be necessary to correlate the quantity reduction with varying weed density levels. Tangwongkit et al., (2008) developed a tractor mounted variable rate weedicide applicator. The applicator was tested in constant application mode and the variable rate mode. The field capacity and field efficiency of variable rate weedicide applicator was lowest as compared with the constant rate weedicide application system. This was due to the more processing time of each frame taken by the image processing software. To avoid spraying of weedicide on useful plants guards have been provided on either side of the nozzle.

Tewari et al., (2014) reported that variable rate of spraying contributes 50 % weedicide amount saving over conventional spraying method. Also report that drift and excess weedicide application was eliminated with the incorporation of contact roller type weedicide applicator technique. Chandel et al., (2018) developed contact type weed eradicator. The average weeding efficiency was reported as 90.30 %. The plant damage was reported as 5.74 % and 7.91 % for groundnut and maize plantation. The weedicide saving amount was reported as 79.50 %. Field performance of the developed system equipped with the quadratic DM-HSISD classifier indicated no significant difference between variable rate (VR) and uniform application (UA) in terms of mean percentage area coverage (PAC) for the targeted goldenrod spots in both fields (Rehman et al., 2019). However, a significant difference was observed between mean PAC of VR and UA applications for the non-targeted wild blueberry spots. The potential and actual chemical savings were in ranged between 46.71 % and 74.83 % and 30.12 % and 60.58 % depending on the weed and sprayed area, respectively. These results demonstrated that the developed weed detection system has potential for targeted application of agrochemicals to control goldenrod in wild blueberry fields.

2.8 Review summary

Advances in high resolution vision systems, image processing techniques and embedded computing devices were finding direct application in smart agriculture and have generated scope and opportunities for precise application of inputs such as pesticides, fertilizers, seeds, etc. through VR application technology. Factors such as small land holdings, moderate labour charges, negligible on farm computer use and costly imported high tech equipment advocate less adoption and lag in site specific weed management technology the farmers in developing countries. Application of weedicide on site-specific manner leads to saving of costly chemical apart from achieving desired goal of weed control. The simplest way of site-specific weedicide application was turning-off the sprayer, wherever no weeds were detected. However, several attempts made by various researchers developing site specific weedicide applicator at various parts of world, there was a need of location specific research.

It was observed from previous studies that there were several factors need to be considered to develop a successful field deployable site specific weedicide applicator. Variable illumination, camera parameters, feature selection and plant segmentation methods were to be considered. Visible spectral colour indices (ExG, ExR, ExGR, CIVE, COM, NDI) and colour

models (HSV, CIELAB, YC_rC_b) have been employed for weed and soil pixels classification. Moreover, selection of optimal threshold value for weed and soil pixels classification was also challenging task. It was observed from literature that several dynamic threshold techniques also employed for weed and soil pixels classification. Forward speed of prime mover also one significant factor that to be considered while deploying site specific weedicide applicator at field level. It was observed from previous literature that processing time of image segmentation algorithm also plays vital role maintaining distance between weed detection sensor and spraying nozzle and forward speed of prime mover.

There is need of image processing software and high computing power for colour transformation, colour feature extraction and performing real time site specific weedicide application. Matlab software was used for developing colour based image segmentation algorithm (Tewari et al., 2014). Sujaritha et al., (2017) developed a weed detection robot for weeds detection in sugarcane field using Raspberry Pi, Raspbian operating system (OS) and Python software based coding. Power requirement of hardware components is also significant factor because during field operations either power to be taken from prime mover or additional batteries to be used. Hence low power consumption, compact and robust hardware components are a necessary for field applications.

Keeping in view the above factors, the present study was undertaken in three distinct phases. The first phase was related to optimization of factors affecting colour based weed identification. A semi supervised machine learning approach was investigated to create ground truth image. The second phase was related to selection of hardware components like microcontroller, spraying unit and development of laboratory setup. Develop a decision making algorithm and deploy on Raspberry Pi 4 model B as edge device. Python, an open-source programming language was used for building image segmentation algorithm. The second phase also includes optimization of operational parameters. The third phase was related to a tractor mounted a real time camera based weedicide applicator development and field evaluation.

Chapter 3

Materials and Methods

Chapter-3

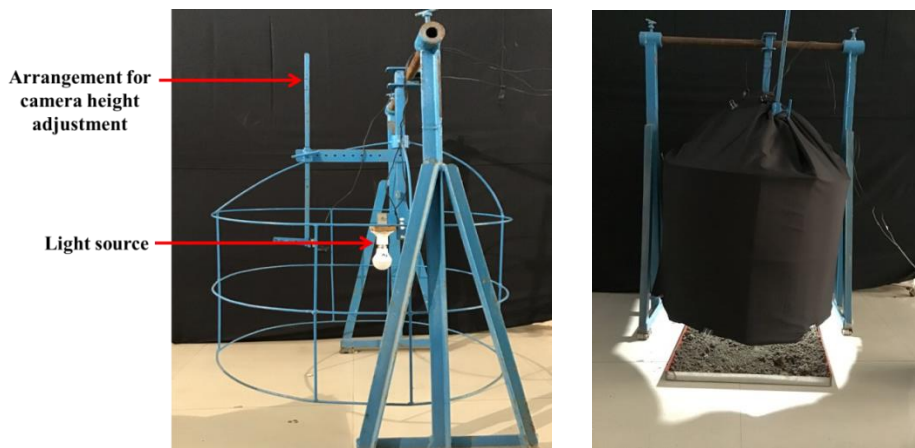
Materials and Methods

This chapter deals with materials used and methodology followed to conduct the research work. The research work was chronologically carried out as per objectives. This research work makes an attempt to develop a real time camera based weedicide applicator, this attempt plants present in between the crop rows were considered as weeds. In this work a webcam was employed as a weed detection sensor. The research work has been conducted with three objectives. In the first objective factors affecting weed detection in a camera-based image acquisition system such as illumination intensity, image resolution, working height, visible spectral colour indices and colour models on colour based weed and soil pixels classification were studied. In the second objective algorithms for weed and soil pixel classification and weedicide application was developed. In addition, the processing time of developed software and the response time of solenoid valve were measured. Pump, nozzle, solenoid valve, hose and hose connections were selected. The distance between weed detection sensor and spraying nozzle, frame grab interval and quantity of weedicide applied were optimized. A prototype of camera based weed detection system and real time weedicide applicator was developed and evaluated in field as third objective. The various methods employed and materials used are presented in below under following subheadings:

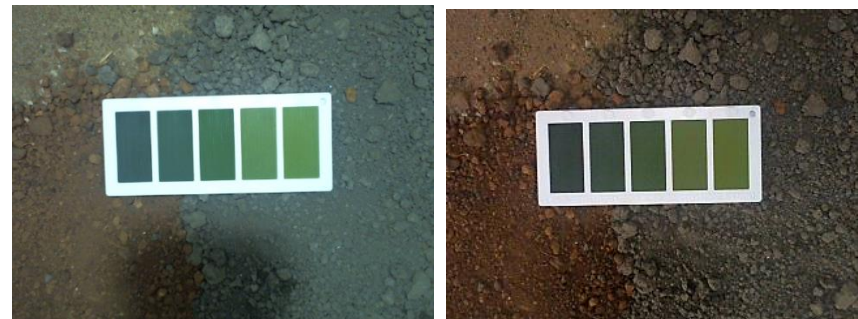
- 3.1 Development of light source testing platform
- 3.2 Effect of illumination intensity and image resolution on colour difference (ΔE_{ab})
- 3.3 Effect of illumination intensity and image resolution on R, G, B, ExG and ExGR intensity values of green and soil pixels
- 3.4 Microcontroller unit
- 3.5 Effect of working height, image resolution and plant segmentation methods on weed and soil pixels classification accuracy
- 3.6 Effect of soil type on weed and soil pixels classification accuracy
- 3.7 Spraying unit
- 3.8 Optimization of constructional and operational parameters
- 3.9 Development of a real time camera based weedicide applicator
- 3.10 Field evaluation of developed a real time camera based weedicide applicator

3.1 Development of light source testing platform

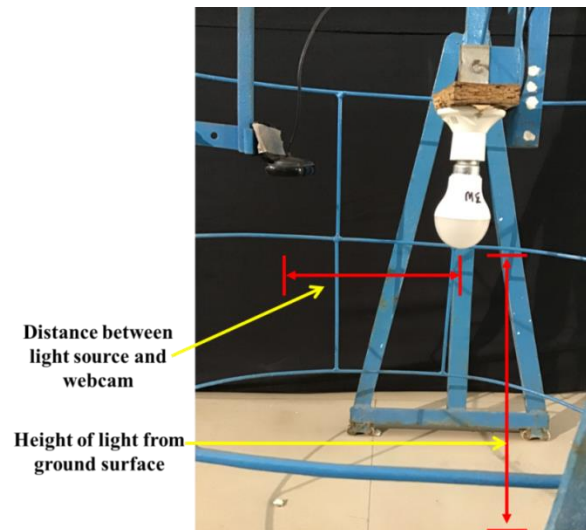
Colour-based weed and soil pixel classification was severely affected by outdoor light especially sun light and clouds. The illumination intensity varies throughout the day and this factor profoundly affects colour and texture based weed identification process (Mahmud et al., 2019). The image quality of digital colour camera was greatly affected by external illumination since the camera works on reflected light. Under field condition there were several factors affecting the performance of imaging sensors. They were variable illumination (Chandler, 2003), camera parameters (Mahmud et al., 2019), image acquisition speed (Esau et al., 2017) and image inappropriate feature selection (Chang et al., 2012; Rehman et al., 2018). To overcome problem of outside light effect on weed detection sensor performance several studies suggested use of artificial light source and protective cloth (Kazmi et al., 2015; Mahmud et al., 2019; Sujaritha et al., 2017; Tangwongkit et al., 2008; Tewari et al., 2014). Concerning the previous studies to tackle or minimize illumination intensity effect on colour based weed and soil pixels classification; the present study developed a light source testing platform. The testing platform consisted of a weed detection sensor, DC LED bulb (Colour temperature: 6000 K), 12 V DC battery and a protective cloth (black). The testing platform was covered with black cloth to eliminate outside light entering the sensor field of view, as shown in Plate 3.1 (a). The artificial light source can illuminate the field of view of the weed detection sensor. The artificial light source should able to provide sufficient illumination at camera field of view. If the light source was too close to the web camera, there was a problem of shadow (Plate 3.1 (b)). Otherwise, if light source was too far from weed detection sensor, there may be insufficient illumination at camera field of view. The bulb was placed in a position such that the shadow of the sensor should not fall inside the camera field of view. The bulb was fixed to testing platform vertically at the height of 600 mm from the ground surface. The distance between sensor and light source was kept 200 mm (Plate 3.1 (c)).



(a)



(b)



(c)

- (a) Light source testing platform, (b) Shadow problem at sensor field view,
 (c) Location of bulb

Plate 3.1: Development of light source testing platform

3.1.1 Weed detection sensor

A Logitech (C525) webcam was used as a weed detection sensor (Plate 3.2). It was a compact digital colour camera to broadcast video in real time. Similar to a digital colour camera, it captures light through a small lens at the front using a grid of microscopic light-detectors that built into an image-sensing microchip. Unlike a digital colour camera, a webcam has no built-in memory chip. The webcam transmits captured images immediately to a computer or microcontroller. The webcam consists of USB 2.0 port cable. The USB cable supplies power to the webcam from the computer/microcontroller and takes the digital information captured by the webcam to the computer. Logitech C525 webcam specification is given in Table 3.1.



Plate 3.2: Webcam (Logitech C525)

Table 3.1: Logitech C525 webcam specification

Image sensor	C525 webcam
Frame rate	30fps @ 640 x 480 pixels
Connector	1x USB 2.0
System Requirements	
Computer	512MB RAM or more 200MB hard drive space USB 1.1 port (2.0 recommended)
Operating System	Windows XP (SP2 or higher), Windows Vista or Windows 7 (32-bit or 64-bit)

3.2 Effect of illumination intensity and image resolution on colour difference (ΔE_{ab})

The aim of experiment was to test weed detection sensor performance at different illumination intensity and image resolution. The colour difference (ΔE_{ab}) commonly used to assess camera performance was taken as dependent parameter for this study. The colour difference of weed detection sensor was tested with help of standard test chart at four illumination intensities and four image resolutions. It was reported that very high or low illumination intensity affects RGB pixels values of colour image (Sojodishjani et al., 2010) and this leads to poor weed and soil pixel classification accuracy. Hence good quality images were

utmost important in computer-vision based system. It was necessary to maintain optimum illumination intensity of light source and image resolution of weed detection sensor for better results at image segmentation process. The plan of experiment to test colour difference (ΔE_{ab}) of weed detection sensor is given in Table 3.2.

Table 3.2: Plan of experiment to test colour difference (ΔE_{ab}) of weed detection sensor

Variables	Level	Description
Independent		
Illumination intensity	4	$L_1: 89 \pm 4.4 \text{ lx}; L_2: 188.9 \pm 6.4 \text{ lx};$ $L_3: 259.3 \pm 12.7 \text{ lx}; L_4: 359.3 \pm 7.5 \text{ lx}$
Image resolution	4	$S_1: 320 \times 240 \text{ pixels}; S_2: 640 \times 480 \text{ pixels};$ $S_3: 800 \times 600 \text{ pixels}; S_4: 1280 \times 720 \text{ pixels}$
Dependent		
Colour difference (ΔE_{ab})		
Total treatments	16	
Replications	3	
Total number of experiments	48	

3.2.1 Illumination intensity of light source

It was observed from previous studies that protective cloth and artificial light source protect weed detection sensor performance from outside extreme light illumination intensity. Hence, in present study light source testing platform as shown in plate 3.1(a) was developed. The main task was what illumination intensity should be maintained at field of view of weed detection sensor so that colour saturation would not happen. From previous studies, it was observed that researchers have used different illumination intensities based on application (Esau et al., 2017; Mahmud et al., 2019; Tewari et al., 2014). Hence, in the present study our goal was to test effect of different levels of illumination intensities on satisfactory performance of weed detection sensor.

There were wide varieties of light sources commercially available in the market for the purpose of illumination in the computer vision applications. Paying attention to illumination may result in enhanced images. Due to flexibility and long life span, LED was the first choice as machine-vision light source (Adelkhani et al., 2012). Two 12 V (3W, 5W) DC LED bulbs (Colour temperature: 6000 K) were used in the present study (Plate 3.3). The illumination intensity was measured using lux meter (LI-250). The technical details of light meter are shown

in Table 3.3. A photometric sensor was placed exactly below light source. The minimum illumination intensity was maintained as 89 ± 4.4 lx. The illumination intensity less than 89 ± 4.4 lx did not provide sufficient illumination for image processing applications. The difference between two consecutive illumination intensities readings was tried to maintain as 100 lx. The illumination intensity was adjusted during the experiment by a voltage regulator. Four range of illumination intensity levels were taken for the study. The illumination intensity was recorded and averaged. The illumination intensities that maintained during experiment were 89 ± 4.4 (L_1), 188.9 ± 6.4 (L_2), 259.3 ± 12.7 (L_3) and 359.3 ± 7.5 (L_4) lx. Plate 3.4 shows photometric sensor and LCD display. While measuring light illumination intensity the testing platform was covered with black cloth. All experiments were conducted while testing platform was covered with black cloth.

Table 3.3: Technical details of lux meter

Measurement unit	lx
Accuracy	± 0.4 % of reading [± 3 counts on the least significant digit displayed]
Range and Resolution	0-1999 lx (0.1 lx); 0-19999 (1 lx); 0-199 klx (0.001 lx)
Power requirement	9W



Plate 3.3: LED bulbs



Plate 3.4: Lux meter

Procedure to use lux meter

- 1) Use the 5 key keyboard of LI-250.
- 2) Attach the desired sensor.

- 3) Press and hold the ON key for about 2 seconds and then release to turn the instrument ON. The instrument will be in measurement mode. Press the OFF key to turn the power off if lux meter is not in measurement mode. Again, press and hold the ON key for about 2 seconds.
- 4) Press CAL to enter configuration mode, the display will show CA. The calibration multiplier currently in use can be displayed or changed.
- 5) Press UNITS until the units label on the display matches the sensor type. Readings will be incorrect if the Units Label does not match the sensor type.
- 6) Press the UP and DOWN arrow keys to change the displayed multiplier values. Press and hold the arrow keys down to scroll the values rapidly.
- 7) Press CAL again to store the displayed multiplier value and units label and use them to take measurements.
- 8) While in measurement mode you can press HOLD to retain the current reading on the display, until the HOLD key is pressed again.
- 9) Press AVG to perform a 15 second average, which will be displayed in Hold mode. Press the HOLD key to resume measurements.
- 10) Press the OFF key to turn the power off. The LI-250 will automatically shut off after 25 minutes of inactivity in measurement mode.

3.2.2 Image resolutions of weed detection sensor

Various researchers have reported that camera type (Cubero et al., 2011; Mendoza et al., 2006; Menesatti et al., 2012) has significant effect on colour difference (ΔE_{ab}). It also reported that an image resolution (Mahmud et al., 2019) has significant effect on weed and soil pixel classification accuracy. The different image resolutions supported by Logitech (C525) webcam is presented in Table 3.4. Among them four commonly used image resolutions i.e., 320×240, 640×480, 800×600 and 1280×720 pixels were used to study effect of different image resolutions on colour reproduction quality of weed detection sensor. A python code was developed to acquire images of different image resolutions.

Table 3.4: Supported image resolution (pixels) of Logitech (C525) webcam

1024×576	1184×656	1280×720	1280×960
1392×768	1504×832	1600×896	160×120
176×144	320×176	320×240	352×288
432×240	544×288	640×360	640×480
752×416	800×600	864×480	960×544

3.2.3 Colour difference (ΔE_{ab})

The color reproduction accuracy was determined through the CIE total colour difference (ΔE_{ab}). The equation 3.1 for colour difference (ΔE_{ab}) is given below. The value of colour difference (ΔE_{ab}) was calculated using below given equation 3.1.

$$\Delta E_{ab} = \sqrt{(\Delta L^*)^2 + (\Delta a^*)^2 + (\Delta b^*)^2} \quad \dots(3.1)$$

$$\Delta L^* = L_{Reference}^* - L_{Processed}^*$$

$$\Delta a^* = a_{Reference}^* - a_{Processed}^*$$

$$\Delta b^* = b_{Reference}^* - b_{Processed}^*$$

The L^* indicates the lightness and darkness of the product; it varies from 0 to 100, 0 indicates the black and 100 indicates white. Increase in L^* value of the product indicates the lightness increasing and decrease in L^* value indicates the product becomes darker. The a^* indicates the greenness and redness of the product. The b^* represents the blue and yellow of the product. Based on CIE (1931) XYZ, CIE $L^*a^*b^*$ was developed to measure the colour differences consistently with the perceived colour differences. It has been found that the Euclidian distance in $L^*a^*b^*$ space provides better match to the human visual perception of colour.

3.2.3.1 Standard test chart

Standard test charts have employed to ascertain the colour reproduction quality of digital camera. For this, ISO 12233 eSFR test chart was used (Plate 3.5). The standard RGB values of the chart were published by the manufacturer; hence the same values used as reference colour values. In addition, Imatest software automatically locates and analyses colour accuracy of camera. Imatest eSFR ISO charts can be printed in a variety of sizes to suit different cameras.

The following chart specifications (Table 3.5) were used to test different image resolutions of sensor. The dimensions of test chart at different megapixels are given in Table 3.5. The standard resolution of Logitech (C525) webcam was 640×480 pixels. Hence, recommended test chart as per megapixel of imaging sensor was chart size 1x ($200 \text{ mm} \times 305 \text{ mm}$).

Table 3.5: Dimensions of test chart and megapixels suitability

Chart size	Chart dimensions (mm)	Megapixels suitability (MP)
1x	200×305	1.6
2x	400×610	6.2
4x	800×1224	24.9

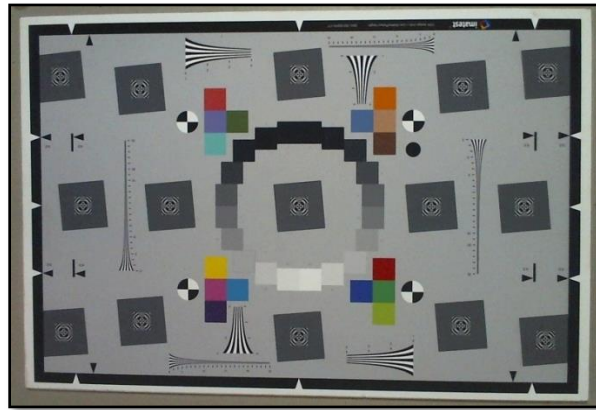


Plate 3.5: ISO12233 edge spatial frequency response (eSFR) test chart

3.2.3.2 Measurement of colour difference (ΔE_{ab})

The test chart was placed inside light source testing platform at weed detection sensor field of view. The weed detection sensor was placed orthogonally upward to a height such that the field of view sensor should exactly cover the boundary of chart. The test chart image was acquired at 89 ± 4.4 , 188.9 ± 6.4 , 259.3 ± 12.7 and 359.3 ± 7.5 lx illumination intensities and 320×240 , 640×480 , 800×600 and 1280×720 pixels image resolutions. Each experiment was repeated thrice. After acquiring colour chart images with a weed detection sensor, the images were analysed for its colour difference (ΔE_{ab}) using Imatest master software. The average colour difference (ΔE_{ab}) value was reported as colour reproduction quality of weed detection sensor. Lower colour difference (ΔE_{ab}) values were desirable for better colour reproduction of the original scene.

3.2.4 Statistical analysis and optimization

Full factorial experiment with three replications was conducted to see the significant effect of illumination intensity (4 levels) and image resolution (4 levels) on colour difference (ΔE_{ab}) as given in Table 3.2. To compare the influence of illumination intensity and image resolution on colour difference (ΔE_{ab}), a two-way analysis of variance (ANOVA) was performed, followed by post-hoc test Tukey's honestly significant difference test (Tukey's HSD). Tukey's HSD test identifies significant differences in the mean values by pairwise comparisons while adjusting the p-values for multiple comparisons. The illumination intensity and image resolution were considered as first and second factors, respectively. The data of colour difference (ΔE_{ab}) was subjected to analysis of variance (ANOVA) in OriginPro 2021 software to determine the significance of main treatments and intercation effects. The significance based on F-value and the null hypothesis was accepted/rejected at a 5% level of signfcance.

The selection of illumination intensity and image resolution was done by a numerical optimization technique based on desirability value. The desirability was a unitless numerical measure (Varies from 0 to 1) to identify best combination of peak performance of response variable (Dependent variable). The set of constraints for illumination intensity and image resolution were applied as “in range”. The “minimize” goal was assigned to colour difference.

Table 3.6: Selection of illumination intensity and image resolution based on desirability value

Name	Goal	Lower Limit	Upper Limit
Illumination intensity	is in range	89 ± 4.4	359.3 ± 7.5
Image resolution	is in range	320×240	1280×720
Colour difference (ΔE_{ab})	minimize	9.04	19.21

3.3 Effect of illumination intensity and image resolution on R, G, B, ExG and ExGR intensity values of green and soil pixels

In the previous experiment, effect of illumination intensity and image resolution on colour reproduction quality of imaging sensor was studied. In this experiment, effect of illumination intensity and image resolution on red (R), green (G), blue (B), excess green index (ExG) and excess green minus red index (ExGR) intensity values of green and soil pixels was studied. The output of digital colour camera was a RGB image. The red, green and blue channel intensity values of weed and soil pixels have been used for weed and soil pixels classification.

Red, green and blue channels intensity values were employed (El-Faki et al., 2000; Tewari et al., 2014) for weeds and soil background pixels classification. It was mentioned that for each pixel if the green intensity value greater than red and blue channel intensity ($G > R$ and $G > B$) that pixel classified as green object otherwise soil object. Similarly, visible spectral colour indices have been commonly used for weed and soil pixels classification (Meyer & Neto, 2008). Excess green index (ExG) and excess green minus red index (ExGR) colour indices have been most commonly used for weed and soil pixels classification. There was a need to fix threshold value for ExG and ExGR for weed and soil pixels classification. It was mentioned that ExG and ExGR values were sensitive to illumination intensities and other factors. Because of varying outside light condition, the pre-defined threshold value results either under segmentation or over segmentation. Hence, it was necessary to study effect of illumination intensity and image resolution on red (R), green (G), blue (B), excess green index (ExG) and excess green minus red index (ExGR) intensity values of green and soil pixels. Details of variables considered in present study are shown in Table 3.7.

Table 3.7: Plan of experiment to test sensitivity of R, G, B, ExG and ExGR values of green and soil pixels

Variables	Level	Description
Independent		
Illumination intensity	4	$L_1: 89 \pm 4.4 \text{ lx}; L_2: 188.9 \pm 6.4 \text{ lx};$ $L_3: 259.3 \pm 12.7 \text{ lx}; L_4: 359.3 \pm 7.5 \text{ lx}$
Image resolution	4	$S_1: 320 \times 240 \text{ pixels}; S_2: 640 \times 480 \text{ pixels};$ $S_3: 800 \times 600 \text{ pixels}; S_4: 1280 \times 720 \text{ pixels}$
Dependent		
		1. Red channel intensity values 2. Green channel intensity values 3. Blue channel intensity values 4. ExG intensity values 5. ExGR intensity values
Replications		
		1. Foliage 2. Yellow green 3. Green 4. Dark skin 5. Moderate red 6. Magenta
Total treatments	16	
Total number of experimental evaluations	96	

3.3.1 Standard colour chart

The X-Rite colour chart checker was used as standard colour chart for present experiment. Suh et al., (2014) used a standard X-Rite colour chart as a reference test chart for colour indices testing at field level. Also, ISO 17321 suggested using an X-Rite colour chart for RGB colour camera calibration. Menesatti et al., (2012) reported that three colour charts were employed for RGB colour camera calibration. The colour charts were GretagMacbeth colour checker SG 140 colour-patches, the GretagMacbeth colour checker 24 colour patches and the IFRAO standard colour checker 7 colour patches. The experimental results suggested that the use of color checker with 24 patches (X-Rite colour chart) was sufficient to resume the entire colour space, while 7 patches were insufficient and 140 patches oversamples. The X-Rite colour chart checker was a standard colour chart consists of 24 colour patches (Plate 3.6). The standard red, green and blue channel intensity values of all 24 colour patches were provided with test chart. A total of six colour patches out of 24 colour patches were selected for the present study. The foliage, yellow-green and green colour patches were used instead of actual plant samples, whereas dark-skin, moderate-red, and magenta colour patches were used for soil samples (Suh et al., 2014).



Plate 3.6 X-Rite colour chart checker

3.3.2 Excess green index and excess green minus red index values of green and soil colour patches

Excess green index (ExG) and excess green minus red index (ExGR) are formed by combining red, green and blue intensity values. Colour indices job is to accentuate particular colour so that feature extraction process becomes easy. The most commonly used colour indices were excess green index (ExG), excess red index (ExR) and excess green minus red index (ExGR). Excess green index (ExG) (El-Faki et al., 2000), excess red index (ExR) (Meyer et al.,

1999) and excess green minus red index (ExGR) (Meyer & Neto, 2008) segments the images into foreground pixels and background pixels based on threshold values.

$$\text{Excess green index (ExG)} = 2 \times G - R - B \quad \dots(3.2)$$

$$\text{Excess red index (ExR)} = 1.4 \times R - G \quad \dots(3.3)$$

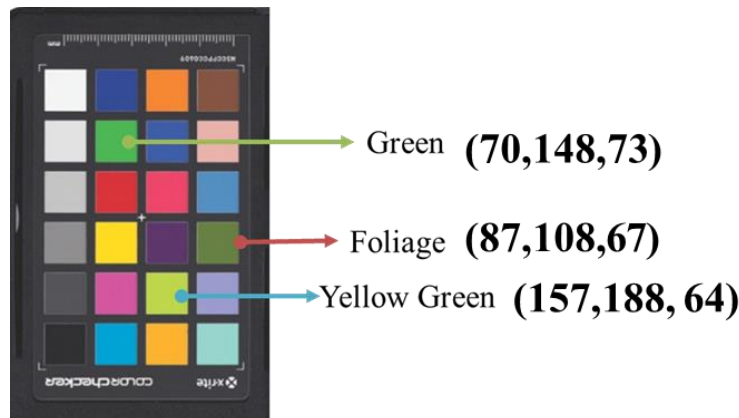
$$\text{Excess green index minus excess red index} = \text{ExG-ExR} \quad \dots(3.4)$$

Where,

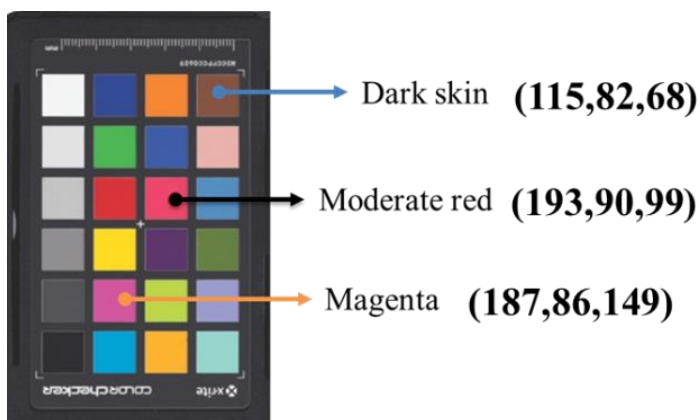
R=Red channel intensity values of RGB image

G=Green channel intensity values of RGB image

B=Blue channel intensity values of RGB image



(a)



(b)

(a) Green colour patches, (b) Soil colour patches

Fig. 3.1: Standard RGB values of green and soil colour patches

The X-Rite colour chart was placed inside light source testing platform. The X-Rite colour chart image was captured using weed detection sensor at four illumination intensities and

four image resolutions. The captured images were stored in the jpg file format. The standard RGB values of green and soil colour patches are shown in Fig 3.1. A sample of 10 pixels colour information from each colour patch were extracted and averaged. The foliage, yellow-green, green, dark skin, moderate red and magenta colour patches RGB intensity values were extracted using *ImageJ* software and stored in the MS excel sheet for further analysis. The RGB values of six colour patches were converted into ExG and ExGR values. Actual ExG and ExGR intensity values of green and soil colour patches are given in Table 3.8. Procedure to compute ExG, ExR and ExGR is shown in Fig 3.2 to Fig 3.4.

It was also important to check ExG and ExGR intensity values of actual leaves and soil samples. Fresh and healthy plant leaves and soil samples were collected from the field for this analysis. The collected leaves were of different shades of green from light to dark green. The leaves and soil sample images were captured at room lighting condition. The RGB intensity values of soil and leaves were extracted with help of *ImageJ* software and stored. The RGB values of leaves and soil samples were converted into ExG and ExGR values.

Table 3.8: ExG and ExGR intensity values from RGB channels intensity values of green and soil colour patches

Colour patches	Intensity values			Excess green index (ExG)	Excess green minus red index (ExGR)
	Red	Green	Blue		
Foliage	87	108	67	62	48.2
Yellow green	157	188	64	155	123.2
Green	70	148	73	153	203
Dark skin	115	82	68	-19	-98
Moderate red	193	90	99	-112	-292
Magenta	187	86	149	-164	-339

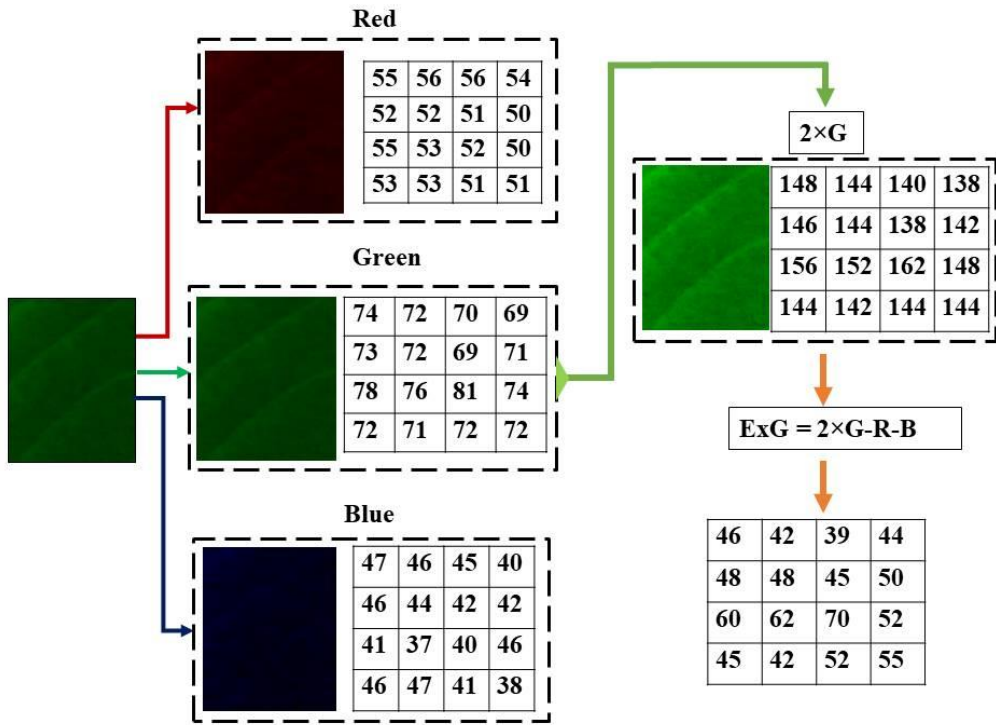


Fig. 3.2: Excess green index (ExG) values of selected leaf

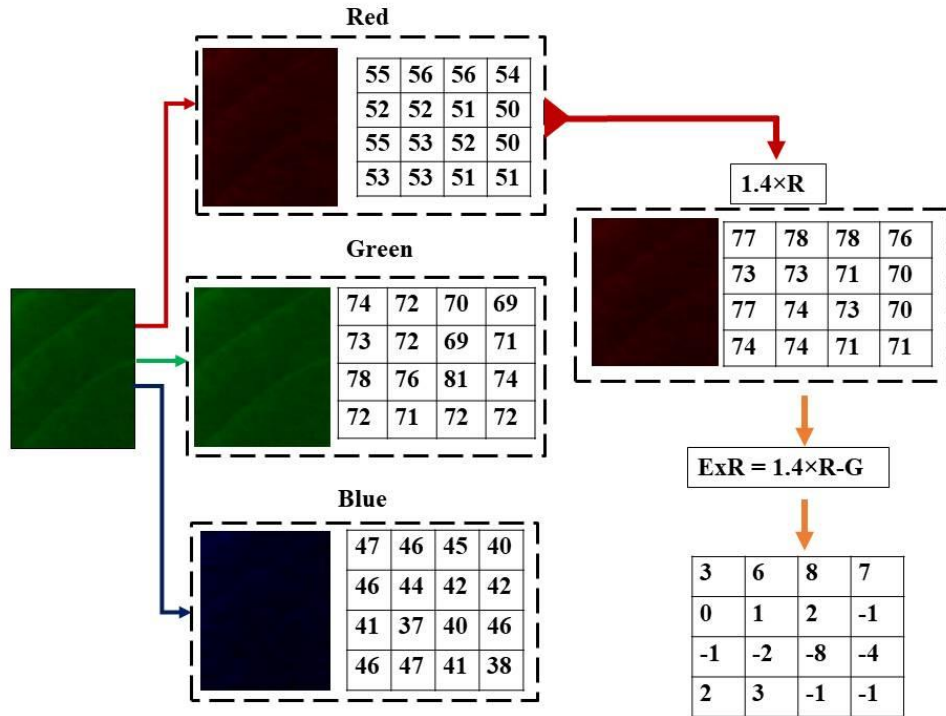


Fig. 3.3: Excess red index (ExR) values of selected leaf

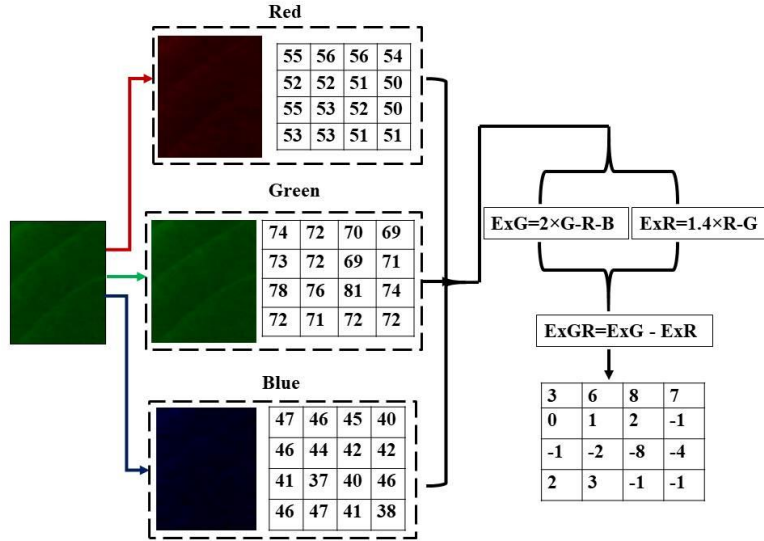


Fig. 3.4: Excess green minus red index (ExGR) values of selected leaf

3.3.3 Statistical analysis

Full factorial experiment with six replications was conducted to see the significant effect of illumination intensity (4 levels) and image resolution (4 levels) on red, green, blue, excess green index (ExG) and excess green minus red index (ExGR) channels intensity values of green and soil patches is given in Table 3.7. The red, green blue, excess green index (ExG) and excess green minus red index (ExGR) channels intensity values were subjected to three way analysis of variance (ANOVA) in OriginPro 2011 software to determine the significance of main treatments ($L-(L_1, L_2, L_3, L_4)$, $S-(S_1, S_2, S_3, S_4)$) and intercation effects ($L_1 S_1, L_1 S_2, L_1 S_3, L_1 S_4, L_2 S_1, L_2 S_2, L_2 S_3, L_2 S_4, L_3 S_1, L_3 S_2, L_3 S_3, L_4 S_1, L_4 S_2, L_4 S_3, L_4 S_4$). The illumination intensity, image resolution and type of colour patches were considered as first, second and third factors, respectively. The significance based on F- value and the null hypothesis was accepted/rejected at a 5% level of significance.

3.4 Microcontroller unit

The microcontroller acts like a human brain for sensing, interpretation and action. Similarly, in present study a microcontroller takes information from the imaging sensor (weed detection sensor), interprets the image information and sends signal to actuator for closing or opening the spraying nozzle. In present study Raspberry Pi 4B model was used as microcontroller. The Raspberry pi was a small single-board computer developed in the UK by the Raspberry Pi Foundation (Plate 3.7). It was a single-board computer with Wi-Fi and

Bluetooth functionality built-in. It consists of general purpose input and output (GPIO) pins, which provide the ability to connect the interface with external sensors and electrical components. It has 4 universal serial bus (USB) ports, enabling it to connect to peripherals like a mouse, keyboard, microphone, speakers and camera. There was an HDMI port that enables Raspberry Pi to connect to a monitor for displaying contents. There was a 15 pin camera interface connector that can be used with the Raspberry Pi camera. Power cable supplies 5 V and 3 A to the Raspberry pi board. The SD card contains the operating system.



Plate 3.7: Microcontroller (Raspberry Pi)

3.4.1 Raspberry Pi - general purpose input and output (GPIO) pins

General Purpose Input and Output (GPIO) pins help to connect external sensors and electrical components to Raspberry Pi. A powerful feature of the Raspberry Pi was the row of GPIO pins mounted along the board's top edge. A 40-pin GPIO header was found on all current Raspberry Pi boards stacked in a 20×2 array. Any GPIO pins can be assigned (in code) as an input or output pin and used for a wide range of purposes. Layout out of GPIO pins is shown in Fig 3.5. Concerning functionality, each pin has its specialty. Except for power and ground pins, rest were general-purpose input and output pins. These power and ground pins provide constant power when Raspberry Pi is turned ON. Moreover, these power and ground pins were not programmable by any means. Among 40 pins of Raspberry Pi, 6, 9, 14, 20, 25, 30, 34 and 39 pins provide the ground connection. Colour coding and significance of each pin are shown in Fig.3.5. When a GPIO pin was used in output mode, it gives 3.3V constant power when it is turned ON.

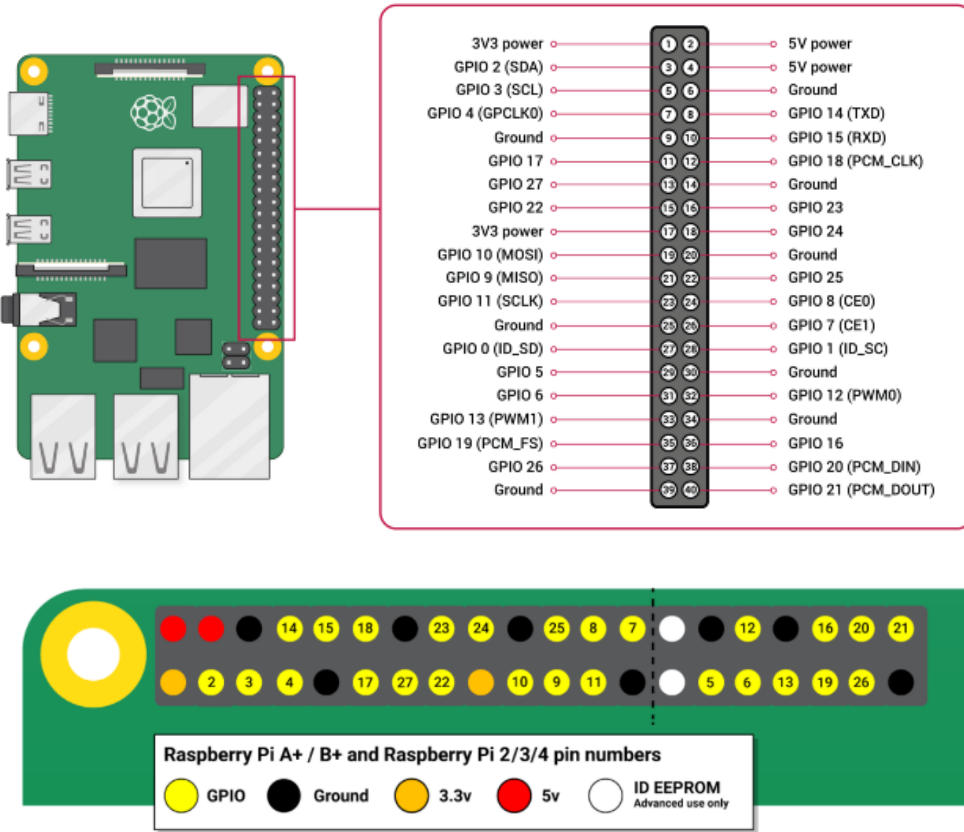


Fig.3.5: GPIO pin layout and colour coding of each pin of Raspberry Pi

3.4.2 Raspberry Pi operating system

There were many operating systems available for Raspberry Pi. The most popular and commonly used operating system was Raspbian operating system. NOOBS file was to be downloaded from internet. NOOBS was designed to make it easy to select and install operating systems for the Raspberry Pi. It's a program that facilitates the installation of an operating system. Raspberry Pi OS (formerly known as Raspbian) was a Debian-based operating system for Raspberry Pi. Since 2013, it has been officially provided by the Raspberry Pi foundation as the primary operating system for the Raspberry Pi family of compact single-board computers. The stages of operating system installation are shown in Fig 3.6. The zip file of NOOBS operating system was downloaded from the official site (www.raspberrypi.org) and the same file was unzipped. A memory card of 16 GB was used to store operating system. Before installing the Raspbian operating system on the memory card, the memory card needs to be formatted using SD card formatter. The SD card adapter was used to read micro SD card. Then the SD card

reader was inserted into the SD card reader slot on a personal computer (PC). The unzipped OS file was flashed into the memory card. Once the SD card was ready and flashed with the operating system, the SD card was removed from the laptop and the SD card adapter and inserts it into the backside of Raspberry Pi.

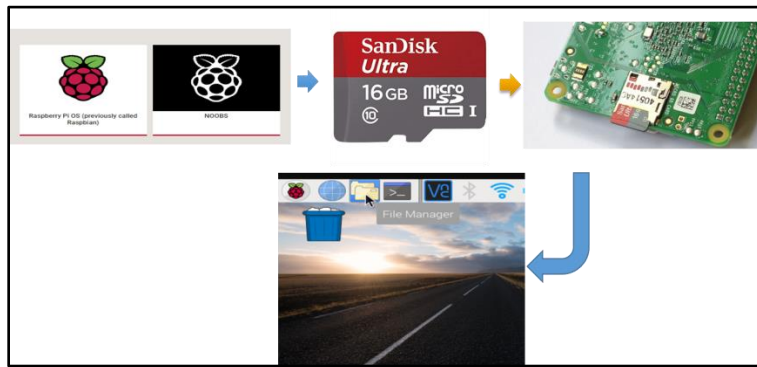


Fig.3.6: Operating system installation procedure

3.5 Effect of working height, image resolution and plant segmentation methods on weed and soil pixels classification accuracy

For an imaging system capable of detecting weeds underneath a camera (weed detection sensor), the field of view (FoV) of the camera should be at least as large as the area covered by spray produced by the nozzle. For an imaging system to recognize small objects within field of view the image resolution should be such that small objects get thresholded. Each pixel of the image representing higher area on the ground may result in low detection accuracy and small objects may get omitted. To achieve better accuracy, the field of view (FoV) would have to be reduced by reducing the distance between the weed detection sensor and the objects or increase the resolution of image. Thus, a study was conducted to test effect of image resolution and working height on classification accuracy of weeds and soil pixels.

Visible spectral colour indices and colour models have been commonly used for weed and soil pixels classification (Meyer & Neto, 2008). There was a need to fix/pre-define threshold value for visible spectral colour indices and colour models for weed and soil pixels classification. Effect of pre-defined threshold value and dynamic threshold value of visible spectral colour indices and colour models on weed and soil pixels classification accuracy was studied. The list of parameters considered testing effect of working height, image resolution and plant segmentation methods on classification accuracy are given in Table 3.9.

Table 3.9: Experimental plan to measure the effect of image resolution, working distance and plant segmentation methods on response variables

Variables	Level	Description
Independent		
Working height	4	H ₁ : 400 mm; H ₂ : 500 mm; H ₃ : 600 mm; H ₄ : 700 mm
Image resolution	4	S ₁ : 320×240 pixels; S ₂ : 640×480 pixels; S ₃ : 800×600 pixels; S ₄ : 1280×720 pixels
Plant segmentation method	8	M ₁ : ExG +pre-defined threshold value; M ₂ : ExGR+pre-defined threshold value; M ₃ : HSV+pre-defined threshold value; M ₄ : CIELAB+pre-defined threshold value; M ₅ : ExG +dynamic threshold value; M ₆ : ExGR+dynamic threshold value; M ₇ : HSV+dynamic threshold value; M ₈ : CIELAB+dynamic threshold value
Dependent		
	1.	Precision
	2.	Recall
	3.	False positive rate
Replications	10	(Test images)
Total treatments	128	
Total number of experimental evaluations	1280	
Fixed variable	Illumination intensity	

3.5.1 Working height

To ascertain effect of working height of weed detection sensor on weed and soil pixel classification an experiment was conducted at four working height of weed detection sensor. The selected working heights were 400, 500, 600 and 700 mm. The working height was adjusted by setting the adjustable camera mount. Working height was the distance between weed detection sensor to the object. The graphical definition of working height is shown in Fig 3.7. The working height was measured using steel ruler scale. Images of plants (Test images) at different working heights were acquired under light source testing platform at optimized illumination intensity.

The graphical definition of field of view is shown in Fig 3.8. The field of view (width and height of the image) of the weed detection sensor was measured at two heights from the ground surface. The field of view of weed detection sensor at 400 and 700 mm was measured and linear

regression model was developed, so that field of view of weed detection sensor on remaining heights can be estimated easily from the developed linear regression model.

The linear regression model for the image width estimation was
 Width of image = $0.869 \times \text{Height of camera} + 1.7$... (3.5)

The linear regression model for the image height estimation was
 Height of image = $0.625 \times \text{Height of camera} + 2.5$... (3.6)

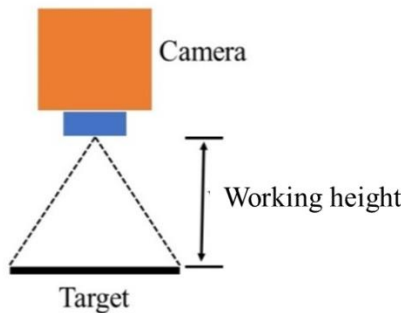


Fig. 3.7: Working height

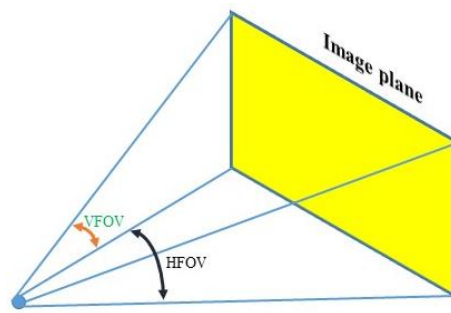


Fig. 3.8: Field of view of camera

3.5.2 Image resolution of weed detection sensor

The effect of image resolution on weed and soil pixels classification accuracy was studied. The image resolutions used were 320×240 , 640×480 , 800×600 and 1280×720 pixels. The same image resolutions were used during testing colour reproduction quality of weed detection sensor.

3.5.3 Plant segmentation methods

The plant segmentation method includes classifier and threshold value. Visible spectral colour indices and colour models used as a classifier for weed and soil pixel classification are formed by combining the RGB values through simple arithmetic operations. In present study excess green index (ExG), excess green minus red index (ExGR), hue-saturation-value (HSV) and CIELAB colour model models were used for weed and soil pixel classification. The HSV and CIELAB colour models consist of three channels. Hue, saturation and value were three channels. In CIELAB colour model, “L” channel represents lightness; “A” channel contains green to red colour information, whereas “B” channel contains blue to yellow colour information. These plant segmentation methods need threshold value for weed and soil pixel

classification. Hence, the effect of pre-defined threshold value and dynamic threshold value of colour indices and colour models on weed and soil pixels classification accuracy was studied. Total eight methods were used for weed and soil pixels classification. ExG, ExGR, HSV and CIELAB with pre-defined threshold value and dynamic threshold value were used.

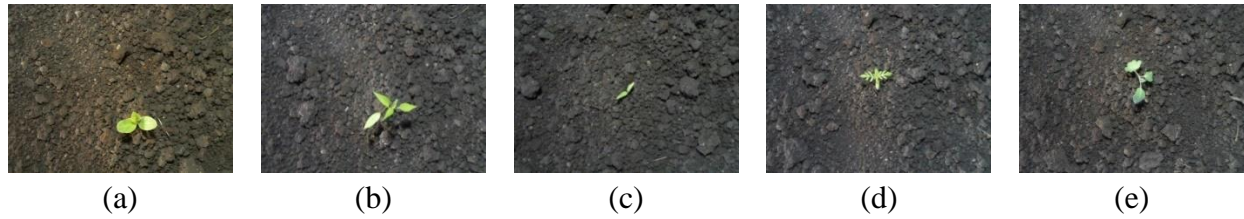


Plate 3.8: Test images (a-e)

To test the weed and soil pixel classification accuracy of colour indices and colour models seedlings of brinjal, cabbage, green gram and chilli were procured from nearby nursery (Plate 3.8). These seedlings were used as a test images. Black cotton soil was used as a background material. At different combination of working distances (400, 500, 600, 700 mm) and image resolutions (320×240, 640×480, 800×600, 1280×720 pixels) the test images were captured at finalized illumination intensity.

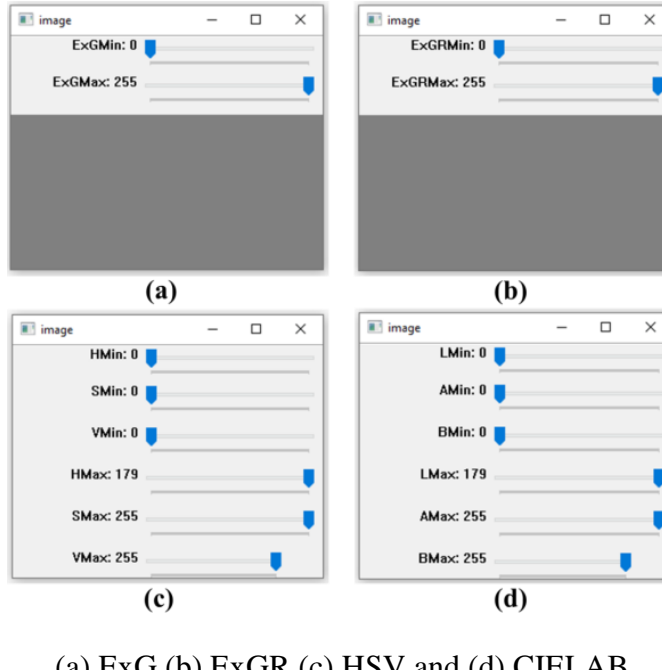
3.5.3.1 Threshold value selection

3.5.3.1.1 Pre-defined threshold value

A suitable threshold value needs to be selected for weed and soil pixel classification using ExG, ExGR, HSV and CIELAB methods. The ExG, ExGR, HSV and CIELAB are derived from red, green and blue channel intensity values. ExG and ExGR consist of single channel, whereas HSV and CIELAB consist of three channels. For ExG and ExGR indices threshold value was to be selected for single channel, whereas for HSV and CIELAB three threshold values were to be selected for three channels. Each channel was grayscale image and 8 bit image. Hence, grayscale intensity values were ranges from 0 to 255.

The optimal threshold value lies between 0 and 255. The aim was find best threshold value that yields better classification accuracy. Using python *range()* function the start, end and step size of threshold values were selected. The start, end and step size of threshold value were 0, 255, 5 respectively. Fresh and healthy plant leaves were collected. The fresh and healthy leaves and plant images with soil as background material were captured with help of light source testing platform. Effect of threshold values on image weed and soil pixel classification was observed.

Moreover, a graphical user interface (GUI) using python has been developed to select the lower boundary and upper boundary of colour indices and colour models for weed and soil pixel classification. ExG, ExGR, HSV and CIELab GUI's were developed (Fig 3.9). With the help these GUI's final lower and upper threshold values boundary were selected for each method.



(a) ExG (b) ExGR (c) HSV and (d) CIELAB

Fig.3.9: Track bars window

3.5.3.1.2 Dynamic threshold value

Among the various dynamic thresholding methods Otsu method has been most commonly used dynamic image thresholding technique. In this method the threshold value was to be selected automatically based on grayscale histogram (Meyer & Neto, 2008; Yang et al., 2015). It travels from the lowest gray level of an image to the highest to find the optimal threshold. Each time it uses the current gray level as the threshold and partition the whole image into two groups, and then calculates the between group variance. When the travel ends, the right gray level which makes the maximal between-group variance was the optimal threshold. The pixels become white if the intensity values of pixels greater than the threshold values otherwise black. HSV and CIELAB colour models consists of three channels. In case of dynamic threshold selection method, the Otsu method was applied on hue channel of HSV colour model and "A" channel of CIELAB colour model. The core idea was separating the image histogram into two

clusters with a threshold defined as a result of minimization the weighted variance of these clusters denoted by $\sigma_w^2(t)$. The probabilities of the two clusters were divided by a threshold t and threshold value was within the range from 0 to 255. The objective was to minimize the within-class variance($\sigma_w^2(t), w_1(t), w_2(t)$).

$$\sigma_w^2(t) = w_b(t)w_f(t) (\mu_b - \mu_f)^2 \quad \dots(3.7)$$

$$w_b(t) = \sum_{i=1}^t P(i)$$

$$w_f(t) = \sum_{i=t+1}^I P(i)$$

$$W_b = \frac{\text{Number of pixels in background}}{\text{Total number of pixels}}$$

$$W_f = \frac{\text{Number of pixels in foreground pixels}}{\text{Total number of pixels}}$$

μ_b = Mean intensity of background

μ_f = Mean intensity of foreground

3.5.3.2 Development of weed and soil pixels classification algorithm

Software was developed using python programming language. In order to access weed detection sensor and performing few operations like resizing of images, reshaping of images and acquiring frames, the computer vision library called Open-CV Python (cv2) was installed. A library called numerical python (numpy) was used for handling three dimensional colour images. This library stores the RGB image colour information in matrix format. So that working with each colour channel separately (R, G, B) was possible. Gaussian smoothing with kernel size 5×5 and standard deviation of 2 was applied on input image to remove noise as pre-processing of an image.

In the present study, weed coverage percentage (WCP) in the input image was extracted using excess green index (ExG), excess green minus red index (ExGR), HSV and CIELAB. There were no inbuilt python modules to compute ExG and ExGR intensity values from input image, but there were python libraries for computation of HSV and CIELAB from input image. Since OpenCV represents images as NumPy arrays in reverse order, the input image in a BGR format. The ExG and ExGR were computed using python code from BGR image. OpenCV-

Python library consists of one separate module for colour model conversion. The BGR image was converted to HSV image using `cv2.cvtColor(image, cv2.COLOR_BGR2HSV)`. The BGR image was converted to CIELAB using `cv2.cvtColor(image, cv2.COLOR_BGR2LAB)`. If intensity value of particular pixels $I(i,j)$ satisfied the threshold value that pixels were classified as weed pixels and the remaining pixels were classified as soil pixels. The image was masked using cv2 inbuilt function called `cv2.threshold()`. The `cv2.threshold()` function takes four arguments. The first argument should be an array of size 8 bit format. The second argument was threshold value. The third argument was highest intensity value. The fourth argument was binary threshold. If particular pixel intensity values satisfied the threshold value that pixel value assigned as 255 otherwise zero. The `cv2.threshold()` function return two parameters; one was threshold value and second one was segmented image. To fix the lower and upper limits of four methods, a built-in `cv2.inRange()` function was used. This function returned binary image (mask) where white pixels belong to foreground and black pixels belongs to background. In case of dynamic threshold value selection a built in `cv2.threshold()` function was used to automatically segment an image into foreground pixels (white) and background pixels (black). Then number of white pixels i.e., weed pixels in segmented image was counted by a built in `np.sum()` function.

3.5.4 Performance metrics

Precision, recall and false positive rate (FPR) were used as performance metrics to evaluate image segmentation accuracy of plant segmentation methods at different image resolutions and working heights. The details of metrics are given below.

True positives (TP) – It indicates correctly predicted positive class labels i.e., green pixels. It means that actual pixel belongs to green class and the model predicted it as green class label.

True negatives (TN) – It indicates correctly predicted negative class labels i.e., background pixels. The actual pixel belongs to background class and the model predicted it as background class.

False positives (FP) – Actually, when pixel class belongs to negative class i.e., soil background pixels but the model predicted the pixel as positive class i.e., green pixels.

False negatives (FN) – Actually, when pixel class belongs to positive class i.e., green pixels but the model predicted that pixel as negative i.e., soil background pixel.

Precision: It is the ratio of correctly predicted positive observations to the total predicted positive observations.

Recall (Sensitivity or True positive rate): Recall is the ratio of correctly predicted positive observations to all observations in actual class.

False positive rate (FPR): It corresponds to the proportion of negative data points that are mistakenly considered as positive, with respect to all negative data points. In other words, the higher the FPR, the more negative data points we will misclassify.

$$\text{Precision} = \frac{\text{TP}}{\text{TP} + \text{FP}} \quad \dots(3.8)$$

$$\text{Recall} = \frac{\text{TP}}{\text{TP} + \text{FN}} \quad \dots(3.9)$$

$$\text{False positive rate (FPR)} = \frac{\text{FP}}{\text{FP} + \text{TN}} \quad \dots(3.10)$$

3.5.4.1 Development of machine learning algorithm for ground truth image creation

The performance metrics were used for quantifying performance of plant segmentation methods. Before going to the computation of TP, TN, FN, FP metrics, the actual pixels labels of image were to be identified. The each pixel in a given image was classified as weed or soil class. If the actual pixels labels in the input image were known, then it can be compared with the output image that was segmented by the image segmentation methods. Finally, performance metrics was computed. In the present work, the weed and soil images were captured at four image resolutions and four working heights at finalized illumination intensity. Ground truth image creation for all combination was time consuming. Moreover, manually painting each pixel was prone to error. To overcome this problem, an attempt was made to automate the ground truth image creation process. It consists of two steps. In the first stage the image pixels were partially annotated. In the second stage the development of supervised machine learning model was done.



(a)



(b)

(a) Test image (b) Partially labelled image

Plate 3.9: Preparation of ground truth image

Assigning labels to pixels

In the first stage using APEER annotate software the image pixels were painted partially. Annotate tool assign 1 to weed pixels and 2 to soil background pixels. The pixels that were not painted manually assign a 0 value to them. The test image is shown in Plate 3.9 (a). The partially labelled image is shown Plate 3.9 (b).

Supervised machine learning algorithm

The approach was followed to create ground truth image using supervised machine learning approach. In case of supervised learning approach user has to provide feature and target variable to the classification algorithm. Features from image was extracted using traditional image processing techniques. A Gabor filter, named after Dennis Gabor, a linear filter was used for texture analysis in image processing. It typically means that it analyzes any specific frequency content in the image in particular directions in a localized region around the point or area of analysis. Total 42 features were used as an input to machine learning model. The features dataset were extracted from each image using Gabor filter, Sobel filter, Median filter, Gaussian filter and Canny edge filters. All the mentioned filters works on grayscale image (8 bit image). Each channel in RGB, HSV and CIELAB colour model was grayscale image. The intensity of grayscale image was used as a one feature variable. For extracting texture and edge features “A” channel of CIELAB was employed.

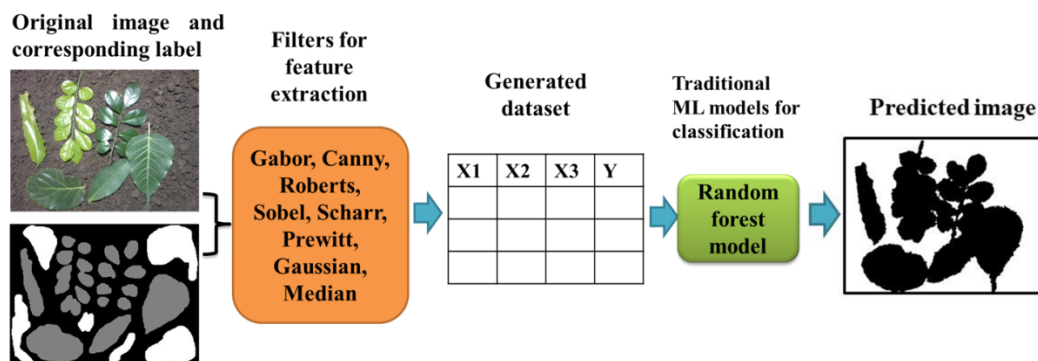


Fig. 3.10: Feature extraction using filters, model development and prediction

Fig 3.10 shows the feature extraction using filters, model development and prediction. All these 42 features were used as input to supervised machine learning approach. The dataset was divided into training and testing set. For training purpose 80 % of dataset, while testing purpose 20 % of dataset was used. During the training phase the feature variables and target

variable were to be sent through the classification algorithm. One of the supervised machine learning technique called random forest classifier was employed in the present study. The python code was developed for creating groundtruth image using 42 features and random forest machine learning algorithm.

3.5.4.2 Development of software for weed and soil pixels classification and performance metrics computation

There were inbuilt python libraries for performance metrics computation of given features and labeled data. These libraries support popular machine learning algorithm like linear regression, K-nearest neighbors (KNN) and support vector machine (SVM). But, present study used simple colour indices and colour models for weed and soil pixels classification. Hence, there was a need to develop dedicated software for performance metric computation. To compute the performance metrics of weed and soil pixels classification algorithm mainly four stages were involved. In the first stage, an image was captured by weed detection sensor and pre-processing of the captured image takes place. In the second stage, the computation of colour indices and colour models values from RGB colour information takes place. The third stage was the threshold value fixing. Final stage was computation of performance metrics.

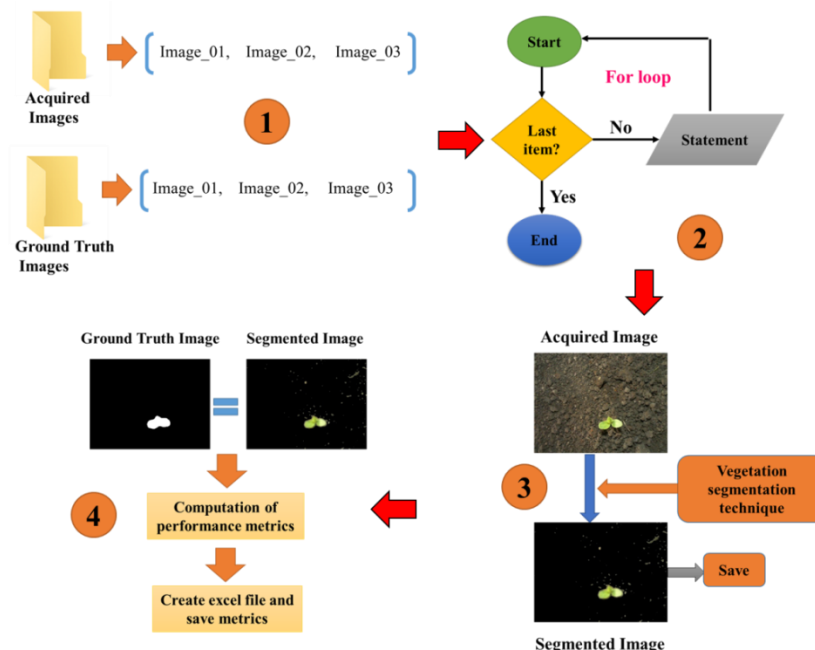


Fig. 3.11: Weed and soil pixels classification and performance metrics computation

Dedicated software was developed using python for calculating the performance metrics of each plant segmentation methods at different threshold values. The original image and ground truth images were stored in working directory. The software takes original image and ground truth image from working directory. Once an original image was passed through the software, it computes the ExG, ExGR, HSV and CIELAB values from the RGB values of the original image. Then compute the performance metrics by comparing the ground truth image with the segmented image. Finally stores the results in an excel file. The working flow of developed software is shown in Fig.3.11.

3.5.5 Statistical analysis

Full factorial experiment with 10 replications as indicated in Table 3.9 conducted to ascertain the effect of image resolution, working height and plant segmentation methods on weed and soil pixels classification accuracy. To compare the influence of image resolution, working height and plant segmentation methods on classification accuracy, a three-way analysis of variance (ANOVA) was performed. OriginPro 2021 software was used to determine the significance of main treatments and intercation effects. The significance based on F-value and the null hypothesis was accepted/rejected at a 5 % level of signifcance.

3.6 Effect of soil type on weed and soil pixels classification accuracy

In the previous section the soil type was black cotton soil. The effect of image resolution, working height and plant segmentation methods on weed and soil pixels classification accuracy was studied. Hence, in this section the effect of soil type on weed and soil pixels classification accuracy was studied. The plant experiment is given in Table 3.10.

3.6.1 Soil type

The soil type varies from one region to other region. Three types of soil were considered. Black cotton soil, sandy soil and red soil were collected from nearby field. Plants and tree leaves were used as foreground material. The test images were acquired using weed detection under with help of developed light source testing platform. The finalized lighting intensity, plant segmentation method, image resolution and working height were used.

Table 3.10: Experimental plan to test effect of soil type on response variables

Variables	Level	Description
Independent		
Soil type	3	B ₁ : Black cotton soil; B ₂ : Sandy soil; B ₃ : Red soil
Working height	4	H ₁ : 400 mm; H ₂ : 500 mm; H ₃ : 600 mm; H ₄ : 700 mm
Dependent		
	1.	Precision
	2.	Recall
	3.	False positive rate
Replications		
	4	(Test mages)
Total treatments		
	3	
Total number of experimental evaluations		
Fixed variable		
		Illumination intensity, Plant segmentation method, Image resolution

3.6.2 Statistical analysis

An experiment with 4 replications was conducted to ascertain the significant effect of soil type on weed and soil pixels classification accuracy. The data of performance metrics was subjected to analysis of variance (ANOVA) in OriginPro 2021 software to determine the significance of main treatment effect. The significance based on F-value and the null hypothesis was accepted/rejected at a 5 % level of significance.

3.7 Spraying unit

The spraying unit consists of a pump, chemical tank, solenoid valve, pressure gauge, flat-fan nozzle, hose and hose connections.

3.7.1 Pump

The ASPEE-BiLi HTP pump was used and its power requirement was 1.45 kW. The pump revolution, discharge rate and maximum pressure were 900 rev/min, 50 l/min and 3.44 MPa, respectively. A chemical tank of 100 litres was used to carry chemical solution. It was mounted on tractor at rear side of tractor seat. Hose and hose connections of diameter 10 mm were used to supply chemical from tank to solenoid valve with help of pump. Pressure gauge

was fitted to pump that indicates operating pressure. The operating pressure of pressure gauge is 0-1372 kPa.

3.7.2 Flat-fan nozzle

Even flat fan type nozzles were most suitable for the weedicide application at a uniform and width. A flat fan nozzle (ASPEE make-60500) was used.

3.7.3 Solenoid valve

Normally closed type solenoid vale was used for controlling flat fan nozzle opening and closing based on control signal generated from microcontroller. In the present study a DC solenoid valve (24V DC, diversion type, 1000 kPa max) of normally closed type was employed to regulate flow. The solenoid valve has two components a solenoid and a valve body (G). The Fig 3.12 shows the components of solenoid valve. The center called the plunger (E) in the solenoid consists of an electromagnetically inductive coil (A) around the iron core. At rest it was normally open (NO) and normally closed (NC). In a de-energized state, the normally open valve was open and the closed valve was closed. When current flows in the solenoid, the coil was energized and creates a magnetic field. This, together with the plunger, creates magnetic attraction, moves it and overcome the spring (D) force. If the valve was normally closed then the plunger lifts, then the seal (F) opens the orifice and allows media to flow through the valve. If the valve was open, the plunger moves the download which blocks the seal (F) orifice and stops the flow of the media through the valve. The shading ring (C) prevents vibration and humming in AC coils.

The solenoid valve was controlled by electrical signal. It gets power from batteries and gets signal ON or OFF from microcontroller. The valve has a solenoid which was an electric coil with a movable ferromagnetic core in the center (Fig 3.12). The plunger closes OFF a small orifice in the rest position. The electric current in the coil creates a magnetic field. The plunger was forced upward to open the magnetic field exerted. This was the basic principal for opening and closing of solenoid valve.

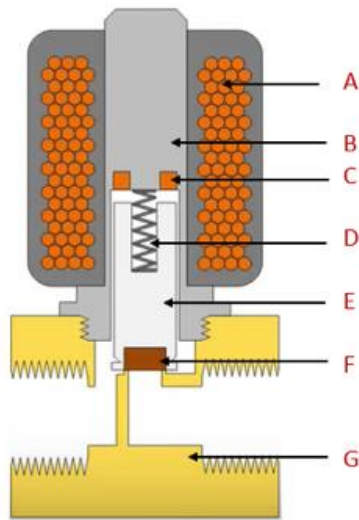


Fig. 3.12: Solenoid valve

3.7.4 Interface microcontroller and motor driver module

The microcontroller (Raspberry Pi) output power was not enough to power the connected devices directly, so Raspberry Pi cannot operate actuator (solenoid valve) directly. Therefore, a single channel L298N motor driver module was used between solenoid valve and Raspberry Pi 4B.

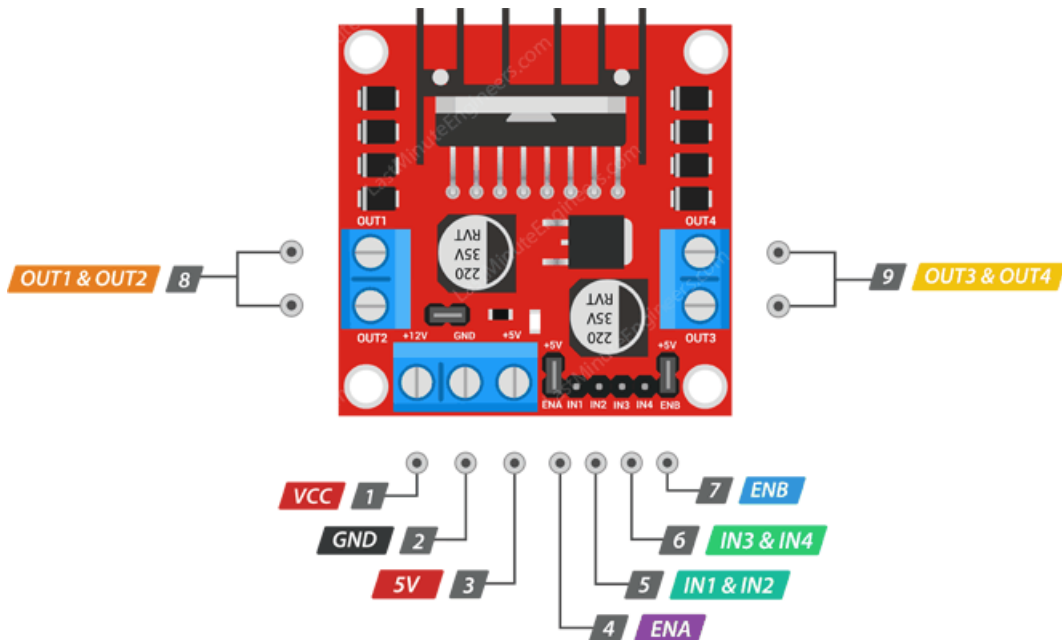
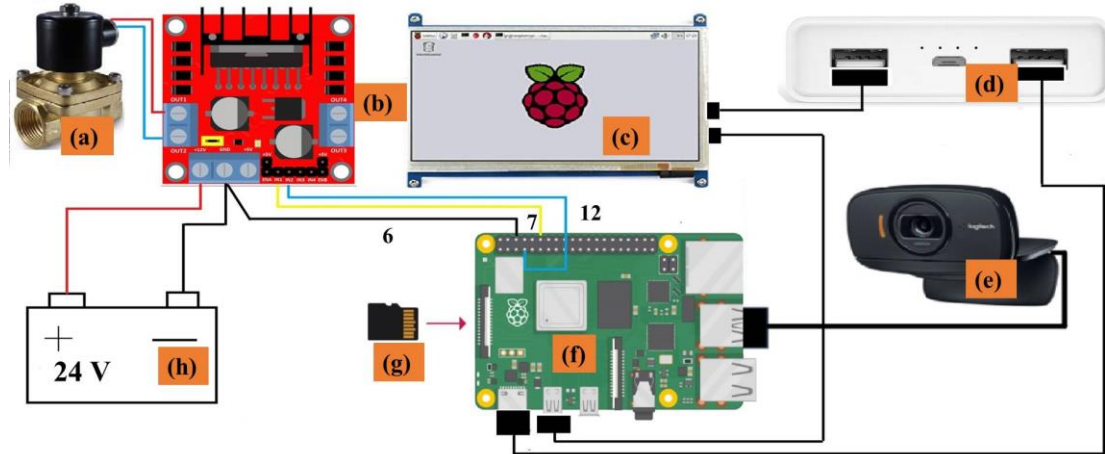


Fig. 3.13: L298N motor driver module

The L298 motor driver module was used most commonly for driving DC motors and stepper motors. It uses the popular L298 motor driver IC and has the on board 5V regulator, which can supply power to an external circuit. It can control 2 DC motors with directional and speed control. The pin diagram of the L298N motor driver IC is shown in Fig 3.13. It contains screw terminals for connecting motors and power supplies, male headers for connecting different pins like enable, IN1, IN2.



(a) Solenoid valve, (b) L298N motor driver module, (c) HDMI 7 inch display, (d) Power bank (20000 mAh), (e) Logitech webcam, (f) Raspberry Pi 4B, (g) Memory card, (h) Battery (24 V)

Fig. 3.14: Circuit diagram of Raspberry Pi 4B and L298N motor driver interface

The circuit diagram and connection of Raspberry Pi and L298N motor driver interface is shown in Fig 3.14. This motor driver module was connected to the 24 V DC power supply. The IN1 and IN2 pins of the L298N motor drive module were connected to Raspberry Pi's physical pins 7 and 12 (GPIO4 and GPIO18). When the motor driver (L298N) gets a true signal i.e. 3.3 V from Raspberry Pi, the motor driver activates the solenoid valve port and the solenoid valve was open. When get false acknowledge through the Raspberry Pi, the solenoid valve was closed.

3.8 Optimization of constructional and operational parameters

Different units of site specific weedicide applicator were optimized. The optimization was utmost important because chemical was to be sprayed on weed detected zone. The distance

between weed detection sensor and spraying nozzle, quantity of weedicide applied and frame grab interval of site specific weedicide applicator were optimized for this purpose.

3.8.1 Optimization of distance between weed detection sensor and spraying nozzle

The distance between the sensing and spraying nozzle was utmost important because chemical was to be sprayed on the weed detected zone, otherwise the purpose of site specific weedicide application was defeated.

3.8.1.1 Processing time of image segmentation and weedicide application algorithm

In real time image segmentation and subsequent application of chemicals, total processing time of weed and soil pixels classification algorithm and weedicide application plays a vital role. The forward speed of prime mover and distance between weed detection sensor and spraying unit depends on algorithm processing time. The image segmentation algorithm involves four major stages. In the first stage, an image was captured by weed detection sensor and preprocessing of the captured image takes place. In the second stage, the computation of selected colour model values from RGB colour information takes place. The third stage was the threshold value fixing. The fourth and final stage was the percentage of weed pixels count in the segmented image.

The weed and soil pixel classification code was developed using Python (Version 3.9). Thonny python integrated development environment (IDE) was used for compiling Python code. The flowchart site specific weedicide applicator is shown in Fig.3.15. Several python packages were used to build decision making software. Open-CV python, RPI.GPIO, numerical python (NumPy) and Time python libraries were used. The developed decision making software acquired the images (I) with help of weed detection sensor. Gaussian smoothing with kernel size 5×5 and standard deviation of 2 was applied on input image to remove noise. The next stage was colour space transformation. Since OpenCV represents images as NumPy arrays in reverse order, the input in a BGR format.

If intensity value of particular pixels $I(i,j)$ satisfied the threshold value that pixels were classified as weed pixels and the remaining pixels were classified as soil pixels. In case of pre-defined threshold value selection a built-in *cv2.inRange()* function was used to fix the lower and upper limits of model. This function returns binary image (mask) where white pixels belong to weed and black pixels belongs to soil. Then number of white pixels i.e., weed pixels in segmented image was counted by a built in *np.sum ()* function. Finally weed coverage percentage

(WCP) computed and generates a control signal for actuating solenoid valve based on WCP threshold value. There were two threshold values as shown in Fig 3.15.

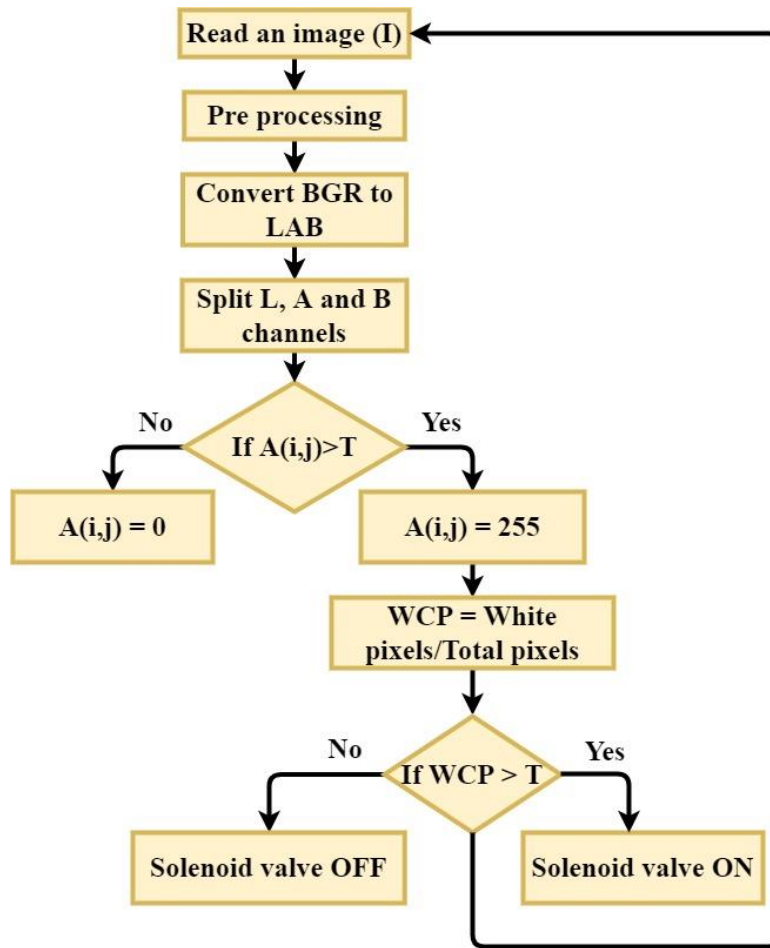


Fig.3.15: Flowchart of site specific weedicide applicator

First threshold value relates to plant segmentation algorithm. The second threshold value relates to nozzle activation. The microcontroller sends signal to solenoid valve only when second threshold value found greater than the pre-defined threshold value of WCP. The developed software was run for 10 minute with the help of python inbuilt time library for testing number of frames passed through image segmentation algorithm. Total run time or processing time of image segmentation algorithm was measured using `time.time()` built in function of time module.

3.8.1.2 Measurement of response time of solenoid valve

An experiment was conducted to measure the solenoid valve response time. The hardware setup was fixed to tractor. During the experiment the forward speed of vehicle was maintained as 1.8 km/h. The test was conducted on tar road. A plastic green patch was used

instead of weed. The dimensions of plastic green patch were $130\text{ mm} \times 200\text{ mm}$. The centre to centre distance between weed detection sensor and spraying nozzle was fixed as 400 mm . Two lines were drawn on tar road at distance of 400 mm between them. The plastic green patch was placed on line B (Plate 3.10). Line B divides green patch into two equal parts i.e. 100 mm . The weed detection sensor field of view was maintained as $400\text{ mm} \times 200\text{ mm}$.

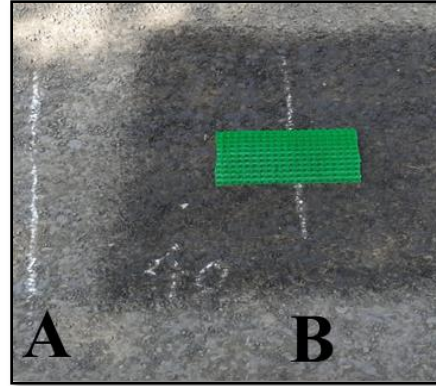
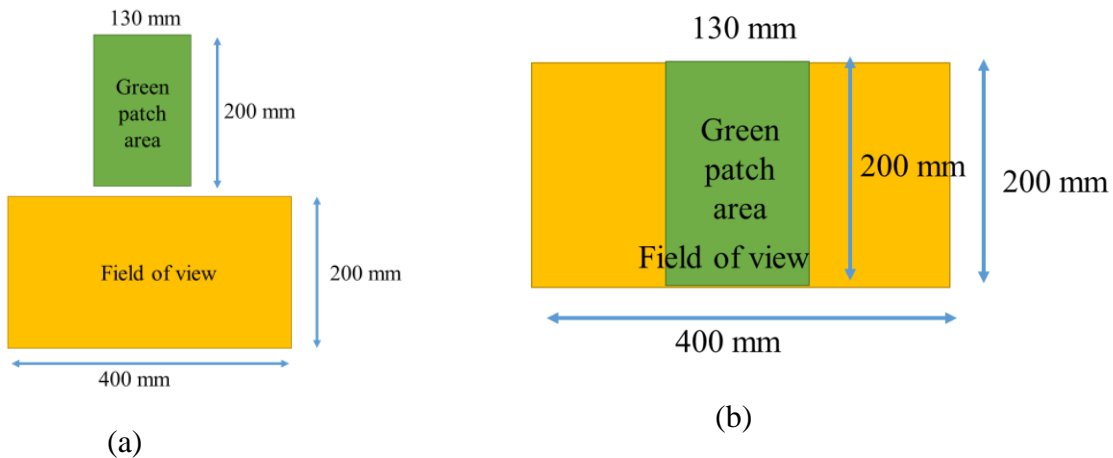


Plate 3.10: Plastic green patch

In this experiment the code was adjusted in such way that the solenoid valve was activated only when weed detection sensor at centre of green patch (Fig 3.16 (b)). To accomplish above task, before conducting the test the weed detection sensor was placed directly over a green patch and then calculated the weed coverage percentage (WCP).



- (a) Microcontroller don't send singal to solenoid valve
- (b) Microcontroller send signals to solenoid valve

Fig.3.16: Green patch area and field of view of weed detection sensor

The software was designed in such way that when weed coverage percentage (WCP) value found greater than the threshold value the microcontroller immediately send signals to the solenoid valve and turn on the solenoid valve. During the test run once weed coverage percentage (WCP) found greater than threshold value, nozzle start spraying liquid solution. After spraying was done the distance between line A and spraying starting point was measured. The amount of time taken to cover such distance was called lag time. This lag time includes processing time (image capturing time, image segmentation) and time taken by solenoid valve to respond to signal generated by microcontroller. Time taken by solenoid valve to respond was obtained subtracting processing time of image segmentation algorithm from lag time.

3.8.1.3 Development of relationship for optimizing distance between weed detection sensor and spraying nozzle

The processing time of image segmentation and weedicide application algorithm was measured. Also, the response time of solenoid valve was measured. As shown in Fig 3.17 that the spraying should be started when point "f" reaches to point "e". The distance between point "e" and point "f" depends on forward speed and lag time. The field of view of weed detection sensor was $200 \times 400 \text{ mm}^2$. Other two factors that affected the centre to centre distance between weed detection sensor and spraying nozzle (c) were field of view of weed detection sensor and nozzle spraying area (length and width). The centre to centre distance between weed detection sensor and spraying nozzle (c) was finalized using equation (3.11).

$$c = a + b + s \quad \dots(3.11)$$

a = Distance travelled in lag time

b = Half of the height of field of view in the forward direction

s = Half of the spraying length of nozzle in the forward direction

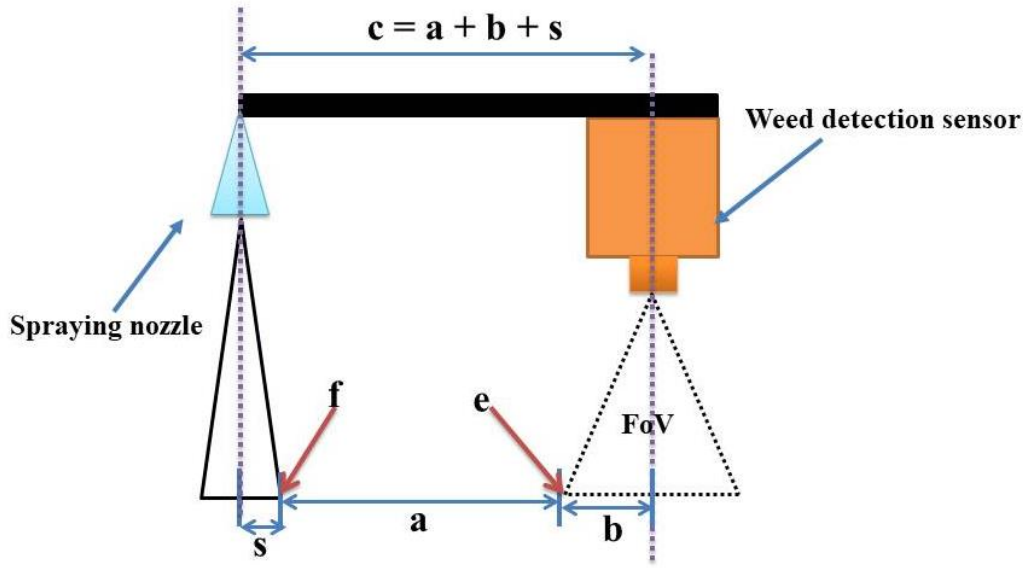
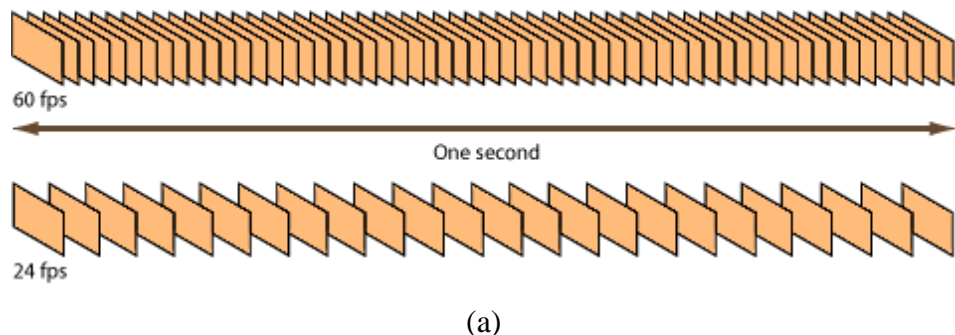
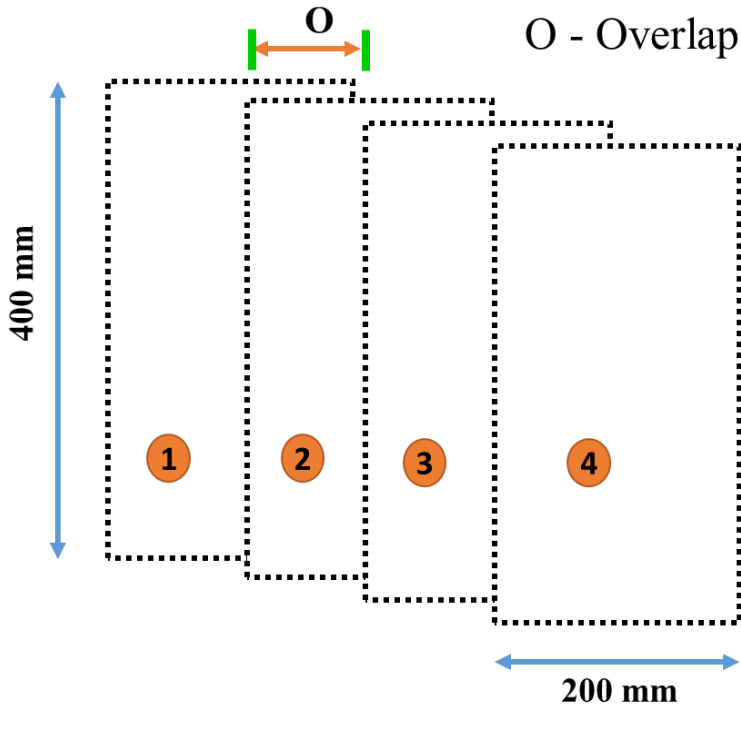


Fig. 3.17: Center to center distance between weed detection sensor and spraying nozzle

3.8.2 Optimization of frame grab interval of weed detection sensor

Weed detection sensor reads video and it was a sequence of frames. The graphical representation of frame rate is shown in Fig 3.18 (a). The graphical representation of overlap between two consecutive frames is shown in Fig 3.18 (b). The overlap between two consecutive frames was indicated by letter “O”. Number of frames to be passed through image segmentation algorithm was depends on processing time and forward speed of prime mover. Lag time includes processing time of image segmentation algorithm and response time of solenoid valve. The number of frames to be discarded between two consecutive frames analyzed was optimized based on lag time and forward speed.





(a) Frame rate, (b) Overlap between two consecutive frames

Fig 3.18: Optimization of frame grab interval of weed detection sensor

3.8.3 Quantity of weedicide applied

Quantity of weedicide to be discharged depends on recommended quantity of chemical to be applied per unit area in a given amount of time. The amount of chemical to be applied in field of view of webcam was calculated using equation (3.12). In present study, flat fan nozzle (ASPEE make-60500), HTP pump of 1.45 kW and solenoid valve of 24 V were employed. The nozzle discharge rate was measured at 196, 294 and 392 kPa operating pressures.

$$\text{Spray amount (I)} = \text{AR} \times \text{A} \quad \dots(3.12)$$

AR = Recommended application rate, l/mm²

A = Field of view of webcam, mm²

$$\text{Discharge rate of nozzle (l/s)} = \frac{\text{Spray amount (I)}}{\text{Duration of solenoid valve opening (s)}} \quad \dots(3.13)$$

3.8.3.1 Measurement of nozzle discharge rate

The test trolley setup was equipped with system to maintain desired pressure of spraying unit and variable frequency (VF) drive with electric motor to control the forward speed of the

trolley. A trolley setup also consists of small soil bin of size 600 mm × 10000 mm. The nozzle discharge rate of the flat fan nozzle was measured at 196, 294 and 392 kPa operating pressures. Using python script duration of solenoid valve opening time was varied. Using built in *time.time()* function of python time library the opening and closing time of solenoid valve was controlled programmatically. The discharge of liquid was collected in jar for 500, 1000, 1500, 2000 ms at operating pressure of 196, 294 and 392 kPa. The total volume of water was measured and discharge rate was calculated.

Table 3.11: Plan of experiment to test effect of operating pressure and solenoid valve opening time on discharge rate

Variables	Level	Description
Independent		
Operating pressure	3	P ₁ : 196 kPa; P ₂ : 294 kPa; P ₃ : 392 kPa
Solenoid valve opening time	4	T ₁ : 500 ms; T ₂ : 1000 ms; T ₃ : 1500 ms; T ₄ : 2000 ms
Dependent :		Nozzle discharge rate (l/min)
Total treatments	12	
Replications	3	
Total number of experimental evaluations	36	

3.8.3.2 Measurement of spray distribution pattern

The spray distribution pattern was measured at plant protection laboratory, ICAR-CIAE, Bhopal. The standard spray patternator was used for the spray distribution pattern investigation. The uniformity of the spray and spray width of flat fan nozzles was measured. The nozzle was mounted at a height of 450 mm so that the entire spray liquid was projected towards the patternator. At the pressure settings of 196, 294 and 392 kPa, sprayed liquid was collected and the volume of collected liquid in the 1000 ml glass tubes from each channel of patternator was noted. All the measuring cylinders were emptied to drain and the tests were repeated thrice to find the mean value of the spray liquid collected in each measuring cylinder.

3.9 Development of a real time camera based weedicide applicator

The major components of a typical computer vision based site specific weedicide applicator with Raspberry Pi 4 model B as micro controller is given in Table 3.12. A 20000 mAh power bank was used to power the Raspberry Pi 4 model B and 7 inch LCD screen. The solenoid valve was powered by two 12 V batteries. Flat fan nozzle (ASPEE make-60500) to generate requisite spray pattern was used. The weed detection sensor and solenoid valve were covered with black cloth. A dedicated light source for illumination at weed detection sensor field of view was provided. The functional block diagram of the site specific weedicide application system is shown in Fig 3.19.

Table 3.12: Hardware components used for site specific weedicide applicator

Weed detection sensor	
Name of sensor	Logitech c525 webcam
Specifications	Standard resolution (640×480 pixels), 30 fps
Microcontroller	
Name of microcontroller	Raspberry Pi 4 model B (4GB RAM, 1.5 GHz processor, USB 3.0, Bluetooth, Wi-Fi)
Storage	32 GB memory card
Display	7 inch LCD screen with HDMI port (800×480 pixels resolution)
Software components	
Operating system	NOOBs (Raspbian)
Integrated development environment (IDE)	Thonny python
Libraries	Computer vision (cv2), numerical python (NumPy), Time module, GPIO and Matplotlib.pyplot libraries
Spraying unit	
Actuator	DC solenoid valve (24 V, 1000 kPa max.)
Position	Normally closed type
Pump	1.45 kW HTP
Spraying nozzle	Flat fan nozzle (ASPEE make-60500)
Motor driver	L298N motor driver module

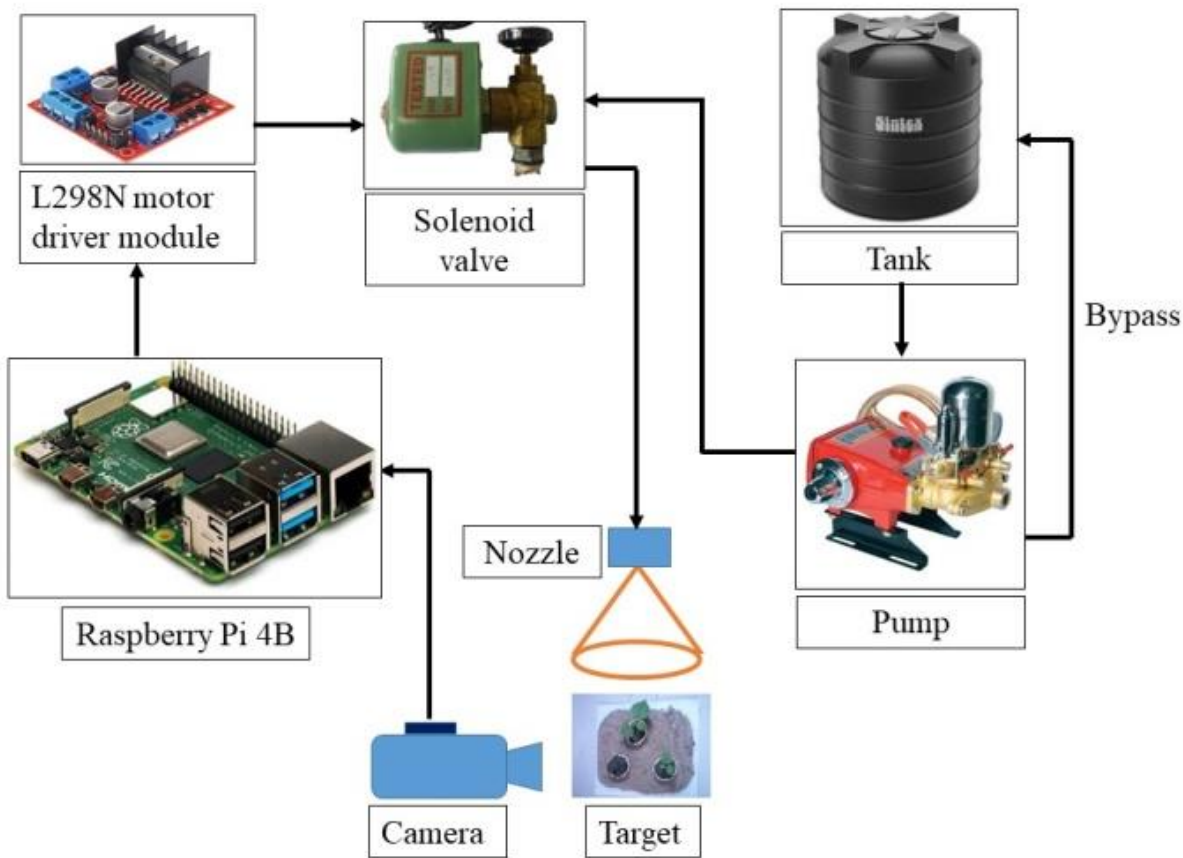
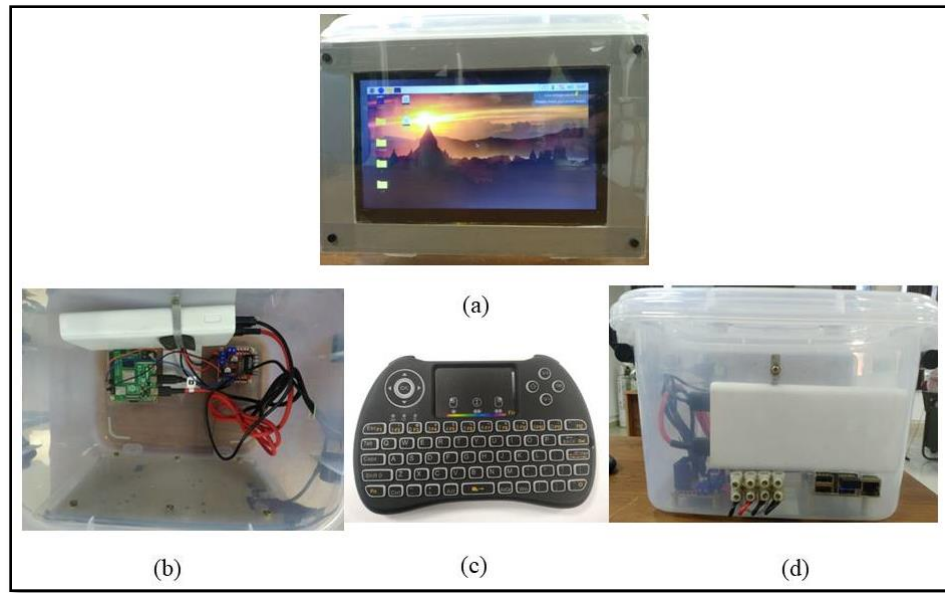


Fig.3.19: Functional block diagram of the site specific weedicide application system

3.9.1 Development of tractor mounted single row site specific weedicide applicator

A tractor of 13.42 kW was used as prime mover. All the components such as microcontroller, HDMI screen, power bank and motor driver module were secured in a box to protect parts (Plate 3.11). To mount a solenoid valve and weed detection sensor a dedicated set up was made (Fig 3.20). The set up was fitted to tractor with the help of three point hitch. The cad model of a single row camera based weedicide applicator is shown in Fig 3.21. The height of the nozzle and weed detection sensor was adjustable so that the field of view of sensor and spray area could be fine-tuned/adjusted to crop conditions. The HTP pump was mounted at front side of tractor. The pump was driven front power take off shaft (PTO) of tractor. A single row tractor mounted site specific weedicide applicator was developed and as shown in Plate 3.12.



(a) Front view, (b) Top view, (c) Wireless keyboard with touchpad, (d) Side view

Plate 3.11: Compact setup for mounting microcontroller, LCD screen, motor driver and power bank

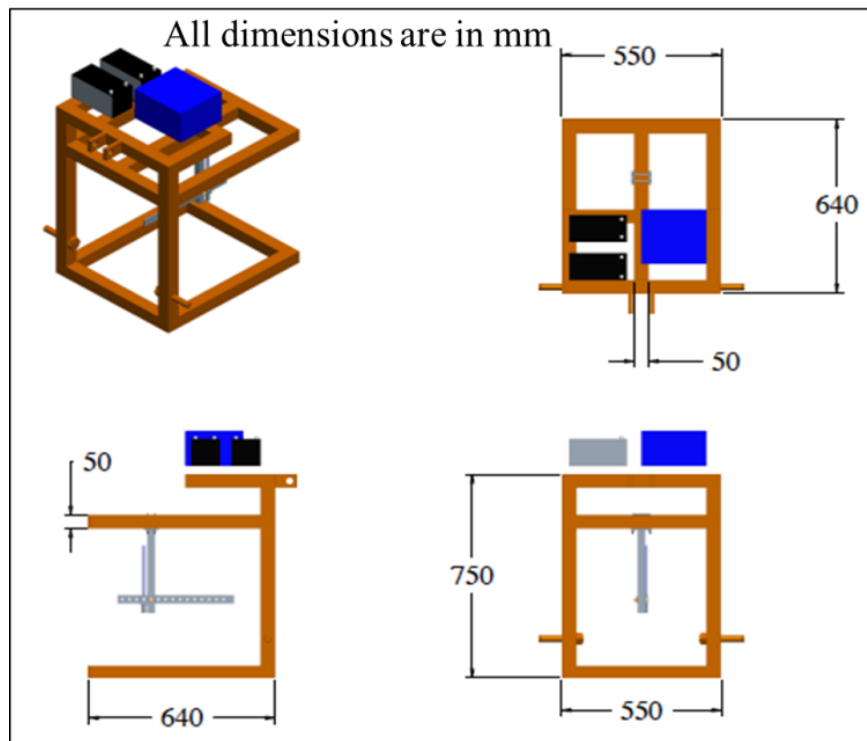


Fig.3.20: Set up for fixing webcam, light, solenoid valve, batteries and microcontroller

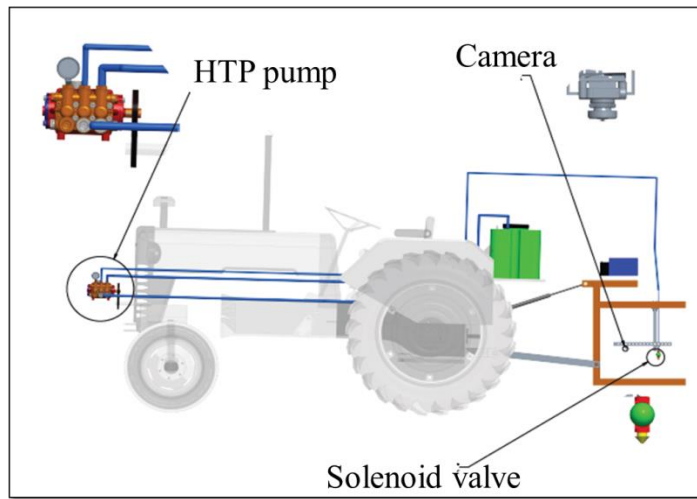


Fig.3.21: Schematic diagram of a single row site specific camera based weedicide applicator



(a) Weed detection sensor, (b) Solenoid valve, (c) Power bank, raspberry pi, motor driver module, (d) HDMI display, (e) Pressure gauge, (f) HTP pump, (g) Chemical tank, (h) Two 12 V batteries

Plate.3.12: Prototype and components of single row site specific camera based weedicide applicator

A preliminary experiment was conducted to evaluate effectiveness of plant segmentation and site specific spraying of developed system with optimized operational parameters in an agriculture field (open field). The forward speed of tractor was maintained as 1.2 km/h. The height of weed detection sensor and flat fan nozzle were 400 and 450 mm, respectively. Plant leaves were used as weeds. Soil type was black cotton soil (vertisol). Decision making algorithm consists of finalized plant segmentation method for weed and soil pixels classification. The screen recorder was installed in Raspberry Pi. With the help of screen recorder the decision making algorithm weed and soil pixels classification performance was recorded in real time. A second webcam was fitted inside system setup for recording the spraying performance. Field set up of site specific weedicide applicator is shown in Plate 3.13.



Plate 3.13: Field set up of tractor mounted site specific weedicide applicator

An experiment was conducted to check the effectiveness of spray coverage of the developed system on tar road. Intersection section over union was used as a performance metric to report the spray coverage of developed system (Fig 3.22). Green patch of size 200 mm × 130 mm was considered for this study. The length of green patch was considered as A. The length of spraying was considered as B. The intersection over union value ranges between 0 and 1. If the IoU value was near to 1 that means that developed system able to spray on green patch detected zone. If the IoU value was near to 0 that means that developed system start spraying before or after green patch. While conducting this experiment all optimized operational parameters (distance between weed detection sensor and nozzle unit) were kept constant except duration of solenoid valve opening time. To show significant effect of duration of solenoid valve opening on target spraying, the solenoid valve was opened for 150, 250 and 450 ms. Each test was replicated three times to confirm the reliability of the system.

$$\text{Intersection over union (IoU)} = \frac{A \cap B}{A \cup B} \quad \dots(3.14)$$

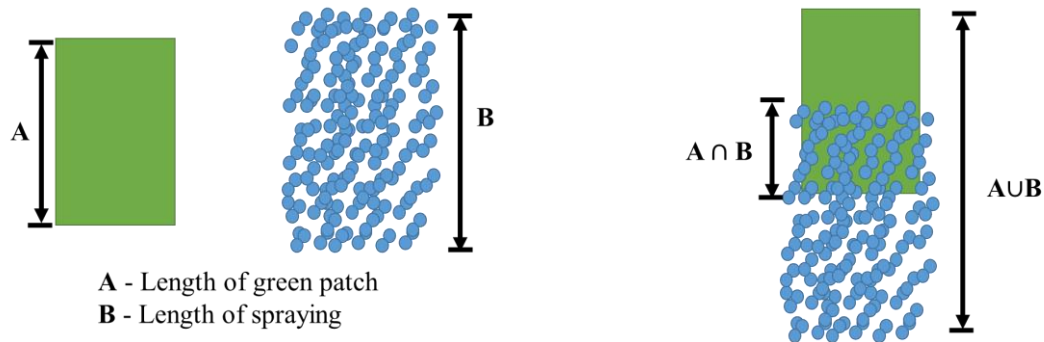


Fig.3.22: Illustration of intersection over union (IoU) metric

3.10 Field evaluation of developed real time camera based weedicide applicator

The developed real time camera based weedicide applicator was evaluated in cotton field. Soil type was black cotton soil (vertisol). The field test was conducted with the optimized operational parameters. The forward speed of tractor was maintained as 1.2 km/h. The height of weed detection sensor and flat fan nozzle was 400 and 450 mm, respectively. A graphical user interface (GUI) was developed in Python environment for easy monitoring of the developed site specific spraying system by the operator. This GUI displays the original image, segmented image and weed coverage percentage (WCP). Also, there was an option to adjust the threshold limits of weed coverage percentage for solenoid valve activation. Field set up of site specific weedicide applicator is shown in Plate 3.14. The test was conducted after 45 days of sowing. The lower limit of threshold value of WCP was selected 2 %. The solenoid valve was to be activated only when weed coverage percentage in each frame was greater than 2 %. Glyphosate was used as weedicide. The chemical solution was made by mixing 100 g of Glyphosate with 15 litre of water. The performance of developed system was expressed in weeding efficiency, chemical saving and field capacity.



Plate 3.14: Field evaluation of developed system (Cotton field)

3.10.1 Weedicide application rate

Initially the tank was filled up to the mark. The amount of weedicide used was measured by refilling the tank up to the mark. The weedicide application amount of site specific weedicide applicator was compared with fixed rate weedicide applicator. In fixed rate weedicide application method, the webcam was stopped and solenoid valve position was set as normally open, the system sprayed chemical to known distance. In site specific weedicide application method, the developed system sprayed chemical to known distance on only weed infested zone. The speed of operation was maintained as constant for both methods. The amount of chemical saving was reported by comparing amount chemical applied by fixed rate weedicide application with site specific weedicide application method.

3.10.2 Weeding efficiency

Weeding efficiency is number of weeds present in a given area before weedicide application to number of weeds present in a given area after weedicide application (Chandel et al., 2018). Five places were randomly selected and $400\text{ mm} \times 400\text{ mm}$ area was marked to see the weed count before and after weedicide application. After 5 days weeds count was measured from same locations. Water sensitive papers were placed on bare soil and weed infested zone. The water sensitive paper was visually examined after testing site specific weedicide applicator.

$$\text{Weeding efficiency} = \frac{A-B}{A} \times 100 \quad \dots(3.15)$$

A = Average number of weeds present in each plot before weedicide application

B = Average number of survived weeds in each plot five days after weedicide application

3.10.3 Plant damage

The water sensitive paper was attached to cotton plants to test if any weedicide was sprayed on main crop.

3.10.4 Statistical analysis

Experimental design, a completely randomized design (CRD) with three replications was used to show significant effect of site specific weedicide application and fixed rate weedicide application on weeding efficiency and weedicide application amount. One way analysis of variance (ANOVA) was to see significance effect of weedicide application methods on chemical saving amount and weeding efficiency. The significance based on F-value and the null hypothesis was accepted/rejected at a 5% level of significance.

As per plan of work all experiments mentioned in section 3.2, section 3.3, section 3.5, section 3.6, section 3.8, section 3.9 and section 3.10 were conducted. The experimental results of effect of illumination intensity and image resolution on colour difference, illumination intensity and image resolution on R, G, G, ExG and ExGR intensity values of green and soil pixels, effect of working height, image resolution and plant segmentation methods on weed and soil pixels classification accuracy, effect of soil type on weed and soil pixels classification accuracy and field evaluation of developed a real time camera based weedicide applicator is presented in chapter 4 from section 4.1 to 4.9.

Chapter 4

Results

Chapter-4

Results

This chapter presents the results pertaining to illumination intensity, image resolution, working height, plant segmentation methods, optimization of threshold values of plant segmentation methods, development and field evaluation of a real time camera based weedicide applicator. The contents are organized in following subheadings:

- 4.1 Effect of illumination intensity and image resolution on colour difference (ΔE_{ab})
- 4.2 Effect of illumination intensity and image resolution on R, G, B, ExG and ExGR intensity values of green and soil pixels
- 4.3 Development of software for ground truth image creation and performance metrics computation
- 4.4 Effect of threshold value of plant segmentation methods on weed and soil pixels classification accuracy
- 4.5 Effect of working height, image resolution, plant segmentation methods on classification accuracy of weed and soil pixels
- 4.6 Effect of soil type on classification accuracy of weed and soil pixels
- 4.7 Optimization of constructional and operational parameters
- 4.8 Development of a real time camera based weedicide applicator
- 4.9 Field evaluation of developed real time camera based weedicide applicator

4.1. Effect of illumination intensity and image resolution on colour difference (ΔE_{ab})

The colour difference (ΔE_{ab}) was used a metric to represent the colour reproduction quality of weed detection sensor. The colour difference (ΔE_{ab}) of weed detection sensor was evaluated at four illumination intensities and four image resolutions as per methodology stated in section 3.2. The effect of different illumination intensities and image resolutions on colour difference (ΔE_{ab}) values is given in Fig 4.1. Perusal of Fig 4.1 indicates that lowest colour difference (ΔE_{ab}) value 9.07 ± 0.04 was observed at interaction effect of illumination intensity of 89 ± 4.4 lx and image resolution of 1280×720 pixels. The highest colour difference (ΔE_{ab}) value 19.16 ± 0.06 was observed at interaction effect of illumination intensity of 359.3 ± 7.5 lx and image resolution of 320×240 pixels. It was observed that increasing illumination intensity from 89 ± 4.4 lx to 359.3 ± 7.5 lx, there was an increasing trend in the average colour difference (ΔE_{ab}) values

all image resolutions. It was also observed that increasing image resolution from 320×240 pixels to 1280×720 pixels; there was a decreasing trend in the average colour difference (ΔE_{ab}) values at all illumination intensities.

The analysis of variance (ANOVA) presented in Table 4.1 indicated that the variation caused in colour difference (ΔE_{ab}) values due to change in illumination intensity was found to be significantly different ($F_{3,32} = 1265.99$, $p=0.005$). Similarly, the variation caused in colour difference (ΔE_{ab}) values due to change in image resolution was found to be significantly different ($F_{3,32} = 1543.34$, $p=0.001$). Likewise, the variation caused in colour difference (ΔE_{ab}) values due to the interaction effect of the illumination intensity and image resolution was also found to be significantly different ($F_{9,32} = 7.73$, $p=0.001$).

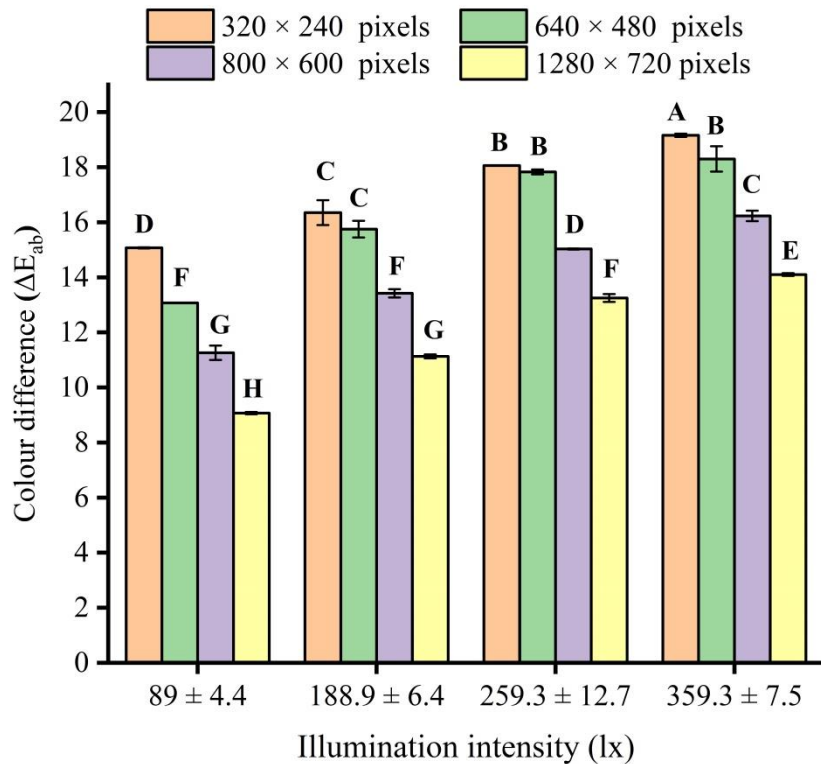


Fig. 4.1: Effect of illumination intensity and image resolution on colour difference (ΔE_{ab})

All treatment means of colour difference (ΔE_{ab}) values at illumination intensity of 89 ± 4.4 lx shared different letters (D, F, G, H); it implies that colour difference (ΔE_{ab}) values of weed detection sensor were found to be significantly different at four image resolutions. Similarly at illumination intensity of 359.3 ± 7.5 lx, all treatments means of colour difference (ΔE_{ab}) values

shared different letters (A, B, C, E); it implies that colour difference (ΔE_{ab}) values of weed detection sensor were found to be significantly different at four image resolutions.

Table 4.1: Analysis of variance (ANOVA) of colour difference (ΔE_{ab})

Source of variation	DF	F-value
Illumination intensity (L)	3	1265.99**
Image resolution (S)	3	1543.34**
L×S	9	7.73**
Error	32	
Total	47	

Note: DF:Degree of freedom; “**” = Significant at 1% level of significance; “*” = Significant at 5% level of significance; “ns”=non-significant

Table 4.2: Desirability values of 16 combinations of categorical factor levels

Number	Illumination intensity (lx)	Image resolution (pixels)	Colour difference (ΔE_{ab})	Desirability
1	89±4.4	1280×720	9.07	0.957
2	188.9±6.4	1280×720	11.13	0.794
3	89±4.4	800×600	11.26	0.781
4	89±4.4	640×480	13.07	0.604
5	259.3±12.7	1280×720	13.25	0.586
6	188.9±6.4	800×600	13.42	0.569
7	359.3±7.5	1280×720	14.10	0.502
8	259.3±12.7	800×600	15.03	0.410
9	89±4.4	320×240	15.07	0.407
10	188.9±6.4	640×480	15.75	0.340
11	359.3±7.5	800×600	16.23	0.293
12	188.9±6.4	320×240	16.35	0.281
13	259.3±12.7	640×480	17.83	0.135
14	259.3±12.7	320×240	18.06	0.113
15	359.3±7.5	640×480	18.30	0.089
16	359.3±7.5	320×240	19.16	0.005

At illumination intensity of 188.9 ± 6.4 lx, the image resolutions 320×240 and 640×480 pixels shared same letter (C). Similarly, at illumination intensity of 259.3 ± 12.7 lx, the image resolutions 320×240 and 640×480 pixels shared same letter (B). It implies that at illumination

intensities 188.9 ± 6.4 and 259.3 ± 12.7 lx, image resolutions 320×240 and 640×480 pixels performed similarly.

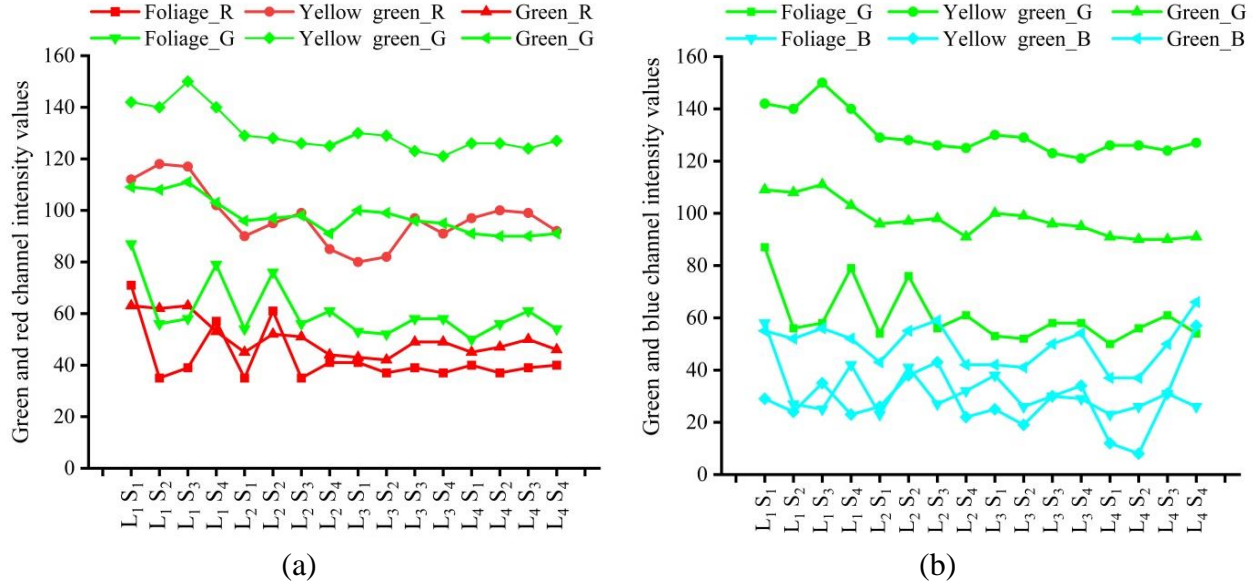
The desirability values of 16 treatment combination are given in Table 4.2. From numerical optimization it was observed that the desirability value 0.957 was found to be highest at interaction effect of 89 ± 4.4 lx and 1280×720 pixel (Table 4.2). At this interaction the colour difference (ΔE_{ab}) value was observed as 9.07. The lowest desirability value 0.005 was observed at illumination intensity of 359.3 ± 7.5 lx and image resolution of 320×240 pixels.

4.2 Effect of illumination intensity and image resolution on R, G, B, ExG and ExGR intensity values of green and soil pixels

The effect of illumination intensity and image resolution on red, green and blue intensity values of six colour patches is shown in Fig 4.2 and Fig 4.3. It was observed from Fig 4.2 and Fig 4.3 that there was a variation in red, green and blue intensity values of green and soil colour patches with different levels of illumination intensity as well as image resolution. This means that red, green and blue channels grey level intensity values of six colour patches were sensitive to illumination intensity as well as image resolution. Hence, even keeping illumination intensity constant and changing image resolution there was variation in the red, green and blue channels intensity values. Similarly, keeping image resolution constant and changing illumination intensity there was variation in the red, green and blue channels intensity values.

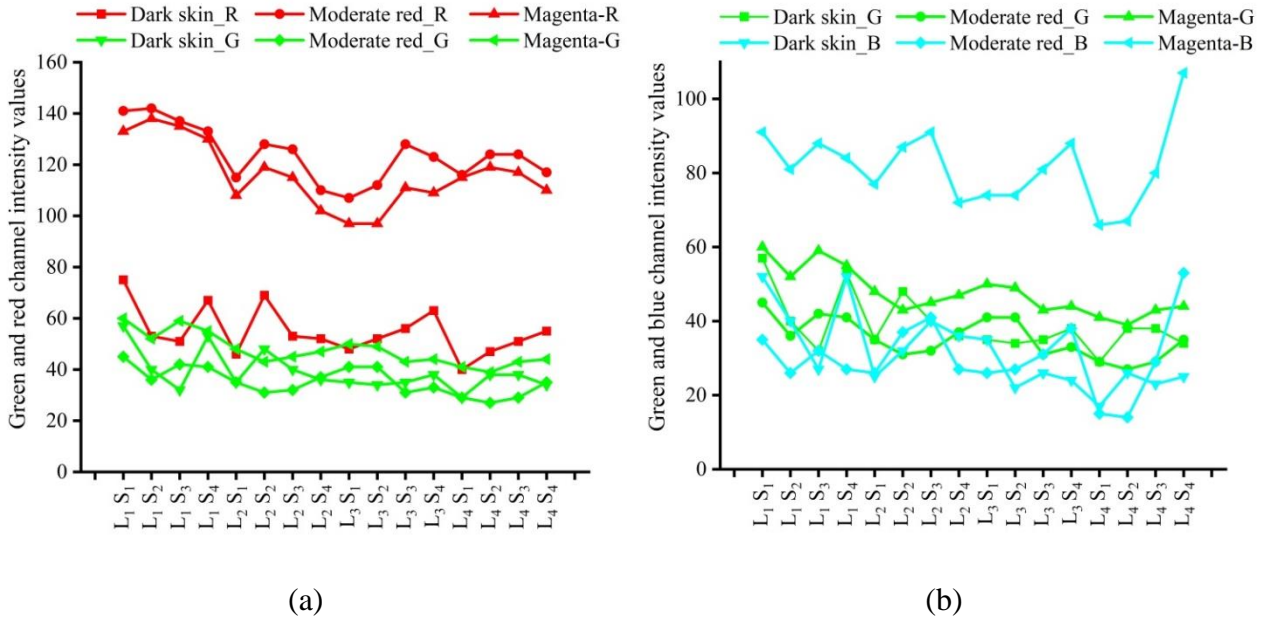
The green and red channel intensity values of green patches are shown in Fig 4.2 (a). The green and blue channel intensity values of green patches are shown in Fig 4.2 (b). It was observed from Fig 4.2 (a) that there was an overlap between green and red channels intensity values of green colour patches. Similarly, there was an overlap between green and blue channel intensity values of green colour patches (Fig 4.2 (b)). The green and red channel intensity values of soil patches are shown in Fig 4.3 (a). The green and blue channel intensity values of soil patches are shown in Fig 4.3 (b).

It was observed from Fig 4.3 (a) that there was an overlap between green and red channel intensity values of soil patches. Similarly, there was an overlap between green and blue channel intensity values of soil patches. This indicates that there was overlap among red, green and blue channel intensity values of green and soil colour patches with variation of illumination intensity and image resolution.



(a) Green and red channels intensity values of green patches, (b) Green and blue channel intensity values of green patches

Fig. 4.2: Red, green and blue channel intensity values of green patches



(a) Green and red channel intensity values of soil patches (b) Green and blue channel intensity values of soil patches

Fig. 4.3: Red, green and blue channel intensity values of soil patches

The red, green and blue channel intensity values of six colour patches were subjected to analysis of variance (ANOVA) (Table 4.3). The variation in red, green and blue intensity values

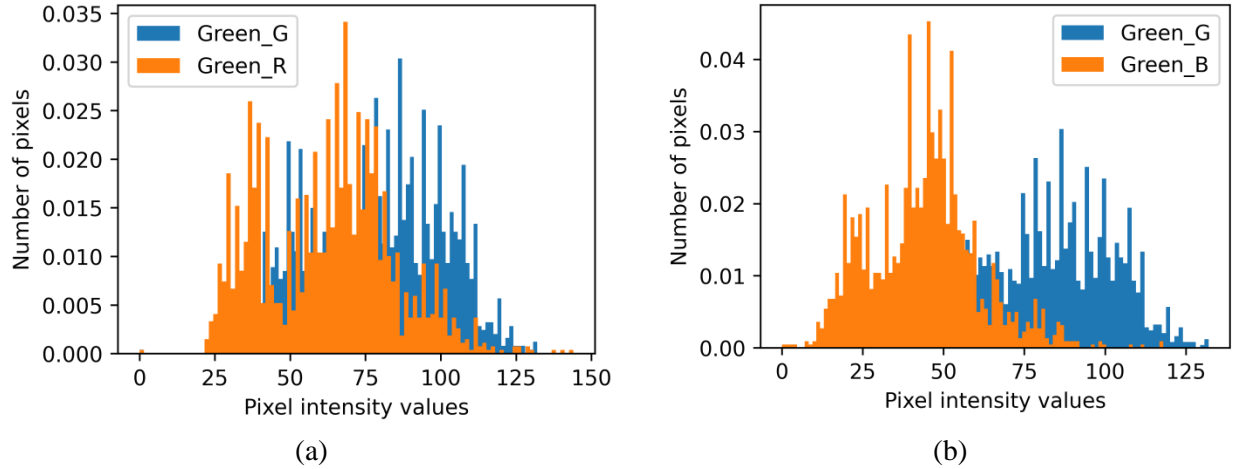
due to variation in illumination intensity (L), image resolution (S) and colour patches (C) were found to be significantly different. The interaction effect of illumination intensity (L) and image resolution (S) on red, green and blue channel intensity values was found to be significantly different. The interaction effect of illumination intensity (L) and colour patch (C) on red and green channel intensity values was found to be significantly different. The interaction effect of illumination intensity (L) and colour patch (C) on blue channel intensity was found to be significantly different. The interaction effect of image resolution (S) and colour patches (C) on red, green and blue channel intensity values was found to be significantly different. The interaction effect of illumination intensity (L), image resolution (S) and colour patches (C) on red, green and blue channel intensity values was found to be significantly different.

Table 4.3: Analysis of variance (ANOVA) of red, green and blue channel intensity

Source of variation	DF	F-value		
		Red channel	Green channel	Blue channel
Illumination intensity (L)	3	310.60 **	312.56 **	16.13 **
Image resolution (S)	3	32.68 **	20.38 **	48.24 **
Colour patches (C)	5	3290.21 **	8850.81 **	755.94 **
L×S	9	18.81 **	23 **	57.28 **
L×C	15	7.10 **	8.34 **	1.39 * *
S×C	15	8.67 *	10.44 *	10.68 *
L×S×C	45	9.45 *	7.75 *	9.92 *
Error	192			
Total	287			

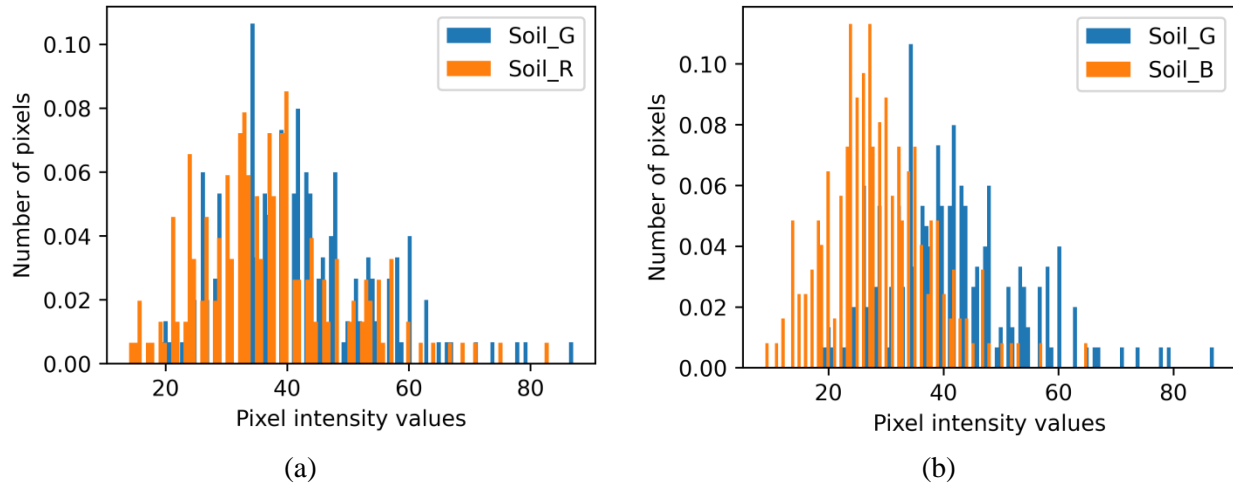
Note: DF: Degree of freedom; “**” = Significant at 1% level of significance; “*” = Significant at 5% level of significance; “ns” = non-significant

The red, green and blue channel intensity values of fresh and healthy green leaves, and soil sample are shown in Fig 4.4 and Fig 4.5. Green, red and blue channel intensity values of green leaves were labeled as Green_G, Green_R and Green_B (Fig 4.4). It was observed from Fig 4.4 that there was an overlap between green and red channel intensity values of green leaves (Fig 4.4(a)). Similar trend was observed between green and blue channel intensity values of green leaves (Fig 4.4(b)). Green, red and blue channel intensity values of soil were labeled as Soil_G, Soil_R and Soil_B (Fig 4.5). It was observed from Fig 4.5 (a & b) that there was an overlap between green and red channel intensity values of soil as well as green and blue channel intensity values of soil.



(a) Green and red channels intensity values of green leaves, (b) Green and blue channel intensity values of green leaves

Fig 4.4: Red, green and blue channel intensity values of green leaves



(a) Green and red channels intensity values of soil sample, (b) Green and blue channel intensity values of soil sample

Fig 4.5: Red, green and blue channel intensity values of soil sample

The variation in excess green index (ExG) intensity values at different illumination intensities and image resolutions is shown in Fig 4.6. It was observed that there was a variation in excess green index intensity values with illumination intensity as well as image resolution. There was small overlap among excess green index intensity values of three green colour patches (foliage, yellow green, green). Similarly, there was small overlap among excess green index intensity values of three soil colour patches (dark skin, moderate red, magenta). However, there was no overlap between excess green index intensity values of green (foliage, yellow green, green) and soil (dark skin, moderate red, magenta) colour patches. The similar behavior was

observed with the excess green minus red index (ExGR) intensity values of green and soil colour patches. The trend in excess green minus red index (ExGR) values at different illumination intensities and image resolutions is shown in Fig 4.7. It was observed from Fig 4.6 and Fig 4.7 that the ExG and ExGR channel intensity values were found to be different at different illumination intensities and image resolutions. Due to this issue a pre-defined threshold value that was to be used for weed and soil pixel classification may not be feasible solution for all conditions.

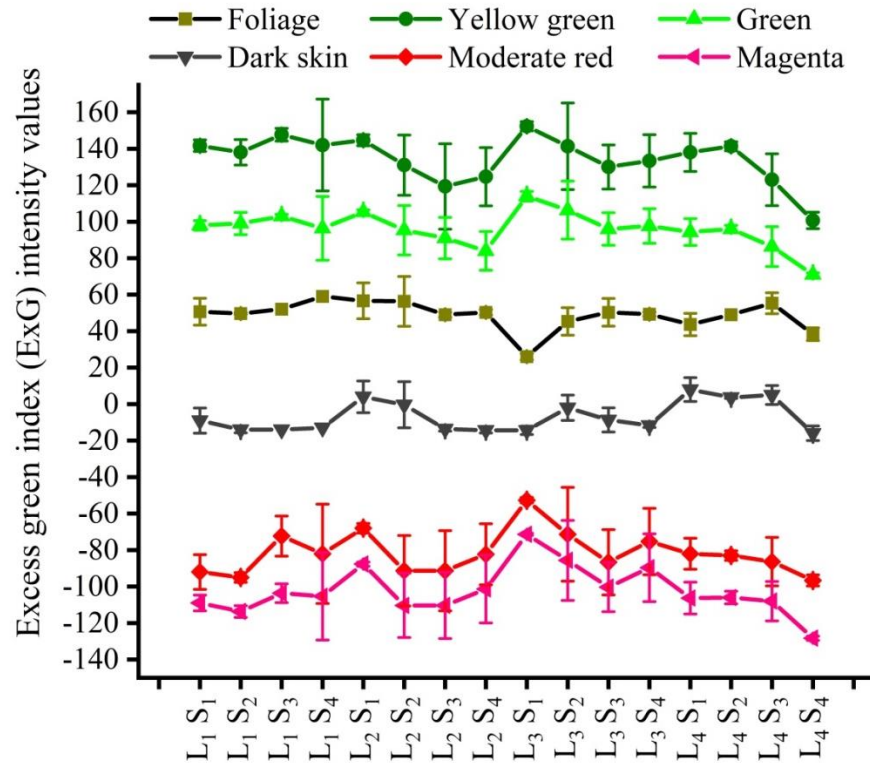


Fig. 4.6: Effect of illumination intensity and image resolution on ExG intensity values

The ExG and ExGR channel intensity values of six colour patches were subjected to analysis of variance (ANOVA) (Table 4.4). The variation in ExG and ExGR channel intensity values due to variation in illumination intensity (L), image resolution (S) and colour patches (c) was found significantly different. The interaction effect of illumination intensity (L) and image resolution (S) and the interaction effect of illumination intensity (L) and colour patches (C) on ExG and ExGR channel intensity values were found to be significantly different. The interaction effect of image resolution (S) and colour patches (C) on ExG and ExGR channel intensity values was found to be significantly different. The interaction effect of illumination intensity (L), image

resolution (S) and colour patches (C) on ExG and ExGR channel intensity values was found to be significantly different.

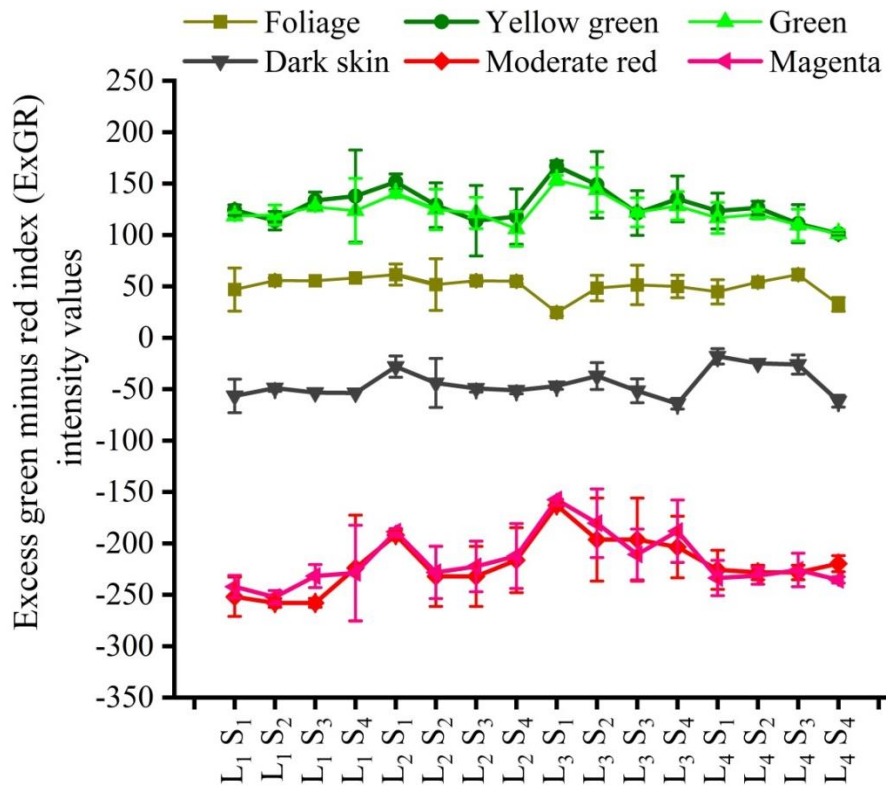


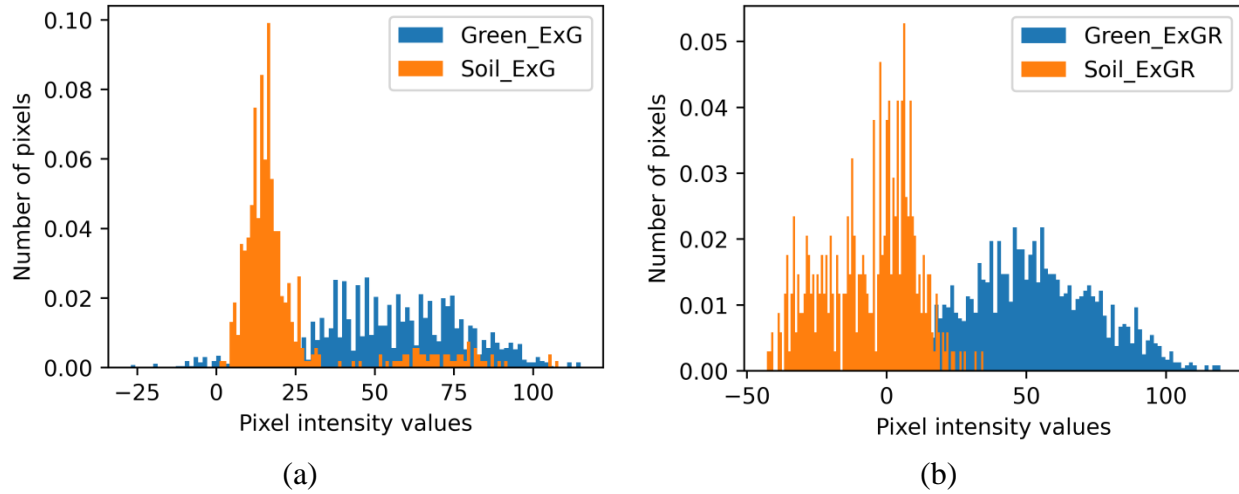
Fig. 4.7: Effect of illumination intensity and image resolution on ExGR intensity

Table 4.4: Analysis of variance of ExG and ExGR channel intensity

Source of variation	DF	F-value	
		Excess green index (ExG)	Excess green minus red index (ExGR)
Illumination intensity (L)	3	8.99 **	16.25 **
Image resolution (S)	3	11.59 **	5.71 **
Colour patches (C)	5	3503.27 **	3498.13 **
L×S	9	6.43 **	5.62 **
L×C	15	4.71 **	5.12 **
S×C	15	1.86 *	1.68 *
L×S×C	45	1.82 *	1.73 *
Error	192		
Total	287		

Note: DF: Degree of freedom; “**” = Significant at 1% level of significance; “*” = Significant at 5% level of significance; “ns” = non-significant

The excess green index and excess green minus red index values of fresh and healthy leaves and soil sample are shown in Fig 4.8 (a & b). There was a separate histogram for each class (leaves and soil). There was some overlap was observed between ExG and ExGR values of leaves and soil sample. There was more overlap among ExG values of leaves and soil sample than ExGR intensity values.



(a) ExG intensity values of fresh and healthy leaves and soil sample (b) ExGR intensity values of fresh and healthy leaves and soil sample

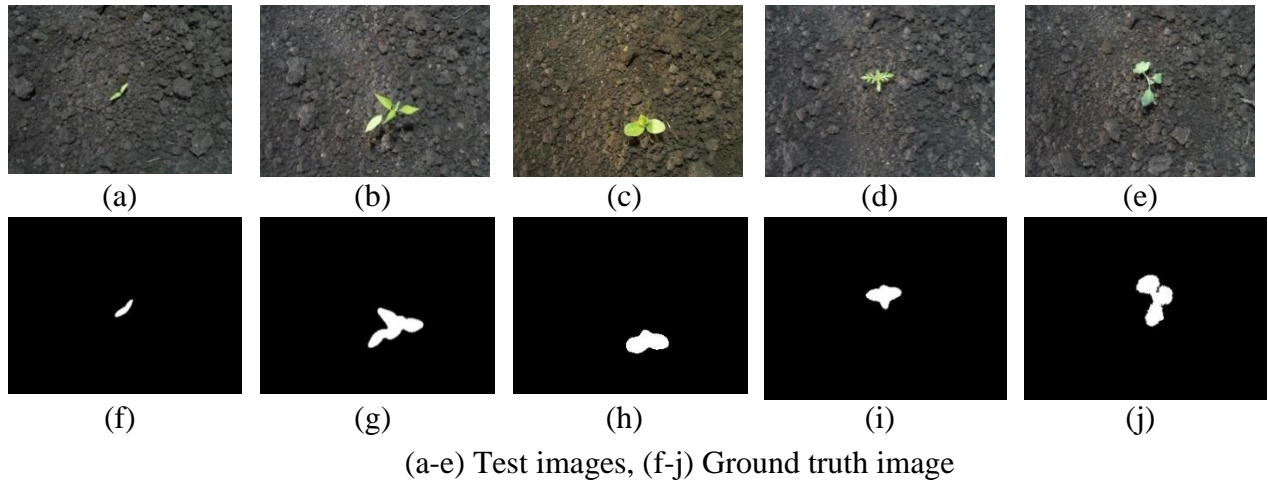
Fig. 4.8: ExG and ExGR intensity values of green leaves and soil sample

4.3 Development of software for ground truth image creation and performance metrics computation

The performance metrics were used to quantify green and soil pixel classification accuracy of plant segmentation methods. Before going to the computation of true positive (TP), true negative (TN), false negative (FN), false positive (FP) metrics, the actual pixels labels of image were to be identified. The performance metrics were calculated by comparing actual pixels labels with pixels of segmented image obtained from plant segmentation methods.

4.3.1 Development of machine learning algorithm for ground truth image creation

The Random forest classifier was employed for ground truth creation process. The performance of random forest model was expressed in terms of precision, recall and false positive rate. The precision, recall and false positive rate were found to be 99.87 %, 99.56 % and 0 %, respectively. The test images and ground truth images are shown in Fig 4.9.

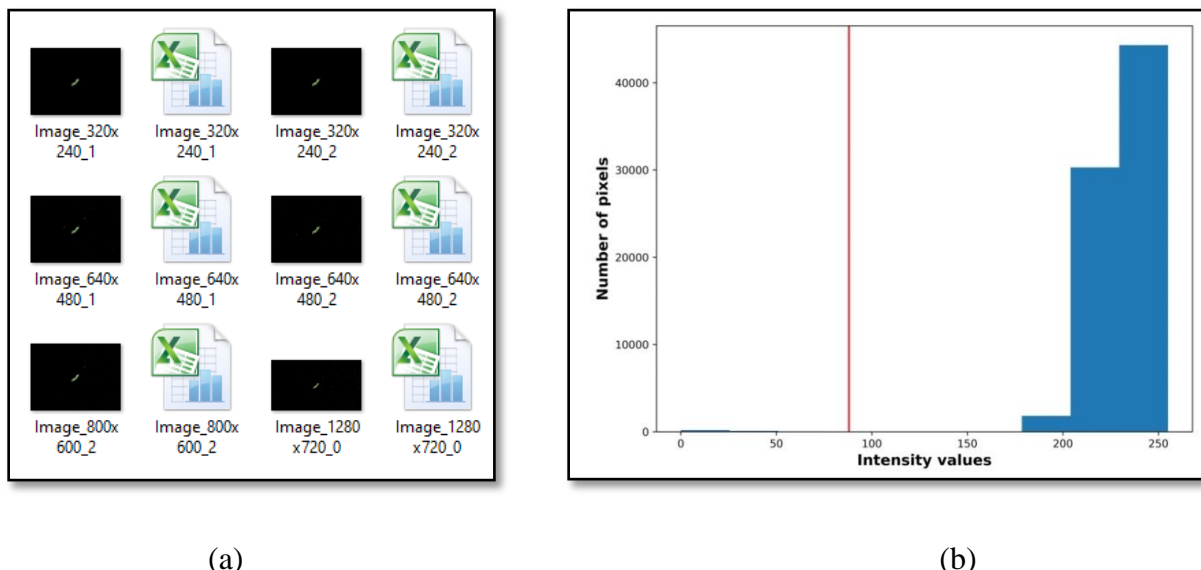


(a-e) Test images, (f-j) Ground truth image

Fig. 4.9: Test images and corresponding ground truth images

4.3.2 Development of Python module to automate performance metrics computation

Specialized software was developed using python module for calculating the performance metrics of each plant segmentation methods at different threshold values. The developed software generates separate excel file for each test image. The excel file contains performance metrics information and threshold value. In case of Otsu method, based on grayscale histogram the Otsu threshold value was generated. This threshold value was also saved in excel file for each test image. The outcome of developed software is shown in Fig 4.10.



(a)

(b)

The figure consists of two side-by-side screenshots of Microsoft Excel. Both screenshots show a table with columns A through E and rows 1 through 8. The tables represent performance metrics for two different images: 'Image_3...' on the left and 'Image_6...' on the right.

Table for Image_3... (Left):

	A	B	C	D	E
1		20			
2	TP	910			
3	TN	75304			
4	FP	3			
5	FN	48			
6	Precision	100			
7	Recall	95			
8	FPR	0			

Table for Image_6... (Right):

	A	B	C	D	E
1			127		
2	TP		1918		
3	TN		45028		
4	FP		257129		
5	FN		2082		
6	Precision		1		
7	Recall		48		
8	FPR		85		

(c)

(d)

- (a) Segmented image and excel file (b) Histogram shows dynamic threshold value generated by Otsu technique (c) Performance metrics of pre-defined threshold method (d) Performance metrics of dynamic threshold method

Fig. 4.10: Output of developed software to compute performance metrics

4.4 Effect of threshold value of plant segmentation methods on classification accuracy of weed and soil pixels

After finalizing illumination intensity of light, threshold values of plant segmentation methods for weed and soil pixel classification were optimized. Four plant segmentation methods were used for weed and soil pixels classifications in the present study. Excess green index (ExG), excess green minus red index (ExGR), hue-saturation-value (HSV) and CIELAB were used as plant segmentation methods. Fresh and healthy leaves and soil sample were collected. The images of these leaves and soil samples were captured at four working heights and four image resolutions under light source testing platform at finalized illumination intensity of 89 ± 4.4 lx. Four working heights 400, 500, 600 and 700 mm were considered. Four image resolutions 320×240, 640×480, 800×600 and 1280×720 pixels were considered as stated in section 3.5.

The test image weed and soil pixels classification results of ExG method at different threshold values are shown in Appendix-I. The corresponding threshold value of segmented image was given in name of image file itself. It was observed that at each threshold value there was either over segmentation or under segmentation. The trend in precision, recall and false positive rate of ExG method at different threshold values are shown in Fig 4.11. It was observed from Fig 4.11 that when ExG threshold value was greater than 0, the recall was found to be 100%. That means all weed pixels were correctly classified as weed pixels. But at same threshold value the false positive rate was found to be 90.56 %. that means 90.56 % soil pixels were misclassified as weed pixels. Further increasing threshold value from 0 to 150, there was gradual decreasing trend in recall. The recall was found to be almost 0 after threshold value 150. But there was sharp decrease in false positive rate when threshold value increased from 0 to 25. Further increasing threshold value from 25 to 240, there was no change was observed in false positive rate. There was slight decline in false positive rate observed at threshold value of 250. The similar behaviour was observed in case of ExGR method. Test image segmentation results of ExGR, HSV and CIELAB methods at different threshold values are shown in Appendix-I. The trend in precision, recall and false positive rate of ExGR, HSV and CIELAB methods at different threshold values are shown in Fig 4.12, Fig 4.13 and Fig 4.14.

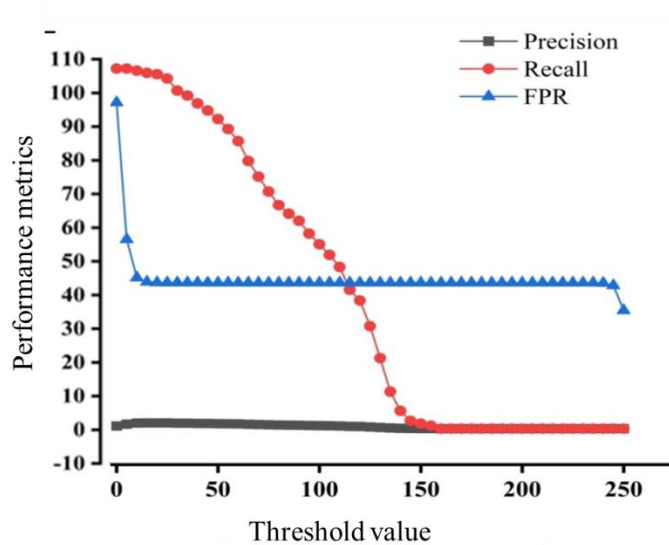


Fig. 4.11: Performance metrics of excess green index (ExG) method at different threshold values

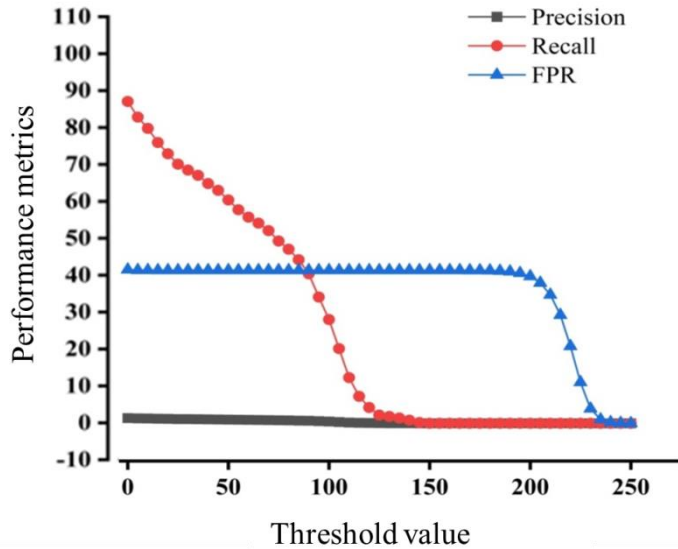


Fig. 4.12: Performance metrics of excess green minus red index (ExGR) method at different threshold values

It was observed from Fig 4.14 that when hue channel threshold value was greater than 0, the recall was found to be 100 %. That means all weed pixels were correctly classified as weed pixels. Increasing threshold value from 0 to 50, there was sudden decrease in recall. It reaches to 4.94 % at threshold value 50. Similarly, when hue channel threshold value was greater than 0, the false positive rate was found to be 93.69 %. That means 93.69 % soil pixels were misclassified as weed pixels. Further increasing threshold value from 0 to 255, there was a gradual decline in false positive rate. The false positive rate was approached to 0 when threshold value reached to 200. That means all soil pixels were correctly classified as soil pixels. It was observed from Fig 4.15 that when A channel threshold was set greater than 0, the recall was found to be 100 %. That means all weeds pixels were classified correctly as weed pixels. This trend was continued upto threshold value 95. But at same time when A channel threshold was set greater than 0, false positive rate was found to be 100 %. That means all soil pixels were misclassified as weed pixels. This trend was continued upto threshold value 125. The precision was followed same trend in all threshold values because at every threshold value either weed classified as soil (FN) or soil classified as weed (FP) was happened. When A channel threshold was set greater than 135, the false positive rate became 0. That means all soil pixels were correctly classified as soil pixels. But same threshold value all weed pixels were misclassified as soil pixels.

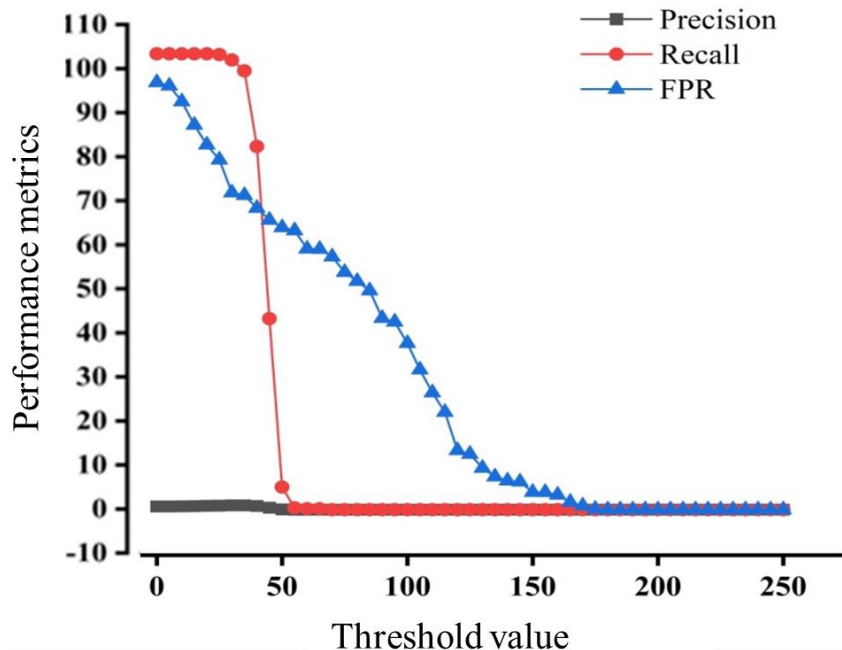


Fig. 4.13: Performance metrics of HSV method at different threshold values

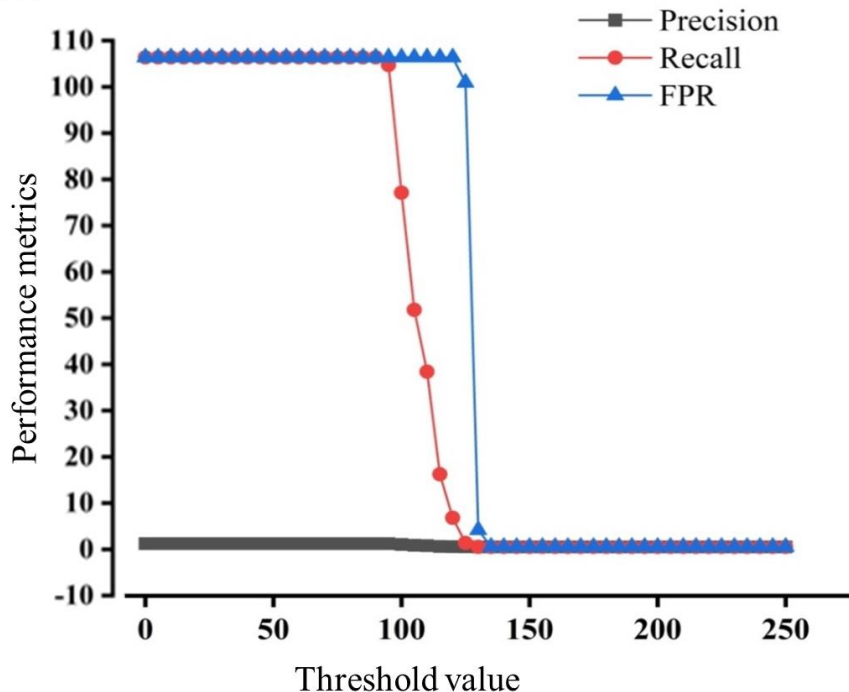
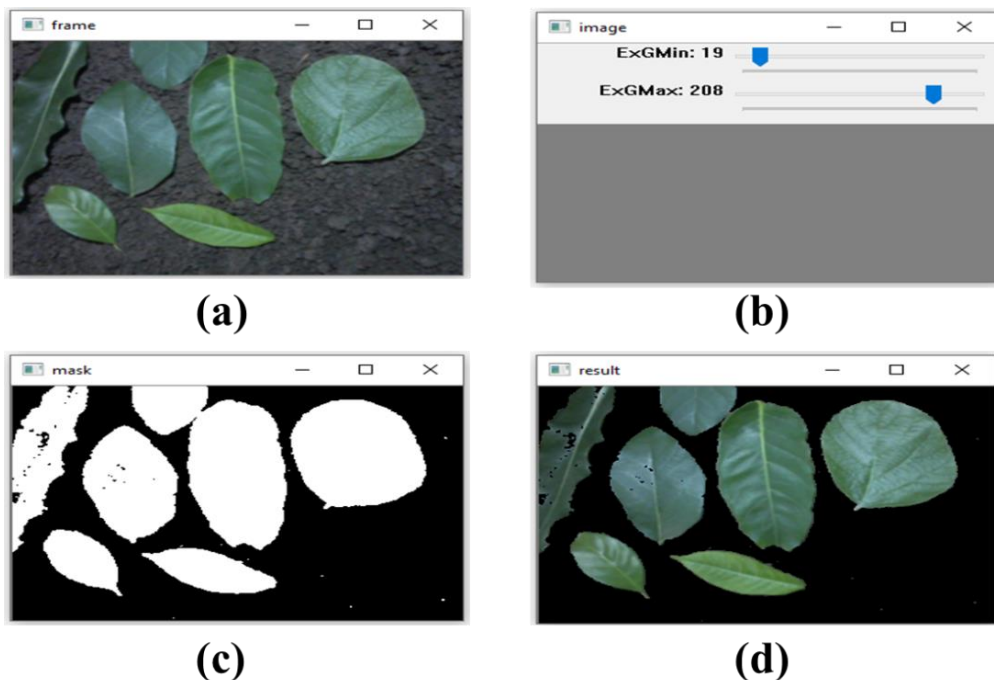


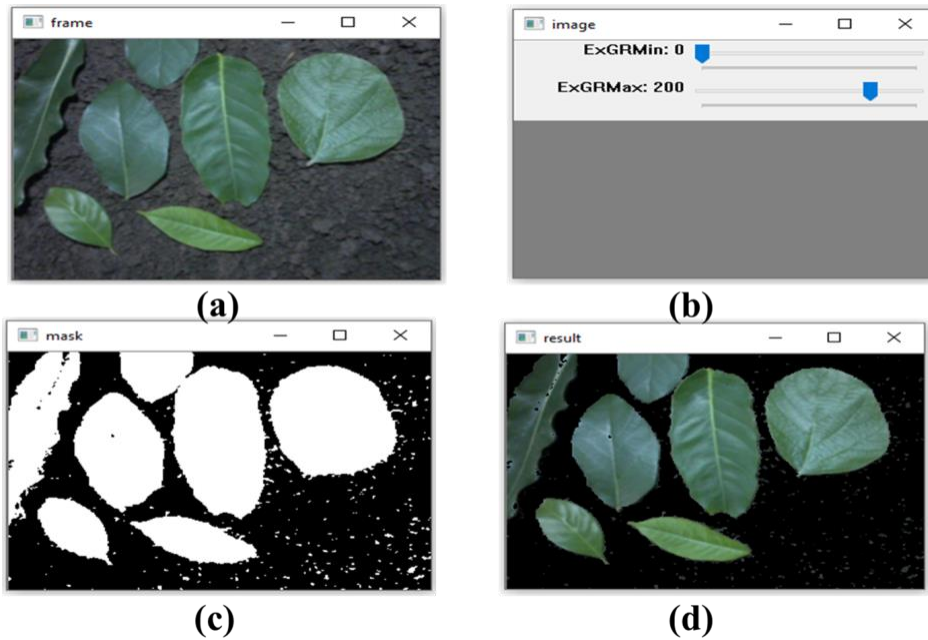
Fig. 4.14: Performance metrics of CIELAB method at different threshold values

Graphical user interface (GUI) using python has been developed to select the lower boundary and upper threshold values of colour indices and colour models for weed and soil pixel classification. ExG, ExGR, HSV and CIELAB GUI's were developed (Fig 4.15 to Fig 4.18). The excess green index (ExG) and excess green minus red index (ExG) were single channel images, hence two track bars were used, whereas HSV and CIELAB methods consists of three channels, hence, six track bars were used. "V" channel of HSV colour represents lighness. In present study same illumination intensity was maintained throughout experiment, hence, default values were used for V channel. The lower limit and upper of V channel were 0 and 255, respectively. Similarly, "L" channel of CIELAB colour model represents lighness, hence default values were used for L channel. The lower limit and upper of L channel were 0 and 255, respectively. Moreover, "B" channel of CILAB colour model consists of blue and yellow colour information, hence, this channel intensity values were set as default values. The lower limit and upper of B channel were 0 and 255, respectively.



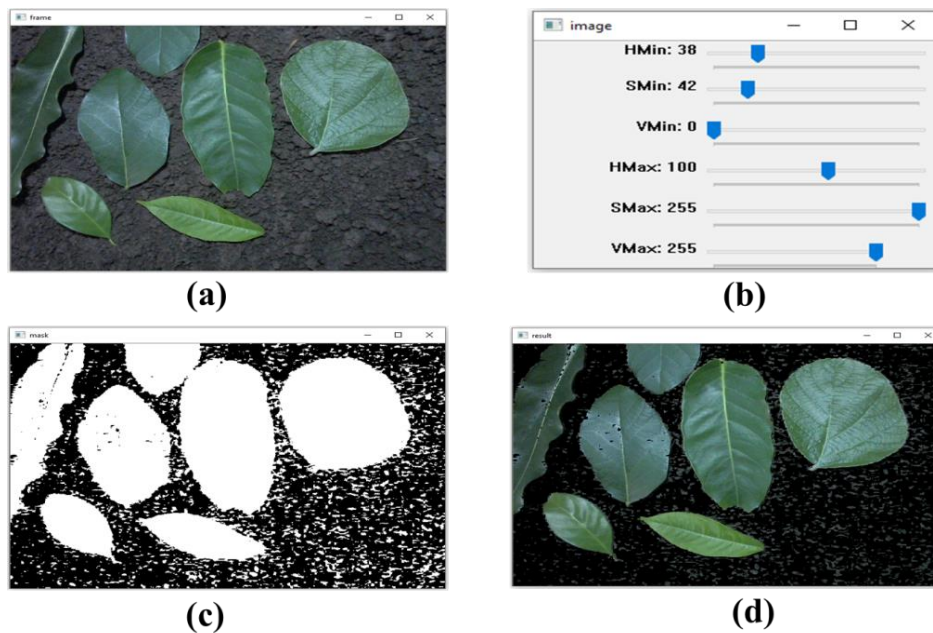
a) Acquired image (b) ExG track bar (c) Segmented image (d) Masked image

Fig. 4.15: GUI of excess green index



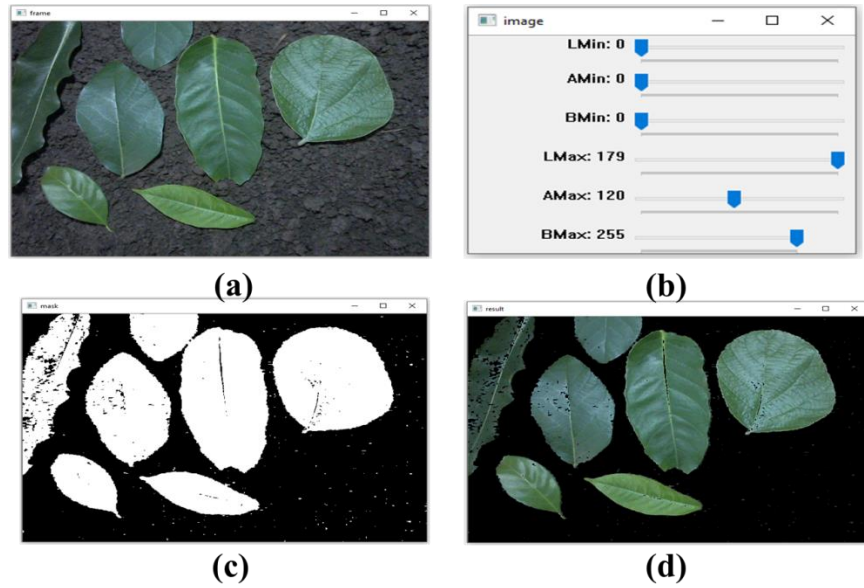
(a) Acquired image (b) ExGR track bar (c) Segmented image (d) Masked image

Fig. 4.16: GUI of excess green minus red index (ExGR)



(a) Acquired image (b) HSV track bar (c) Segmented image (d) Masked image

Fig. 4.17: GUI of HSV method



(a) Acquired image (b) CIE LAB track bar (c) Segmented image (d) Masked image

Fig. 4.18: GUI of CIELAB method

The lower limit and upper limit of ExG, ExGR, HSV and CIELAB methods of different leaves were analysed. Using the trackbar window the lower and upper threshold limits of ExG were adjusted till get better foreground and background pixels classification. By visual inspection of masked image and segmented image, the final lower and upper threshold limits of particular image was adjusted. Similar way lower and upper threshold limits of ExGR, HSV and CIELAB were computed. The lower and upper limit of different leaves ExG, ExGR, HSV and CIELAB methods are shown in Table 4.5. Finally, the lower limit and upper limit were selected as 20 and 210 for ExG, 0 and 190 for ExGR, 30 and 100 for HSV, 0 and 120 for CIELAB, respectively.

Table 4.5: Threshold values of ExG, ExGR, HSV and CIELAB models

S. No.	ExG		ExGR		HSV		CIELAB	
	Lower	Upper	Lower	Upper	Lower	Upper	Lower	Upper
1	20	200	0	190	47	104	0	120
2	18	205	0	185	31	108	0	115
3	18	205	0	183	31	99	0	115
4	21	228	0	190	53	99	0	119
5	17	213	0	190	53	99	0	123
6	19	235	0	189	48	99	0	120

4.5 Effect of working height, image resolution, plant segmentation methods on classification accuracy of weed and soil pixels

In section 4.4, the threshold values of plant segmentation methods were optimized. The lower and upper threshold limits were finalized as 20 and 210 for ExG, 0 and 190 for ExGR, 30 and 100 for HSV, 0 and 120 for CIELAB, respectively. The effect of optimized threshold values on weed and soil pixel classification accuracy was studied in this section. Along with optimized threshold values, the effect of dynamic threshold value on weed and soil pixel classification accuracy was studied. Along with two threshold methods of plant segmentation methods, the effect of working height and image resolution on weed and soil pixel classification was studied. The optimized threshold values and dynamic threshold value of ExG, ExGR, HSV and CIELAB methods were tested on images captured at four working heights and four image resolutions under illumination intensity of 89 ± 4.4 lx. The weed and soil pixels classification accuracy of ExG, ExGR, HSV and CIELAB methods at four working heights and four image resolutions is shown in Fig 4.19 to 4.24. The precision, recall and false positive rate values of plant segmentation methods at different working heights and image resolutions were computed and tabulated (Table 4.6).

It was observed from experimental results (Table 4.6) that the optimized threshold value of ExG method showed the highest precision (>90 %), recall (>90 %) and lowest false positive rate (<5 %) for image resolutions of 640×480, 800×600 and 1280×720 pixels at working height of 500 mm, for image resolutions of 640×480, and 800×600 at working height of 600 mm and for image resolutions of 640×480, 800×600 and 1280×720 at working height of 700 mm. Similarly, the optimized threshold value of ExGR method showed the highest precision (>90 %), recall (>90 %) and lowest false positive rate (<5 %) for image resolutions of 320×240, 640×480, 800×600, 1280×720 pixels at working height of 400 mm and for image resolution of 1280×720 pixels at working height of 600 mm.

The optimized threshold value of HSV method showed the highest precision (>90 %), recall (>90 %) and lowest false positive rate (<5 %) for image resolutions of 320×240, 640×480 and 800×600 pixels at working height of 400 mm, for image resolutions of 800×600 and 1280×720 pixels at working height of 500 mm and for image resolutions of 1280×720 pixels at

working height of 600 mm. It was observed from performance metrics of plant segmentation methods at different working height and image resolution that the optimized threshold values of CIELAB method showed the highest precision (>90 %), recall (>90 %) and lowest false positive rate (<5 %) in all four working heights and four image resolutions (Fig 4.19, Fig 4.21 and Fig 4.23).

It was observed from experimental results (Table 4.6) that dynamic threshold value of ExG, ExGR and HSV method showed under segmentation or over segmentation of weed and soil pixels in all four working heights and four image resolutions (Fig 4.20, Fig 4.22 and Fig 4.24). The dynamic threshold value of CIELAB method showed the highest precision (>90 %), recall (>90 %) and lowest false positive rate (<5 %) in all four image resolutions at working height of 400 and 500 mm (Fig.4.20). The dynamic threshold value of CIELAB method showed under segmentation or over segmentation at in all image resolutions at working height of 600 and 700 mm (Fig.4.20).

The precision, recall and false positive value of ExG + Pre-defined threshold method were subjected to three way analysis of variance (ANOVA) (Table 4.7). It was also observed from ANOVA that variation caused in precision, recall and false positive rate due to test image, working height and image resolution were found to be significantly different. Similarly, variation caused in precision, recall and false positive rate due to interaction effect of test image, working height and image resolutions were also found to be significantly different. The same trend was observed in ExGR+ Pre-defined threshold, HSV+ Pre-defined threshold, CIELAB + Pre-defined threshold, ExG+ Dynamic threshold, ExGR+ Dynamic threshold, HSV+ Dynamic threshold, CIELAB + Dynamic threshold (Table 4.8 to Table 4.10).

Table 4.6: Performance metrics of plant segmentation methods at different working height and image resolution

Working height(mm)	Image resolution	M ₁	M ₂	M ₃	M ₄	M ₅	M ₆	M ₇	M ₈	
400	320×240	Precision (%)	53±12	95±2	96±1.2	95±3	0	32±18	0	87±10
		Recall (%)	98±1.5	96±3	95±2.2	96 ±2	39±14	9 ±4	92±2	89±3
		FPR (%)	3±2	0	0	3 ± 1.2	95±4	0	70±8	0
	640×480	Precision	63±12	97±1.2	95±3	97±2	5±1.2	65±16	10±5	91±3
		Recall	95±2	94±4	97±2	91±3	48±20	94±2	95±4	91±4
		FPR	2.5 ±2	0	0	5± 3	85±15	20±12	88±8	0
	800×600	Precision	82±4	97±1.2	95±2	94±2	8±4	60±20	15±2	90±2
		Recall	94±2	95±2	97±3	90±4	51±18	9 ±4	94±5	93±4
		FPR	2.5±2	0	0	0	75±10	20±10	89±3	0
	1280×720	Precision	82±5	95±2	95±2.3	36±10	42±10	47±21	10±2.8	90±5
		Recall	95±2	94±4	83±7	96±3	63±14	9 ±2.3	83±9	94±3
		FPR	4±2	2.1±2.1	0	0	51±17	20±10	44±20	0
500	320×240	Precision (%)	94±2.1	79±13	90±4	95±2.6	20±8	64±12	20±10	88±10
		Recall (%)	87±7	90±4	79±12	9 ±1.5	82±12	91±5	79±12	91±3
		FPR (%)	0	2.5±2.2	0	3 ±1.2	61±14	0	43±20	0
	640×480	Precision	95±3	82±12	94±2	95±2.2	42±21	76±12	45±12	92±2
		Recall	92±4	94±2	82±8	92±2.3	63±20	95±2	82±8	93±3
		FPR	0	2.1±1.2	0	0	59±12	10±5	60±12	0
	800×600	Precision	97±1.2	80±5.2	93±2.5	95±2.1	12±3.1	69±15	20±14	91±4.1
		Recall	93±2.3	93±4.2	80±7	92±3.2	66±14	93±13.2	80 12	94±2.2
		FPR	0	3.2±2.1	0	0	49±20	20±7	46±20	0
	1280×720	Precision	95±2	78±12	92±3	96±2	20±12	75±12	3±1.2	95±2
		Recall	93±3	92±3	78±12	96±2	79±11	92±4	78±12	94±2.2
		FPR	0	3.5±2	0	0	49±17	20	45±14	0
600	320×240	Precision (%)	97±2.2	66±22	81±9	93 ± 4	20±12	57±14	27±3.2	93±2.5
		Recall (%)	77±12	81±8	66±14	92 ±4	97±2.2	82±7	66±12	91±3.5
		FPR (%)	0	8.2±4	0	0	25±14	0	2±1.2	46±12
	640×480	Precision	95±4.2	76±15	91±2.2	97±2	10±2.5	83±7.2	7±2.2	93±2.2
		Recall	90±5	91±14	76±12	94±2	83±4	92±3	76±14	92±4.2
		FPR	0	2.5±1.2	0	0	46±12	10±4.5	12±2.2	44±14
	Precision	97±1.2	86±12	92±2.2	95±5	20±13	96±2	40±15	94±1.1	

	800×600	Recall	93±2.2	92±4	86±10	97±1.2	76±12	93±2.2	86±3.3	94±2.5
		FPR	0	1.8±1.1	0	0	53±22	10±2.2	32±8.7	45±15
	1280×720	Precision	96±2.2	94±1.2	92±5	97±1.1	10±5.2	76±15	20±12	94±2.2
		Recall	93±2.3	92±2.3	94±2.5	97±1.2	74±12	93±4	94±2	93±2.2
		FPR	0	0	0	0	58±15	20±12	41±12	61±14
	320×240	Precision (%)	97±1.1	97±1.2	86±12	93±2.2	22±1.2	95±2.2	10±8	92±2.2
		Recall (%)	85±2.5	86±10	96±2.2	91±3.6	78±12	86±3.6	93±2.2	86±4.4
		FPR (%)	0	0	0	0	88±2.3	22±2.2	90±2.2	56±14
	640×480	Precision (%)	96±1.2	97±2.2	87±5.6	97±1.1	10±2.2	93±2.3	10±2.5	9 ±2.1
		Recall (%)	93±3.2	87±4.2	97±1.1	97±2.2	61±5.2	88±3.2	97±1.2	93±3.2
		FPR (%)	0	0	0	0	65±12	20±12	90±3.5	71±14
700	800×600	Precision (%)	92±2.8	97±1.2	88±2.3	95±3.1	10±2.2	88±2.5	15±2.5	94±2.2
		Recall (%)	93±3.9	88±2.2	97±1.2	96±1.2	61±12	89±5.2	92±5	92±3.6
		FPR (%)	0	0	0	0	74±14	10±2.3	84±10	59±15
	1280×720	Precision (%)	95±1.2	96±2.2	89±3.5	94±2.2	18±2.2	67±17	18±2.3	94±2.2
		Recall (%)	94±2.2	89±5.2	96±2.2	92±2.2	60±12	90±3.2	96±1.2	93±1.5
		FPR (%)	0	0	0	0	67±14	10±3.2	70±12	58±17

Note: M_1 : ExG + Pre-defined threshold; M_2 : ExGR + Pre-defined threshold; M_3 : HSV + Pre-defined threshold; M_4 : CIELAB + Pre-defined threshold; M_5 : ExG + Dynamic threshold; M_6 : ExGR + Dynamic threshold; M_7 : HSV+ Dynamic threshold; M_8 : CIELAB + Dynamic threshold

Table 4.7: Analysis of variance (ANOVA) of precision, recall and false positive rate of ExG method

Source of variation	DF	F-value		F-value		
		Pre-defined threshold value		Dynamic threshold value		
		Precision	Recall	Precision	Recall	FPR
Test image (A)	9	558.80 **	6.80 **	533.69 **	5.55 **	479.97 **
Working height (B)	3	234.21 **	234.21 **	12.07 **	17.01 **	26.19 **
Image resolution (C)	3	742.10 **	742.10 **	113.54 **	22.01 **	15.21 **
A×B	27	2.1 **	1.64 *	2.29 **	3.46 **	1.64 *
A×C	27	206.19 **	206.19 **	2.99 **	28.81 **	17.30 **
B×C	9	39.39 **	39.39 **	15.01 **	12.43 **	26.35 **
A×B×C	81	16.36 **	16.36 **	1.58 **	3.73 **	2.46 **
Error	320					
Total	479					

Note: DF: Degree of freedom; “**” = Significant at 1% level of significance; “*” = Significant at 5% level of significance; “ns”=non-significant

Table 4.8: Analysis of variance (ANOVA) of precision, recall and false positive rate of ExGR method

Source od variation	DF	F-value		F-value		
		Pre-defined threshold value		Dynamic threshold value		
		Precision	Recall	Precision	Recall	FPR
Test image (A)	9	26.25 **	5.20 *	2505.46 **	4.96 **	85.10 **
Working height (B)	3	1086.95 **	167.82 **	325.56 **	180.70 **	6.16 **
Image resolution (C)	3	6713.20 **	20.20 **	10584.68 **	40.95 **	7.14 **
A×B	27	20.98 **	3.12 *	670.16 **	2.79 *	7.64 **
A×C	27	1499.59 **	103.10 **	1668.38 **	137.00 **	19.59 **
B×C	9	461.53 **	10.58 **	351.35 **	14.12 **	3.73 **
A×B×C	81	104.59 **	8.20 **	182.04 **	11.26 **	3.91 **
Error	320					
Total	479					

Note: DF: Degree of freedom; “**” = Significant at 1% level of significance; “*” = Significant at 5% level of significance; “ns”=non-significant

Table 4.9: Analysis of variance (ANOVA) of precision, recall and false positive rate of HSV method

Source of variation	DF	F-value			F-value	
		Pre-defined threshold value		Dynamic threshold value		
		Precision	Recall	Precision	Recall	FPR
Test image (A)	9	43.34 **	34.10 **	1879.81 **	50.67 **	267.87 **
Working height (B)	3	38.06 **	24.98 **	58.61 **	49.80 **	19.85 **
Image resolution (C)	3	154.80 **	12.65 **	46.49 **	135.48 **	269.54 **
A×B	27	2.03 **	2.028 **	94.27 **	10.75 **	16.15 **
A×C	27	51.19 **	37.57 **	14.76 **	6.61 **	20.30 **
B×C	9	8.26 **	2.26 *	4.20 **	35.64 **	7.90 **
A×B×C	81	4.63 **	3.48 **	4.63 **	13.04 **	4.81 **
Error	320					
Total	479					

Note: DF: Degree of freedom; “**” = Significant at 1% level of significance; “*” = Significant at 5% level of significance; “ns”=non-significant

Table 4.10: Analysis of variance (ANOVA) of precision, recall and false positive rate of CIELAB method

Source of variation	DF	F-value			F-value	
		Pre-defined threshold value		Dynamic threshold value		
		Precision	Recall	Precision	Recall	
Test image (A)	9	66.46 **	46.11 **	131.86 **	173.26 **	
Working height (B)	3	22.88 **	16.96 **	37.61 **	43.69 **	
Image resolution (C)	3	40.63 **	3.99 **	26.72 **	37.81 **	
A×B	27	2.08 **	1.56 *	5.37 **	6.49 **	
A×C	27	37.78 **	23.66 **	55.93 **	78.95 **	
B×C	9	5.75 *	8.18 *	4.01 **	7.54 **	
A×B×C	81	3.19 **	2.24 **	4.85 **	7.69 **	
Error	320					
Total	479					

Note: DF: Degree of freedom; “**” = Significant at 1% level of significance; “*” = Significant at 5% level of significance; “ns”=non-significant

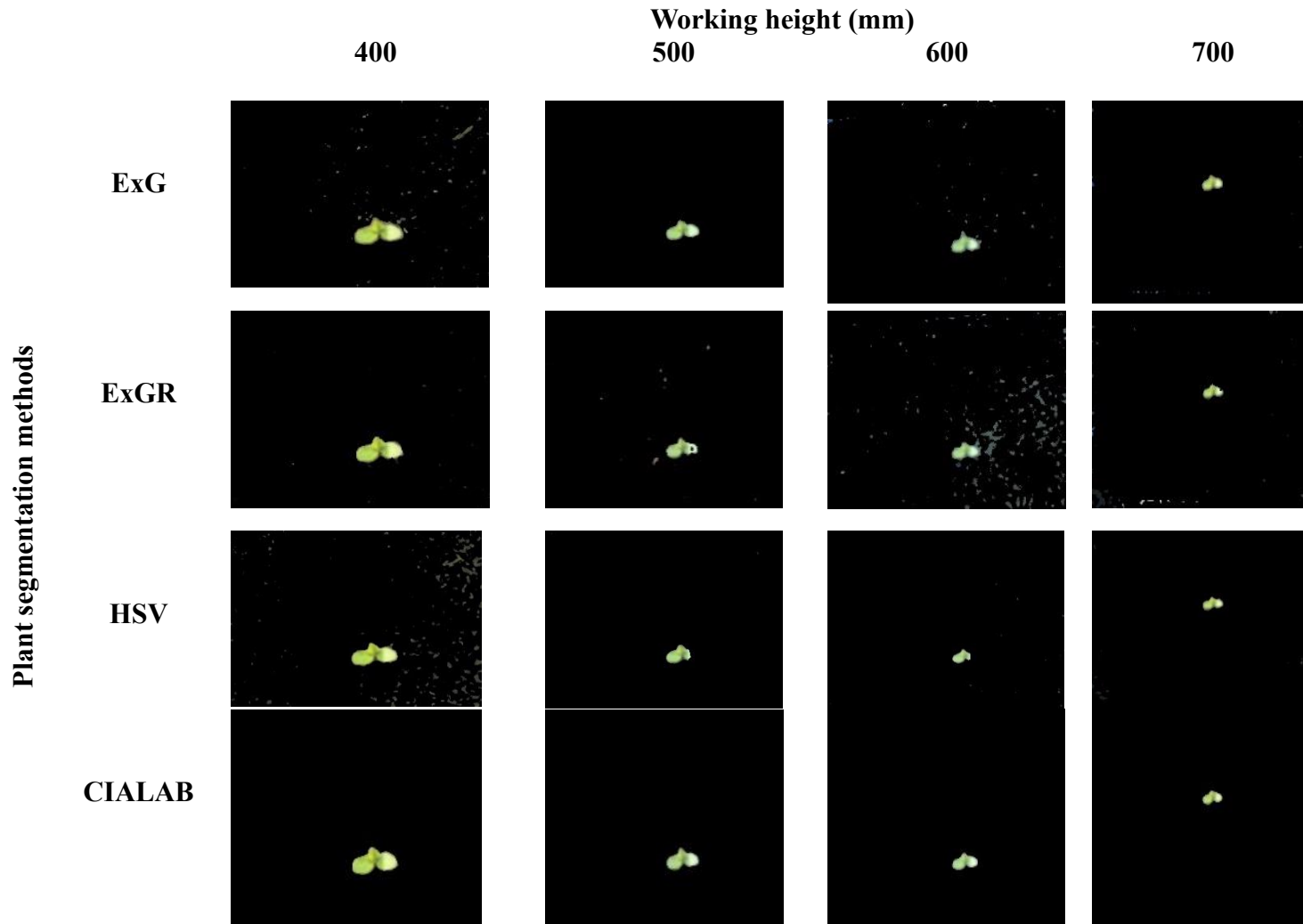


Fig.4.19: Effect of plant segmentation methods with pre-defined threshold value and working height on weed and soil pixels classification accuracy

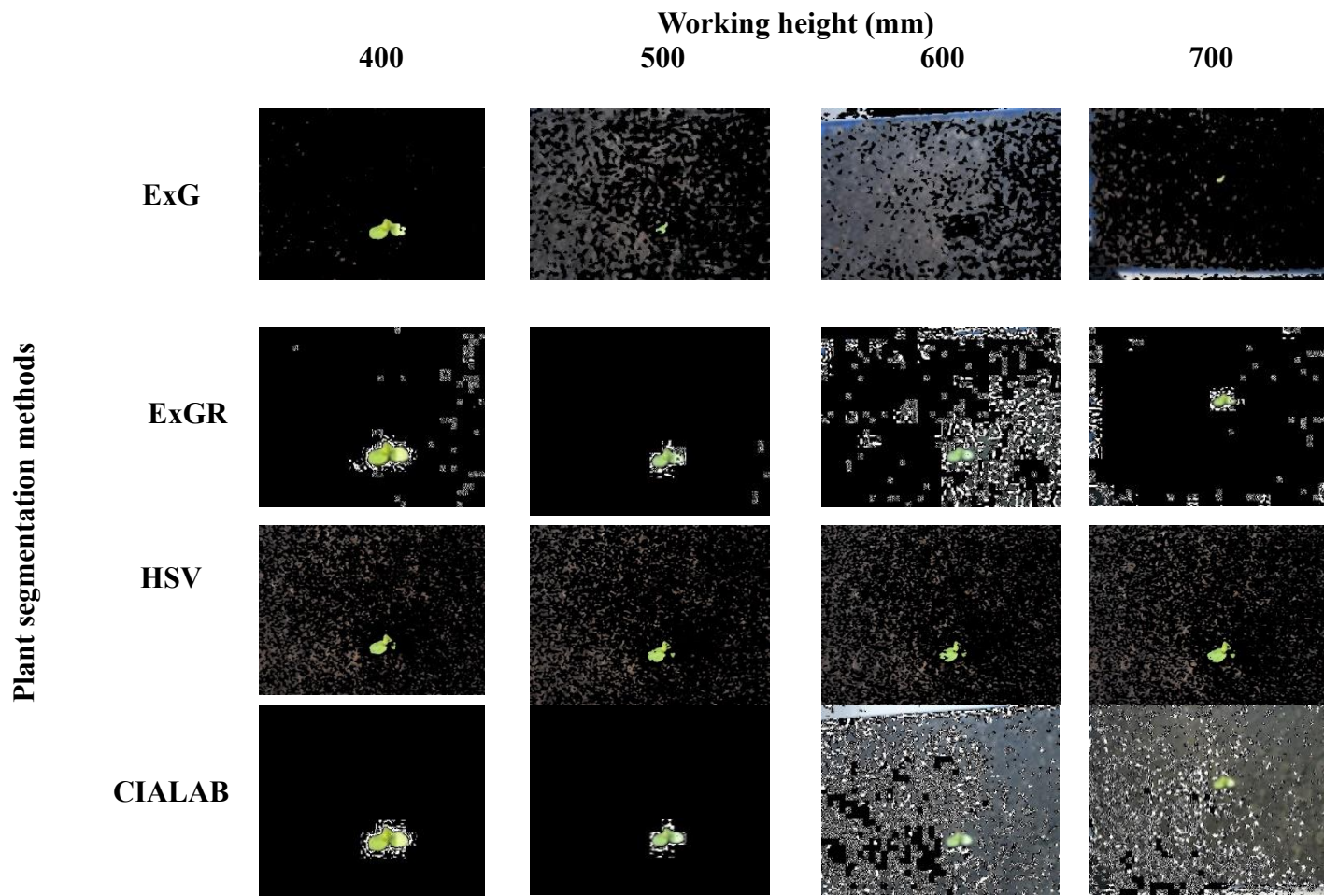


Fig.4.20: Effect of plant segmentation methods with dynamic threshold value and working height on weed and soil pixels classification accuracy

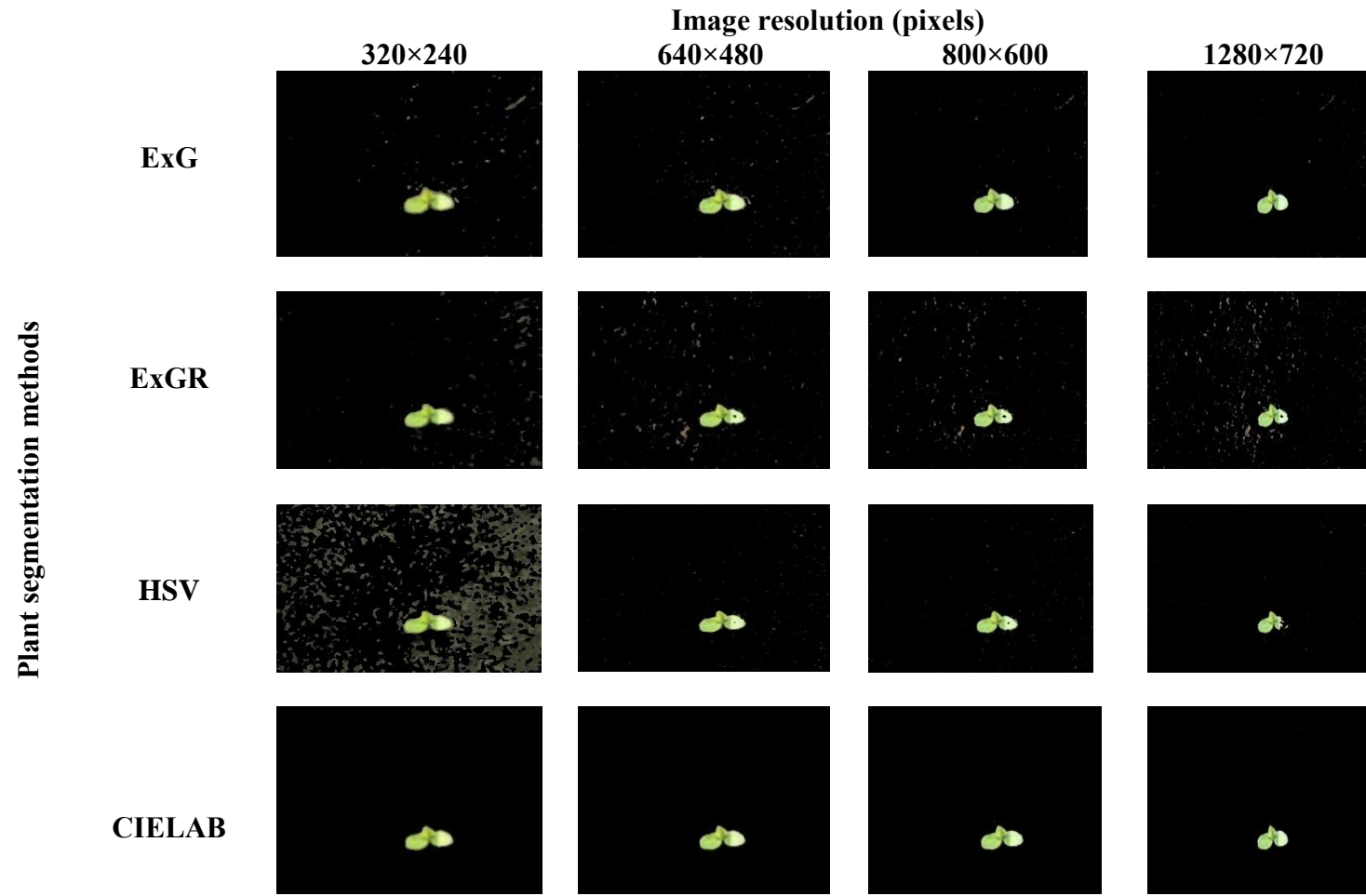


Fig.4.21: Effect of plant segmentation methods with pre-defined threshold value and image resolution on weed and soil pixels classification accuracy

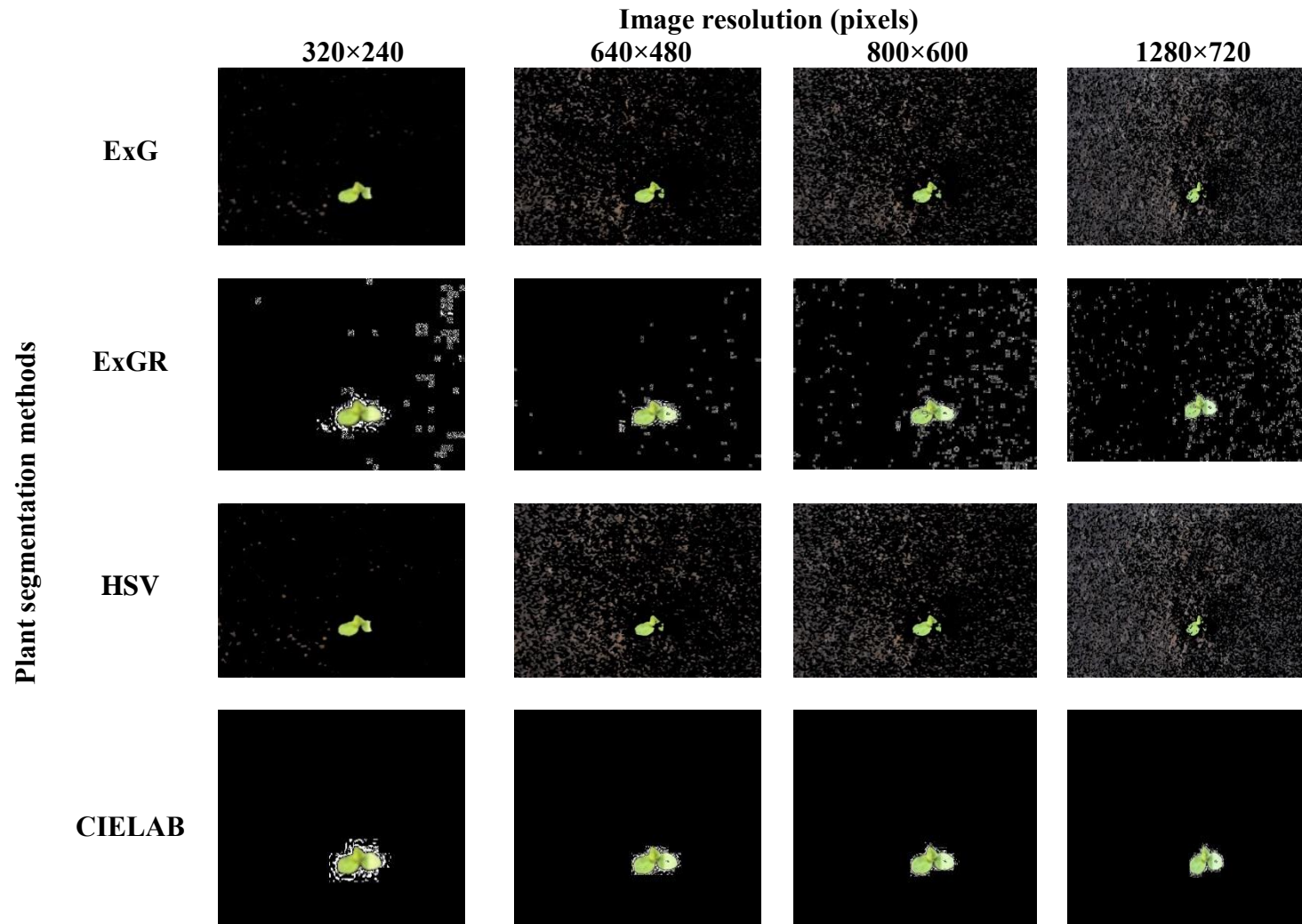


Fig.4.22: Effect of plant segmentation methods with dynamic threshold value and image resolution on weed and soil pixels classification accuracy



Fig.4.23: Effect of plant segmentation methods with pre-defined threshold value and test images on weed and soil pixels classification accuracy

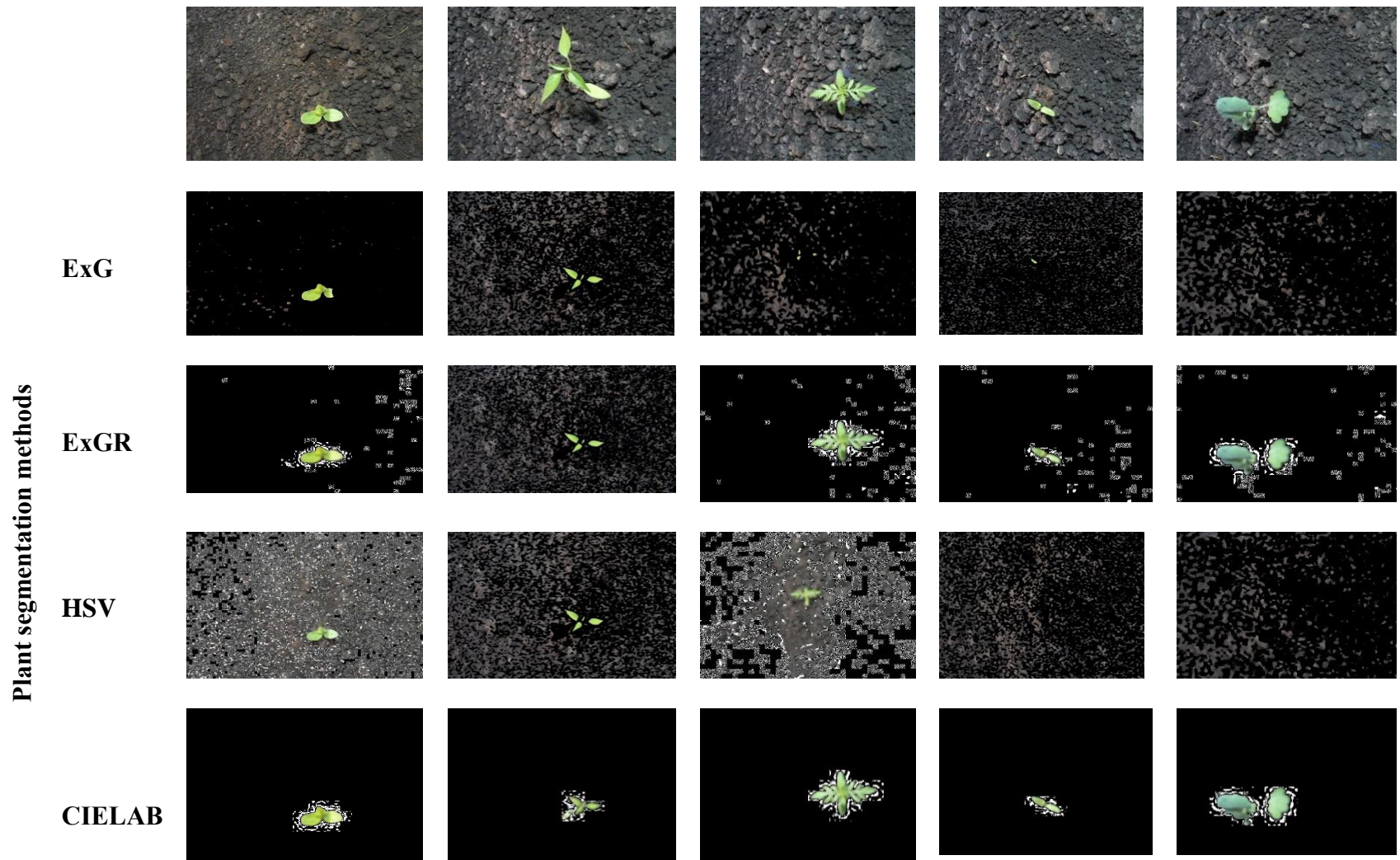


Fig.4.24: Effect of plant segmentation methods with dynamic threshold value and test images on weed and soil pixels classification accuracy

Table 4.11: Dynamic threshold values of plant segmentation methods at four working heights and image resolutions

Working height (mm)	Image resolution (pixels)	Dynamic threshold values			
		ExG	ExGR	HSV	CIELAB
400	320×240	113±18	111±18	75±15	117±1
400	640×480	131±22	129±22	76±14	118±3
400	800×600	121±25	119±25	72±17	118±3
400	1280×720	145±22	143±22	67±17	118±3
500	320×240	121±19	115±19	78±15	120±3
500	640×480	153±14	147±14	74±13	119±1
500	800×600	120±33	114±33	72±11	120±3
500	1280×720	138±20	132±20	70±8	119±1
600	320×240	147±30	139±30	76±14	121±1
600	640×480	158±20	150±20	77±13	122±3
600	800×600	161±20	153±20	72±17	122±3
600	1280×720	176±27	168±27	67±17	122±3
700	320×240	117±17	114±17	79±16	126±3
700	640×480	150±20	147±20	74±14	125±1
700	800×600	137±21	134±21	73±12	126±3
700	1280×720	170±26	167±26	70±9	125±1

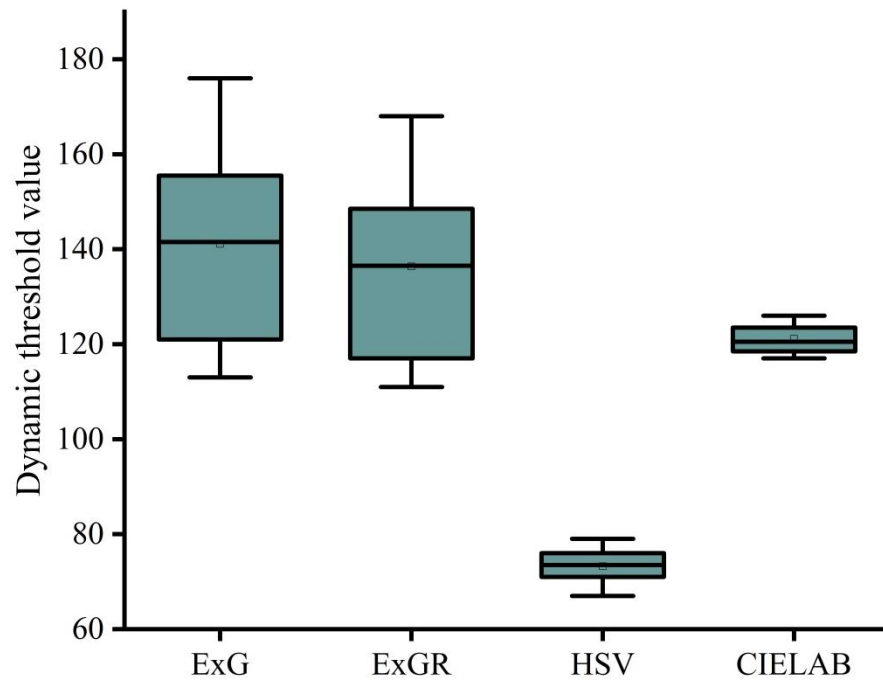


Fig. 4.25: Dynamic threshold values of plant segmentation methods

The dynamic threshold values of ExG, ExGR, HSV and CIELAB is shown in Fig 4.25. The dynamic threshold values range between 110 and 175 for ExG, 105 and 170 for ExGR, 65 and 80 for HSV and 117 and 126 for CIELAB, respectively.

4.6 Effect of soil type on classification accuracy of weed and soil pixels

The effect of soil type and working height on classification of weed and soil pixel was studied. The illumination intensity, plant segmentation method and image resolution were 89 ± 4.4 lx, CIELAB and 640×480 pixels used in this study. The CIELAB with optimized pre-defined threshold values was used. Performance metrics of CIELAB color model with optimized threshold value are given in Table 4.12.

In all combinations of soil type and working height, the CIELAB colour model with optimized threshold value showed highest precision ($>90\%$), recall ($>90\%$) and lowest false positive rate ($<5\%$). The optimized threshold value was able to separate weed and soil pixels accurately under three soil types (Fig 4.26).

Table 4.12: Performance metrics of CIELAB method with pre-defined threshold value

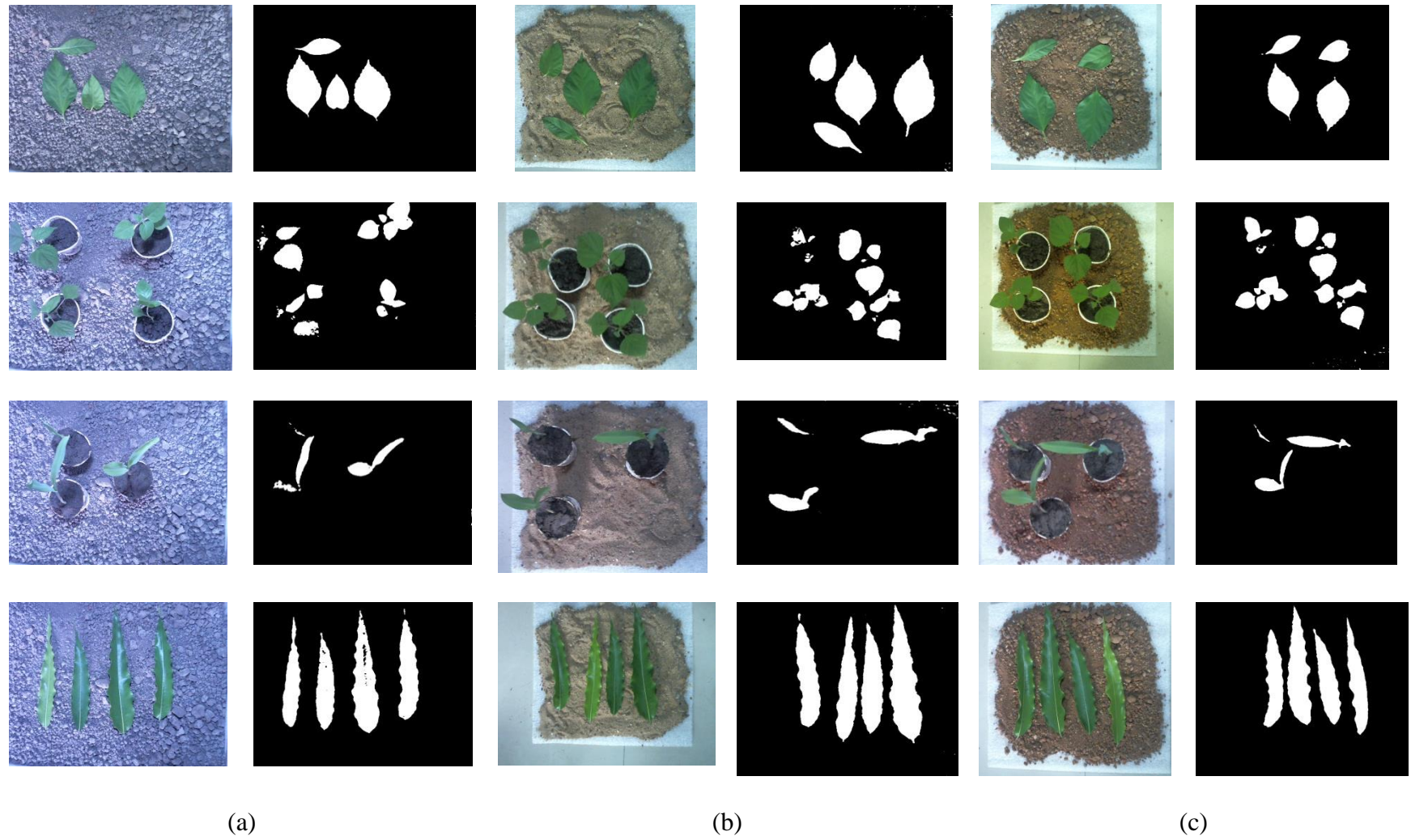
Soil type	Working height (mm)	Image resolution (pixels)	Precision (%)	Recall (%)	FPR (%)
Clay	400	640×480	97 ± 2.2	95 ± 2.2	1.3 ± 0.5
Clay	500	640×480	92 ± 5.2	97 ± 1.2	2.3 ± 1.2
Clay	600	640×480	95 ± 5.5	93 ± 2.1	1.2 ± 0.2
Clay	700	640×480	95 ± 2.5	93 ± 2.2	1.2 ± 0.5
Sandy	400	640×480	97 ± 1.5	95 ± 2.2	2.5 ± 1.2
Sandy	500	640×480	95 ± 2.3	97 ± 1.2	3.2 ± 2.2
Sandy	600	640×480	97 ± 3.3	97 ± 2.2	2.3 ± 1.2
Sandy	700	640×480	96 ± 2.2	96 ± 2.3	2.8 ± 1.2
Red	400	640×480	92 ± 5.6	93 ± 2.1	3.4 ± 1.5
Red	500	640×480	94 ± 3.2	94 ± 2.3	1.8 ± 0.2
Red	600	640×480	95 ± 2.2	95 ± 1.5	2.8 ± 1.8
Red	700	640×480	93 ± 1.2	93 ± 4.5	1.2 ± 0.5

The variation in precision and recall due to change in soil type was found to be significant. Similarly, the variation caused in precision and recall due to change in working height was found to be significantly different. Moreover, the interaction effect of soil type and working height on precision and recall was found to be significantly different.

Table 4.13: Analysis of variance of precision and recall of CIELAB with pre-defined threshold value

Source of variation	DF	F-value	
		Precision	Recall
Soil type (A)	2	204.11**	91.32**
Working height (B)	3	37.29**	64.49**
A×B	6	6.38**	2.74*
Error	24		
Total	35		

*Note: DF: Degree of freedom; “**” = Significant at 1% level of significance; “*” = Significant at 5% level of significance; “ns”=non-significant*

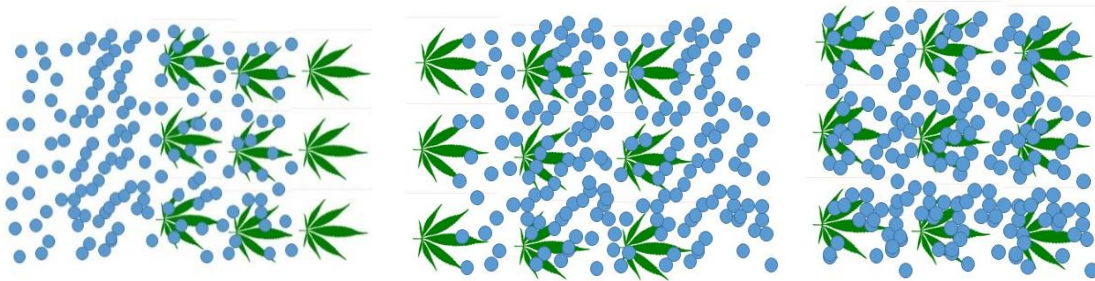


(a) Black cotton soil (b) Sandy soil (c) Red soil

Fig.4.26: CIELAB method performance at three soil type

4.7 Optimization of constructional and operational parameters

The distance between weed detection sensor and spraying nozzle depends on processing time of decision making algorithm, time taken by solenoid valve to respond to signal generated by microcontroller and forward speed of prime mover. The processing time of decision making algorithm and solenoid valve response time combinedly called as lag time. In section 4.5, the highest weed and soil pixels classification accuracy at different working heights and image resolutions was showed by optimized threshold value of CIELAB method. The CIELAB method showed best weed and soil pixels classification even for three soil types. Hence, CIELAB was used for weed and soil pixels classification in further studies. The CIELAB method showed best weed and soil classification accuracy in all four image resolutions. Any image resolution may be used for further experiments. The standard resolution of webcam was 640×480 pixels. Hence, it was decided to use this image resolution for further experiments.



(a) Spraying starts before reaching the weed detection area (b) Spraying starts after crossing the weed detection area (c) Spraying exactly on weed detection area

Fig.4.27. Effect of optimization of operational parameters on detection and spraying

The following three situations can be observed if the operational parameters were not optimized properly. The situation in Fig 4.27 (a) happens when the distance between the weed detection sensor and the nozzle was closer and the solenoid valve responds quickly. The Fig 4.27 (b) condition occurs when the distance between the weed detection sensor and nozzle was wider and the response time of the solenoid valve was too slow. Fig 4.27 (c) depicts precise spraying on weed patches detected by the weed detection sensor. The forward speed was also show significant effect on precise spraying on weed patches. If forward speed was more than optimized forward speed, then the spray happens after crossing weed detection area (Fig 4.27

(b)). Similarly, if forward speed was less than optimized forward speed, then the spray happens before reaching weed detection area.

4.7.1 Optimization of distance between weed detection sensor and spraying nozzle

Python script was developed for weed and soil pixels classification and subsequent herbicide application. The average processing time of weed and soil pixel classification algorithm with an image resolution of 640×480 for CIELAB method was found to be 150 ± 7 ms. It was observed from processing time that microcontroller can process 6 frames per second. An experiment was conducted to find response time of solenoid valve. It was observed from experimental results that the average response time of solenoid valve was found to be 250 ± 50 ms. The summation of solenoid valve response time and processing time was called as lag time. The lag time was found to be 400 ± 57 ms. It was already reported that the distance between weed detection sensor and spraying nozzle depends on forward speed of prime mover.

The minimum forward speed was considered as 1.0 km/h. The prime mover travels a distance of 278 mm/s. Hence, the prime mover travels 111 mm distance in a span of 400 ms lag time. That means the value “a” was 111 mm (Fig. 3.17). Other two factors that affected the centre to centre distance between weed detection sensor and spraying nozzle were field of view of weed detection sensor (length and height) and nozzle spraying area (length and width). The weed detection sensor was mounted at height of 500 mm.

Table 4.14: Distance between weed detection sensor and spraying nozzle at different forward speed

Forward speed (km/h)	Center to center distance between weed detection sensor and spraying nozzle (mm)
1.0	286
1.2	307
1.5	341
2.0	395
2.5	452

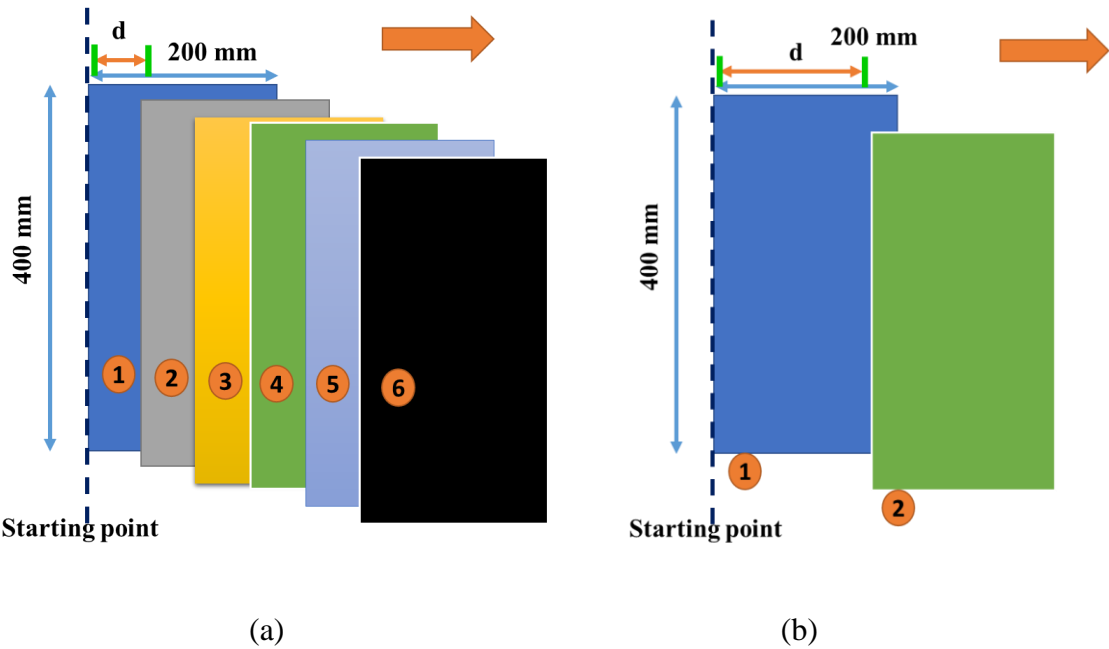
The field of view of weed detection sensor was $400 \text{ mm} \times 200 \text{ mm}$ at 500 mm working height. The height of flat fan nozzle over a ground surface was 450 mm. The nozzle spraying

area was measured and it was found to be $400\text{ mm} \times 150\text{ mm}$. The center to center distance between weed detection sensor and spraying nozzle was distance travelled in lag time, half of the height of field of view in the forward direction and half of the spraying length of nozzle in the forward direction. Finally, the center to center distance between weed detection sensor and spraying nozzle was found to be 286 mm. The same procedure was followed to measure center to center distance between weed detection sensor and spraying nozzle at forward speed of 1.2, 1.5, 2.0 and 2.5 km/h. The center to center distance between weed detection sensor and spraying nozzle at different forward speeds is given in Table 4.14

4.7.2 Optimization of frame grab interval of weed detection sensor

The average processing time of weed and soil pixel classification algorithm for CIELAB colour model with optimized threshold value was found to be 150 ± 7 ms. Hence, time interval between two consecutive frames captured by weed detection sensor was 150 ± 7 ms. The microcontroller was able to process approximately 6 frames per second.

If prime mover forward speed was 1.0 km/h, then it travels a distance of 277 mm in a period of one second. The field of view of weed detection sensor was maintained as $400\text{ mm} \times 200\text{ mm}$ in this study. According to processing time image segmentation algorithm, the microcontroller captures six frames in distance of 277 mm. Due to this reason weed detection sensor acquire frame from the same area and again send signal to the solenoid valve. The prime mover travels a distance of 41 mm in a time span of 150 ms if forward speed of prime mover as 1.0 km/h. Hence, the value of “d” in Fig 4.28 (a) was 41 mm. The overlap among success frames was 159 mm. To overcome the problem of overlap a delay was provided in the python script. The overlap among successive frames was reduced to 118 mm by providing delay of 150 ms. The overlap among success frames was reduced to 77 mm by providing delay of 300 ms. As per calculation two frames needs be discarded between two consecutive frames in order to maintain an overlap of 77 mm at forward speed of 1.0 km/h (Fig 4.28 (b)). Using *time.time()* built python function a delay of 300 ms was provided in the python script. So that time interval between two consecutive frames captured by weed detection sensor was became 450 ms. The frame grab interval of weed detection sensor at different forward speed is given in Table. 4.15.



(a) Overlap between successive frames, (b) Frames discarded between successive frames

Fig. 4.28 Overlap among successive frames of weed detection sensor

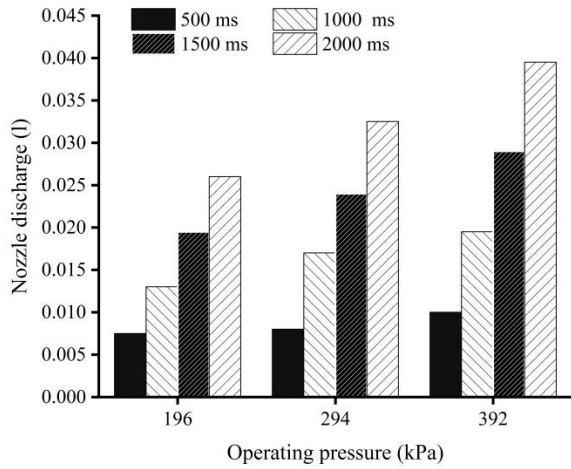
Table 4.15: Frame grabbing interval of weed detection sensor at different forward speed

Forward speed (km/h)	Delay (mm)	Overlap (mm)	Frames to be discarded
1.0	300	77	2
1.2	300	50	2
1.5	150	76	1
2.0	150	28	1
2.5	0	96	0

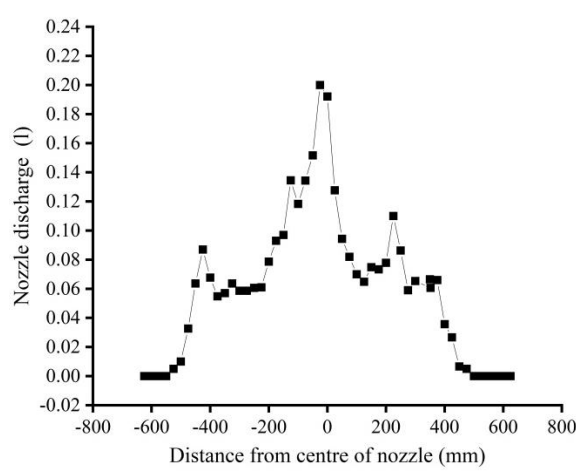
4.7.3 Quantity of herbicide applied

The nozzle discharge rate at three operating pressures and four solenoid valve operating times is shown in Fig 4.29 (a). The discharge rate of nozzle was found to be 0.78, 1.02 and 1.2 l/min at operating pressure of 196, 294 and 392 kPa. The spray distribution patterns of flat fan nozzle at three operating pressures are shown in Fig 4.29 (b), Fig 4.29 (c) and Fig 4.29 (d). The nozzle discharge was analyzed statistically using two way analysis of variance (ANOVA). The

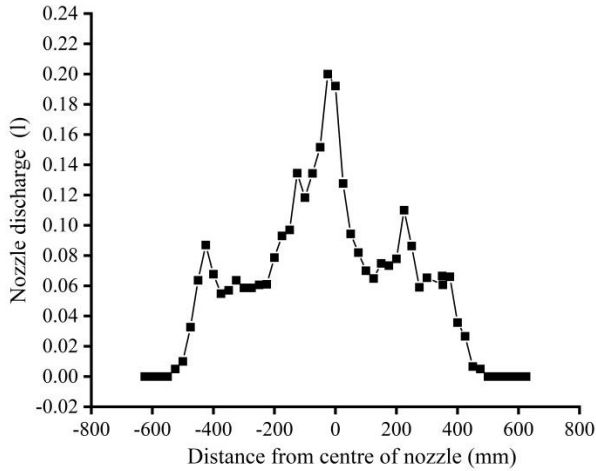
population means of operating pressure were significantly different. Similarly, the population means of solenoid valve opening time were significantly different. Similarly, the interaction between operating pressure and solenoid valve opening time was significantly different. It was observed from results that discharge of nozzle depends on operating pressure as well as duration of solenoid valve opening.



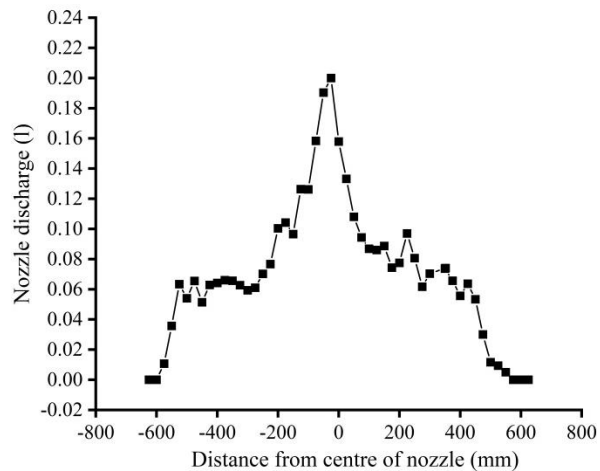
(a)



(b)



(c)



(d)

- (a) Nozzle discharge at different operating pressures and solenoid valve opening time, (b) Spray distribution pattern of flat fan nozzle at 196 kPa operating pressure, (c) Spray distribution pattern of flat fan nozzle at 294 kPa operating pressure, (d) Spray distribution pattern of flat fan nozzle at 392 kPa operating pressure

Fig.4.29: Measurement of nozzle discharge and spray distribution pattern

It was confirmed from experimental results that the solenoid was responding to signal generated by microcontroller and able to open or close for duration as mentioned in the code. It was also proven that solenoid valve opening or closing time can be controlled using python time library.

4.8 Development of a real time camera based weedicide applicator

In the previous sections an illumination intensity, image resolution and plant segmentation method were finalized. Moreover, distance between weed detecting sensor and spraying nozzle and frame grab interval of weed detection sensor at different forward speeds were optimized. An illumination intensity of 89 ± 4.4 lx was finalized. A webcam (Logitech C525) was used as weed detection sensor. The weed detection sensor image resolution was maintained as 640×480 pixels. The CIELAB method was selected for weed and soil pixel classification. The optimized lower and upper threshold values were (0, 0, 0) and (255, 120, 255) for L, A, B channels of CIELAB method. The DC solenoid valve (24 V, 1000 kPa max.) a normally closed type was used.

A tractor of 13.42 kW was used as prime mover in this study. The HTP pump was mounted at front side of tractor generates required operating pressure for satisfactory performance of nozzle. A dedicated set up was made and covered with black cloth. The weed detection sensor, light, solenoid valve and nozzle were placed inside of setup. The setup was attached to tractor with the help of three point hitch. A single row tractor mounted site specific herbicide applicator was developed and is shown in Plate 3.12

4.8.1 Target detection and site specific spraying

An experiment was conducted to check the effectiveness of target detection and spray coverage of the developed system on tar road. Intersection section over union was used as a performance metric to report the spray coverage of developed system. The weed detection sensor image resolution was 640×480 pixels and was mounted at working height of 500 mm. The field of view of weed detection sensor was 400 mm \times 200 mm at 500 mm working height. The illumination intensity of light was maintained as 89 ± 4.4 lx. The flat fan nozzle of operating pressure and discharge rate were 294 kPa and 0.78 l/min used. The height of flat fan nozzle over a ground surface was 450 mm. The prime mover moved at a constant speed of 1.2 km/h. As per calculation the solenoid valve was to be in ON position for a period of 450 ms. An experiment

was conducted to test whether 450 ms duration was sufficient to spray field of view weed detection sensor ($400\text{ mm} \times 200\text{ mm}$). The length of spray of flat fan nozzle was measured for 450 ms duration of solenoid valve opening. With the help of Python `time.time()` the solenoid valve opening time was set as 450 ms. It was observed from experimental results that the length of spray of flat fan nozzle was found to be 210 ± 30 mm (Plate 4.1). It was confirmed that the duration of solenoid valve opening time was sufficient to cover field of view of weed detection sensor.



Plate 4.1: Measurment of spray foot print at different duration of solenoid valve opening

In case of CIELAB method with pre-defined threshold value, the maximum soil misclassification rate was observed less 2 % in all test images at different working height and image resolution. Hence, the minimum threshold value of weed coverage percentage was provided as 2 %. The microcontroller sends signals to solenoid only when weed coverage percentage greater than 2 %. The spraying unit apply constant amount of liquid whenever weeds were detected by sensing unit. To conduct a conceptual test before moving to an actual field, a rectangular green patch was used to represent weeds in a field. During test, the prime mover moved at a constant speed of 1.2 km/h. The distance between weed detection sensor and spraying unit was 307 mm. The delay provided between two successive frames of weed detection sensor was 300 ms.

While conducting experiment all optimized operation parameters (distance between weed detection sensor and spraying unit, weed detection sensor and nozzle height, forward speed of

vehicle and operating pressure) were kept constant except duration of solenoid valve opening time. The duration of solenoid valve opening was varied to show its relevance on target spraying. The duration of solenoid valve opening was kept as 150, 250 and 450 ms. Plate 4.2 (a) shows the inter section over union ($\text{IoU}=0$) for 150 ms and Plate 4.2 (b) shows the inter section over union ($\text{IoU}=0.45$) for 250 ms. Plate 4.2 (c) shows inter section over union ($\text{IoU}=0.74$) when the duration of solenoid valve opening is kept as 450 ms.

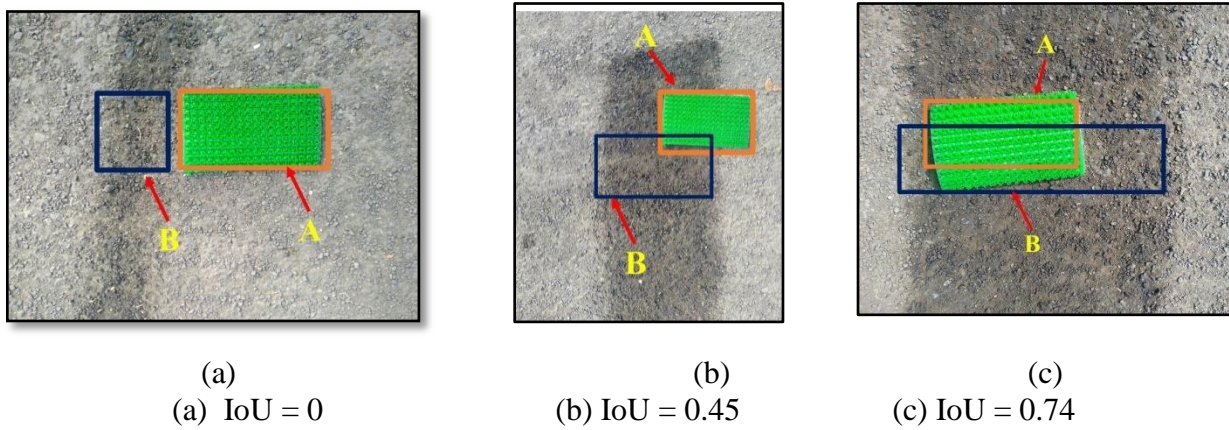


Plate 4.2: Effect of solenoid valve opening time spray coverage

The developed site specific herbicide applicator was tested at agriculture field. Plant leaves were used as weeds. Fig 4.30 shows the real time weed and soil pixel classification. Fig 4.30 (a,b,c) shows percentage of weed coverage or percentage of green as zero, because the green objects were not found in the image. No soil pixel was misclassified as green pixel. Fig 4.30 (d,e,f, g, h,i) shows weed coverage percentage as 0.21, 0.72, 0.33, 2.92, 3.38, 4.17 and 0.33 %. Fig 4.31 (a-d) shows real time weeds detection and site specific weedicide application. The CIELAB colour model with optimized threshold values was able to differentiate weed and soil pixels in real time. The minimum weed coverage percentage in given frame was fixed as 2%. Based on threshold value of weed coverage percentage (WCP) in a given frame, the developed system sprayed only on those frames. The solenoid valve was activated only when percentage of weed pixel was found to be greater than this threshold value

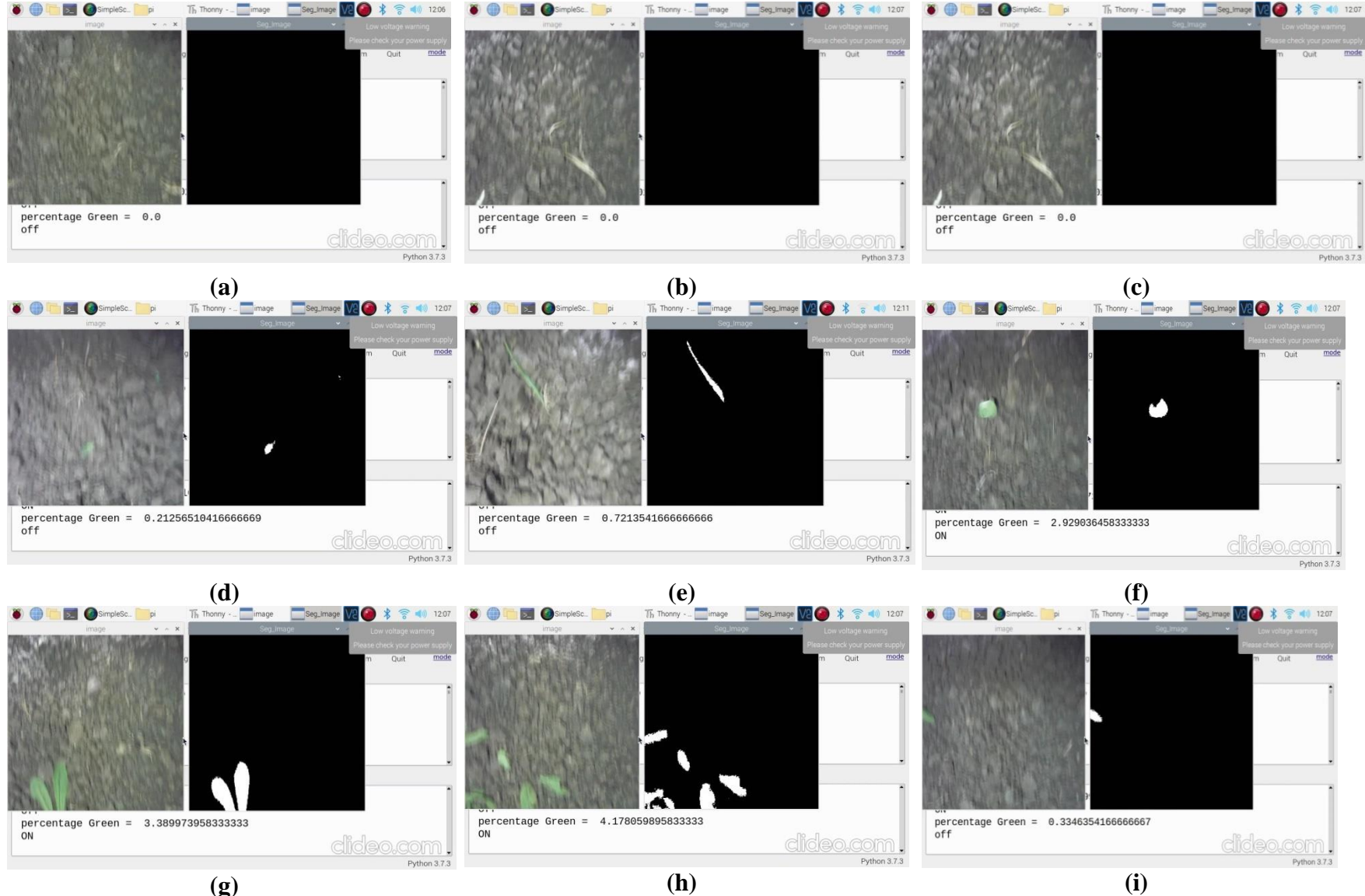


Fig 4.30: Input image and segmented image (a-i)



(a)



(b)



(c)



(d)

Fig. 4.31: Real time site specific weedicide application (a-d)

4.9 Field evaluation of developed real time camera based weedicide applicator

The developed site specific weedicide applicator was tested in the cotton field. The amount herbicide recommended for sugarcane, maize, potato, groundnut, mustard, jute and cotton crops was 500-550 l/ha. The average herbicide application rate was considered as 550 l/ha. In present study, the field of view of webcam was 400 mm × 200 mm. The amount of herbicide required for 400 mm × 200 mm was calculated using formula (Eq. 3.13) and was found to be 5 ml. The duration of solenoid opening was 450 ms, it includes processing time of single frame and delay period of 300 ms. The recommended chemical was to be applied within 450 ms. According to chemical application and solenoid valve opening time, the nozzle discharge rate should be 0.66 l/min. The nozzle discharge rate was measured at three operating pressures. The discharge rate of nozzle was found to be 0.78, 1.02 and 1.2 l/min at operating pressure of 196, 294 and 392 kPa. The discharge rate of nozzle was 0.78 l/min at operating pressure 294 kPa and it was close to desire discharge rate of nozzle. Hence, the operating pressure of 294 kPa was considered for present study. After finalizing operating pressure, the developed system was tested in cotton field. The weed distribution percentage of cotton field is shown in Fig 4.32.

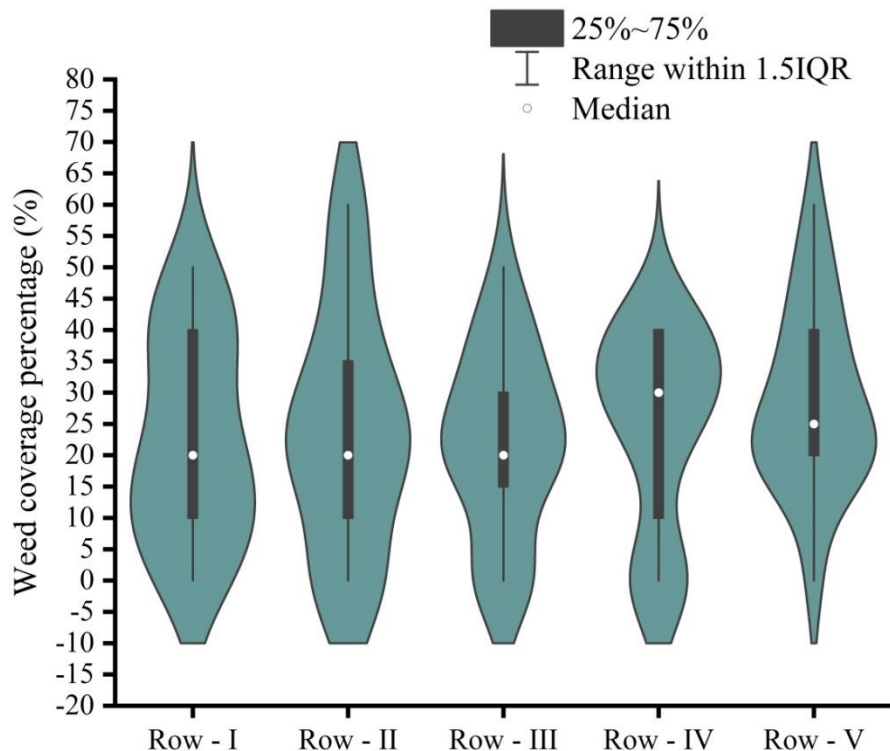


Fig. 4.32. Variation of weed coverage percentage at different location of cotton field

The average weedicide application rate by fixed rate and site specific weedicide application methods were found to be 537.85 ± 14.96 l/ha and 400.87 ± 17.01 l/ha (Table 4.16), respectively. The herbicide saving amount was found to be 25.43 ± 3.52 l/ha. One way analysis of variance (ANOVA) of the average values of the herbicide application data showed that the two spraying methods (site specific herbicide spraying and fixed rate spraying) were significantly different ($F_{1,9}=182.86$).

Table 4.16: Calculation of reduction in weedicide use by site specific weedicide application

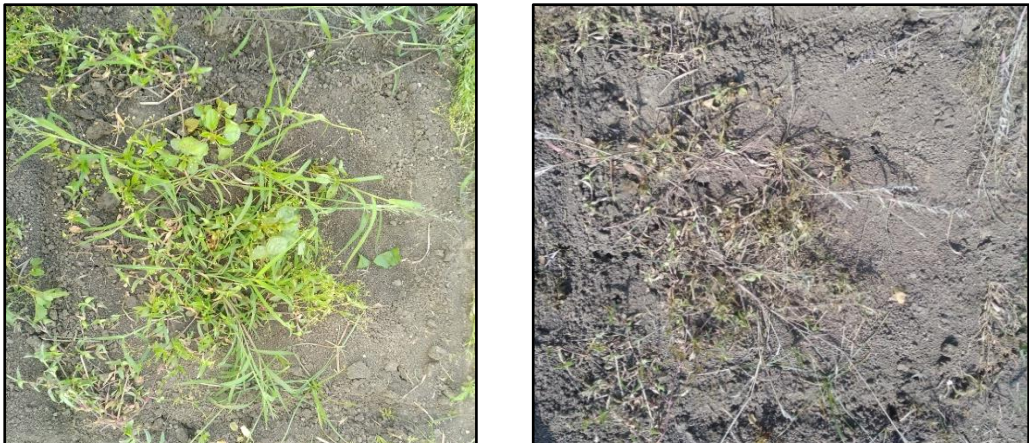
Sl.No.	Application rate (l/ha)		Reduction in herbicide use (%)
	Site specific weedicide application	Fixed rate weedicide application	
1	380.96	535.93	28.92
2	410.37	560.52	26.79
3	407.4	518.52	21.43
4	385.19	535.93	28.13
5	420.41	538.33	21.90
Mean	400.87	537.85	25.43
Std	17.01	14.96	3.52

Plate 4.3 shows weed coverage percentage of plot before and after spraying weedicide. The average weeding efficiency was to be 86.74 ± 1.95 for site specific weedicide application and 87.81 ± 3.70 for fixed rate weedicide application (Table 4.17). The average values of weeding efficiency were not significantly different for the two weedicide application methods indicating that site specific weedicide spraying application was as effective as the conventional (fixed rate) application method in the eradication of weeds ($F_{1,29}=0.5821$, $p=0.4518$). Moreover, it was evidence from plate 4.4 that the weedicide was applied only on weed infested zone rather than whole field. The water sensitive paper appeared in blue colour at weed infested zone because chemical was sprayed. There was no spray was happened at bare soil hence, the water sensitive paper was yellow colour. It was also evident from water sensitive papers that were attached to main crop (cotton) that no chemical was sprayed on main plant (plate 4.5).

Table 4.17: Weeding efficiency of two spraying methods

SI. No.	Site specific weedicide application			Fixed rate weedicide application		
	W ₁	W ₂	WE (%)	W ₁	W ₂	WE (%)
1	20	2	90.00	18	2	88.89
2	15	2	86.67	24	3	87.50
3	41	5	87.80	40	4	90.00
4	40	5	87.50	30	3	90.00
5	30	4	86.67	34	4	88.24
6	21	3	85.71	36	6	83.33
7	25	4	84.00	35	5	85.71
8	32	4	87.50	35	6	82.86
9	30	4	86.67	37	6	83.78
10	18	3	83.33	18	3	83.33
11	20	3	85.00	21	3	85.71
12	28	4	85.71	33	4	87.88
13	14	2	85.71	32	2	93.75
14	18	2	88.89	28	2	92.86
15	20	2	90.00	30	2	93.33
Mean			86.74			87.81
Std			1.95			3.70

Note: W₁: No. weeds before weedicide application; W₂: No. weeds after weedicide application; WE: Weeding efficiency

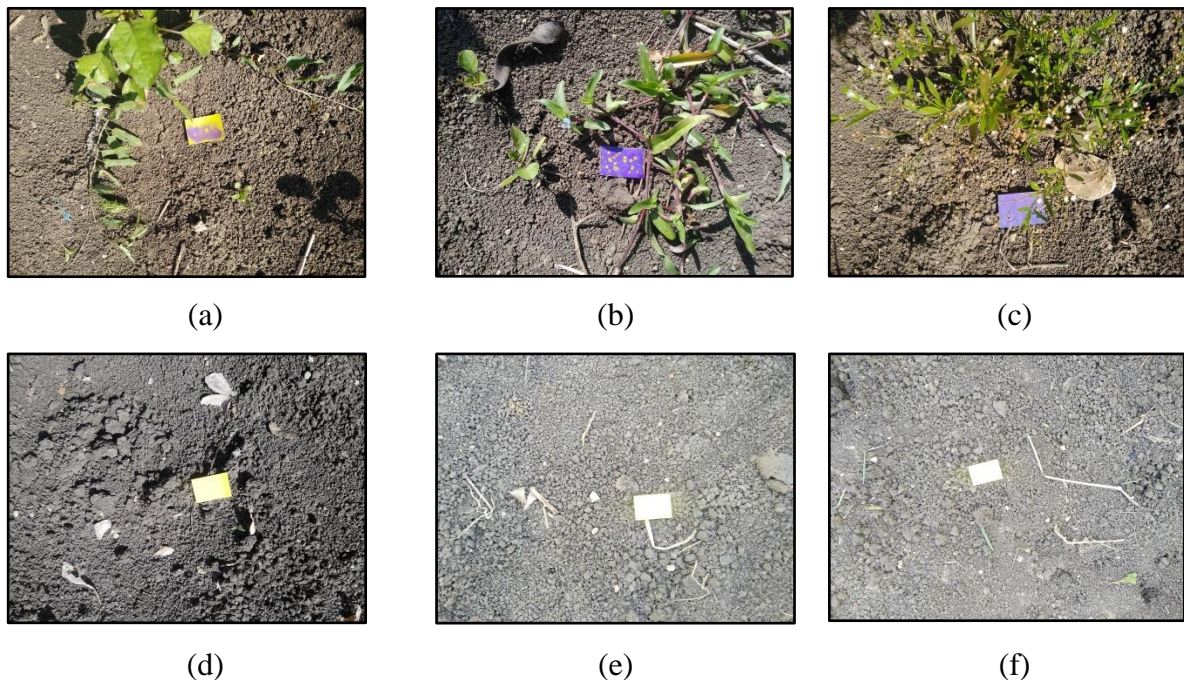


(a)

(b)

(a) Before weedicide application, (b) After 5 days of weedicide application

Plate 4.3: Weeding efficiency



(a)

(b)

(c)

(d)

(e)

(f)

(a-c) Weed detected zones-chemical applied, (d-f) Bare soil zones- chemical not applied

Plate 4.4: Water sensitive paper



Plate 4.5: Water sensitive paper attached to cotton plants

The discussion of effect of illumination intensity and image resolution on colour difference, illumination intensity and image resolution on R, G, B, ExG and ExGR intensity values of weed and soil pixels, plant segmentation methods, threshold values, working height, image resolution and soil type on weed and soil pixels classification and field evaluation of developed real time camera based weedicide applicator is presented in chapter 5 from section 5.1 to section 5.5.

Chapter 5

Discussion

Chapter-5

Discussion

In this chapter, the discussion about results with factors affecting colour difference (ΔE_{ab}), optimization of threshold values, weed and soil pixels classification efficiency of plant segmentation methods, development and field evaluation of a real time single row weedicide applicator are given in the following sequence:

- 5.1 Effect of illumination intensity and image resolution on colour difference (ΔE_{ab})
- 5.2 Effect of illumination intensity and image resolution on R, G, B, ExG and ExGR intensity values of green and soil pixels
- 5.3 Effect of working height, image resolution and plant segmentation methods on classification accuracy of weed and soil pixels
- 5.4 Effect of processing time and forward speed on frame grab interval and distance between weed detection sensor and spraying nozzle
- 5.5 Field evaluation of single row real time site specific weedicide applicator

5.1 Effect of illumination intensity and image resolution on colour difference (ΔE_{ab})

It can be observed from Fig 4.1 that increasing illumination intensity of light from 89 ± 4.4 lx to 359.3 ± 7.5 lx, there was an increasing trend in the average colour difference (ΔE_{ab}) values in all image resolutions. Similarly, an increasing image resolution from 320×240 pixels to 1280×720 pixels there was a decreasing trend in the average colour difference (ΔE_{ab}) values in all illumination intensities. It was observed from numerical optimization that the desirability value 0.957 was found to be highest at interaction effect of 89 ± 4.4 lx and 1280×720 pixel (Table 4.2). The second highest desirability value was found to be 0.794 at interaction effect of 188.9 ± 6.4 lx and 1280×720 pixels. It was also observed from Fig 4.1 that in all four illumination intensities the lowest colour difference (ΔE_{ab}) value was observed at 1280×720 pixels, whereas the highest colour difference (ΔE_{ab}) value was observed at 320×240 pixels. It was observed that with increase of image resolution better was the colour reproduction quality of weed detection sensor.

Out of top four smallest colour difference (ΔE_{ab}) values, three smallest colour difference (ΔE_{ab}) values were observed at illumination intensity of 89 ± 4.4 lx. These three smallest ΔE_{ab}

values were 9.07, 11.26 and 13.07 observed at image resolution of 1280×720, 800×600 and 640×480 pixels, respectively. The weed detection sensor was able to produce lowest colour difference (ΔE_{ab}) values in three image resolutions except 320×240 pixels at illumination intensity of 89 ± 4.4 lx. The second lowest colour difference (ΔE_{ab}) value was observed at illumination intensity of 188.9 ± 6.4 lx and image resolution of 1280×720 pixels. However, three remaining image resolutions of weed detection sensor i.e., 320×240, 640×480, 800×600 pixels showed higher colour difference (ΔE_{ab}) values at illumination intensity of 188.9 ± 6.4 lx than 89 ± 4.4 lx. The weed detection sensor reported higher colour difference (ΔE_{ab}) values in all four image resolutions at illumination intensity of 259.3 ± 12.7 and 359.3 ± 7.5 lx than 89 ± 4.4 and 188.9 ± 6.4 lx illumination intensities. Hence, it was decided to use an illumination intensity of 89 ± 4.4 lx to conduct further experiments.

In all four illumination intensities the lowest colour difference (ΔE_{ab}) was observed at image resolution of 1280×720 pixels than 320×240, 640×480, 800×600 pixels. This was obvious that more the number of pixels the better was colour reproduction quality of imaging sensors. Similar study, the effect of illumination intensity on camera performance was studied (Esau et al., 2017). It was reported that illumination intensity above 2500 lx causes hot spots due to high intensity of illumination and illumination intensity below 500 lx not sufficient for proper camera working. Esau et al., (2017) conducted experiments without a protective cloth and designed system for night operation due to problem of wind during day time. Mahmud et al., (2019) employed protective cloth and artificial light for disease detection. Illumination intensity of 800 to 900 lx was maintained during field evaluation.

In present study, the lowest colour difference (ΔE_{ab}) was noticed at illumination intensity of 89 ± 4.4 lx. The weed detection sensor performance was found better at an illumination intensity of 89 ± 4.4 lx. The previous studies (Esau et al., 2017; Mahmud et al., 2019) used different illumination intensities and obtained better results. In the present study, the weed detection sensor colour difference (ΔE_{ab}) was found to be different at different illuminations and image resolutions. As it was reported (Cubero et al., 2011; Mendoza et al., 2006; Menesatti et al., 2012) that the colour reproduction quality was device dependent, this may be reason for different sensing devices showing different response at different illumination intensities.

An image resolution of 1280×720 pixels was found to be better than remaining image resolutions in all illumination intensities. This image resolution may be used to conduct further experiments. But, it was reported that the processing time of pixel level image segmentation algorithm depends on image resolution (Mahmud et al., 2019). The processing time of image segmentation algorithm limits forward speed of prime mover and distance between weed detection sensor and spraying nozzle. Hence, there was need to compromise between image quality and processing time of image segmentation algorithm. It was decided that average colour difference (ΔE_{ab}) value alone was not sufficient to finalize image resolution. The image resolution to be used was decided based on weed and soil pixels classification performance at different image resolutions of the weed detection sensor.

5.2 Effect of illumination intensity and image resolution on R, G, B, ExG and ExGR intensity values of green and soil pixels

It was observed from Fig 4.2 and Fig 4.3 that the red, green and blue channels intensity values were affected by illumination intensity and image resolution. It was also observed from Fig 4.4 and Fig 4.5 that fresh and healthy leaves and soil samples red, green and blue channel intensity values were overlapped. When red, green and blue intensity values used for green and soil pixel classification, there was a need to select optimum threshold value. It was observed from Fig 4.2 and Fig 4.3 that it was not possible to use single threshold value of red, green and blue channel for green and soil pixel classification because of overlap among red, green and blue channel intensity values. There was also overlap among red, green and blue channel intensity values of green and soil samples (Fig 4.4 and Fig 4.5). Intensity values of red, green and blue channel were employed for weeds and soil background pixel classification (El-Faki et al., 2000; Tewari et al., 2014). It was mentioned that for each pixel if the green intensity value greater than red and blue channel intensity ($G > R$ and $G > B$) that pixel was classified as green object otherwise soil object. They reported that red, green and blue channel intensity values of weed and soil background were sensitive to illumination intensity and hence, the condition ($G > R$ and $G > B$) prone to misclassification of weed and soil background pixels. The same trend was noticed in the present study. Due to an overlap among red, green and blue channel intensity values of green and soil patches at different illumination intensities and image resolutions (Fig 4.2 and Fig 4.3), this condition ($G > R$ and $G > B$) may not be feasible in all cases for weed and soil pixels classification.

Under varying lighting conditions and image resolutions, direct use of the red, green and blue channel intensity values for weed and soil pixel classification may sometimes result in erroneous conclusions. Due to huge variation in red, green and blue channel intensity values of digital colour image, finalizing fixed threshold value for soil and weed separation was not a viable solution. Hence, to overcome the problem with factors affecting colour based weed and soil segmentation using RGB intensity values; plant segmentation methods (visible spectral colour indices and colour models) can be an acceptable solution. Visible spectral colour indices and colour models are formed by combining the RGB values through simple arithmetic operations to produce relative colour indices which were less sensitive to illumination or other factors affecting the RGB gray levels (El-Faki et al., 2000; Meyer & Neto, 2008).

In present study illumination intensity and image resolution showed significant effect on ExG and ExGR intensity values. Even interaction effects of both factors were found to significantly different. It was also reported (El-Faki et al., 2000) that colour indices values of primary colour plates (red, green and blue) were found to be significantly different at various illumination intensities. It was observed from experimental results of present study that unlike red, green and blue channel intensity values; there was no overlap among ExG and ExGR channel intensity values of green and soil colour patches (Fig 4.6 and Fig 4.7). Similarly, there was small percentage overlap among ExG and ExGR channel intensity values of fresh and healthy leaves and soil samples (Fig 4.8).

The clear cut boundary between the index values of green and soil colour patches under different illumination intensities and image resolutions supported the assumption that the relative colour indices (ExG and ExGR) were less sensitive to illumination change. Use of these colour indices would, therefore, greatly improve the effectiveness of the classifiers in colour recognition when illumination was not completely controllable. It was an advantage of ExG and ExGR methods for weeds and soil pixel classification over red, green and blue channel intensity values. Hence, ExG and ExGR can be used for vegetation and non-vegetation pixels separation. Selection of suitable threshold value was trivial for ExG and ExGR method of weed and soil pixels segmentation. In order to use visible spectral colour indices for image segmentation the threshold value of ExG and ExGR methods need to be calibrated under fixed illumination intensity.

In previous experiment the colour difference (ΔE_{ab}) value was found to be lowest at 89 ± 4.4 lx than remaining illumination intensities. There were high colour difference (ΔE_{ab}) values observed at 188.9 ± 6.4 lx, 259.3 ± 12.7 and 359.3 ± 7.5 lx. It was recommended (El-Faki et al., 2000) that imaging under dimmer illumination shows more separation among red, green and blue colour plates than high illumination. Kazmi et al., (2015) reported that creeping thistle detection in sugar fields using visible spectral colour indices was found highest under shade condition than direct sun.

This finding was very important because it provided an alternative solution for the illumination effect on weed detection. If illumination was difficult to control at field level, colour indices threshold values can be calibrated to the standard red, green and blue intensity values at standard light intensity before classification (El-Faki et al., 2000). Thus, for field applications, a device to protect the detected area from natural light might be needed to insure more accurate weed detection. Hence, an artificial light source needed. Along with illumination intensity, an image resolution of weed detection sensor needs to be fixed because changing image resolution there was change in colour difference (ΔE_{ab}) values and it affects ExG and ExGR values.

5.3 Effect of working height, image resolution and plant segmentation methods on classification accuracy of weed and soil pixels

Effect of different threshold values of ExG, ExGR HSV and CIELAB methods on weed and soil pixels classification was studied in the experiment as presented in Fig. 4.11 to Fig 4.14. At threshold value 0 of ExG, ExGR, HSV and CIELAB methods, all pixels related to weed object correctly were classified but many background pixels were misclassified as weed pixels. As increasing threshold value, there was a drastic decreasing trend in the false positive rate. It means soil pixels misclassification rate was decreasing. It was also observed that there was also decreasing trend in recall because weed pixels were also misclassified as soil pixels. A linear trend was observed in precision metric. It was because as increasing threshold value there was two things happening simultaneously. As increasing threshold value false positive (soil pixels classified as weed pixels) decreased, but false negative (weed pixel as soil pixel) increased. Similar trend was observed with ExGR, HSV and CIELAB methods. The optimum threshold value was at which highest recall and precision and lowest false positive rate observed. Total of 51 threshold values were used for classification of weed and soil pixels, but, no threshold value

of ExG, ExGR HSV and CIELAB reported highest recall and precision, and lowest false positive rate.

One important phenomena was observed in Fig 4.11 to 4.14. At threshold value 0, all weed pixels were correctly classified as weed pixels, but all soil pixels were misclassified as weed pixels. Similarly, when threshold value between 135 to 200, all soil pixels were correctly classified as soil but all weed pixels were misclassified as soil pixels. From these trend it was observed that only single threshold value was not sufficient for weed and soil pixel classification. The condition (ExG or ExGR or HSV or CIELAB >threshold) was not sufficient for weed and soil pixel classification. Two boundary conditions were needed to be defined for weed and soil pixel classification instead of single threshold value. With help of developed graphical user interface (GUI) (Fig 4.15 to 4.18), the lower and upper threshold limits of different leaves were obtained. The lower and upper limits of different leaves are given in Table 4.5. There was small variation in lower and upper threshold limit of different leaves. Finally, lower and upper threshold values of ExG, ExGR, HSV and CIELAB methods were selected. The lower and upper threshold limits were 20 and 210 for ExG, 0 and 190 for ExGR, 30 and 100 for hue channel of HSV, 0 and 120 for “A” channel of CIELAB, respectively.

The effect of optimized threshold values and dynamic threshold value of ExG, ExGR, HSV and CIELAB on weed and soil pixels classification is given in Table 4.6. It was observed from weed and soil pixel classification accuracy of optimized threshold value of ExG, ExGR, HSV and CIELAB methods that the false positive rate was found to be almost less than 5 % ($FPR<5\%$) excluding two or three instances ($FPR>5\%$) at all levels of working heights and image resolutions. The threshold values that were optimized were able to correctly classify all soil pixels as soil pixels. Among four plant segmentation methods, the optimized threshold value of CIELAB method showed highest precision ($>90\%$), recall ($>90\%$) and lowest false positive rate ($<5\%$) at all working heights (400, 500, 600 and 700 mm) and image resolutions (320×240, 640×480, 800×600 and 1280×720 pixels). The optimized threshold values of ExG, ExGR and HSV also reported precision ($>90\%$), recall ($>90\%$) and lowest false positive rate ($<5\%$) on few combinations of working height and image resolutions but failed to provide same results at another pair of working height and image resolution.

The dynamic threshold values of ExG, ExGR, HSV and CIELAB method at different working heights and image resolutions are given in Table 4.11. It was observed from dynamic

threshold values of ExG, ExGR, HSV and CIELAB methods that there was more variation in dynamic threshold values of ExG and ExGR than HSV and CIELAB with variation of working heights and image resolutions. This implies that there was more variation in grayscale intensity values of ExG, ExGR than “H” channel of HSV and “A” channel of CIELAB channels with changing working height and image resolution. This may be reason for better classification accuracy reported by CIELAB method. HSV also reported less sensitive to working heights and image resolutions, the optimized threshold values of HSV method failed to report highest precision, recall and lowest false positive rate. The green objects contains dominant colour is green, whereas red objects dominant colour is red. Green leaves contain green channel intensity higher than red and blue channel intensities, whereas soil contains red channel intensity higher than green and blue channel intensity values. “A” channel of CIELAB consists of green and red colour information. This “A” channel consists of only green and red colour information. This may be reason for highest weed and soil pixels classification accuracy observed for CIELAB method than ExG, ExGR and HSV. In order to get best weed and soil pixels segmentation results with ExG, ExGR and HSV methods at particular working height and image resolution, the lower and upper threshold values were to be fine-tuned for particular working height and image resolution. This approach may show better results for ExG, ExGR and HSV methods.

The dynamic threshold value of ExG, ExGR and HSV generated by Otsu method failed classifying weed and soil pixels in all image resolutions and working heights (Fig 4.20, Fig 4.22 and Fig 4.24). But, the dynamic threshold value of “A” channel of CIELAB showed best classification accuracy in all image resolutions at working heights of 400 and 500 mm. The dynamic threshold value of “A” channel of CIELAB showed under segmentation and over segmentation at working heights of 600 and 700 mm. The Otsu works on grayscale image. It works well only when histogram was bimodal. Hue channel of HSV colour model consists of all colours. There was colour range defined for each colour spectrum. i.e. red, yellow, green, blue. ExG and ExGR are single channel image. They are simple grayscale images. The ExG, ExGR, hue channel of HSV of soil and weed pixels were may not be a bimodal. This may be the reason for failure of Otsu technique on ExG, ExGR and hue channel of HSV. The dynamic threshold value of CIELAB showed good classification accuracy when there was equal proportion of weed and soil pixel in an image. When image contains only soil pixels or percentage of weed pixels very small in such condition Otsu method showed under segmentation i.e. classification of soil

pixels as weed pixels. This may be reason for the CIELAB model with dynamic threshold value showed misclassification (soil as green) at working heights of 600 and 700 mm (Fig 4.20). These were main disadvantage of Otsu method of automatic thresholding. In order to use Otsu method for weed and soil pixels classification there must be presence of weed and soil samples in each image. Hence, Otsu method may be applied for soil background separation when images contains main crop, weed and soil background. Similarly, to provide path to robotic vehicles crop rows were to be identified. In that case Otsu method may be applied for soil background separation from main crop to identify crop rows. Identification of crop plants positional information for a mechanical intra row weeding was performed by modified excess green feature along with Otsu threshold method (Nan et al., 2015).

The effect of soil type and working height on classification of weed and soil pixel is given Table 4.12. It was observed that the weed and soil pixel classification accuracy (precision and recall) of CIELAB model under three soil type (black cotton soil, sandy soil, red soil) was found to more than 90 %. However, the background was changed (soil type) there was not much variation observed in recall and precision. It was concluded from experimental results that CIELAB model with optimized threshold values was able to classify weed and soil pixel accurately with more than 90 % in three soil types and four working heights. It was also proved that the CIELAB model and optimized threshold values were robust to soil type as well as working height.

The optimized lower and upper threshold values of “A” channel of CIELAB colour model showed highest precision, recall and lowest false positive rate. The CIELAB method with an all image resolutions showed high precision (>90 %) and recall (>90 %) at all working heights. Another interesting thing observed in this study was that the ground truth images were created using several image processing filters (Gabor, Canny, Sobel and Gaussian) and random forest algorithm. The binary images generated by CIELAB method were very similar to ground truth images and it was also proved from the performance metrics i.e., recall, precision, false positive rate of CIELAB method. The single channel of CIELAB colour model i.e. “A” channel was able to segment weed and non-weed pixels correctly if lighting condition and threshold values were optimized accordingly. From results of present study it was decided to use CIELAB method for further weed and soil pixel classification. The CIELAB method showed almost equal results in all image resolutions. The lowest and highest colour difference (ΔE_{ab}) values were

reported by 1280×720 and 320×240 pixels image resolutions of weed detection sensor. However, the weed and soil pixels classification accuracy of CIELAB method was almost equal in all image resolutions. The weed detection sensor default image resolution was 640×480 pixels. Hence, 640×480 pixels image resolution was considered for further weed and soil pixel classification.

Meyer & Neto, (2008) also conducted similar study. They used excess green index (ExG), excess green minus excess red (ExG-ExR) and normalised difference index (NDI) for weed and soil pixels segmentation. The threshold value to excess green index (ExG) and normalised difference index (NDI) was set by Otsu method, whereas, the threshold value of excess green minus excess red (ExG-ExR) was fixed as zero. The performance of HSV colour model for plant and soil pixels segmentation was tested on images captured under different environmental conditions (Yang et al., 2015). The image dataset consists of maize seedlings, dark green leaf, tender green leaf, red soil, yellow soil, black soil, corn straw and wheat straw. The lower and upper limits were used (Yang et al., 2015). It was observed from previous studies that based on background materials different threshold values were set for plant segmentation methods. Mahmud et al., (2019) reported that the working height significantly affected the image quality of imaging sensor.

5.4 Effect of processing time and forward speed on frame grab interval and distance between weed detection sensor and spraying nozzle

The distance between weed detection sensor and spraying nozzle and frame grab interval of weed detection sensor at different forward speed were optimized. It was observed that processing time and response time of solenoid valve were found to be 150 ± 7 and 250 ± 50 ms respectively. Electromechanical components i.e. solenoid valve take time to activate once signal received from microcontroller for nozzle opening or closing. Therefore, the weed detection sensor cannot be attached adjacent to the nozzle. Hence, there was a need to provide a suitable gap between the weed detection sensor and nozzle, so that at particular forward speed of prime mover the nozzle sprays the chemical precisely at weed detected area. The distance between weed detection sensor and spraying nozzle was 307, 341, 395 and 452 mm at 1.2, 1.5, 2.0 and 2.5 km/h forward speeds.

As compared to previous studies (Tangwongkit et al., 2008; Tewari et al., 2014), in the present study the field of view of weed detection sensor was maintained small ($400\text{ mm} \times 200\text{ mm}$). The problem associated with field of view of camera was that the herbicide recommendation was per hectare basis. Even if weeds were present in a corner or middle of camera field of view, the herbicide was to be applied on whole field of view of camera. Even if herbicide was applied based on weed density or weed pressure the same problem was encountered. Due to this reason it was better to use small field view so that above mentioned problems can be eliminated. Another deciding factor to select small field view of camera along with processing time of algorithm was solenoid valve response time. Hence, these two factors were needs to be considered while selecting field of view of camera.

The forward speed of prime mover was kept as 1.2 km/h . A delay of 300 ms to acquire new frame was provided. The intersection over union (IoU) was found to be 0.74 at duration of solenoid valve opening time of 450 ms . It was observed from Plate 4.2 (c) that the spray started at start point of green patch and stopped after passing green patch. It was also observed that the developed system was able to adjust duration of spray according green patch size. It was confirmed from experimental results that solenoid valve opening time of 450 ms was sufficient time to spray detected green zone without missing the detected green zone area. With the help of optimized operational parameters (center to center distance between weed detection sensor and solenoid valve and duration of solenoid valve opening) the spraying started at start of green patch and continued spraying till the end of green patch. Finally, spray stopped only after passing the green patch. It was proven that entire field of view of weed detection sensor was sprayed by the spraying nozzle in given amount of time if green object found in that particular frame.

The weed and soil pixels classification accuracy of developed decision making algorithm is shown in Fig 4.30. It was observed from experimental results that the decision making algorithm was able to discriminate between weed and soil even when the percentage of weed pixels were very small as compared soil background pixels. The optimized threshold value of CIELAB colour model showed better soil and weed pixels classification accuracy. It was observed from field testing of developed a real time weedicide applicator that the optimized illumination intensity of $89\pm4.4\text{ lx}$ was able provide sufficient illumination intensity at field of view of sensor even under field condition.

Moreover, it was observed from field study that the duration of solenoid valve opening of 450 ms was sufficient to cover entire field of view of weed detection sensor if weed present in that frame (Fig 4.31). The entire area of green patch was sprayed by developed system with in stipulated time. The optimized distance between weed detection sensor and spraying unit was able to start spraying at target zone. It was concluded from experimental results that the optimized operational parameters were able to differentiate weed and soil pixels and spray on weed detected zone in real time. It was observed from field experiment that there was no spraying was observed when percentage of weed pixel was less than 2 %. With the help of this technology the herbicide application rate can be controlled successfully. Moreover, with this technology, the pollution caused by excessive herbicide application and non-target weedicide application can be reduced drastically.

5.5 Field evaluation of single row real time site specific weedicide applicator

The developed single row site specific weedicide applicator was tested in the cotton field. The quantity of weedicide to be applied was optimized. It was evident from weed coverage percentage distribution of all frames that weed distribution or weed infestation density was non-uniform in field (Fig 4.32). Therefore, a significant reduction in herbicide application was expected by implementing site specific weedicide spraying over a conventional (fixed rate) spraying. The average herbicide application rate by fixed rate and site specific weedicide application methods were found to be 537.85 ± 14.96 l/ha and 400.87 ± 17.01 l/ha, respectively. The herbicide saving amount was found to be 25.43 ± 3.52 l/ha. One way analysis of variance (ANOVA) of the average values of the herbicide application data showed that the two spraying methods (site specific weedicide spraying and fixed rate spraying) were significantly different. Plate 4.3 shows weed coverage percentage of plot before and after spraying weedicide. The average weeding efficiency was to be 86.74 ± 1.95 % for site specific weedicide application and 87.81 ± 3.70 % for fixed rate weedicide application. The average values of weeding efficiency were not significantly different for the two weedicide application methods indicating that site specific weedicide spraying application was as effective as the conventional (fixed rate) application method in the eradication of weeds. The field capacity of developed system was 0.048 ha/h. Since one row unit therefore field capacity was low, the multiple units may lead to higher field capacity.

Similar study was conducted by Tangwongkit et al., (2008). They reported that the developed weedicide applicator reduced the application rate by 20.6 %. They also reported that the operating speed of the site specific weedicide application system was lower than the fixed rate application system. However, the site specific weedicide application system cuts down the use of weedicides and saves the environment from the damage that comes from using too many chemicals. Similar study was conducted (Esau et al., 2017; Rehman et al., 2018). It was reported that about 65 % chemical was saved with the help site specific weedicide application technology and the amount of chemical saving depends on weed and weed coverage. This reduction of liquid amount could be stochastic and depending upon the amount of weed density in the field. It was an advantage and emphasizes the need to develop cost-effective and reliable systems for targeted application of agrochemicals on an as needed basis (Zaman et al., 2011). The actual herbicide savings with help of site specific weedicide application not only lower the cost of production but also help to lower environmental hazards (Esau et al., 2017). Future studies are needed to optimize quantity of weedicide to be applied based on weed pressure or weed density.

Chapter 6

Summary and Conclusions

Chapter-6

Summary and conclusions

Precision Agriculture uses several technologies, such as sensors, information systems, improved machinery and informed management, to maximize production while considering the variability and uncertainty of agricultural systems (Molin et al., 2015). This precision agriculture technology uses the idea that a production area was not homogeneous; it varies greatly. Thus, using agricultural inputs such water, chemicals and fertilizers and management techniques equal for areas with different characteristics was not appropriate (Gibbons, 2000). The development and convergence of numerous technologies, such as remote sensing, microcomputers, control automation, mobile computing, advanced information processing and telecommunications, have largely benefited precision agriculture. These technologies made it possible to analyze spatial and temporal variability by collecting data, managing information, applying inputs at different rates, and then evaluating the results in terms of their economic and environmental effects (Soares et al., 2015).

Weeds grow in the fields where they compete with main crop for nutrients, water, light and space and thus reduce the crop yield. It was estimated that reduction in yield due to weeds alone was 20-30% depending on the crops, weed infestation intensity and location, which might increase up to 50% if adequate crop management practices were not observed. The methods to control the weeds were generally classified into two types (1) pre-emergence and (2) post emergence. The pre-emergence methods include primary tillage and application of the pre-emergence herbicides to the field. The post emergence weed control measures were mechanical, chemical, thermal and biological. The mechanical measures were labour consuming and energy intensive. Chemical measure of weed control includes use of weedicide as selective or nonselective at various stages of plant growth. A great advantage of chemical spraying method lies in killing weeds in the crop row or in the immediate vicinity of crop plants. Traditional approaches to weedicide application were based on an assumption that weeds were distributed uniformly in fields. However, the distribution of weeds was often non-uniform or random rather than uniform. Therefore, site specific herbicide spraying may prove to be effective and could reduce the amount of herbicide applied. Site-specific weedicide application technology

eliminates the blanket application of weedicides by spraying only on weed-infested areas; a potential weedicide-saving amount was reported as 30-75 %.

Several types of sensors have been engaged for weed detection in agriculture field. Detect-Spray, Green-Seeker, Weed-IT and Weed-Seeker sensors have been developed and deployed for patch spraying to detect and extract herbaceous plants. The field of view these sensors were very low. In order to work with these sensors the weeds needed to be well developed or there needed to be a lot of weed coverage, making it easier to identify weeds and apply weedicides. Distance measurement sensors (laser and ultrasonic) were engaged in plant/weed identification. The disadvantage of distance measurement sensors was that target weeds need to be taller to be sensed using ultrasonic sensors. If weeds were too small, an ultrasonic sensor detects ground surface as weed. To overcome the problem with opto-electric sensors and distance sensors, imaging sensors have been employed for weed detection in agriculture field. Colour, shape and texture features have been commonly employed for weed detection in agriculture field. The present study focused only on weeds that were present in between crop rows, hence, colour feature was employed for weed and soil pixels classification. Visible spectral colour indices and colour models have been commonly employed by researchers for weeds and soil pixels classification.

In real time weed detection and subsequent application of agrochemicals, more attention was required towards total processing time of image segmentation algorithm. Image processing task was to be performed to extract salient features from digital colour image. There was a need of image processing software and high computing power for colour transformation, colour feature extraction and performing real time site specific herbicide application.

The present investigation therefore was aimed to develop an image based crop weed identification system with following objectives.

1. To optimize the factors affecting weed detection in a camera based image acquisition system
2. To develop an algorithm and real time validation of image acquisition and spraying system
3. To develop a camera based real time weedicide applicator

In the first objective factors affecting weed detection in a camera-based image acquisition system were studied. Considering the previous studies to tackle or minimize illumination intensity effect on colour based weed and soil pixels classification, a light source testing platform was developed. The artificial light source testing platform consists of light, light blocking screen and weed detection sensor. The artificial light illuminates the field of view of the weed detection sensor. The light source was placed in a position such that the shadow of the detection sensor should not fall inside the detection sensor field of view.

The major aim was to select illumination intensity at field of view of weed detection sensor so that colour saturation should not happen. Two separate experiments were conducted to finalize illumination intensity. In the first experiment effect of illumination intensity and image resolutions on colour reproduction quality of imaging sensor was studied. In first experiment, colour difference (ΔE_{ab}) was used as a metric to report colour reproduction quality of weed detection sensor. The illumination intensities that maintained during experiment were 89 ± 4.4 (L₁), 188.9 ± 6.4 (L₂), 259.3 ± 12.7 (L₃) and 359.3 ± 7.5 (L₄) lx. The image resolutions maintained during experiment were 320×240, 640×480, 800×600 and 1280×720 pixels. It was observed from experimental results that an increasing illumination intensity of light from 89 ± 4.4 lx to 359.3 ± 7.5 lx, there was an increasing trend in the average colour difference (ΔE_{ab}) values in all image resolutions. Similarly, an increasing image resolution from 320×240 pixels to 1280×720 pixels there was a decreasing trend in the average colour difference (ΔE_{ab}) values in all illumination intensities of light.

In second experiment effect of illumination intensity and image resolutions on red, green blue, excess green index (ExG) and excess green minus red index (ExGR) intensity values of green and soil pixels intensity values was studied. The X-Rite colour chart checker was used as standard colour chart. The X-Rite colour chart checker consists of 24 colour patches. A total of six colour patches out of 24 colour patches were selected for the present study. The foliage, yellow-green and green colour patches were used instead of actual plant samples, whereas dark skin, moderate red, and magenta colour patches were used for soil samples. The red, green and blue channel intensity values of green and soil colour patches were subjected to three way analysis of variance. The six colour patches (foliage, yellow-green, green, dark skin, moderate red, magenta) were considered as replications.

The variation in red, green, blue, ExG and ExGR intensity values due to illumination intensity (L), image resolution (S) and colour patches (C) and interaction effect of three factors (illumination intensity, image resolution, colour patches) were found to be significantly different. When red, green and blue intensity values used for green and soil pixel classification, there was a need to select optimum threshold value. It was observed from experimental results that it was not possible to use single threshold value of red, green and blue channel for green and soil pixel classification because of overlap among red, green and blue channel intensity values. It was observed from present experimental results that like red, green and blue channel intensity values, the excess green index (ExG) and excess green minus red index (ExGR) channel intensity values were also affected by illumination intensity and image resolution. Unlike red, green and blue channel intensity values; there was no overlap among ExG and ExGR channel intensity values of green and soil colour patches. These two experiments helped finalizing the illumination intensity.

After finalizing illumination intensity of light, threshold values of plant segmentation methods for weed and soil pixel classification were optimized. Four plant segmentation methods were used for weed and soil pixels classifications in the present study. Excess green index (ExG), excess green minus red index (ExGR), hue-saturation-value (HSV) and CIELAB were used as plant segmentation methods. Fresh and healthy leaves and soil sample were collected. The images of these leaves and soil samples were captured at four working heights and four image resolutions under light source testing platform with finalized illumination intensity of 89 ± 4.4 lx. Four working heights 400, 500, 600 and 700 mm were considered. Four image resolutions 320×240 , 640×480 , 800×600 and 1280×720 pixels were considered.

Different threshold values of ExG, ExGR, HSV and CIELAB ranges from 0 to 255 were tested on few images. There was no single threshold value of ExG, ExGR, HSV and CIELAB methods showed best weed and soil pixels classification accuracy. The problem of under segmentation or over segmentation was observed at different threshold values. Instead of single threshold value, lower and upper threshold limits of ExG, ExGR, HSV and CIELAB methods were employed for weed and soil pixels classification. This experiment helped to optimize the lower and upper threshold limits of ExG, ExGR, HSV and CIELAB methods. The lower and upper threshold limits were 20 and 200 for ExG, 0 and 190 for ExGR, 30 and 100 for hue channel of HSV, 0 and 120 for A channel of CIELAB, respectively. After this experiment, the

effect of optimized threshold values (pre-defined threshold values), dynamic threshold values, working height and image resolutions on weed and soil pixels classification was studied. Precision, recall and false positive rate were used as a performance metrics. There was a need of ground truth image to compute performance metrics. Manually annotating each pixel of image was time consuming and prone to human error. Hence, a supervised machine learning approach was followed to create ground truth image. A dedicated software was developed to compute performance metrics i.e., precision, recall, false positive rate.

The precision, recall and false positive rate of ExG+Pre-defined threshold were subjected to three way analysis of variance (ANOVA). It was observed from ANOVA that variation caused in precision, recall and false positive rate due to individual and interaction effect of test image, working heights and image resolutions were found to be significantly different. The same trend was observed on remaining plant segmentation methods. The dynamic threshold value of ExG, ExGR and HSV showed under or over segmentation at all working heights and image resolutions. But, the dynamic threshold value of CIELAB method showed best results in all image resolutions at working height of 400 and 500 mm. It was observed from experimental results that plant segmentation methods and two threshold value approaches (pre-defined threshold and dynamic threshold) showed more effect on precision, recall and false positive rate than image resolution and working height. With help above experimental results, plant segmentation method, image resolution and working height were finalized. After finalizing the plant segmentation method, image resolution and working height from above experiment, the effect of soil type on weed and soil pixels classification accuracy was also studied.

. In the second objective hardware components required for development site specific herbicide application were finalized. A microcontroller for image processing and actuator for spray control were selected. In present study Raspberry Pi 4B model 4GB RAM was used as microcontroller. The spraying unit consists of a HTP pump (1.45 kW), DC solenoid valve (24V DC, diversion type, 1000 kPa max), pressure gauge (0-1372 kPa), flat-fan nozzle, motor driver module, hose and hose connections. The microcontroller (Raspberry Pi) output power was not enough to power the connected devices directly, so Raspberry Pi cannot operate actuator (solenoid valve) directly. Therefore, a single channel L298N motor driver module was used between solenoid valve and Raspberry Pi 4B. A 20000 mAh power bank was used to power the

Raspberry Pi 4 model B and 7 inch LCD screen. The processing time of weed and soil pixel segmentation algorithm with finalized image resolution and plant segmentation method was computed. The response time of solenoid valve was measured.

Performance of weedicide applicator and spraying systems was to be synchronized. The distance between weed detection sensor and spraying nozzle, frame grab interval of weed detection sensor and quantity of herbicide discharge were optimized. The effect of operating pressure of flat fan nozzle and durations of opening of solenoid valve on discharge was studied. There operating pressures 196, 294 and 392 kPa and four durations of solenoid valve opening were used. The discharge rate of nozzle was found to be 0.78, 1.02 and 1.2 l/min at operating pressure of 196, 294 and 392 kPa. The nozzle discharge was analyzed statistically using two way analysis of variance (ANOVA). It was observed from ANOVA that variation caused in liquid discharge due to individual and interaction effect of operating pressure and solenoid valve opening time were found to be significantly different. The relationship for optimizing distance between weed detection sensor and spraying nozzle was developed. The distance between weed detection sensor and spraying nozzle was 307, 341, 395 and 452 mm at 1.2, 1.5, 2.0 and 2.5 km/h forward speeds. After optimizing operational parameters dedicated software using python programming language.

In the third objective prototype of single row tractor mounted site specific weedicide applicator was developed. A small 13.42 kW tractor was selected as power source. A setup was made to connect camera, spraying unit and light to tractor. The developed herbicide applicator was mounted at rear side of the tractor with help of three point hitch of tractor. HTP pump was powered by tractor front mounted PTO. The weedicide tank was placed at rear of driver seat. The real time potentiality of the developed weedicide applicator was tested and the target spraying accuracy was reported in terms of intersection over union (IoU). The performance of the developed system was tested in cotton field and performance was reported in terms of application rate, chemical saving, weeding efficiency and field capacity.

Completely randomized design (CRD) was used to show relative significance of site specific weedicide application and fixed rate weedicide application on weeding efficiency and application rate. One way analysis of variance (ANOVA) of the average values of the weedicide application data showed that the two spraying methods (site specific and fixed rate spraying)

were significantly different. The average values of weeding efficiency were not significantly different for the two weedicide application methods indicating that site specific weedicide spraying application was as effective as the conventional (fixed rate) application method in the eradication of weeds.

Some of the major conclusions drawn from the present investigation are given below

- ❖ Colour-based weed and soil pixel classification was severely affected by sun light and clouds. Illumination intensity and image resolution have shown significant effect on colour difference (ΔE_{ab}). Considering smallest colour difference (ΔE_{ab}) value (9.07) at illumination intensity of 89 ± 4.4 lx and image resolution of 1280×720 pixels, these illumination intensity and image resolutions were finalized. Considering no overlap among ExG and ExGR channel intensity values of green and soil colour patches, these ExG and ExGR colour indices were advisable for weed and soil pixels classification instead direct use of red, green and blue intensity values.
- ❖ Considering, weed and soil pixels classification accuracy of different threshold values of ExG, ExGR, HSV and CIELAB, the lower and upper threshold limits were finalized as 20 and 200 for ExG, 0 and 190 for ExGR, 30 and 100 for hue channel of HSV, 0 and 120 for A channel of CIELAB, respectively. Considering, highest precision (>90 %), recall (>90 %) and lowest false positive rate (<5 %) of CIELAB method with optimized threshold value in all image resolutions, working heights and soil type, the CIELAB method with optimized threshold value and 640×480 pixels image resolution were selected.
- ❖ The processing time of weed and soil pixels classification algorithm with an image resolution of 640×480 pixels and CIELAB method was found to be 150 ± 7 ms. The response time of solenoid valve was found to be 250 ms respectively.
- ❖ The forward speed of prime mover and distance between weed detection sensor and spraying unit depends on processing time of weed and soil pixels classification algorithm and response time of solenoid valve. Considering processing time and response time of solenoid valve, the distance between weed detection sensor and spraying unit was finalized as 307, 341, 395 and 452 mm at 1.2, 1.5, 2.0 and 2.5 km/h forward speeds. Considering processing time and forward speed, the frames to be discarded was finalized as 2, 2, 1, 1, and 0 at 1.0, 1.2, 1.5, 2.0 and 2.5 km/h of forward speed.

- ❖ The main goal of site specific weedicide applicator was to spray weedicide at weed detected zone. Considering intersection over union, the solenoid valve opening time of 450 ms was sufficient time to spray detected green zone without missing the detected green zone. The intersection over union (IoU) was found to be 0.74 at forward speed of 1.2 km/h, distance between weed detection sensor and spraying unit of 307 mm and number of frames discarded was 2.
- ❖ Site-specific weedicide application technology can successfully replace the blanket application of weedicide by spraying only on weed-infested areas without sacrificing the weeding efficiency. The weeding efficiency of site specific weedicide applicator was found to be 86.74 ± 1.95 % over fixed rate weedicide applicator (87.81 ± 3.70 %) and the different was non-significant.
- ❖ The field capacity of the developed real time site specific weedicide applicator was found to be 0.048 ha/h. The average application rate of site specific weedicide applicator (400.87 ± 17.01 l/ha) was against fixed rate weedicide application (537.85 ± 14.96 l/ha) with an overall saving of 25.43 ± 3.52 %.

Recommendation for future work

Based on the findings of this work further research activity can be recommended as follows

1. The developed system can be modified for multiple rows along with proper integration of solenoid valves and microcontroller.
2. The developed system can be further modified to vary herbicide application rate based on weed pressure or intensity.

Bibliography

BIBLIOGRAPHY

- Adelkhani, A., Beheshti, B., Minaei, S., & Javadikia, P. (2012). Optimization of lighting conditions and camera height for citrus image processing. *World Applied Sciences Journal*, 18(10), 1435–1442.
- Agrawal, K., Singh, K., Tiwari, P., & Chandra, M. (2012). *Laser sensor based tractor mounted herbicide applicator*. 183–185.
- Anonymous, (2022). *Reserve Bank of India—Publications*. (n.d.). Retrieved December 28, 2022, from <https://m.rbi.org.in/scripts/PublicationsView.aspx?id=21037>
- Basavaraj, A., Surendrakumar, C., & Divaker, D. (2016). Study of agronomical and soil parameters in paddy field for development of paddy weeder. *International Journal of Agricultural Sciences*, 8(30), 1627–1631.
- Biswas, H. (1990). Soil tool interaction for mechanical control of weeds in black soils. *Unpublished Ph. D. Thesis, Indian Institute of Technology, Kharagpur*.
- Bruno, T. J., & Svoronos, P. D. (2005). *CRC handbook of fundamental spectroscopic correlation charts*. CRC Press.
- Burgos-Artizzu, X. P., Ribeiro, A., Guijarro, M., & Pajares, G. (2011). Real-time image processing for crop/weed discrimination in maize fields. *Computers and Electronics in Agriculture*, 75(2), 337–346. <https://doi.org/10.1016/j.compag.2010.12.011>
- Campbell, J. B., & Wynne, R. H. (2011). *Introduction to Remote Sensing, Fifth Edition*. Guilford Press.
- Chandel, A. K., Tewari, V., Kumar, S. P., Nare, B., & Agarwal, A. (2018). On-the-go position sensing and controller predicated contact-type weed eradicator. *Current Science*, 1485–1494.
- Chandler, R. (2003). *Autonomous agent navigation based on textural analysis (Doctoral dissertation, University of Florida, 2003)*.
- Chang, Y., Zaman, Q., Schumann, A., Percival, D., Esau, T., & Ayalew, G. (2012). Development of color co-occurrence matrix based machine vision algorithms for wild blueberry fields. *Applied Engineering in Agriculture*, 28(3), 315–323.
- Chattha, H. S., Zaman, Q. U., Chang, Y. K., Farooque, A. A., Schumann, A. W., & Brewster, G. R. (2015). Effect of lighting conditions and ground speed on performance of intelligent

- fertilizer spreader for spot-application in wild blueberry. *Precision Agriculture*, 16(6), 654–667. <https://doi.org/10.1007/s11119-015-9400-2>
- Cubero, S., Aleixos, N., Moltó, E., Gómez-Sanchis, J., & Blasco, J. (2011). Advances in Machine Vision Applications for Automatic Inspection and Quality Evaluation of Fruits and Vegetables. *Food and Bioprocess Technology*, 4(4), 487–504. <https://doi.org/10.1007/s11947-010-0411-8>
- Deng, J. (2009). A large-scale hierarchical image database. *Proc. of IEEE Computer Vision and Pattern Recognition, 2009*.
- DiTomaso, J. (1997). *Risk analysis of various weed control methods*. California Exotic Pest Plant Council. 1997 Symposium Proceedings. California Invasive Plant Council, Berkeley, California.
- Dowling, K. J., Mueller, G. G., & Lys, I. A. (2003). *Systems and methods for providing illumination in machine vision systems*.
- Dryden, I. L., Scarr, M. R., & Taylor, C. C. (2003). Bayesian texture segmentation of weed and crop images using reversible jump Markov chain Monte Carlo methods. *Journal of the Royal Statistical Society: Series C (Applied Statistics)*, 52(1), 31–50. <https://doi.org/10.1111/1467-9876.00387>
- Earl, R., Wheeler, P. N., Blackmore, B. S., & Godwin, R. J. (1996). Precision farming—The management of variability. *Landwards*.
- Eaton, L. J. (1989). *Nitrogen cycling in lowbush blueberry stands*. Dalhousie University.
- Economic_survey_2021-2022. (n.d.). Retrieved December 28, 2022, from https://www.indiabudget.gov.in/economicsurvey/ebook_es2022/files/basic-html/page262.html
- Edwards-Jones, G. (2008). Do benefits accrue to ‘pest control’ or ‘pesticides?’: A comment on Cooper and Dobson. *Crop Protection*, 27(6), 965–967. <https://doi.org/10.1016/j.cropro.2007.11.018>
- El-Faki, M., Zhang, N., & Peterson, D. (2000). Factors affecting color-based weed detection. *Transactions of the ASAE*, 43(4), 1001.
- Esau, T., Zaman, Q., Groulx, D., Chang, Y., Schumann, A., & Havard, P. (2017). Supplementary light source development for camera-based smart spraying in low light conditions. *Applied Engineering in Agriculture*, 33(1), 5–14.

- Farooque, A. A., Chang, Y. K., Zaman, Q. U., Groulx, D., Schumann, A. W., & Esau, T. J. (2013). Performance evaluation of multiple ground based sensors mounted on a commercial wild blueberry harvester to sense plant height, fruit yield and topographic features in real-time. *Computers and Electronics in Agriculture*, 91, 135–144. <https://doi.org/10.1016/j.compag.2012.12.006>
- Font, D., Tresanchez, M., Martínez, D., Moreno, J., Clotet, E., & Palacín, J. (2015). Vineyard yield estimation based on the analysis of high resolution images obtained with artificial illumination at night. *Sensors*, 15(4), 8284–8301. <https://doi.org/10.3390/s150408284>
- Ford, A., & Roberts, A. (1998). Colour space conversions. *Westminster University, London, 1998*, 1–31.
- Gebhardt, S., & Kühbauch, W. (2007). A new algorithm for automatic Rumex obtusifolius detection in digital images using colour and texture features and the influence of image resolution. *Precision Agriculture*, 8(1), 1–13. <https://doi.org/10.1007/s11119-006-9024-7>
- Gianessi, L. P., & Reigner, N. P. (2007). The value of herbicides in U.S. crop production. *Weed Technology*, 21(2), 559–566.
- Gong, L., Yu, C., Lin, K., & Liu, C. (2022). A Lightweight Powdery Mildew Disease Evaluation Model for Its In-Field Detection with Portable Instrumentation. *Agronomy*, 12(1), 97. <https://doi.org/10.3390/agronomy12010097>
- Guijarro, M., Pajares, G., Riomoros, I., Herrera, P. J., Burgos-Artizzi, X. P., & Ribeiro, A. (2011). Automatic segmentation of relevant textures in agricultural images. *Computers and Electronics in Agriculture*, 75(1), 75–83. <https://doi.org/10.1016/j.compag.2010.09.013>
- Hague, T., Marchant, J. A., & Tillett, N. D. (2000). Ground based sensing systems for autonomous agricultural vehicles. *Computers and Electronics in Agriculture*, 25(1), 11–28. [https://doi.org/10.1016/S0168-1699\(99\)00053-8](https://doi.org/10.1016/S0168-1699(99)00053-8)
- Hamuda, E., Glavin, M., & Jones, E. (2016). A survey of image processing techniques for plant extraction and segmentation in the field. *Computers and Electronics in Agriculture*, 125, 184–199. <https://doi.org/10.1016/j.compag.2016.04.024>
- Hassanein, M., Khedr, M., & El-Sheimy, N. (2019). Crop row detection procedure using low-cost uav imagery system. *ISPRS - International Archives of the Photogrammetry, Remote*

Sensing and Spatial Information Sciences, 42(13), 349–356. <https://doi.org/10.5194/isprs-archives-XLII-2-W13-349-2019>

Haug, S., & Ostermann, J. (2015). A crop/weed field image dataset for the evaluation of computer vision based precision agriculture tasks. In L. Agapito, M. M. Bronstein, & C. Rother (Eds.), *Computer Vision—ECCV 2014 Workshops* (pp. 105–116). Springer International Publishing. https://doi.org/10.1007/978-3-319-16220-1_8

Hecht, K. (2005). *Integrating LED illumination system for machine vision systems*.

Hennessy, P. J., Esau, T. J., Schumann, A. W., Zaman, Q. U., Corscadden, K. W., & Farooque, A. A. (2022). Evaluation of cameras and image distance for CNN-based weed detection in wild blueberry. *Smart Agricultural Technology*, 2, 100030. <https://doi.org/10.1016/j.atech.2021.100030>

Hernández-Hernández, J. L., García-Mateos, G., González-Esquiva, J. M., Escarabajal-Henarejos, D., Ruiz-Canales, A., & Molina-Martínez, J. M. (2016). Optimal color space selection method for plant/soil segmentation in agriculture. *Computers and Electronics in Agriculture*, 122, 124–132. <https://doi.org/10.1016/j.compag.2016.01.020>

Hong, S., Minzan, L., & Qin, Z. (2012). Detection system of smart sprayers: Status, challenges, and perspectives. *International Journal of Agricultural and Biological Engineering*, 5(3), 10–23. <https://doi.org/10.25165/ijabe.v5i3.585>

Hunt, E. R., Cavigelli, M., Daughtry, C. S. T., McMurtrey, J. E., & Walthall, C. L. (2005). Evaluation of digital photography from model aircraft for remote sensing of crop biomass and nitrogen status. *Precision Agriculture*, 6(4), 359–378. <https://doi.org/10.1007/s11119-005-2324-5>

India Agrochemical Industry Outlook 2022–2026. (n.d.). Retrieved December 27, 2022, from <https://www.reportlinker.com/clp/country/11/726396>

Ishak, W., Hudzari, R., & Ridzuan, M. (2011). Development of variable rate sprayer for oil palm plantation. *Bulletin of the Polish Academy of Sciences. Technical Sciences*, 59(3), 299–302.

ISO 17321-1:2006 Graphic technology and photography Color characterization of digital still cameras-Part 1: Stimuli, metrology and test procedures

ISO-17321-2:2006 Graphic technology and photography Color characterization of digital still cameras Part 2: Considerations for determining scene analysis transforms

- Ji, R., & Qi, L. (2011). Crop-row detection algorithm based on Random Hough Transformation. *Mathematical and Computer Modelling*, 54(3), 1016–1020. <https://doi.org/10.1016/j.mcm.2010.11.030>
- Jinglei, T., Ronghui, M., Zhiyong, Z., Jing, X., & Dong, W. (2017). Distance-based separability criterion of ROI in classification of farmland hyper-spectral images. *International Journal of Agricultural and Biological Engineering*, 10(5), 177–185. <https://doi.org/10.25165/ijabe.v10i5.2264>
- Kamilaris, A., & Prenafeta-Boldú, F. X. (2018). Deep learning in agriculture: A survey. *Computers and Electronics in Agriculture*, 147, 70–90. <https://doi.org/10.1016/j.compag.2018.02.016>
- Karkanis, A., Bilalis, D., Efthimiadou, A., & Katsenios, N. (2012). The critical period for weed competition in parsley (*Petroselinum crispum* (Mill.) Nyman ex A.W. Hill) in Mediterranean areas. *Crop Protection*, 42, 268–272. <https://doi.org/10.1016/j.cropro.2012.07.003>
- Kataoka, T., Kaneko, T., Okamoto, H., & Hata, S. (2003). Crop growth estimation system using machine vision. *Proceedings 2003 IEEE/ASME International Conference on Advanced Intelligent Mechatronics (AIM 2003)*, 2, b1079-b1083 vol.2. <https://doi.org/10.1109/AIM.2003.1225492>
- Kazmi, W., Garcia-Ruiz, F. J., Nielsen, J., Rasmussen, J., & Jørgen Andersen, H. (2015). Detecting creeping thistle in sugar beet fields using vegetation indices. *Computers and Electronics in Agriculture*, 112, 10–19. <https://doi.org/10.1016/j.compag.2015.01.008>
- Kirk, K., Andersen, H. J., Thomsen, A. G., Jørgensen, J. R., & Jørgensen, R. N. (2009). Estimation of leaf area index in cereal crops using red-green images. *Biosystems Engineering*, 104(3), 308–317. <https://doi.org/10.1016/j.biosystemseng.2009.07.001>
- Knezevic, S. Z., Weise, S. F., & Swanton, C. J. (1994). Interference of Redroot Pigweed (*Amaranthus retroflexus*) in Corn (*Zea mays*). *Weed Science*, 42(4), 568–573.
- Kumawat, N., Yadav, R. K., Bangar, K., Tiwari, S., Morya, J., & Kumar, R. (2019). Studies on integrated weed management practices in maize-A review. *Agricultural Reviews*, 40(1).
- Lan, Y., Huang, Y., Martin, D., & Hoffmann, W. (2009). Development of an airborne remote sensing system for crop pest management: System integration and verification. *Applied Engineering in Agriculture*, 25(4), 607–615.

- Lee, K.-J., & Lee, B.-W. (2013). Estimation of rice growth and nitrogen nutrition status using color digital camera image analysis. *European Journal of Agronomy*, 48, 57–65. <https://doi.org/10.1016/j.eja.2013.02.011>
- Lee, W. S., Slaughter, D. C., & Giles, D. K. (1999). Robotic Weed Control System for Tomatoes. *Precision Agriculture*, 1(1), 95–113. <https://doi.org/10.1023/A:1009977903204>
- Li, J., & Tang, L. (2018). Crop recognition under weedy conditions based on 3D imaging for robotic weed control. *Journal of Field Robotics*, 35(4), 596–611. <https://doi.org/10.1002/rob.21763>
- Limsripraphan, P., Kumpan, P., Sathongpan, N., & Phengtaeng, C. (2019). Algorithm for mango classification using image processing and naive bayes classifier. *Industry Technology Lampang Rajabhat University*, 12(1), 112–125.
- Llorens, J., Gil, E., Llop, J., & Escolà, A. (2011). Ultrasonic and LIDAR Sensors for Electronic Canopy Characterization in Vineyards: Advances to Improve Pesticide Application Methods. *Sensors*, 11(2), 2177–2194. <https://doi.org/10.3390/s110202177>
- Mahmud, M. S., Zaman, Q. U., Esau, T. J., Chang, Y. K., Price, G. W., & Prithiviraj, B. (2020). Real-Time Detection of Strawberry Powdery Mildew Disease Using a Mobile Machine Vision System. *Agronomy*, 10(7), 1027. <https://doi.org/10.3390/agronomy10071027>
- Mahmud, Zaman, Q. U., Esau, T. J., Price, G. W., & Prithiviraj, B. (2019). Development of an artificial cloud lighting condition system using machine vision for strawberry powdery mildew disease detection. *Computers and Electronics in Agriculture*, 158, 219–225. <https://doi.org/10.1016/j.compag.2019.02.007>
- Mao, W., Wang, Y., & Wang, Y. (2003). *Real-time detection of between-row weeds using machine vision*. 1.
- Matas, J., Marik, R., & Kittler, J. (1995). Colour-based object recognition under spectrally non-uniform illumination. *Image and Vision Computing*, 13(9), 663–669. [https://doi.org/10.1016/0262-8856\(95\)98861-M](https://doi.org/10.1016/0262-8856(95)98861-M)
- Mathanker, S. K., Weckler, P. R., & Taylor, R. K. (2007). *Effective spatial resolution for weed detection*. 1.

- Mendoza, F., Dejmek, P., & Aguilera, J. M. (2006). Calibrated color measurements of agricultural foods using image analysis. *Postharvest Biology and Technology*, 41(3), 285–295. <https://doi.org/10.1016/j.postharvbio.2006.04.004>
- Menesatti, P., Angelini, C., Pallottino, F., Antonucci, F., Aguzzi, J., & Costa, C. (2012). RGB color calibration for quantitative image analysis: The “3D thin-plate spline” warping approach. *Sensors (Basel, Switzerland)*, 12(6), 7063–7079. <https://doi.org/10.3390/s120607063>
- Meng, Q., Qiu, R., He, J., Zhang, M., Ma, X., & Liu, G. (2015). Development of agricultural implement system based on machine vision and fuzzy control. *Computers and Electronics in Agriculture*, 112, 128–138. <https://doi.org/10.1016/j.compag.2014.11.006>
- Meyer, G. E., Hindman, T. W., Jones, D. D., & Mortensen, D. A. (2004). Digital camera operation and fuzzy logic classification of uniform plant, soil, and residue color images. *Applied Engineering in Agriculture*.
- Meyer, G. E., Hindman, T. W., & Laksmi, K. (1999). *Machine vision detection parameters for plant species identification*. 3543, 327–335.
- Meyer, G. E., & Neto, J. C. (2008). Verification of color vegetation indices for automated crop imaging applications. *Computers and Electronics in Agriculture*, 63(2), 282–293. <https://doi.org/10.1016/j.compag.2008.03.009>
- Meyer, G., Hindman, T., & Laksmi, K. (1999). *Machine vision detection parameters for plant species identification*.
- Michaud, M.-A., Watts, C., & Percival, D. (2006). *Precision pesticide delivery based on aerial spectral imaging*. 1.
- Milioto, A., Lottes, P., & Stachniss, C. (2018). *Real-time semantic segmentation of crop and weed for precision agriculture robots leveraging background knowledge in CNNs*. 2229–2235.
- Molin, J. P., Menegatti, L., Pereira, L., Cremonini, L., & Evangelista, M. (2002). *Testing a fertilizer spreader with VRT*. 232.
- Montalvo, M., Guerrero, J. M., Romeo, J., Emmi, L., Guijarro, M., & Pajares, G. (2013). Automatic expert system for weeds/crops identification in images from maize fields. *Expert Systems with Applications*, 40(1), 75–82. <https://doi.org/10.1016/j.eswa.2012.07.034>

- Moran, M. S., Inoue, Y., & Barnes, E. M. (1997). Opportunities and limitations for image-based remote sensing in precision crop management. *Remote Sensing of Environment*, 61(3), 319–346. [https://doi.org/10.1016/S0034-4257\(97\)00045-X](https://doi.org/10.1016/S0034-4257(97)00045-X)
- Muangkasem, A., Thainimit, S., Keinprasit, R., Isshiki, T., & Tangwongkit, R. (2010). Weed detection over between-row of sugarcane fields using machine vision with shadow robustness technique for variable rate herbicide applicator. *Energy Research Journal*, 1(2), 141–145.
- Mulligan, G. A., & Findlay, J. N. (1970). Reproductive systems and colonization in Canadian weeds. *Canadian Journal of Botany*, 48(5), 859–860. <https://doi.org/10.1139/b70-119>
- Nan, L., Chunlong, Z., Ziwen, C., Zenghong, M., Zhe, S., Ting, Y., Wei, L., & Junxiong, Z. (2015). Crop positioning for robotic intra-row weeding based on machine vision. *International Journal of Agricultural and Biological Engineering*, 8(6), 20–29. <https://doi.org/10.25165/ijabe.v8i6.1932>
- National Research Council. (1997). Precision Agriculture in the 21st Century. Committee on Assessing Crop Yield: Site-Specific Farming. *Information Systems, and Research Opportunities*. National Academy Press, Washington DC., USA, 149.
- Nayar, S. K., & Mitsunaga, T. (2000). High dynamic range imaging: Spatially varying pixel exposures. *Proceedings IEEE Conference on Computer Vision and Pattern Recognition. CVPR 2000 (Cat. No.PR00662)*, 1, 472–479 vol.1. <https://doi.org/10.1109/CVPR.2000.855857>
- Neto, J. C. (2004). *A combined statistical-soft computing approach for classification and mapping weed species in minimum-tillage systems*. The University of Nebraska-Lincoln.
- Perez, A., Lopez, F., Benlloch, J., & Christensen, S. (2000). Colour and shape analysis techniques for weed detection in cereal fields. *Computers and Electronics in Agriculture*, 25(3), 197–212.
- Radosevich, S. R., Holt, J. S., & Ghersa, C. (1997). *Weed Ecology: Implications for Management*. John Wiley & Sons.
- Rasmussen, J., Nørremark, M., & Bibby, B. (2007). Assessment of leaf cover and crop soil cover in weed harrowing research using digital images. *Weed Research*, 47(4), 299–310. <https://doi.org/10.1111/j.1365-3180.2007.00565.x>

- Rehman, T. U., Zaman, Q. U., Chang, Y. K., Schumann, A. W., Corscadden, K. W., & Esau, T. J. (2018). Optimising the parameters influencing performance and weed (goldenrod) identification accuracy of colour co-occurrence matrices. *Biosystems Engineering*, 170, 85–95. <https://doi.org/10.1016/j.biosystemseng.2018.04.002>
- Schmittmann, O., & Schulze, L. P. (2017). A True-Color Sensor and Suitable Evaluation Algorithm for Plant Recognition. *Sensors (Basel, Switzerland)*, 17(8), 1823. <https://doi.org/10.3390/s17081823>
- Schmoldt, D. L. (2001). Precision agriculture and information technology. *Computers and Electronics in Agriculture*. 30 (2001): 5-7.
- Smith, L. A., & Thomson, S. J. (2003). United States Department of Agriculture-Agricultural Research Service research in application technology for pest management. *Pest Management Science*, 59(6–7), 699–707. <https://doi.org/10.1002/ps.697>
- Sojodishijani, O., Abd, R. R., Rostami, V., Samsudin, K., & Saripan, M. I. (2010). Just-in-time outdoor color discrimination using adaptive similarity-based classifier. *IEICE Electronics Express*, 7(5), 339–345.
- Stevens, M., Párraga, C. A., Cuthill, I. C., Partridge, J. C., & Troscianko, T. S. (2007). Using digital photography to study animal coloration. *Biological Journal of the Linnean Society*, 90(2), 211–237. <https://doi.org/10.1111/j.1095-8312.2007.00725.x>
- Steward, B. L., & Tian, L. F. (1999). Machine-vision weed density estimation for real-time, outdoor lighting conditions. *Transactions - American Society of Agricultural Engineers: General Edition*, 42(6), 1897–1909.
- Sudars, K., Jasko, J., Namatevs, I., Ozola, L., & Badaukis, N. (2020). Dataset of annotated food crops and weed images for robotic computer vision control. *Data in Brief*, 31, 105833. <https://doi.org/10.1016/j.dib.2020.105833>
- Suh, H., Hofstee, J., & Van Henten, E. (2014). *Shadow-resistant segmentation based on illumination invariant image transformation*.
- Sujaritha, M., Annadurai, S., Satheeshkumar, J., Kowshik Sharan, S., & Mahesh, L. (2017). Weed detecting robot in sugarcane fields using fuzzy real time classifier. *Computers and Electronics in Agriculture*, 134, 160–171. <https://doi.org/10.1016/j.compag.2017.01.008>
- Swain, K. C., Nørremark, M., Bochtis, D., Olsen, H. J., Sørensen, C. G., Green, O., & Hameed, I. A. (2009). Automated blob spraying system for agricultural robots. *Proceedings of the*

10th International Agricultural Engineering Conference, Bangkok, Thailand, 7-10 December, 2009. Role of Agricultural Engineering in Advent of Changing Global Landscape. <https://www.cabdirect.org/cabdirect/abstract/20103032349>

Tangwongkit, B., Tangwongkit, R., Salokhe, V. M., Jayasuriya, H. P. W., & Nakashima, H. (2008). Field evaluation of a variable rate herbicide applicator. *Agricultural Information Research (Japan)*, 17(1), 1-5.

Tangwongkit, R., Salokhe, V., & Jayasuriya, H. (2006). Development of a tractor mounted real-time, variable rate herbicide applicator for sugarcane planting. *Agricultural Engineering International: The CIGR Ejournal*, 8, 1–11.

Tewari, V. K., Ashok Kumar, A., Nare, B., Prakash, S., & Tyagi, A. (2014). Microcontroller based roller contact type herbicide applicator for weed control under row crops. *Computers and Electronics in Agriculture*, 104, 40–45. <https://doi.org/10.1016/j.compag.2014.03.005>

Tian, L. F., & Slaughter, D. C. (1998). Environmentally adaptive segmentation algorithm for outdoor image segmentation. *Computers and Electronics in Agriculture*, 21(3), 153–168. [https://doi.org/10.1016/S0168-1699\(98\)00037-4](https://doi.org/10.1016/S0168-1699(98)00037-4)

Triantafyllou, A., Sarigiannidis, P., & Bibi, S. (2019). Precision Agriculture: A Remote Sensing Monitoring System Architecture. *Information*, 10(11), Article 11. <https://doi.org/10.3390/info10110348>

Utstumo, T., Urdal, F., Brevik, A., Dørrum, J., Netland, J., Overskeid, Ø., Berge, T. W., & Gravdahl, J. T. (2018). Robotic in-row weed control in vegetables. *Computers and Electronics in Agriculture*, 154, 36–45. <https://doi.org/10.1016/j.compag.2018.08.043>

Varghese, D., Wanat, R., & Mantiuk, R. (2014). Colorimetric calibration of high dynamic range images with a ColorChecker chart. *Proceedings of the HDRi*.

Vidović, I., Cupec, R., & Hocenski, Ž. (2016). Crop row detection by global energy minimization. *Pattern Recognition*, 55, 68–86. <https://doi.org/10.1016/j.patcog.2016.01.013>

Wang, A., Zhang, W., & Wei, X. (2019). A review on weed detection using ground-based machine vision and image processing techniques. *Computers and Electronics in Agriculture*, 158, 226–240. <https://doi.org/10.1016/j.compag.2019.02.005>

- Wang, N., Zhang, N., Wei, J., Stoll, Q., & Peterson, D. E. (2007). A real-time, embedded, weed-detection system for use in wheat fields. *Biosystems Engineering*, 98(3), 276–285. <https://doi.org/10.1016/j.biosystemseng.2007.08.007>
- Winterhalter, W., Fleckenstein, F. V., Dornhege, C., & Burgard, W. (2018). Crop Row Detection on Tiny Plants With the Pattern Hough Transform. *IEEE Robotics and Automation Letters*, 3(4), 3394–3401. <https://doi.org/10.1109/LRA.2018.2852841>
- Woebbecke, D. M., Meyer, G. E., Von Bargen, K., & Mortensen, D. A. (1995). Color indices for weed identification under various soil, residue, and lighting conditions. *Transactions of the ASAE*, 38(1), 259–269.
- Wu, Z., Chen, Y., Zhao, B., Kang, X., & Ding, Y. (2021). Review of Weed Detection Methods Based on Computer Vision. *Sensors*, 21(11), 3647. <https://doi.org/10.3390/s21113647>
- Yang, W., Wang, S., Zhao, X., Zhang, J., & Feng, J. (2015). Greenness identification based on HSV decision tree. *Information Processing in Agriculture*, 2(3), 149–160. <https://doi.org/10.1016/j.inpa.2015.07.003>
- Yao, Y., Harner, T., Blanchard, P., Tuduri, L., Waite, D., Poissant, L., Murphy, C., Belzer, W., Aulagnier, F., & Sverko, E. (2008). Pesticides in the Atmosphere Across Canadian Agricultural Regions. *Environmental Science & Technology*, 42(16), 5931–5937. <https://doi.org/10.1021/es800878r>
- Zaman, Q. U., Esau, T. J., Schumann, A. W., Percival, D. C., Chang, Y. K., Read, S. M., & Farooque, A. A. (2011). Development of prototype automated variable rate sprayer for real-time spot-application of agrochemicals in wild blueberry fields. *Computers and Electronics in Agriculture*, 76(2), 175–182. <https://doi.org/10.1016/j.compag.2011.01.014>
- Zhang, N., Wang, N., Wei, J., & Stoll, Q. (2003). A real-time, embedded, weed-detection and spray-control system. 1064–1080.
- Zhang, W., Miao, Z., Li, N., He, C., & Sun, T. (2022). Review of Current Robotic Approaches for Precision Weed Management. *Current Robotics Reports*, 3(3), 139–151. <https://doi.org/10.1007/s43154-022-00086-5>
- Zimdahl, R. L. (2018). *Fundamentals of weed science*. Academic press.

Abstract

Development of a Camera Based Real Time Weedicide Applicator

ABSTRACT

Weeds are undesired plants which grow with the main crop and compete with main crop for sunlight, water, nutrients, provide shelter for crop pests and reduce crop yield. The conventional method of fixed rate weedicide application on whole area basis leads to wastage of agrochemicals and cause environmental pollution. The site specific weedicide application technology apart from saving costly chemicals, also save environment. In the present study an attempt has been made to develop computer vision based site specific weedicide applicator. Colour feature has been employed for weed and soil pixels classification. Traditional image processing approaches fails at field level because of variable illumination intensity throughout the day. To tackle outside variable illumination intensity, an artificial light source testing platform was developed. An artificial light source testing platform covered with light blocking screen and LED bulb. The illumination intensity that to be maintained at field of view of weed detection sensor was finalized based on colour reproduction quality of weed detection sensor and behavior of excess green index (ExG) and excess green minus red index (ExGR) intensity values of green and soil colour patches. Based on experimental results an illumination intensity of 89 ± 4.4 lx was finalized to maintain at weed detection sensor field of view. Red, green and blue channel intensity values of green and soil colour patches were sensitive to both illumination intensity and image resolution and there was overlap among red, green and blue channel intensity values of green and soil colour patches. Hence, direct use of red, green and blue channel intensity values of weed and soil were not suitable for weed and soil pixels classification. There was no overlap was observed between excess green index (ExG) and excess green minus red index (ExGR) intensity values of green and soil colour patches. So ExG and ExGR indices may be employed for weed and soil pixels classification. Excess green index (ExG), excess green minus red index (ExGR), hue-saturation-value (HSV) and CIELAB methods were used for weed and soil pixels classification at four working heights and image resolutions. The threshold values of ExG, ExGR, HSV and CIELAB methods were optimized under controlled illumination intensity of 89 ± 4.4 lx. The lower and upper limits were finalized as 20 and 210 for ExG, 0 and 190 for ExGR, 30 and 100 for HSV, 0 and 120 for CIELAB, respectively. Among four plant segmentation methods, the optimized threshold values of

CIELAB methods showed highest precision and recall more than 90 % and false positive rate less than 5 % in four working heights (400, 500, 600, 700 mm) and four image resolutions (320×240, 640×480, 800×600, 1280×720 pixels). The OTSU thresholding technique was also employed for dynamic thresholding of weed and soil pixels. The dynamic threshold value of CIELAB method showed better weed and soil pixels classification at working heights of 400 and 500 mm. The optimized threshold value of ExG, ExGR and HSV methods also showed highest precision and recall more than 90 % in few combinations of working height and image resolution. These three methods failed to show highest weed and soil pixels classification accuracy on remaining pair of working height and image resolution. The dynamic threshold value of ExG, ExGR and HSV methods always showed under segmentation or over segmentation at four working heights and four image resolutions. Python programming language was used to develop weed and soil pixels classification algorithm. After finalizing illumination intensity, image resolution, working height and plant segmentation methods, a tractor (13.42 kW) mounted single row real time camera based weedicide applicator was developed. The main components of developed weedicide applicator were weed detection sensor, Raspberry Pi 4 model B, 7 inch HDMI screen, L298N motor driver module, artificial light, 24 V solenoid valve, flat fan nozzle and prime mover. The discharge rate of flat fan nozzle was found to be 0.78, 1.02 and 1.2 l/min at operating pressure of 196, 294 and 392 kPa. The distance between weed detection sensor and spraying unit and frame grab interval of weed detection sensor were optimized with respect to forward speed of prime mover. After optimizing operational parameters, target detection and spraying accuracy of tractor mounted single row real time camera based weedicide applicator was tested on tar road. The mean intersection over union (IoU) was found to be 0.74. The developed single row real time camera based weedicide applicator performance was tested in cotton field. The average weeding efficiency was found to be 86.74 ± 1.95 % for site specific weedicide application against 87.81 ± 3.70 % for fixed rate weedicide application. The average weedicide application rate by site specific and fixed rate weedicide application methods were found to be 537.85 ± 14.96 l/ha and 400.87 ± 17.01 l/ha, respectively for cotton crop. The average weedicide saving amount was found to be 25.43 ± 3.52 %. The field capacity of developed single row system was 0.048 ha/h. A multi row unit may lead to higher field capacity. The developed technology could detect the inter row weeds successfully with saving in chemical without affecting weeding efficiency.

Key words: Weed detection, Site specific chemical applicator, Spot weedicide applicator, Weed-soil identification, Image processing, Image segmentation

सारांश

खरपतवार अवांछित पौधे हैं जो मुख्य फसल के साथ उगते हैं और प्रकाश, पानी एवं पोषक तत्वों के लिए मुख्य फसल के साथ प्रतिस्पर्धा करते हैं, फसल के कीटों को आश्रय प्रदान करते हैं और फसल की उपज को कम करते हैं। कुल क्षेत्र के आधार पर निश्चित दर पर खरपतवारनाशी के प्रयोग की पारंपरिक विधि में कृषि रसायनों की बर्बादी होती है और पर्यावरण प्रदूषित होता है। स्थल-विशिष्ट खरपतवारनाशी के प्रयोग की तकनीक महंगे रसायनों को बचाने के अलावा पर्यावरण को भी बचाती है। वर्तमान अध्ययन में कंप्यूटर विजन आधारित स्थल-विशिष्ट पर्यावरण खरपतवारनाशी के प्रयोग हेतु छिड़काव यंत्र विकसित करने का प्रयास किया गया है। रंग वैशिष्ट्य को खरपतवार और मिट्टी पिक्सेल वर्गीकरण के लिए उपयोग किया गया है। परिवर्तनीय प्रकाश की तीव्रता के कारण खेतों में कार्य करते समय पारंपरिक इमेज प्रसंस्करण विधि कारगर नहीं रहती है। बाहरी परिवर्तनीय प्रकाश की तीव्रता से निपटने के लिए, एक कृत्रिम प्रकाश स्रोत परीक्षण मंच विकसित किया गया एलईडी बल्ब के कृत्रिम प्रकाश द्वारा प्रकाश एवं अवरोधक स्क्रीन के द्वारा वाह्य प्रकाश को कवर किया गया। खरपतवार का पता लगाने वाले संवेदक के दृश्य क्षेत्र में प्रकाश की तीव्रता को बनाए रखने के लिए अंतिम रूप दिया गया जो कि खरपतवार का पता लगाने वाले संवेदक की रंग पुनरूत्पादन गुणवत्ता और अतिरिक्त ग्रीन इंडेक्स (ExG) के व्यवहार और हरे और मिट्टी के रंग के धब्बे के अतिरिक्त ग्रीन माइनस रेड इंडेक्स (ExGR) तीव्रता मूल्यों के आधार पर तय किया गया था। प्रयोगात्मक परिणामों के आधार पर 89 ± 4.4 ल्यूमन की प्रकाश की तीव्रता को अंतिम रूप दिया गया हरे और मिट्टी के रंग के धब्बों के लाल, हरे और नीले चैनल की तीव्रता मान, प्रकाश की तीव्रता और इमेज रिज़ॉल्यूशन दोनों के प्रति संवेदनशील थे तथा हरे और मिट्टी के रंग के धब्बे के लाल, हरे और नीले चैनल तीव्रता मूल्यों के बीच ओवरलैप था। इसलिए खरपतवार और मिट्टी के लाल, हरे और नीले चैनल तीव्रता मूल्यों का प्रत्यक्ष उपयोग खरपतवार और मिट्टी पिक्सेल वर्गीकरण के लिए उपयुक्त नहीं था। अतिरिक्त ग्रीन इंडेक्स (ExG) और अतिरिक्त ग्रीन माइनस रेड इंडेक्स (ExGR) के हरे और मिट्टी के रंग पैच के तीव्रता मूल्यों के बीच कोई ओवरलैप नहीं पाया गया, इसलिए खरपतवार और मृदा पिक्सेल वर्गीकरण के लिए ExG और ExGR सूचकांकों का

उपयोग किया गया। अतिरिक्त ग्रीन इंडेक्स (ExG), अतिरिक्त ग्रीन माइनस रेड इंडेक्स (ExGR), ह्यू-सैचुरेशन-वैल्यू (HSV) और CIELAB विधियों का उपयोग चार कार्यकारी ऊँचाई और इमेज रेजोल्यूशन में खरपतवार और मृदा पिक्सेल वर्गीकरण के लिए किया गया। ExG, ExGR, HSV और CIELAB विधियों के थ्रेशोल्ड मूल्यों को 89 ± 4.4 1x की नियंत्रित प्रकाश तीव्रता के तहत अनुकूलित किया गया था। थ्रेशोल्ड की ऊपरी एवं निम्न सीमा को ExG के लिए क्रमशः 20 और 210, ExGR के लिए क्रमशः 0 और 190, HSV के लिए क्रमशः 30 और 100, CIELAB के लिए क्रमशः 0 और 120 के रूप में अंतिम रूप दिया गया था। चार पौधे एवं मृदा वर्गीकरण विधियों के बीच, CIELAB विधि के अनुकूलित थ्रेशोल्ड मूल्यों में उच्चतम सटीकता पाई गई और चार कार्यकारी ऊँचाईयों (400, 500, 600, 700 मिमी) और चार इमेज रिज़ॉल्यूशन (320×240, 640×480, 800×600, 1280×720 पिक्सेल) में 90 प्रतिशत से अधिक रिकाल और 5 प्रतिशत से कम झूठी सकारात्मक दर प्राप्त हुई। ओटीएसयू थ्रेशोल्डिंग तकनीक को खरपतवार और मिट्टी के पिक्सेल की गतिशील थ्रेशोल्ड मूल्य के लिए भी नियोजित किया गया था। CIELAB विधि के गतिशील थ्रेशोल्ड मूल्य ने 400 और 500 मिमी की कार्यकारी ऊँचाई पर बेहतर खरपतवार और मिट्टी पिक्सेल का वर्गीकरण दिखाया। ExG, ExGR और HSV विधियों का अनुकूलित थ्रेशोल्ड मान भी उच्चतम सटीकता दिखाता है और काम करने की ऊँचाई और इमेज रिज़ॉल्यूशन के कुछ संयोजनों में 90 प्रतिशत से अधिक रीकाल दर प्राप्त हुई। काम करने की ऊँचाई और इमेज रिज़ॉल्यूशन की शेष जोड़ी पर उच्चतम खरपतवार और मिट्टी पिक्सेल वर्गीकरण सटीकता दिखाने में अन्य तीनों विधियाँ विफल रहीं। ExG, ExGR और HSV विधियों का गतिशील थ्रेशोल्ड मूल्य, हमेशा चार कार्यकारी ऊँचाई और चार इमेज रिज़ॉल्यूशन पर कम वर्गीकरण या अधिक वर्गीकरण के तहत पाया गया। पायथॉन प्रोग्रामिंग भाषा का उपयोग, खरपतवार और मृदा पिक्सेल वर्गीकरण एल्गोरिथम विकसित करने के लिए किया गया था। प्रकाश की तीव्रता, इमेज रेजोल्यूशन, काम करने की ऊँचाई और पौधों के वर्गीकरण के तरीकों को अंतिम रूप देने के बाद, एक ट्रैक्टर (13.42 kW) आरोहित एकल कतार वास्तविक समय कैमरा आधारित खरपतवारनाशी छिड़काव यंत्र का विकास किया गया। विकसित यंत्र के मुख्य घटक थे खरपतवार का पता लगाने वाला संवेदक रासपब्रेरी पाई 4 मॉडल बी) कंट्रोलर 7 इंच एचडीएमआई स्क्रीन, एल298एन मोटर ड्राइवर मॉड्यूल, कृत्रिम प्रकाश हेतु एलईडी बल्ब, 24 वोल्ट सोलनोइड वाल्व, फ्लैट फैन नोजल और ट्रैक्टर (प्राथमिक ऊर्जा स्रोत)। 196,294 और 392 किलो पास्कल के परिचालन दबाव पर फ्लैट फैन नोजल की साव

दर 0.78, 1.02 और 1.2 ली/मिनट पाई गई। खरपतवार डिटेक्शन संवेदक और छिड़काव यूनिट के बीच की दूरी और खरपतवार डिटेक्शन संवेदक के फ्रेम गैबिंग अंतराल को प्राथमिक ऊर्जा स्रोत की आग गति के संबंध में अनुकूलित किया गया। परिचालन मापदंडों का अनुकूलन करने के बाद, चार कोल की सड़क पर ट्रैक्टर आरोहित एकल कतार रो वास्तविक समय कैमरा आधारित खरपतवारनाशी छिड़काव यंत्र का परीक्षण छिड़काव स्टीकता हेतु किया गया। माध्य प्रतिच्छेदन यूनियन (IOU) 0.74 पर पाया गया। विकसित एकल कतार वास्तविक समय कैमरा आधारित खरपतवारनाशी छिड़काव यंत्र का परीक्षण कपास के खेत में किया गया। स्थल-विशिष्ट खरपतवारनाशी यंत्र की औसत निराई दक्षता 86.74 ± 1.95 प्रतिशत पाई गई, जबकि निश्चित दर खरपतवारनाशी यंत्र की निराई दक्षता 87.81 ± 3.70 प्रतिशत थी। कपास की फसल के लिए स्पाट स्थल और निश्चित दर खरपतवारनाशी प्रयोग विधियों द्वारा औसत खरपतवारनाशी प्रयोग दर क्रमशः 537.85 ± 14.96 ली/हेक्टेयर और 400.87 ± 17.01 ली/हेक्टेयर पाई गई एवं औसत खरपतवारनाशी की बचत मात्रा 25.43 ± 3.52 प्रतिशत पाई गई। विकसित एकल पंक्ति प्रणाली की क्षेत्र क्षमता 0.048 हेक्टेयर/घंटा थी। विकसित तकनीक निराई दक्षता को प्रभावित किए बिना रासायन बचत के साथ पंक्ति के बीच के खरपतवारों का सफलतापूर्वक पता लगा सकती है। एक बहु कतारी ईकाई के द्वारा इस यंत्र की क्षेत्र क्षमता बढ़ाई जा सकती है।

संकेतक शब्द: खरपतवार नियंत्रक खरपतवार की खोज, स्थल-विशिष्ट रासायन छिड़काव यंत्र खरपतवार-मिट्टी की पहचान, इमेज प्रसंस्करण, इमेज का वर्गीकरण, स्पॉट शाकनाशी छिड़काव यंत्र

Appendices

Appendix-I

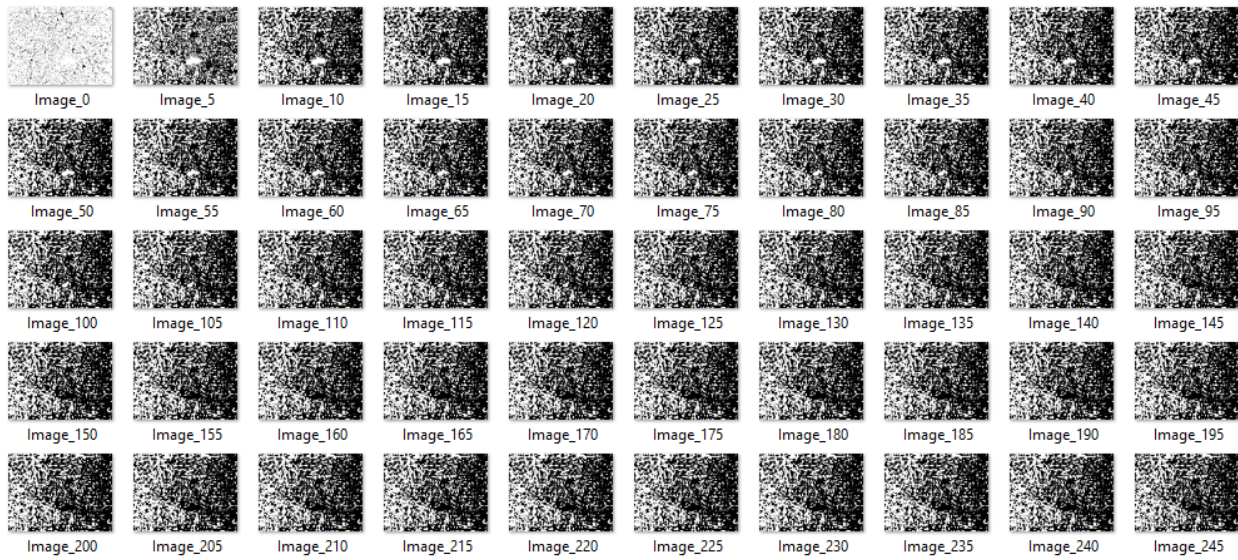


Fig. 1: Test image segmentation results at different threshold values of ExG method

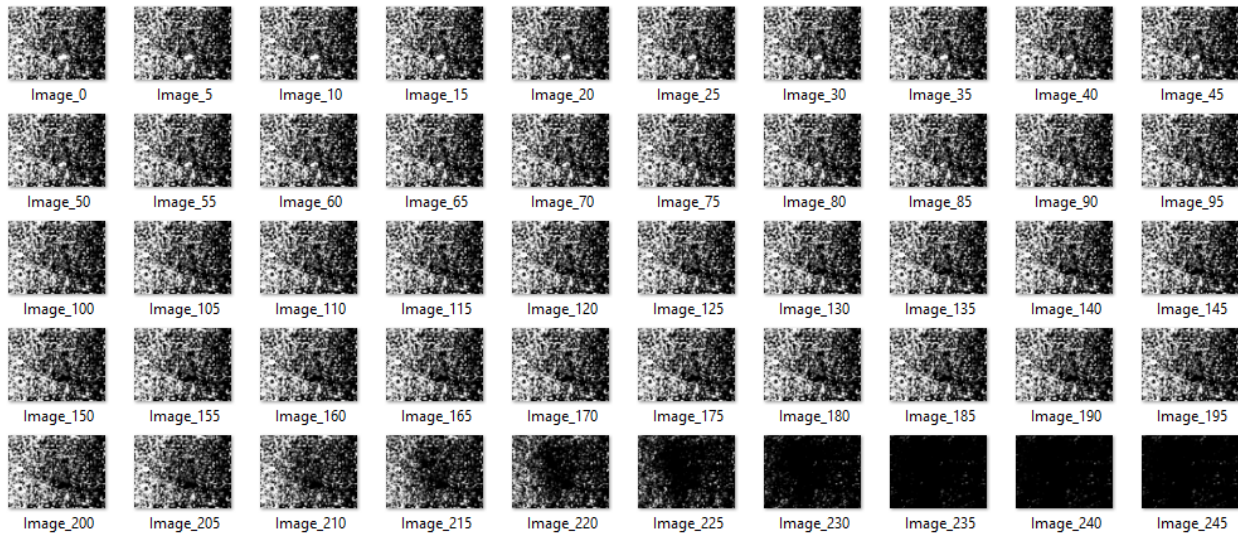


Fig. 2: Test image segmentation results at different threshold values of excess green minus red index (ExGR) method

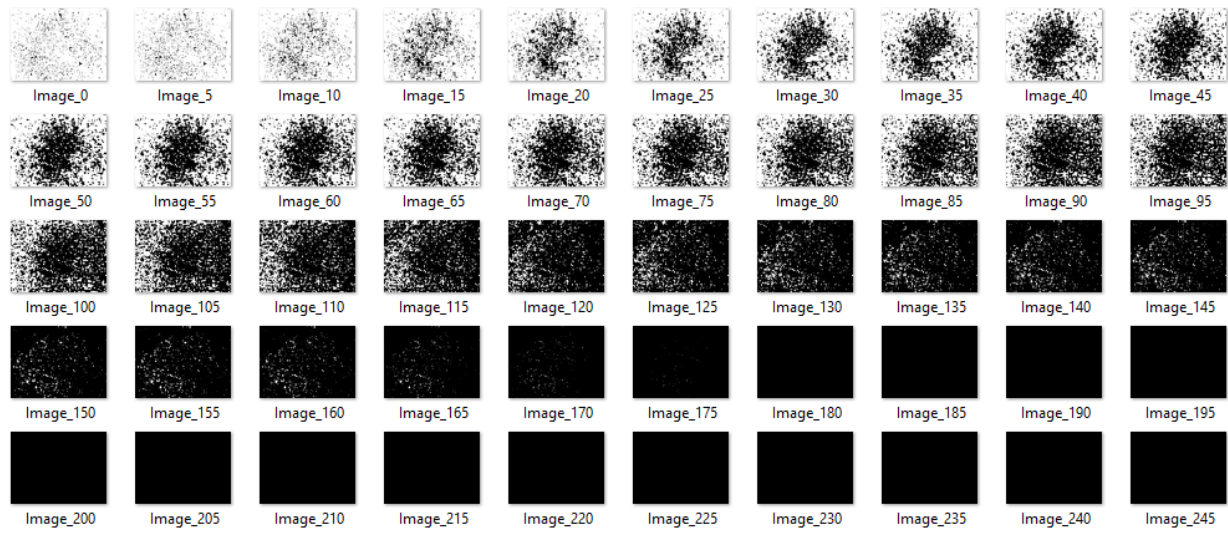


Fig. 3: Test image segmentation results at different threshold values of Hue-Saturation-Value (HSV) method

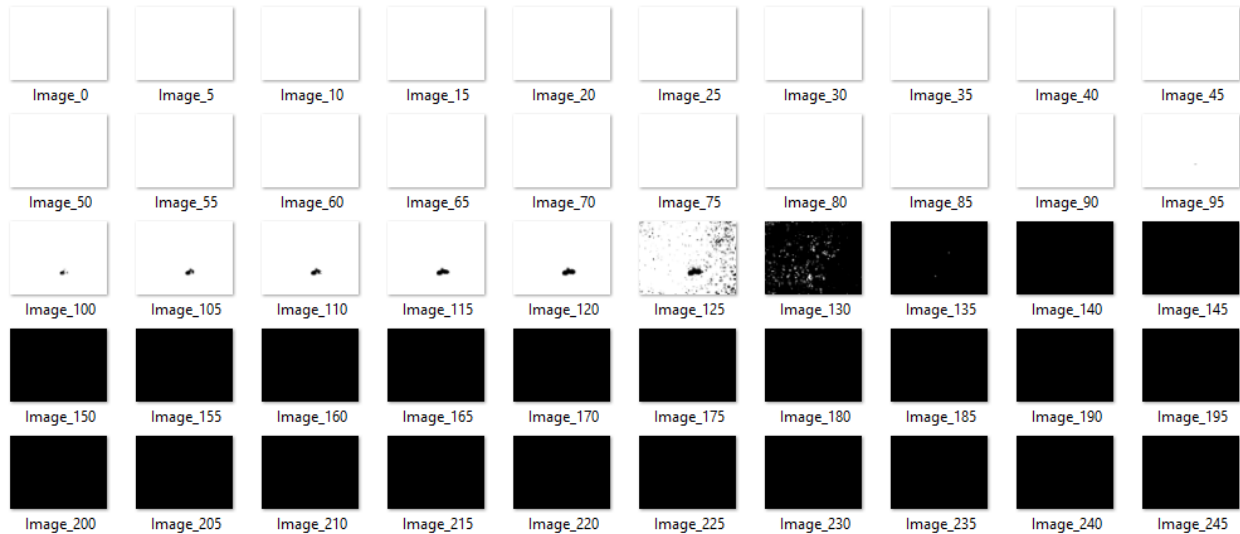


Fig. 4: Test image segmentation results at different threshold values of CIELAB method

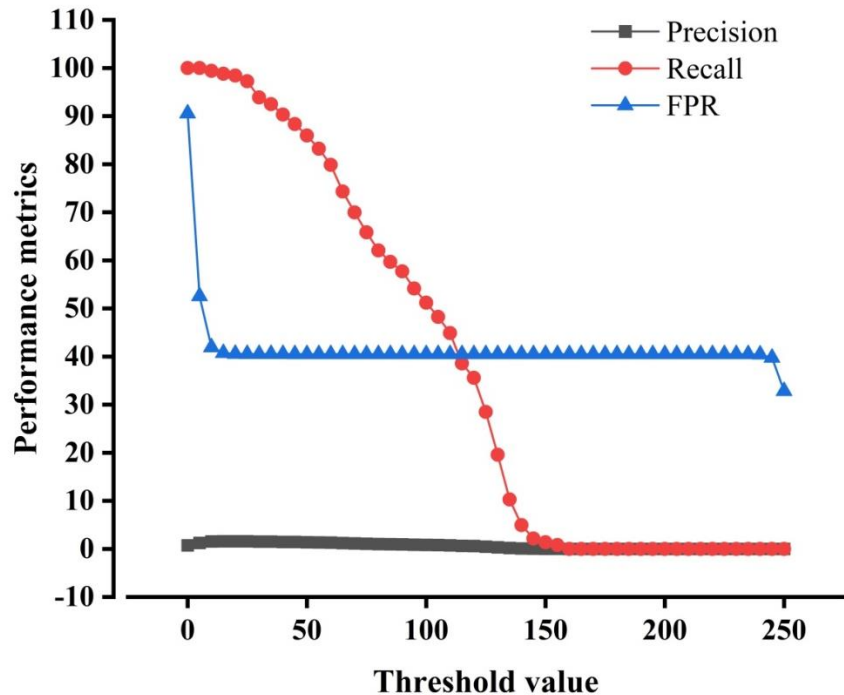


Fig. 5: Performance metrics of excess green index (ExG) method at different threshold values

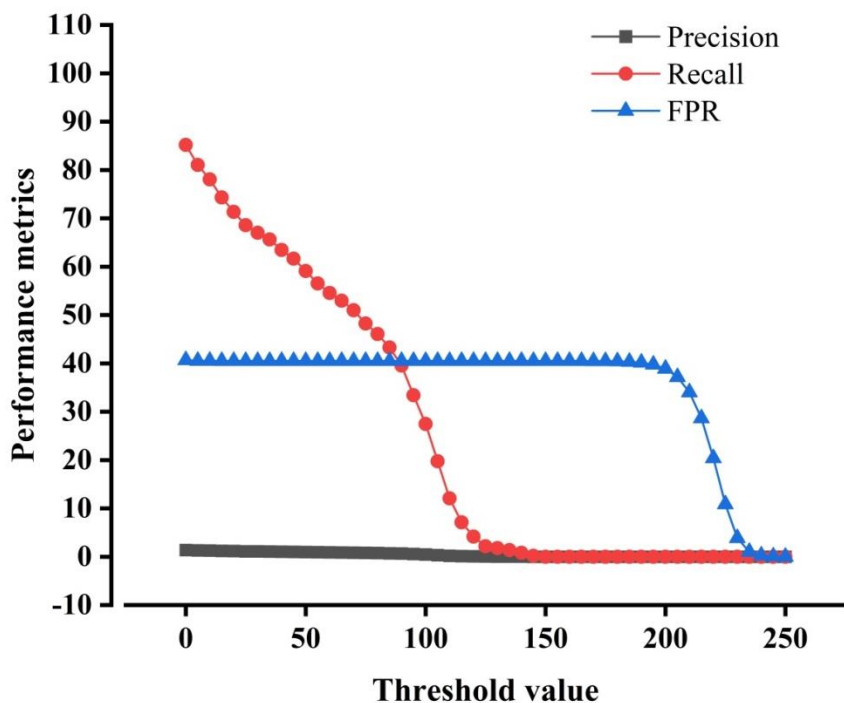


Fig. 6: Performance metrics of ExGR method at different threshold values

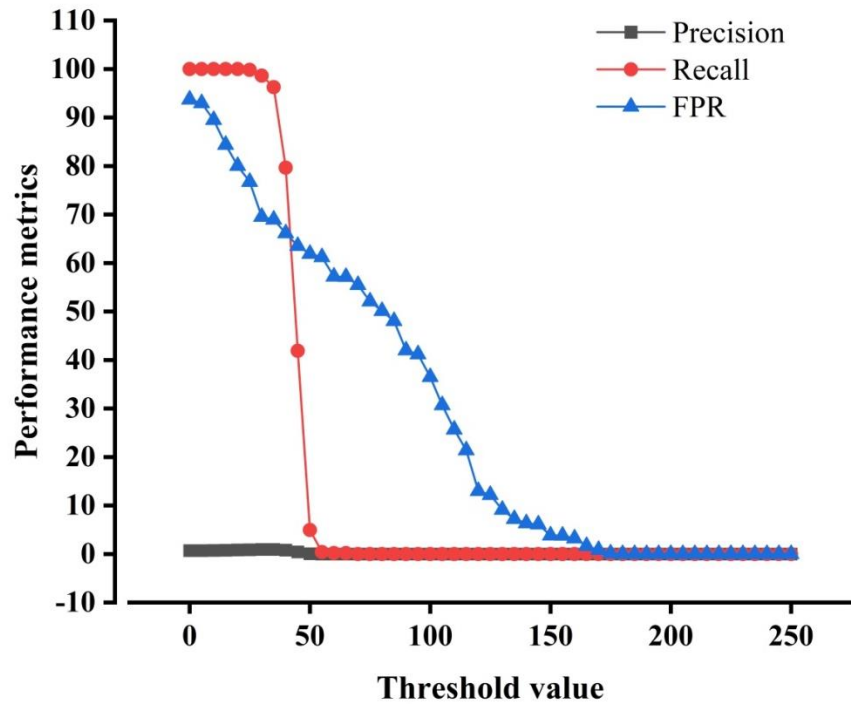


Fig. 7: Performance metrics of HSV method at different threshold values

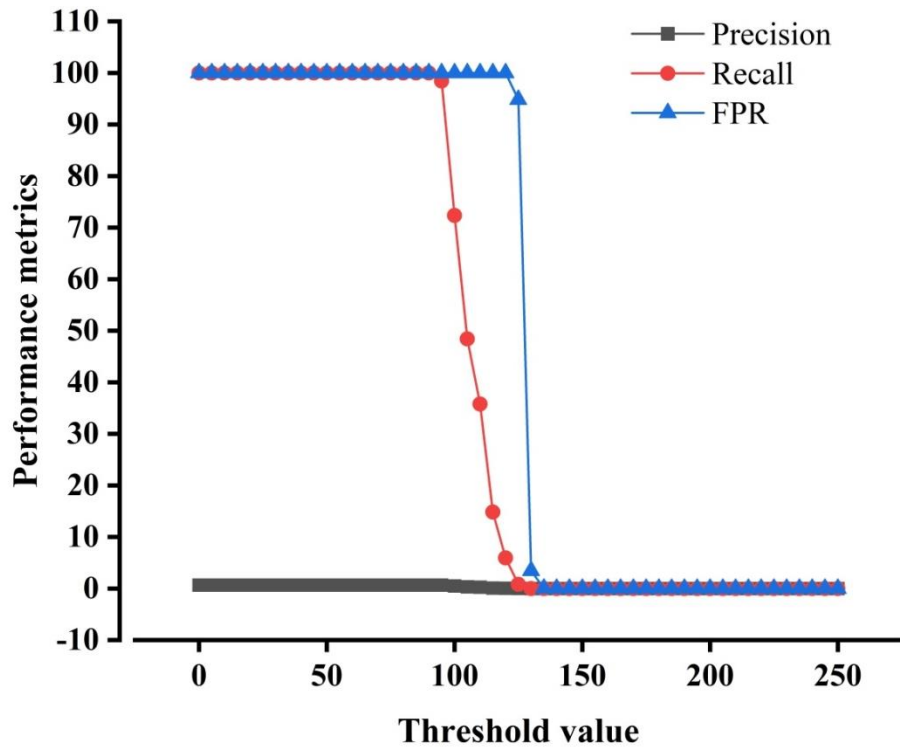


Fig. 8: Performance metrics of CIELAB method at different threshold values

Appendix-II



Plate 1: Over head trolley test setup with microcontroller unit



Plate 2: Measurement of spray distribution pattern using patternator

Appendix-III

Table 1: Analysis of variance of discharge rate at different operating pressure and solenoid valve opening time

Source of variation	Degree of freedom	Sum of Squares	Mean Square	F-value	Prob>F
Operating pressure (P)	2	384.12	192.06	1.685	0.0001
Solenoid valve opening time (t)	3	2893.18	964.39	8.46	0.0001
P×t	6	99.87	16.64	1.46	0.0001
Error	24	2.73	1.13		
Corrected Total	35	3377.18			

Table 2: Analysis of variance of weeding efficiency of two spraying methods

Source of variation	Degree of freedom	Sum of Squares	Mean Square	F-value	Prob>F
Method of application	1	5.17	5.17	0.58	0.45184
Error	28	248.75	8.88		
Total	29	253.92			

Table 3: Analysis of variance of weedicide application rate of two spraying methods

Source of variation	Degree of freedom	Sum of Squares	Mean Square	F-value	Prob>F
Method of application	1	47458.32	47458.32	205.94	0.0005
Error	8	1843.45	230.43		
Total	9	49301.81			

Appendix IV

Paper accepted from the current investigation -I

Plant Physiol. Rep. (January–March 2021) 26(1):179–187
https://doi.org/10.1007/s40502-020-00562-0



ORIGINAL ARTICLE

Greenness identification using visible spectral colour indices for site specific weed management

K. Upendar¹ · K. N. Agrawal¹ · N. S. Chandel¹ · K. Singh¹

Received: 2 September 2020 / Accepted: 7 December 2020 / Published online: 29 January 2021
© Indian Society for Plant Physiology 2021

Abstract In the present study an attempt has been made to identify the green vegetation based on colour using visible spectral colour indices such as excess green index (ExG), excess red index (ExR) and excess green minus excess red index (ExGR). At first stage, the performance of colour indices were tested at four illumination intensities using the standard colour patches. The results indicated a clear separation between the ExG, ExR and ExGR values of green colour patches (foliage, yellow green & green) and soil colour patches (dark skin, moderate red & magenta) at illumination intensity of 89.04 ± 8.12 lux than 188.8 ± 6.36 , 259.25 ± 12.73 and 359.28 ± 10.10 lux illumination intensities. This observation suggested that the colour indices might perform better at low lighting condition. In the second stage, the images of original plants and soil were captured at an illumination intensity of 89.04 ± 8.12 lux and classification rate at different threshold were studied. The average correct classification rate of ExGR and ExG colour indices were found to be 93.03% and 86.03% at threshold values 0 and 10, respectively. This indicates that the colour index ExGR could be successfully employed for image based classification of plant and non-plant material.

Keywords Colour indices · Image processing · Image segmentation · Imaging sensor · Machine vision · Weed identification

Introduction

Weed management is a major challenge in agriculture because weeds are spread randomly in the agriculture field (Agrawal et al. 2012). Weeds compete with the primary crop for resources and decrease crop yields (Hamuda et al. 2016; Wang et al. 2007). A secure link has been identified between loss of crop yield and weed competition, with a wide range of crop varieties (Chandel et al. 2018; Hamuda et al. 2016). The invention of new technologies such as sensors, controllers coupled with opto-electronic system (Agrawal et al. 2012), suitable spraying technology and a decision support system enabled precision application of herbicides; a potential herbicide saving amount was reported as 30 to 75% (Hamuda et al. 2016; Heisel et al. 1999). Hence, there is a need for a system to identify the weed patches so that herbicides can be applied only in weed-infested zones rather than the whole field basis (Agrawal et al. 2012). This site-specific weed management has provided one motivation for developing image processing methods for identifying weeds/plants (Hamuda et al. 2016).

Machine vision is one of the first methods to assess agricultural products and its spread has been associated with hardware development. Machine vision application is not just limited to industry sectors but can also be employed in agriculture product grading, colour diagnosis, and texture analysis (Adelkhani et al. 2012). Most of the available machine vision techniques have limitations in field conditions (Hamuda et al. 2016; Slaughter et al. 2008). The output of a digital colour camera depends on the light source (Adelkhani et al. 2012), variable illumination (Chandler 2003; El-Faki et al. 2000; Mahmud et al. 2019; Steward and Tian 1999; Tian and Slaughter 1998) and type of camera (El-Faki et al. 2000). The conventional

✉ K. Upendar
k.upendar007@gmail.com

¹ ICAR- Central Institute of Agricultural Engineering, Nabi Bagh, Berasia Road, Bhopal 462038, India

Paper communicated from the current investigation -2

Journal of Field Robotics - Manuscript number ROB-22-0302

Inbox ×



Queen Melos <onbehalfof@manuscriptcentral.com>

to me, narendracae, singhkaran, manoj_iasri, kn_agr

Mon, Nov 14, 2:00 PM

14-Nov-2022

Dear K,

Your manuscript entitled "Development of a real time computer vision based post emergence site specific herbicide applicator for weed management" has been successfully submitted online and is presently being given full consideration for publication in *Journal of Field Robotics*.

Your manuscript number is ROB-22-0302. Please mention this number in all future correspondence regarding this submission.

You can view the status of your manuscript at any time by checking your Author Center after logging into <https://mc.manuscriptcentral.com/rob>. If you have difficulty using this site, please click the 'Get Help Now' link at the top right corner of the site.

Book Chapter

The Role of Sensing Techniques in Precision Agriculture

 taylorfrancis.com/chapters/edit/10.1201/9781003122401-3/role-sensing-techniques-precision-agriculture-upendar-agrawal-kumar-vinod

Chapter

By K. Upendar, K.N. Agrawal, Kumar S. Vinod

Book [Machine Vision for Industry 4.0](#)

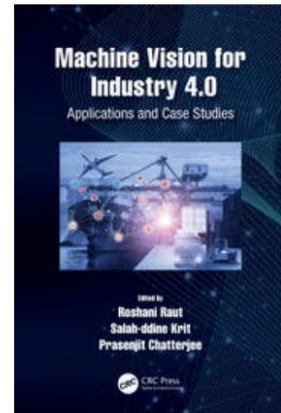
Edition 1st Edition

First Published 2022

Imprint CRC Press

Pages 16

eBook ISBN 9781003122401



ABSTRACT

Industrial Revolution 4.0 refers to how technologies like autonomous vehicles, artificial intelligence (AI) and the Internet of Things (IoT) are uniting with humans' physical lives. Precise application and management of agricultural inputs is a challenging task in present-day agriculture. Green Revolution focused on improving crop productivity through the use of genetically modified seeds, agrochemicals and fertilizers. Due to the excessive dosage of agrochemicals and fertilizers, there are severe environmental concerns and many health problems observed. Moreover, freshwater availability is depleting day by day, and preservation of this natural resource is the need of the hour. In recent years, the prime focus has shifted toward optimizing the agriculture inputs without any adverse effect on crop yield. Upon applying agriculture inputs at the right amount, right time and right place during crop cultivation, there is a chance to reduce the input cost. These things are possible only when we can capture plants' present growth status, information on soil nutrient and moisture status and weather conditions in real time. AI, IoT and autonomous vehicles have become a part of the agriculture sector. The rapid growth and new innovations in the domain of AI for agriculture process control and a variety of monitoring tasks have spawned a parallel growth in the sensor requirements for measuring, recording and controlling the process variable. The present study provides detailed applications of different sensors in the field of precision agriculture, i.e. irrigation, fertilization, pest control and greenhouse.

[Previous Chapter](#)

Poster and Oral presentation from the output of current investigation

Abstract-I

Summary and Abstract

Theme 3: Agricultural Engineering and Technology

Illumination in-variant image transformation and excess green colour index for greenness identification under controlled lightening condition

Upendar K* and Agrawal K.N.

ICAR- Central Institute of Agricultural Engineering, NabiBagh, Berasia Road, Bhopal, M.P.-462038

*Corresponding author : k.upendar007@gmail.com

Identification of crops or weeds from complex soil backgrounds based on colour intensity values is a popular approach in computer vision-based weed identification system. Two approaches were followed to extract vegetation from complex soil backgrounds. Grasses and plant leaf images were captured under a testing platform covered with black cloth and equipped with a light source of illumination intensity of 89.4 ± 8.12 lux. The illumination invariant image transform and excess green colour index values of leaves and soil samples were analyzed. Illumination in-variant image transformation values of plant leaves range from -0.16 to -0.24, whereas soil ranges from -0.025 to -0.125. Excess green index values of plant leaves found more than 60, whereas soil values range from 0 to 50. The threshold value of Illumination in-variant image transformation (IVIT) and excess green index (ExG) was selected as -0.013 and 50, respectively. The classification accuracy of these threshold values was tested on five plant images. The average True Positive Rate (TPR) and False Positive Rate (FPR) were observed as 98% and 96 % for IVIT and 96% and 96% for ExG. Under controlled lighting conditions both methods showed the nearly same segmentation accuracy. However, the execution time of the ExG index was 0.46 milliseconds, whereas 14000 milliseconds for IVIT. The time complexity plays a vital role in real-time weed or plant detection and pesticide or herbicide application, therefore ExG method is more acceptable for crop/weed identification on the go weed identification system.

Abstract-II



International Conference on AAFS Aug. 22 - 24th, 2022

SEMANTIC VEGETATION SEGMENTATION USING VISIBLE SPECTRAL COLOUR INDICES AND COLOUR MODELS

K. Upendar, K. N. Agrawal and N. S. Chandel

ICAR- Central Institute of Agricultural Engineering, Nabi Bagh, Berasia Road, Bhopal, MP, India, - 462038

ABSTRACT

Semantic segmentation of vegetation from the soil background in field images is of great importance for crop weed identification for spot spraying. As detection sensor a Logitech webcam was used. The lower and upper threshold values of excess green index (ExG), excess green minus red index (ExGR) and CIELAB colour model were found to be 20 and 200, 0 and 190, and 0 and 120, respectively. The classification accuracy of ExG, ExGR and CIELAB colour model with finalized threshold values were tested on several plant images captured at fixed illumination intensity. The average precision, recall and F1-score were found to be 0.70, 0.87 and 0.77 for ExG, 0.84, 0.86 and 0.84 for ExGR, 0.96, 0.93 and 0.94 for CIELAB colour model. The CIELAB colour model showed highest classification accuracy than other colour indices. The results of study act as basis for several tasks such as identification of crop rows and crop-weed identification etc.

Keywords: Colour indices, Image processing, Semantic segmentation, Vegetation segmentation, Weed detection sensor

UNIVERSITY OF AGRICULTURAL SCIENCES, BANGALORE
ALL INDIA AGRICULTURAL STUDENTS ASSOCIATION, NEW DELHI
INDIAN COUNCIL OF AGRICULTURAL RESEARCH, NEW DELHI



INTERNATIONAL CONFERENCE ON ADVANCES IN AGRICULTURE AND FOOD SYSTEM TOWARDS SUSTAINABLE DEVELOPMENT GOALS (AAFS-2022) : 22 - 24 AUGUST 2022

Certificate

This is to certify that Dr./Mr./Ms. Konje Upendar, Senior Research Fellow..... of ICAR- Central Institute of Agricultural Engineering..... participated and presented (poster/oral presentation) and delivered their talk on Semantic Vegetation Segmentation Using Visible Spectral Colour Indices and Colour Model..... under the theme entitled 'Role of Agrochemicals, Biological and Technological Interventions Towards Safe Food and Nutritional Security' and secured position in the International Conference on 'Advances in Agriculture & Food System Towards Sustainable Development Goals' held from 22 - 24th, August, 2022 at University of Agricultural Sciences, Bangalore

Ashok Kumar Singh
DDG, Agril. Extension, ICAR
Chairman, Steering Committee

S. Rajendra Prasad
Chairperson, Organising Committee
& Vice-Chancellor, UAS, Bangalore

Vivek Saurabh
Co-Chairperson, Organising Committee
National President, AIASA

Abstract-III

FMPE/PF/023

Development of a real time image based inter row post emergence site specific herbicide applicator

Upendar K^{1*}, Agrawal K.N², Chandel N.S³, and Singh K⁴

¹Senior Research Fellow, ²Project Coordinator, ³Senior Scientist and ⁴Principal Scientist

ICAR-Central Institute of Agricultural Engineering, Nabi Bagh, Berasia Road, Bhopal, India

The efficiency of herbicide use and the effect of herbicide application on the environment and human being have become a critical issue. The conventional method of herbicide application is a blanket application irrespective presence of weeds. Application of herbicide on site-specific manner leads to saving of the costly chemical apart from achieving desired goal of weed control. Hence, an attempt was made to develop a real time image based inter row post emergence site specific herbicide applicator. The developed site specific herbicide applicator consists of Raspberry Pi 4 model B with 4 GB RAM, display (7 inch HDMI screen), L298N motor driver module, weed detection sensor, artificial light source, 24 V solenoid valve and flat fan nozzle. The average precision, recall, false positive rate and F1-score of CIELAB colour model for semantic image segmentation were found to be 96.50%, 96.75 %, 1.5% and 95.61%, respectively. The average processing time of decision-making algorithm was found to be 150 ± 5 ms. Image processing time, delay in acquisition of two successive frames and duration of solenoid valve opening were found to have impact on success of a real time image-based herbicide spraying system. In order to reduce the overlap between two consecutive frames a time delay of 300 ms was employed and optimal centre to centre distance between weed detection sensor and spraying unit was found to be 282 mm. The duration of solenoid opening 450 ms was found to be sufficient to spray recommended amount of chemical at field of view of weed detection sensor.

Keywords: Semantic image segmentation; Site specific weed management; Site specific herbicide applicator; Weed; Weed detection sensor

*Corresponding author:k.upendar007@gmail.com



CERTIFICATE

This is to certify that

Upendar K, SRF, ICAR-CIAE, Bhopal

has presented a paper in the 56th Annual Convention of Indian Society of Agricultural Engineers on "Agricultural Engineering Innovation for Global Food Security" and International Symposium on "India @ 2047: Agricultural Engineering Perspective" held from 09.11.2022 to 11.11.2022 at the Agricultural Engineering College and Research Institute, Tamil Nadu Agricultural University, Coimbatore, Tamil Nadu, India

A handwritten signature in black ink.

Dr. M. Balakrishnan
Organising Secretary

A handwritten signature in black ink.

Dr. A. Raviraj
Convenor

A handwritten signature in black ink.

Dr. S. N. Jha
President, ISAE